Universidad Autónoma de Madrid

Departamento de Bioquímica

Identification of the substrates of the protease MT1-MMP in TNFα-stimulated endothelial cells by quantitative proteomics. Analysis of their potential use as biomarkers in inflammatory bowel disease.

Agnieszka A. Koziol

Tesis doctoral

Madrid, 2013

Departamento de Bioquímica
Facultad de Medicina

Universidad Autónoma de Madrid

Identification of the substrates of the protease MT1-MMP in TNFα-stimulated endothelial cells by quantitative proteomics. Analysis of their potential use as biomarkers in inflammatory bowel disease.

Memoria presentada por Agnieszka A. Koziol licenciada en Ciencias Biológicas para optar al grado de Doctor.

Directora: Dra Alicia García Arroyo
Centro Nacional de Investigaciones Cardiovasculares (CNIC)

Madrid, 2013

- ACKNOWLEDGEMENTS -

First and foremost I would like to express my sincere gratitude to my supervisor Dr. Alicia García Arroyo for giving me the great opportunity to study under her direction. Her encouragement, guidance and support from the beginning to the end, enabled me to develop and understand the subject. Her feedback to this manuscript, critical reading and corrections was inappreciable to finish this dissertation.

Next, I would like to express my gratitude to those who helped me substantially along the way. To all members of MMPs' lab, for their interest in the project, teaching me during al these years and valuable contribution at the seminary discussion. Without your help it would have not been possible to do some of those experiments. Thank you all for creating a nice atmosphere at work and for being so good friends in private. I would like to also thank all of the collaborators and technical units for their support and professionalism.

Finally, I would like to acknowledge Ministerio de Educación, Cultura y Deporte for providing me the financial support for my research, CNIC and Universidad Autonoma de Madrid for all the economical and technological facilities supporting my thesis work and coursework.

- SUMMARY -

Understanding the molecular mechanism regulating angiogenesis is an essential aspect of pathology of many diseases. Recent evidences implicate membrane-type 1 matrix metalloprotease (MT1-MMP), a potent pericellular enzyme expressed by vascular cells, in inflammation and angiogenesis. This work aimed to explore the MT1-MMP's contribution to inflammatory-induced angiogenesis, formation of new vessels from preexisting ones. To accomplish this, we applied quantitative proteomic technique named SILAC to TNFα-activated endothelial cells derived from wildtype and MT1-MMP null mice to identify the substrate repertoire of this protease and identify candidates that might affect capillary sprouting within the inflammatory context. We found that TNFα activated endothelial cells and induced expression of several markers characteristic for endothelial tip cells, the main effectors of sprouting angiogenesis. Moreover, MT1-MMP expression was upregulated after TNFα pulse, accompanied by differences in supernatant glycoproteome between wildtype and MT1-MMP null endothelial cells. Glycoproteins identified as putative MT1-MMP substrates include key extracellular matrix, matricellular and secreted proteins such TSP1, NID1, CYR61, SEM3C or SLIT2 as well as cytokines and growth factors like EGFR and CSF1. Bioinformatic analysis revealed a combinatorial MT1-MMP proteolytic program, in which combined rather than single substrate processing would determine biological decisions by activated endothelial cells, including chemotaxis, cell motility and adhesion, and vasculature development. Processing of TSP1, CYR61, NID1 and SEM3C was impaired in MT1-MMP-deficient animals leading to reduce angiogenic response. The relevance of this MT1-MMP-driven proteolytic program was observed in pathology in aberrant angiogenesis related to chronic inflammatory disorders as inflammatory bowel disease (IBD). Using an experimental model of mouse colitis we showed soluble levels of TSP1 and NID1 were increased and positively correlated with MT1-MMP expression. Impaired processing of these substrates was also observed in human serum samples from patients with low/moderate activity of ulcerative colitis or Crohn's disease.

Taken together, these data illustrate that MT1-MMP is an important regulator of inflammatory-induced angiogenic response in endothelial cells and that substrates processed by this protease, such as TSP1 and NID1 might be used as a biomarkers for the diagnosis or prognosis of chronic inflammatory disorders.

- RESUMEN -

Entender los mecanismos moleculares que regulan la angiogénesis es un aspecto esencial en la patología de numerosas enfermedades. La metaloproteasa de matriz extracelular de membrana tipo 1 (MT1-MMP) es una potente enzima pericelular expresada por las células vasculares. Este trabajo ha explorado la contribución de MT1-MMP en la angiogénesis, formación de nuevos vasos a partir de vasculatura pre-existente, en el contexto inflamatorio. Para ello, se ha aplicado la técnica de proteómica cuantitativa denominada SILAC en células endoteliales derivadas de ratones de genotipo silvestre o deficientes en MT1-MMP; estas células endoteliales se han activado con la citoquina inflamatoria TNFα con objeto de identificar el repertorio de sustratos de MT1-MMP e identificar candidatos que podrían afectar la respuesta angiogénica en inflamación. Hemos demostrado que TNFα activaba las células endoteliales e inducía la expresión de varios marcadores característicos de células endoteliales líder (tip). El tratamiento con TNFα también aumentaba la expresión de la proteasa MT1-MMP en las células endoteliales lo que correlacionaba con diferencias en el glicoproteoma del sobrenadante de cultivo de células endoteliales de genotipo silvestre versus deficientes en MT1-MMP. Las glicoproteínas identificadas como sustratos potenciales de MT1-MMP incluyen proteínas de la matriz extracelular, proteínas matricelulares y proteínas secretadas como TSP1, CYR61, NID1, SEM3C o SLIT2 así como citoquinas y factores de crecimiento como EGFR y CSF1. El análisis bioinformático de los datos proteómicos ha desvelado un programa proteolítico combinatorial, en el cual el procesamiento combinado de varios sustratos por MT1-MMP en vez del procesamiento de sustratos individuales es el que determina las decisiones biológicas de las células endoteliales activadas tales como quimiotaxis, motilidad y adhesión celular, y desarrollo vascular. Hemos confirmado que el procesamiento de TSP1, CYR61, NID1 y SEM3C está disminuido tanto en células como en ratones deficientes en MT1-MMP lo que correlaciona con una reducción de la respuesta angiogénica. Por último, hemos investigado la importancia de este programa proteolítico mediado por MT1-MMP en patologías que cursan con angiogénesis inflamatoria, en concreto en enfermedad inflamatoria intestinal. Utilizando un modelo de colitis experimental en ratón hemos observado que los niveles solubles en suero de los sustratos TSP1 y NID1 aumentan en correlación con la expresión de MT1-MMP a lo largo de la severidad de la colitis. Además, en muestras de suero procedentes de pacientes con colitis ulcerosa o enfermedad de Crohn con actividad baja/moderada también se observa un aumento en los niveles de TSP1 y NID1.

En conclusión, nuestros datos demuestran la importancia de MT1-MMP como proteasa reguladora de la angiogénesis inflamatoria en células endoteliales e indican que sustratos procesados por MT1-MMP como TSP1 o NID1 pueden servir como biomarcadores para el diagnóstico o pronóstico de enfermedades inflamatorias crónicas.

CONTENTS

- NON-STANDARD ABBREVIATIONS AND ACRONYMS -

ADAM(TS)	A Disintegrin and Metalloproteinase (with Thrombospondin Motifs)
BP	Biological Processes
CD	Crohn's Disease
CSUP	Culture supernatant
CXCR4	C-X-C chemokine receptor type 4
CYR61	Cysteine-rich angiogenic inducer 61
DAVID	Database for Annotation, Visualization and Integrated Discovery
Dll4	Delta-like ligand 4
DTT	Dithiothreitol
EC(s)	Endothelial cell(s)
ECM	Extracellular matrix
EDTA	Ethylenediaminetetraacetic acid
GO	Gene Ontology
H/L	Heavy/Light
HUVEC(s)	Human Umbilical Vein Endothelial Cell(s)
IBD	Inflammatory Bowel Disease
ICAM-1	Intracellular adhesion molecule 1
Jag1	Jagged1
MCP-1	Monocyte chemoattractant protein-1
MIP-2	Macrophage inflammatory protein-2
MLEC(s)	Mouse lung endothelial cell(s)
MMP(s)	Matrix metalloprotease(s)
MS	Mass spectrometry
MT1-MMP	Membrane type-1 matrix metalloprotease
NID1	Nidogen 1
PECAM-1	Platelet endothelial cell adhesion molecule 1
PFA	Paraformaldehyde
SDF-1	Stromal cell-derived factor-1
SEM3C	Semaphorin 3C
SILAC	Stable Isotope Labeling by Amino Acids in Cell Culture
TL	Total lysate
TSP1	Thrombospondin 1
UC	Ulcerative colitis
VEGF(R)	Vascular endothelial growth factor (receptor)
VCAM-1	Vascular cell adhesion molecule 1
WGA	Wheat Germ Agglutinin
WT	Wildtype

- MORPHOGENESIS OF THE VASCULAR SYSTEM -

The vascular network penetrates whole body to supply tissues with nutrients and oxygen and provide signaling molecules and immune cells. The mechanism by which blood vessels form involves three main processes: VASCULOGENESIS, ANGIOGENESIS (sprouting and intussusception) and VASCULAR REMODELLING (Risau 1997). VASCULOGENESIS refers mostly to the embryonic stage when the first primitive vascular structures are being formed from endothelial progenitors, although it may also occur in cancer (Carmeliet 2003). It is characterized by primitive vascular endothelial cells (angioblasts) that migrate to the sites of vascularization, differentiate and form the initial vascular plexus (Risau 1995, 1997).

ANGIOGENESIS is referred to formation of new capillaries from pre-existing ones and is driven by highly invasive endothelial cells (ECs), called the tip cells. Once the nascent vascular plexus is formed, these specialized endothelial cells proliferate and migrate forming new capillaries that branch from existing vessels. Tip cells selection is controlled by the Notch pathway (Hellström et al. 2007) and their migration depends on a gradient of VEGF, a master regulator of angiogenesis (Gerhardt et al. 2003). Growth of the vascular network is a highly dynamic process with several main mechanisms including: (1) sprouting, (2) anastomosis, (3) lumenization and (4) pruning. The earliest steps include activation of part of endothelial cells (tip cells), loosening of cell junction integrity, basement membrane degradation and invasion of tip cells to initiate first sprout. Once filopodia-extending tip cells reach other sprout or nearby vessel they connect (anastomose) followed by lumen assembly to create new functional vessel. Subsequent recruitment of mural cells and basement membrane deposition stabilize newly formed connections (R. H. Adams and Eichmann 2010) and excess of redundant branches is removed (pruning). Term "VASCULAR REMODELLING" is commonly used to refer to the later phase of blood vessels formation when vessels increase its luminal diameter in response to increased blood flow and acquires identity as artery, vein or capillary.

Angiogenesis occurs at later embryonic and postnatal stages where appears to be the main process for the formation of the majority of blood vessels. In adult organism in physiologic conditions vasculature is stable, but in situations such as tissue repair or pathological disease processes, ECs become again motile and invasive letting the vessels growth and expand (**Figure 1A**).

Principal cellular players in angiogenesis

Several cell types are actively involved in the process of new vessel formation. Endothelial cells, together with pericytes form a highly specialized, dynamic interface between the blood and the surrounding tissue (**Figure 1A**). Apart of ECs, fibroblasts, epithelial, mesenchymal or

microglial cell can regulate angiogenesis by either releasing pro- or antiangiogenic stimuli or providing physical support by enwrapping nascent tubules and promoting their stability (Rymo et al. 2011). During vessel formation in retinal development astrocytes apart of secreting VEGF-A, the main proangiogenic factor, spread at the vascular front providing a sort of scaffold on which ECs migrate (Gerhardt et al. 2003; Stone et al. 1995). Recent studies demonstrate that also leukocytes and macrophages are universal players associated with physiologic and pathologic angiogenesis acting as suppliers of angiogenic cytokines like M-SCF and placenta growth factor (PlGF) or as physical support for branching and anastomosis (Fantin et al. 2010; Y. Kubota et al. 2009; Luttun et al. 2002; Pipp et al. 2003). Although all these cell types contribute to the correct functioning of the vasculature and directly or indirectly participate in angiogenesis, only the vascular endothelial cells are thought to be the key players regulating the process of vascular network formation.

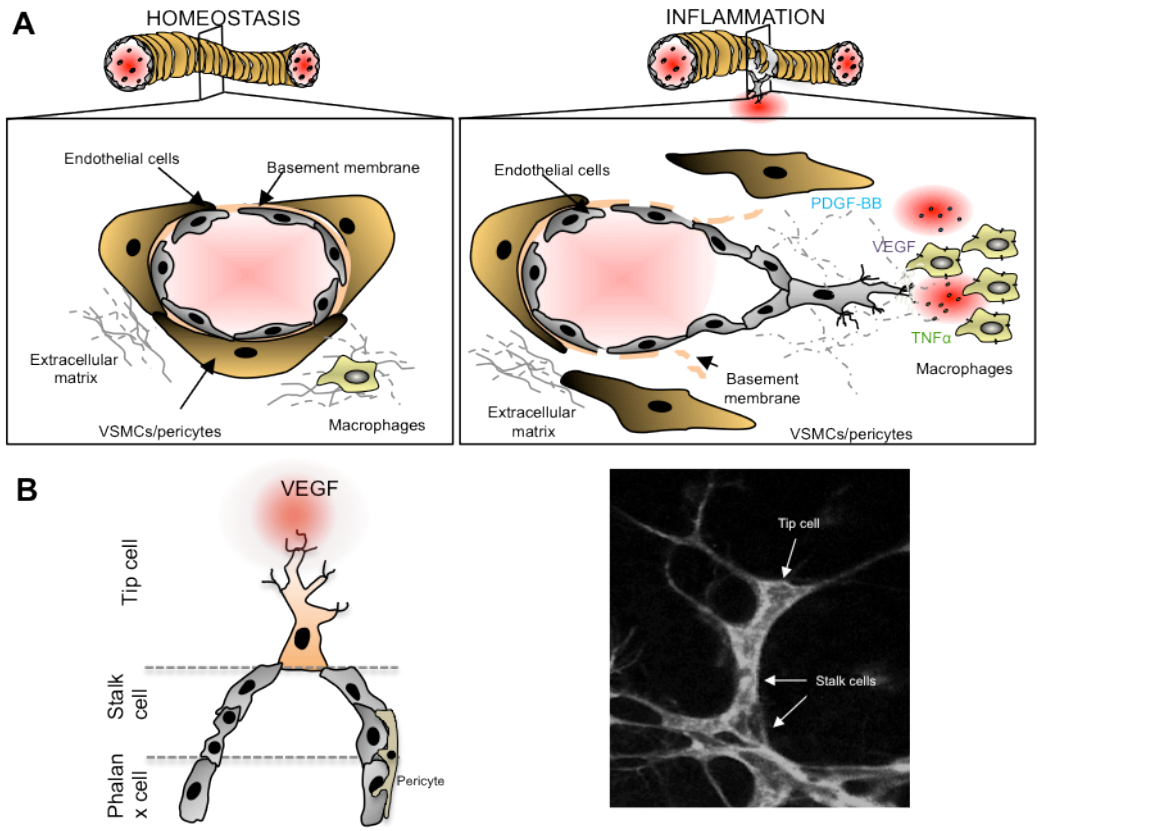

Figure 1. Cell interplay in the vascular system in homeostatic and inflammatory conditions. (**A**) In homeostatic conditions endothelial cells (ECs), vascular smooth muscle cells (VSMCs)/pericytes and macrophages promote normal functioning of the vasculature (left). Upon inflammation, macrophages release soluble cytokines and growth factors such as TNFα that induces morphological and phenotypic changes in ECs, VSMCs and macrophages aimed at resolution of the injury (right). (**B**) Activated endothelium consists of tip cells that lead and guide new sprout, highly proliferative stalk cells and phalanx cells maintaining vessel stability.

In adults ECs maintain plasticity required for specific morphogenetic responses upon proangiogenic stimulus. There are three types of ECs involved in angiogenesis: PHALANX, STALK and TIP endothelial cells (**Figure 1B**). Phalanx cells mostly remain quiescent, resemble cobblestone appearance and together with stalk cells are covered by pericytes and basement membrane to maintain structural and functional integrity of the vessel (Mazzone et al. 2009). Moreover, stalk cells are highly proliferative and provide new ECs for vessel elongation and support lumen formation. In contrast, tip cells, located at the distal end of sprouts are motile and polarized with multiple protrusions. They are attracted by proangiogenic stimuli, which induce directional migration and invasion of surrounding tissue and fuse with neighboring sprouts in process termed anastomosis (Geudens and Gerhardt 2011). Tip cells do not have lumen and usually do not proliferate; they have also different gene expression profile from stalk and phalanx cells, characterized by high levels of VEGFR2 (Gerhardt et al. 2003). The tip/stalk selection is transient and reversible with continuous shuffling regulated by VEGFR-Dll4-Notch signaling (Jakobsson et al. 2010). At final steps of new vessel formation recruitment of mural cells like pericytes and vascular smooth muscle cells stabilize vessel and promote their maturation (Armulik et al. 2005; Betsholtz et al. 2005). Vascular pruning and remodeling finish the process of vascular morphogenesis and convert these new vessels in stable and quiescent vasculature (Baluk et al. 2004; Rocha and Adams 2009).

Molecular regulation of angiogenesis

The master regulator of both physiologic and pathologic vessel growth is VEGF; a mitogen specific to ECs but expressed also by many other cell types including macrophages and cancer cells (Ferrara 1999; Salgado et al. 2001). The effect of VEGF depends on the presence of specific receptors localized on activated endothelium – VEGFR1 on stalk or VEGFR2 and VEGFR3 on tip cells {Phng, 2009, Angiogenesis: a team effort coordinated by notch}. Activation of these receptors causes increased permeability of blood vessels, activation and migration of endothelium (**Figure 1 and 2**). Tip cells migrate towards increased VEGF gradient, whereas stalk cells upregulate proliferation in response to high VEGF concentration (De Smet et al. 2009; Gerhardt et al. 2003). Moreover VEGF induces filopodia formation through Cdc42 activation (De Smet et al. 2009). Other cytokines such as FGF, HGF, IL-8, PDGF and family of CXC chemokines have been also classified as direct proangiogenic factors, stimulating degradation of extracellular matrix, EC migration and proliferation. Another group of angiogenesis stimulating agents in paracrine way are able to stimulate proper ECs to produce and release direct stimulus (Salgado 2001). Among them are IL-6, TGF-β, prostaglandins, angiopoietins, G-CSF, GM-CSF, SCF and other (Heidemann 2003).

Despite high local concentration of VEGF or other proangiogenic stimuli, not all ECs will acquire tip cell phenotype. This fate selection is strongly controlled by the Notch pathway (**Figure 2**) (Eilken and Adams 2010; Phng and Gerhardt 2009; Roca and Adams 2007). VEGF induces high expression levels of Delta-like 4 (Dll4), one of the Notch ligands, in tip cells, which in turn activate Notch in neighboring stalk cells and suppress the tip phenotype by downregulation of VEGFR2 and -3 (Benedito et al. 2009; Hellström et al. 2007; Suchting et al. 2007). Stalk cells in contrast express high levels of another Notch ligand, Jagged1 (Jag1), a Dll4 antagonist, which induces sprouting and inhibit Notch signals in tip cells (R. H. Adams and Eichmann 2010; Benedito et al. 2009). Balanced signaling between Dll4 and Jag1 maintain dynamic and reversible tip/stalk phenotype acquired by vascular endothelial cells.

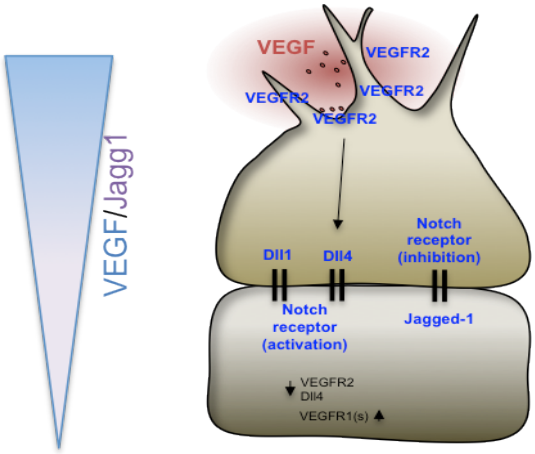

Figure 2. Tip cell selection is controlled through Notch signalling. Tip cells respond to the to high VEGF gradient, which induces high expression levels of Dll4, one of the Notch ligands, in tip cells, which in turn activate Notch in neighboring stalk cells and suppress the tip phenotype by downregulation of VEGFR2 and -3 and increased proliferation of other EC that will become stalk cells. Strong expression of Jagg1 in stalk cell antagonizes Dll4-mediated activation of Notch on neighboring tip ECs.

Inflammation-driven angiogenesis

In the postnatal life of healthy organisms angiogenesis is not a common phenomenon. Proliferation of endothelium is slow and its turnover takes over three years (Denekamp 1984). Activation of the angiogenic process requires local change of equilibrium between stimulating and inhibitory agents of vascular network growth. In healthy adult individuals the balance between pro- and antiangiogenic factors in clearly leaning on the part of the latters (Pepper et al. 1996). Inflammatory response can often activate angiogenesis in several ways. First, vessels permeability and enhanced leukocyte transmigration to the inflamed tissue, which produce angiogenic factors can stimulate vessel growth. Furthermore, released by activated leukocytes/macrophages proinflammatory cytokines stimulate VEGF mRNA expression (Ferrara 1999). Second, increased blood influx itself can stimulate angiogenesis through shear stress on the endothelium (Schaper and Scholz 2003). Finally, hypoxic condition in the inflamed tissue can induce angiogenesis through upregulation of VEGF, TNFα or bFGF (Taylor and Sivakumar 2005). Normally angiogenesis that

occurs in acute inflammation is beneficial to its resolution, however if angiogenesis persists might contribute to induction of chronic inflammatory disease. This pathologic angiogenesis is considered an important indicator of pathogenesis in many diseases like connective tissue disorders such as psoriasis, rheumatoid arthritis, in gastric disorders (inflammatory bowel disease), cardiovascular diseases (artherosclerosis) and neuroinfection, diabetes or cancer (Folkman 1995a, 1995b). Thus the importance of angiogenesis in chronic inflammatory diseases raised a possibility of antiangiogenic therapies. Most of them are based on blocking VEGF or PDGFβ receptors, nonetheless only a part of patients may benefit from antiantiogenic therapies, thus there is a raising need of successful improvement and search of new targets (Crawford and Ferrara 2009; Potente et al. 2011).

- MMP FAMILY OF PROTEASES -

Fundamental to the angiogenic process is the ability of endothelial cells to degrade extracellular matrix and surrounding blood vessels basement membrane. The family of matrix metalloproteases (MMPs) play in this process substantial role principally due to they capability of degrading surrounding tissues during initial steps of sprouting; however new functions for this enzymes have been described recently.

Since their discovery by Gross and Lapierre (GROSS and LAPIERE 1962) matrix metalloproteases have been an object of intensive studies due to their crucial contribution to a variety of physiological and pathological processes. MMP family consists of Zn^{2+}-dependent endopeptidases, composed by at least by 23 members in humans and 24 in mice (Page-McCaw et al. 2007), which share a conserved domain structure and function, and collectively are capable to degrade almost any kind of extracellular matrix (ECM) components.

Nowadays, it is recognized that MMPs functions are extended beyond breaking down the surrounding extracellular matrix. As a result of pericellular proteolysis matrix-bound protein fragments or growth factors can be released from matrix by ectodomain shedding or secreted proteins (e.g. cytokines, other enzymes) can be activated, deactivated or modified their biological activity. Thus MMPs can not only regulate tissue architecture but also can directly alter the availability of bioactive molecules and trigger signaling cascades (Page-McCaw et al. 2007; Sternlicht and Werb 2001). In addition, some of MMP members can impact cellular behavior by regulation of gene transcription in as yet undefined manner (Toriseva et al. 2012). This process is more evident in membrane-inserted MMPs in which their short cytosolic tail can regulate intracellular signaling by interaction with a number of partners or by undergoing posttranslational modifications thus affecting cell migration, invasiveness, intracellular trafficking, gene

transcription and protein expression (Gingras and Béliveau 2010). These aspects will be detailed in further paragraphs.

MMPs as multifunctional enzymes

The ability of cells to migrate into tridimensional complex matrices and invade surrounding tissues is achieved thanks to proteases and protease-like proteins. Among 553 human proteases, the most numerous is the family of metalloproteases and in particular MMPs play a fundamental role in this process (Puente et al. 2003).

Tissue remodeling occurring during embryonic growth and development are events that require MMPs' activity to break basement membrane and ECM to allow cell to proliferate, migrate and growth. Analysis of genetic knockouts of MMPs provided additional information about functions and substrates of each MMP. Surprisingly, no gestation lethality was observed in any of MMPs' knockout mice, suggesting a high grade of compensation and redundancy among the whole family. In contrast, individual MMP adult mutants show serious defects related to failed tissue remodeling. Several MMP knock out mice (MMP-2, -9, -13, -14, -20) present bone and skeletal remodeling defects demonstrated in reduced endochondral ossification, delayed healing of bone fractures, failed transition from cartilage to bone, abnormal bone resorption, secondary ossification centers and defective tooth enamel (Caterina et al. 2002; Colnot et al. 2003; Holmbeck et al. 1999; Holmbeck et al. 2003; Holmbeck et al. 2005; Inada et al. 2004; Stickens et al. 2004; Vu et al. 1998; Zhou et al. 2000). So far the most severe phenotype was decribed for MMP-14 knockout mice that die postnatal (Holmbeck et al. 1999; Zhou et al. 2000). In addition, MMP-2-MMP-14 double knockout mice die at birth indicating that MMP-2 and MMP-14 have overlapping functions (Oh et al. 2001).

In addition to their classical degradative activity, various MMPs are involved in development during embryonic and postnatal life. MMP-2 and -3 are implicated in postnatal mammary development by regulating mammary gland branching morphogenesis during puberty (Wiseman et al. 2003).

Role of MMPs in inflammation and angiogenesis

MMPs are also important in tissue homeostasis, regulating processes like wound healing, inflammation or angiogenesis. MMP-7 knockout mice display defective innate intestinal immunity manifesting susceptibility to bacterial infection due to impaired proteolysis of endogenous antibiotic peptide pro-cryptdin (Wilson et al. 1999). In addition, MMP-7 mutant mice exhibit abnormal chemokine release from lung epithelium (neutrophil attractant CXC-motif ligand-1) resulting in defective recruitment of inflammatory cells after lung injury (Li et al. 2002). Pro- and

anti-inflammatory properties were showed for MMP-2 and MMP-9; which can guide inflammatory cell recruitment and clearance of inflammatory cells by cleaving of inflammatory mediators like MCP3, CXCL1, CXCL4, CXCL6, CXCL8, CXCL12 (D'Haese et al. 2000; Kumagai et al. 1999; McQuibban et al. 2002; Overall 2002; Van den Steen et al. 2000). Finally, several MMP mutant mice exhibit defects in blood vessel remodeling observed only at the postnatal stage both in normal and pathological conditions. Nevertheless, role of MMPs in angiogenesis is complex, and similarly to their impact on inflammation, they may act in both ways: either promoting or inhibiting new vessel formation. It has been widely described the relevance of these enzymes in tumor angiogenesis. Increased MMPs' activity can enhance carcinogenesis by processing and activation of proangiogenic factors like VEGF, bFGF and TGF-β (Belotti et al. 2003; Bergers et al. 2000; Deryugina et al. 2002a; Sounni et al. 2002; Yu and Stamenkovic 2000). In particular, MMP-9 mutant mice have defects in neovascularization at the growth plates of long bones and in response to injury model of retinal degeneration (Lambert et al. 2003; Vu et al. 1998). This latter, was also observed in MMP-2 knockouts and even strongly in MMP-2 MMP-9 double mutant indicating the redundant effect of those two MMPs. The unique exception of this general rule is observed in MMP-8 knockout mice, which in absence of protease strongly increase the evidence of skin tumors (Balbín et al. 2003). Likely mechanism through which MMPs contribute to angiogenesis includes overexpression of protease in vascular cells (macrophages and endothelial cells) under tumorigenic conditions and thus increased processing of basement membrane, in particular collagen I, promoting cell migration, processing and modulation of activity of signaling molecules (e.g. VEGF, PDGF) and regulating perivascular cells coverage (Bergers et al. 2000; Chantrain et al. 2004; Galvez et al. 2001; Hiratsuka et al. 2002; P. H. Huang et al. 2009; Johnson et al. 2004). However, the contrary effect to these proangiogenic MMPs functions was recently described for several proteases. Using again an example of MMP-9, proteolysis of type IV collagen lead to release tumstatin protein with suppressive consequence on pathological angiogenesis (Hamano et al. 2003). Moreover several MMPs are able to cleave precursors of angiostatin, endostatin or thrombospondins known endogenous inhibitors of angiogenesis (J. C. Adams 2004; Cornelius et al. 1998; Rodriguez-Manzaneque et al. 2001).

Lack of any of this angiogenic drawback at the embryonic stage of knock out mice which born with normal vasculature suggest that role of MMPs are mostly attributed to postnatal angiogenesis and remodeling.

MMPs in human disease models

Apart of an evident implication in cancer, diverse human diseases were associated with various MMP-loss-of-function mutations: a rare osteolytic syndrome, Missouri variant of spondyloepimetaphyseal dysplasia (SEMD), and the tooth enamel defect amelogenesis imperfecta,

are caused by point MMP-13, MMP-20 and MMP-2 mutations (Kennedy et al. 2005; Kim et al. 2005; Martignetti et al. 2001). Similarly, homozygous mutations in MMP-14 are responsible for human Winchester syndrome, one of examples of "vanishing bone" disorders (Evans et al. 2012). Other data based on mouse models indicates implication of MMPs to inflammatory-related pathologies such as asthma and lung inflammation, stroke, heart attack, Alzheimer's disease and aortic aneurysm. Also skin, kidney and brain inflammation have been shown the great implications of MMPs (Egeblad and Werb 2002; Page-McCaw et al. 2007; Siefert and Sarkar 2012).

Domain structure and classification

The first classification and nomenclature of MMP family was based on the principal substrate that a particular MMP processed, thus we could distinguish collagenases (MMP-1, MMP-8, MMP-13, MMP-18), gelatinases (MMP-2, MMP-9), stromelysins (MMP-3, MMP-10, MMP-11) and matrilysins (MMP-7, MMP-26). Results of more recent works unified the MMP nomenclature, as it is well known that each MMP degrades a range of substrates, in fact there is considerable substrate overlapping between individual MMPs (Cauwe et al. 2007; GROSS and LAPIERE 1962; Overall et al. 2002; Rawlings et al. 2006).

With minimal variations, all MMPs share the same domain structure that contains from the N-terminus: directing their secretion a SIGNAL PEPTIDE, a PRODOMAIN necessary to maintain enzyme latency, and the conserved CATALYTIC DOMAIN. Depending of each subfamily MMPs optionally possess HEMOPEXIN-LIKE DOMAIN that define substrate specificity, and in case of membrane-tethered members TRANSMEMBRANE DOMAIN or GLYCOSYLPHOPHATIDYLINOSITOL (GPI) LINK and a CYTOSOLIC TAIL at the C-terminus (Folgueras et al. 2004; Overall et al. 2002).

MMPs, like most proteolytic enzymes are synthesized and released as inactive proenzymes or zymogens. MMPs activation occurs through several mechanisms; *in vitro* a variety of agents like mercurial and thiol modifying compounds, reactive oxygen radicals, denaturant agents as well as low pH and high temperature can drive the proenzyme activation (Nagase 1997). This mechanism, known as the cysteine-switch model, where interaction between the thiol group of a pro-domain cysteine residue and the zinc ion of the catalytic site is being disrupted (Van Wart and Birkedal-Hansen 1990). *In vivo*, MMPs form part of proteolytic cascade, where cleavage of N-terminal pro-peptide is done by other protease (Sato et al. 1994; Strongin et al. 1995). In addition, some MMPs possesses a furin-like recognition sequence (RXKR or RRKR) between the pro- and catalytic domains which is cleaved intracellular by furin-like convertases (Yana and Weiss 2000; Zucker et al. 2003).

MMPs are expressed by most of the normal and tumor cells and its expression and activity is regulated at several levels from upon mentioned proteolytic activation, gene transcription (controlled by cytokines and growth factors), by posttranslational modifications (e.g.

phosphorylation, palmitoylation) or directly by interaction with ECM components or other cells (Anilkumar et al. 2005; Biswas et al. 1995; Nagase and Woessner 1999; Nyalendo et al. 2007).

Under physiological conditions exists an equilibrium between proteolytic degradation and inhibition of proteolysis, precisely controlled by a group of specific broad-spectrum inhibitors TIMPs (tissue inhibitors of metalloproteases); those are expressed as soluble proteins (TIMP-1, -2, -4) or associated with ECM (TIMP-3) and block MMPs' activity by forming complexes with their catalytic site (Borden and Heller 1997; Nagase et al. 2006; Visse and Nagase 2003; Westermarck and Kähäri 1999). Apart of TIMPs, MMPs activity can be blocked by binding to plasma proteins such as alpha-2 macroglobulin or membrane-bound glycoprotein RECK (reversion including cysteine-rich protein with kazal motifs (Baker et al. 2002; Oh et al. 2001).

In pathological situations like cancer progression and metastasis this MMP/TIMP axis is disrupted since many of MMPs are upregulated. Moreover studies have shown that MMPs activity is linked to advanced, invasive or metastatic stage of several cancers and thus their expression is often associated with a poor prognosis (Curran et al. 2004; Duffy et al. 2000; Folgueras et al. 2004; Forget et al. 1999; López-Otín and Overall 2002; Stamenkovic 2000). This offered a possibility to use MMPs as targets for anticancer therapy, however different studies demonstrates that relation between MMPs' levels and cancer progression seems not be so linear and thus their use as therapeutics did no fulfilled expectation (Coussens et al. 2002).

This work focused on one particular member of membrane-type (MT-) subfamily of MMPs (**Figure 3**), subdivided in two categories, based on the manner they attach to the cell surface:

1. TRANSMEMBRANE MT-MMPs, with short transmembrane domain inserted in the cellular membrane as a standard type I single pass molecule. Short cytosolic tail is involved in regulation of intracellular trafficking, protein turnover and activity (Lehti et al. 2000; Uekita et al. 2001). Followed members are included here: MT1-MMP (MMP-14), MT2-MMP (MMP-15), MT3-MMP (MMP-16), MT5-MMP (MMP-24) and the unique type II transmembrane protein member MMP-23.
2. GPI-ANCHORED MT-MMPs, which bind to the cell membrane trough GPI-linker and thus lacked transmembrane and cytosolic domain, which is cleaved off in endoplasmic reticulum lumen. Two members compose this group: MT4-MMP (MMP-17) and MT6-MMP (MMP-25) (Itoh et al. 1999; Kojima et al. 2000).

This unique and restricted positioning of MT-MMPs confers them specific properties to regulate extracellular microenvironment and, in the particular case of MT1-MMP, affecting some cellular function by interaction with its intracellular C-terminal.

MT1-MMP as a paradigm of membrane-tethered MMP

MT1-MMP (MMP-14) was discovered as 582 amino acids, 63kDa product expressed by invasive lung carcinoma cells and with potent ability to activate pro-MMP-2 secreted by stromal cells of the same tumor (Sato et al. 1994). cDNA screening identified a protein closely aligned to MMPs' family with a potential 24-amino acid transmembrane domain at the C-terminus (Sato et al. 1994).

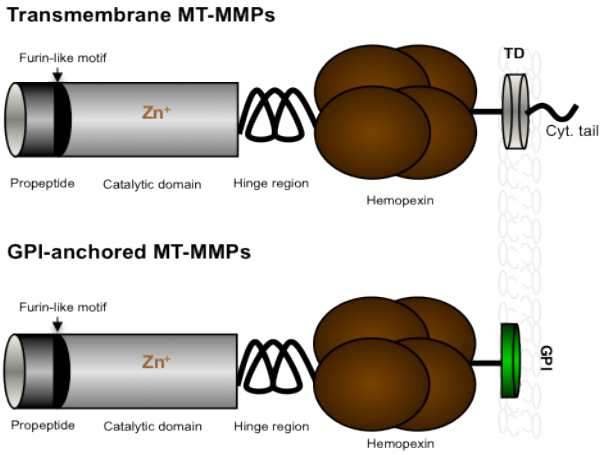

Figure 3. Schematic domain structure of MT-MMPs. MT1-, MT2-, MT3-, MT5-MMP contain short transmembrane domain (TD) followed by an intracellular cytosolic tail. MT4-MMP and MT6-MMP are anchored to the membrane via a glycosylphosphatidylinositol (GPI motif).

MT1-MMP shares a common domain structure with other MMP family members (**Figure 3**), including propetide (M^{1}-R^{111}), catalytic domain (Y^{112}-G^{285}), a hinge region (E^{286}-I^{318}), a hemopexin domain (C^{319}-C^{508}), a stalk region (P^{509}-S^{538}), a transmembrane domain (A^{539}-F^{562}), and a cytoplasmic tail (R^{563}-V^{582}) (Itoh and Nagase 2002; Sato et al. 1994; Zucker et al. 2003). A point mutation in catalytic domain active site of Glu^{240} to Ala (MT1-MMP-E240A) has been shown to be proteolytic inactive and incapable to self-proteolysis (Rozanov et al. 2001).

Like other MMPs, MT1-MMP is produced as an inactive zymogen, with an additional insertion of basic residues ($RRKR^{111}$) between the propeptide and the catalytic domain, which is proteolytically removed by at least four members furin-like serine proteases (Zucker et al. 2003). These protein convertases are transmembrane calcium-dependent protein associated with trans Golgi network; in this manner MT1-MMP activation takes place intracellularly, in the Golgi, and the already mature enzyme is expressed on the cell surface (Itoh and Seiki 2006; Nagase 1997; Yana and Weiss 2000; Zucker et al. 2003).

Regulatory mechanisms controlling MT1-MMP expression

MT1-MMP is ubiquitously expressed in a number of cells and tissues and its regulation is driven by the same mechanisms that in other MMPs i. e. transcriptional and non-transcriptional (e.g. posttranslational modifications, trafficking, dimerization, interaction with cells or ECM

components). Importantly, MT1-MMP in endothelial cells is expressed at low levels in steady-state conditions and may be upregulated upon stimulation. A number of cytokines and growth factors were shown to stimulate MT1-MMP expression; these include IL-1α, IL-1β, TNFα, bFGF, GM-CSF, TGFβ, CCL2, IL-8 and others (Tomita et al. 2000) (Rajavashisth et al. 1999) (Galvez et al. 2005; Han et al. 2001). Tyrosine phosphorylation of c-met activates signaling pathways of MAPK/Erk or PI-2 kinase and STAT components; these factors work as mitogens or migration factors in response to cell-environment stimuli (Han et al. 2001; Zucker et al. 2003). Consensus binding sites for transcription factors such as Sp1, Erg-1, NF-kB were described for endothelial cell MT1-MMP gene promoter (Haas et al. 1999). Traffic to the cell surface and to particular domains is an important stimulating factor. Expression of some members of the claudin family, endothelial tight junction proteins, can directly recruit MT1-MMP to cell surface (Miyamori et al. 2001). In addition, other reports point than many of the extracellular matrix proteins like collagen, fibronectin, laminin, tenascin etc. can regulate MT1-MMP synthesis indirectly by cytoskeletal changes that arise after interaction of these ECM proteins with cell (Galvez et al. 2002; Zucker et al. 2003). Also cell-cell contact also has been reported to modulate MT1-MMP expression; MT1-MMP mRNA levels were showed to decrease in epithelial cells once they reach confluence (Tanaka et al. 1997).

MT1-MMP subcellular location

MT1-MMP is anchored to the plasma membrane but its precise location and compartmentalization at membrane microdomains might vary thus impacting on its accessibility to process certain substrates. Our previous studies and others showed that MT1-MMP is found in endothelial and other cells in different cell compartments in association to distinct molecular partners (**Figure 4**, and (Gonzalo et al. 2010):

1. LAMELLIPODIA and FILOPODIA PROTRUSIONS in association with caveolin-1 and integrin αvβ3 where MT1-MMP is catalytically active (Galvez et al. 2002). Our group has also demonstrated that caveolae-mediated MT1-MMP internalization is required for its proper localization, activity and function in endothelial cell migration (Galvez et al. 2004);

2. CELL-CELL JUNCTIONS IN TSP4 (TETRASPANIN)-ORGANIZED MICRODOMAINS associated with integrin α3β1 where MT1-MMP seems to be proteolytically inactive (Yanez-Mo et al. 2008);

3. FOCAL ADHESIONS likely associated to other integrin β1 members and/or adapter proteins such as p130Cas and FAK where MT1-MMP might be playing additional functions related to signalling,

focal adhesion turnover, and matrix invasion (D'Alessio et al. 2008; Gonzalo and Arroyo 2010; Wang and McNiven 2012);

4. PODOSOMES / INVADOPODIA where MT1-MMP is also a well-characterized component of the invasive machinery and the contribution of MT1-MMP to the formation and function of these protrusive structures is well established (Destaing et al. 2011; Frittoli et al. 2011; Nakahara et al. 1997; Poincloux et al. 2009);

5. INTRACELLULARLY in association with NUCLEUS or GOLGI COMPARTMENTS. Several studies suggest that this intracellular location MT1-MMP can impact gene transcription as shown for VEGF, PI3Kδ, FIH1 and others (**Table 1**), but MT1-MMP may also process nuclear protein pericentrin (Golubkov et al. 2005; Shimizu-Hirota et al. 2012). These findings indicate that under certain circumstances MT1-MMP might unexpectedly be proteolytically active inside cells, through as-yet unclear mechanisms.

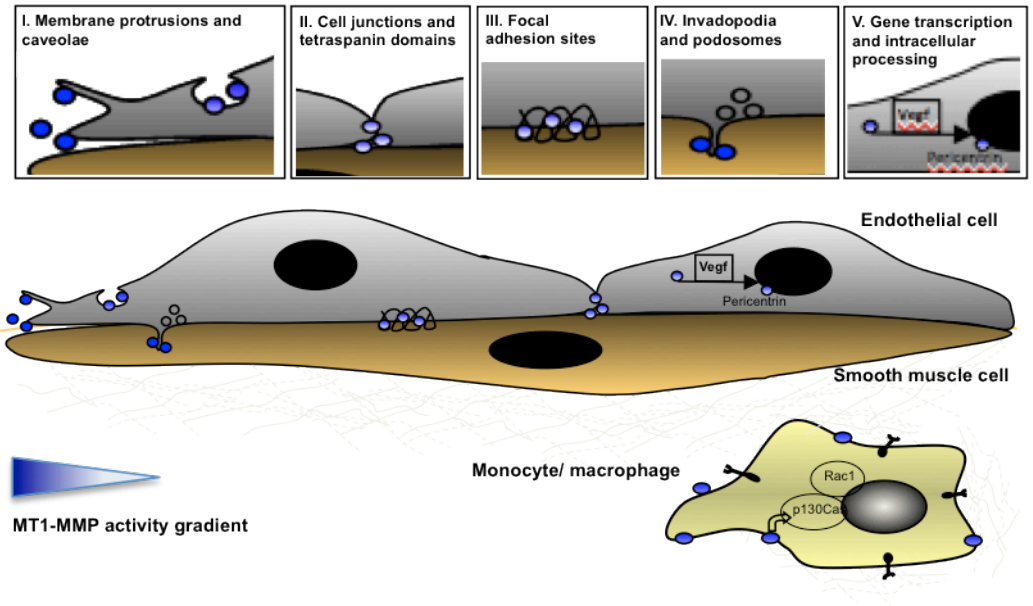

Figure 4. MT1-MMP subcellular localization. MT1-MMP preferentially localizes at the membrane protrusions like filopodia, lamellipodia or invadopodia where it is most active but also in caveolae where associates with integrins or cell-to-cell contact at tetraspanin domains where mostly participate in protein interaction and matrix degradation. Less common is MT1-MMP intracellular localization to Golgi or nucleus. Moreover cytosolic tail interaction with intracellular protein can lead to activation of gene transcription.

Taraboletti and coll. reported that MT1-MMP was found in endothelial microvesicles shed from localized area of the plasma membrane. This shedding was stimulated by some growth factors and addition of this vesicle-enriched medium to the endothelial cells activates cell migration and invasion through basement membrane layers (Taraboletti et al. 2002).

Important role for MT1-MMP cellular localization, invasive activity, trafficking and signalling is assigned to its short cytosolic tail. In fact collection of proteins have been identified as associated to the MT1-MMP cytosolic tail and several signalling pathways are triggered or regulated by MT1-MMP pointing to its contribution in a variety of biological processes. Different groups showed that MT1-MMP required its cytoplasmic tail to localize to the invadopodia of tumor cells; moreover it promotes invasion of several types of tumor cells (Lehti et al. 2000; Nakahara et al. 1997; Rozanov et al. 2001; Shimizu-Hirota et al. 2012).

MT1-MMP subcellular location drives and orchestrates its accessibility to distinct cellular and extracellular substrates contributing to fine-tuned regulation of specific substrate processing and therefore MT1-MMP functionality. As an example, forced location into lipid rafts resulted in limited MT1-MMP-dependent processing of E-cadherin in tumors cells (Rozanov et al. 2004). This information suggests that the compartmentalization of MT1-MMP is linked to proteolytic-dependent and proteolytic-independent functions, through which it can coordinate extracellular cues with cellular responses.

Cleavage preferences and targets of MT1-MMP

In terms of proteolytic activity, MT1-MMP displays a wide substrate repertoire including triple helical collagens and other major ECM components, but also transmembrane receptors, cytokines, growth factors and other proteases such as pro-MMP2, thus being considered one of the most critical modulators of pericellular environment. On top of that it is becoming evident that MT1-MMP can behave as a transmembrane receptor with novel functions in which catalytic activity is dispensable like altering gene expression (Koziol et al. 2012a).

Main MT1-MMP substrates and biological consequences of their processing were briefly summarized in **Table 1** (Baciu et al. 2003; Basile et al. 2006; Belkin et al. 2001; Covington et al. 2006; d'Ortho et al. 1997; Deryugina et al. 2002b; Egawa et al. 2006; Endo et al. 2003; Golubkov et al. 2005; Guo et al. 2012; Hikita et al. 2006; Hiller et al. 2000; Holopainen et al. 2003; Hotary et al. 2002; Karsdal et al. 2002; Koshikawa et al. 2000; Koziol et al. 2012b; Lehti et al. 2002; Lehti et al. 2005; McQuibban et al. 2001; McQuibban et al. 2002; Nishida et al. 2012; Ohuchi et al. 1997; Shimizu-Hirota et al. 2012; Sounni et al. 2004; Strongin et al. 1995).

Table 1. Biological consequences of MT1-MMP catalytic and non-catalytic activity

Changes in matrix proteins and in the tissue architecture
Cleavage of triple helical collagen (I, II and III), laminin, vitronectin, tenascin, fibrin, fibrinogen, aggrecan, PDGFRbeta,
Converting structural matrix proteins to signaling molecules
Fibronectin, nidogen, thrombospondin, semaphorin 4D, CD44, E-cadherin

Changes in protein bioactivity
pro-MMP-2, pro-MMP-8, pro-MMP-13, MT1-MMP, factor XII, pro-TGF-β, αvβ3 integrin, LRP, EMMPRIN, KIM-1

Chemoattraction
SDF1, MCP-3, RANKL,

Proliferation and Motility
Pericentrin, CD44, syndecan-1, laminin-5, E- and N-cadherin, transglutaminase, αvβ3 integrin

Gene expression
VEGF-A, PI3Kδ, FIH1

Kridel and coll. provided studies identifying specific short amino acid motifs recognized by MT1-MMP that defined the degree of substrate specificity for protease cleavage. In this way highly selective MT1-MMP's substrates compromised of the Arg – nonPro – X_{polar} – X_{Hy} motif where Arg at the P_4 position is essential for efficient hydrolysis and lack of Pro which is principally assigned to motif recognized by MMPs in general and poorly selective for MT1-MMP. This combination was shown to bind specifically to the catalytic pocket of MT1-MMP. Therefore selective substrates may become non-selective by insertion of Pro at P_3 position. (Kridel et al. 2002).

MT1-MMP in physiology and pathology

MT1-MMP is expressed in both embryonic and adult tissues, suggesting that MT1-MMP-mediated proteolysis of ECM is important during development and in postnatal tissue remodeling. Increased MT1-MMP mRNA level are found in mesenchymal and mesenchyma-derived cells (fibroblasts, chondrocytes, muscle and neural cells, pulmonary and renal epithelium and endothelial cells) and decreased with postnatal maturation and thus implicates protease in embryogenesis and developmental processes of kidney tubules formation, bone and lung development (Apte et al. 1997; Kadono et al. 1998; Kheradmand et al. 2002; Tanney et al. 1998).

However the role of MT1-MMP is not limited to the developmental homeostasis, but its requirement has been reported in processes like inflammation, injury and wounding. MT1-MMP produced by keratinocytes and stromal cells in granulation tissue is required for cell migration and ECM remodeling during wound healing (Okada et al. 1997). In healthy adult tissues MT1-MMP is expressed in hematopoietic cells – macrophages, neutrophils and lymphocytes, as well as endothelial cells where become upregulated by inflammatory stimuli such as TNFα, chemokines MCP-1/CCL2, IL-8 and SDF-1/CXCL12, nitric oxide and prostaglandin E2, that induces endothelial cells migration and tube formation (Alfranca et al. 2008; Gálvez et al. 2005; Genis et al. 2007; Han et al. 2001). Increased protease expression on the inflamed endothelium leads to

shedding and activation of a number of cytokines, growth factors and adhesion molecules crucial for correct course and resolution of inflammation (**Table 1**). MT1-MMP has temporal expression in endometrial epithelium where it is critical for glandular regeneration (Zhang et al. 2000).

The destructive capability of MMPs initially focused most research onto disease and that includes MT1-MMP, which expression similarly to the rest of MMP family was found in many carcinomas and was directly linked to cancer invasion. Therefore to define better the importance of MT1-MMP as a collagenase, independent groups have generated MT1-MMP-deficient mice (Holmbeck et al. 1999; Zhou et al. 2000), which resulted to be the only lethal MMP null mice. Even though they are apparently normal till birth, postnatal display a severe phenotype with gross developmental problems in skeleton, lung and adipose tissue some of them related to impaired remodelling of connective tissues and die around 3-12 weeks of age (Holmbeck et al. 1999; Zhou et al. 2000). At birth the neonatal null mice are indistinguishable from their wildtype counterparts, but shortly they develop apparent growth and skeletal impartments due to severe fibrosis in soft tissue and delayed in secondary ossification centres caused by failed collagen degradation by osteocytes (Holmbeck et al. 1999; Holmbeck et al. 2005) (**Figure 5**). It was confirmed by *in vitro* experiments that MT1-MMP knockout fibroblasts were not able to degrade type I collagen matrices (Holmbeck et al. 1999). Accordingly, craniofacial and axial skull bones are smaller and deformed. Long bones are severely affected due to impaired chondrocyte proliferation in the growth plates causing dwarfism (Zhou et al. 2000). Concurrently to skeletal development MT1-MMP knockout mice exhibit gross defects in angiogenesis. Defective vascular invasion leads to joints overgrowth and arthritis. MT1-MMP-deficient mice failed to form neovessels in collagen type I matrix (Chun et al. 2004), similarly showed impaired response to FGF-2 in an *in vivo* corneal implantation assay (Zhou et al. 2000).

No other MMP gene KO mice have shown such drastic phenotypes, suggesting that MT1-MMP is an essential cellular collagenase important for organizing the ECM microenvironment, impacting physiologic response as well as disease conditions, and which cannot be substituted for by any other MMP during development.

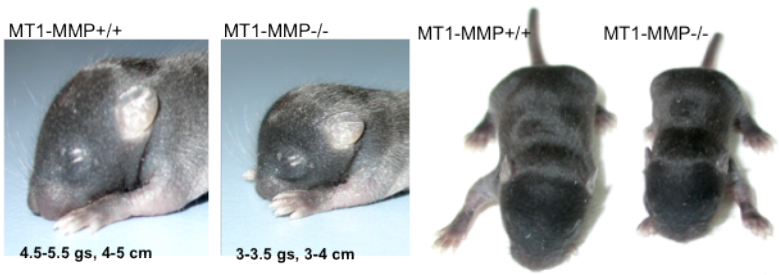

Figure 5. Retarded growth of MT1-MMP-deficient mice. Example of 7-day old littermates. MT1-MMP-deficient mice demonstrates dramatic retardation in the growth, showing a difference in the size and body weight.

Role of MT1-MMP in angiogenesis

MT1-MMP is considered to play important role in the vascular system and, as shown for MT1-MMP-deficient mice, developmental and postnatal angiogenic response in markedly reduced in these animals. However, its function in the cells present in the vasculature still remains poorly defined. MT1-MMP is expressed in smooth muscle cells in the vessel wall during embryonic development in aorta and other vascular territories being required for normal pericyte/VSMC recruitment through regulation of PDGFR signaling pathway (Apte et al. 1997; Lehti et al. 2005). In the adult however, MT1-MMP expression is low in the vasculature and is upregulated by inflammatory stimuli in ECs, VSMCs and macrophages upon injury contributing to angiogenesis and to vascular pathologies e.g. proinflammatory stimuli (IL-1α, TNF-α, and oxidized LDL) upregulate MT1-MMP expression in vascular smooth muscle cells and macrophages in atherosclerotic arteries affecting matrix remodeling and misregulating capillary morphogenesis (Rajavashisth et al. 1999).

MT1-MMP contributes to postnatal vascular development through several independent mechanisms, which include both catalytic and non-catalytic activity:

1. DEGRADATION OF BASAL LAMINA AND ECM PROTEINS is critical initiating step leading to break of the physical barrier, to clear the path and facilitates cell migration. MT1-MMP was shown to be the main and most potent fibrinolysin in endothelial cells during angiogenesis and cells with deleted form of transmembrane MT1-MMP resulted noninvasive (Hiraoka et al. 1998). But also the secondary effect of MT1-MMP on ECM and non-ECM protein processing can promote or inhibit angiogenesis by generation of degradation products of vascular basement membrane components, such as semaphoring-4D, endoglin, thrombospondin, soluble chemokines and growth factors, integrins and cadherins (Covington et al. 2006; Deryugina et al. 2002b; McQuibban et al. 2001; McQuibban et al. 2002; Ratnikov et al. 2002).
2. INVASION AND MIGRATION BY ACTIVATED ENDOTHELIAL CELLS are also essential requirements for the first steps in efficient angiogenesis. Quiescent endothelial cells express low levels of MT1-MMP that become upregulated by their migration and/or invasion within 2D and 3D matrices (Galvez et al. 2001). Highly migratory and invasive endothelial cells localized at the capillary front, so-called tip cells, express high levels of MT1-MMP (Fisher et al. 2009; Yana et al. 2007). In addition MT1-MMP is required for the formation of vascular guidance tunnels, which ECs use to migrate through ECM (Stratman et al. 2009).
3. ACTIVATION OF PROANGIOGENIC GENES; as above-mentioned MT1-MMP enhances the transcriptional activation of VEGF-A via src tyrosine kinase, a master regulator of angiogenesis, which in turn partially increases the proteolytic capacity of MT1-MMP (Deryugina et al. 2002a; Sounni et al. 2004).

4. DIRECTING NEOINTIMA FORMATION BY PERIVASCULAR CELLS (VSMCs). MT1-MMP derived from VSMCs mobilizes pericellular proteolysis, but protease deletion results to exhibit beneficial effect protecting from neointimal hyperplasia and lumen narrowing (Filippov et al. 2005). Other works described MT1-MMP-PDGFβ axis responsible for controlling VSCMs proliferation and chemotaxis leading to decreased mural cell density and abnormal vessel wall morphology (Lehti et al. 2005).
5. REGULATION OF VASCULAR TUBE REGRESSION. Aplin and coll. showed that blocking MT1-MMP expression interferes tube regression, due to impaired collagen degradation along the abluminal surface of neovessels (Aplin et al. 2009).

Taken together, these data suggest that MT1-MMP can actively regulate neovessel formation via different mechanisms starting from initial sprouting to the stabilization and maturation of vessels (**Figure 6**).

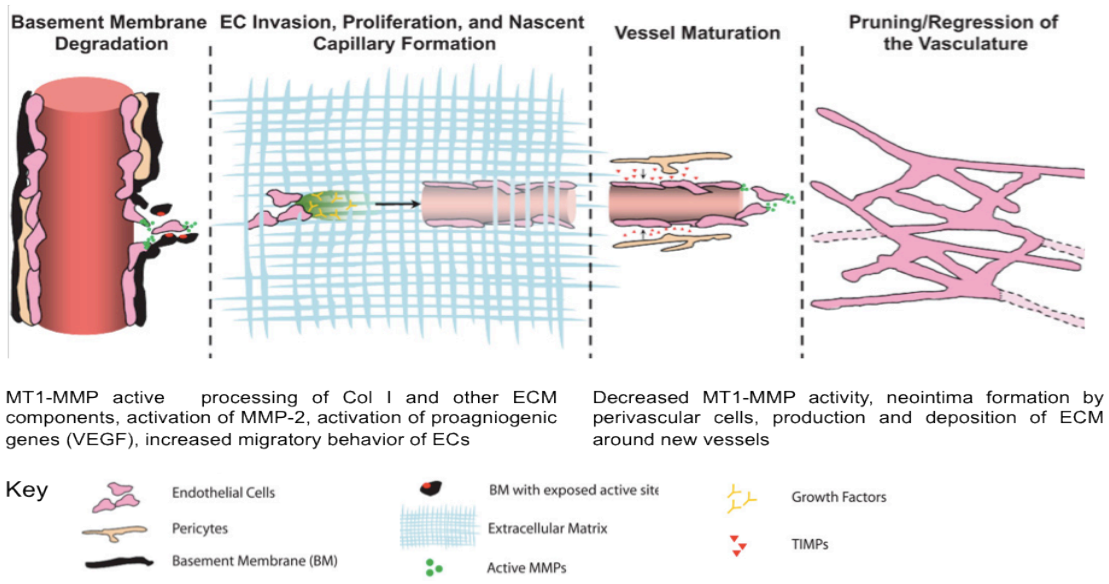

Figure 6. MT1-MMP is important at several steps of neovascularization. MT1-MMP is upregulated during first steps of angiogenesis and its expression on activated endothelial tip cells facilitates basement membrane degradation and EC migration. At following steps crosstalk between EC and pericytes (SMCs) is a key factor in initiating vessel stabilization (adapted from Ghajar et al., 2008).

- PROTEOMIC APPROACHES TO ANALYZE THE PROTEASE SYSTEM -

Traditional *in vitro* and *in vivo* techniques as well as MMP-mutant mouse models have been used for years to investigate the effect of a protease or the type of substrates it can process. However techniques such as these provide only partial information and can mask heterogeneity and dynamical processes of the individual protease, since in many occasions they are focused on single

substrate. In that way by the homology to the first discover MMP later were called interstitial collagenases able to degrade extracellular matrix molecules and thus classified to the same family. Nowadays it is much more elucidate that although many of MMP family members share similar ability to cleave some of the ECM components, the structure and function of each individual MMP can be unique and process substrates beyond matrix proteins. Several powerful approaches that can comprehensively clarify a protease role in a single cell, tissue or even the whole organism are based on genomic and proteomic techniques.

Over the last few years proteomic techniques have advanced significantly, resulting in a variety of powerful tools to complex analysis of biological samples. The group of C. Overall has been pioneered in mass spectrometry (MS)-based proteomic use and other 'omics' techniques for proteases, their inhibitors and substrates. A new term was coined to define these emerging concepts: **DEGRADOMICS** defines "all genomic and proteomic investigations and techniques regarding the genetic, structural and functional identification and characterization of proteases, and their substrates and inhibitors, that are present in an organism" and **DEGRADOME** that encompasses two concepts "first, is the complete set of proteases that are expressed at a specific moment or circumstance by a cell, tissue or organism. Second, the degradome of a protease is the complete natural substrate repertoire of that enzyme in a cell, tissue or organism" (López-Otín and Overall 2002).

One of the most important functions of matrix metalloproteases is the regulation of bioactivity and availability of a number of proteins. That occurs mostly in a process of proteolytic shedding, which is a form of post-translational modification independent of the mRNA expression level (Müllberg et al. 2000; Schlöndorff and Blobel 1999). Thus screening the protease-dependent events require quantitative proteomic techniques, which not only provide the information about identified proteins but also can quantitatively compare two conditions, e.g. effect of an inhibitor, wildtype versus protease-deficient culture, normal and disease-affected tissue, etc.

The identification of MMPs' substrates increased significantly when using proteomic-based techniques. C. Overall's group used ICAT (Isotope-Coded Affinity Tags) applied to breast carcinoma cell line stably transfected with MT1-MMP and discovered several promising candidates, the most important are: secretory leukocyte protease inhibitor, EGF-containing fibulin-like extracellular matrix protein-1, death receptor-6, neuropilin-1 and connective tissue growth factor (Tam et al. 2004). Moreover proteomic analysis of human plasma showed other candidates such as gelsolin and apopoproteins (Hwang et al. 2004). These and other works bring in unparalleled information about how MT1-MMP influences on protein function in pathology and showed how the MT1-MMP substrate degradome changes depending on cell type/condition.

Fundamentals of SILAC approach

SILAC (stable-isotope labeling by amino acids in cell culture) method was developed last decade as an alternative metabolic to standard isotope labeling techniques like ICAT or iTRAQ to label mammalian cells and whole organisms using a non-invasive and efficient method (Ong et al. 2002). By using non-radioactive amino acids, which are indispensable for normal cell growth, all proteins synthesized by the cell are labeled and because isotope analogues are chemically identical, there is no impact on cell behaviour or function (Mann 2006). The incorporation of amino acid isotopes lead to known mass shift compared with the control peptide (**Figure 7**).

A fundamental limitation of this method is the requirement for living cells to proliferate for a several cell cycle doublings. An important advantage of SILAC is that metabolic labeling allows mixing labeled and unlabeled cultured before lysis, which are further processed as one sample thus eliminating possible errors during fractionation or purification steps. The quantification is straightforward; each correctly labeled peptide appears as a pair of fragmentation peaks (for two-condition labeling or more if more than two conditions are considered). The ratio of intensity of each labeled peaks will provide information about abundance of protein, for instance if ratio is close or equal to one then no difference in protein is observed and thus processing of this proteins is not affected between different culture conditions. In contrast, higher intensity of one of peptide suggest higher abundance of protein this that particular condition (for more details see MATERIALS AND METHODS section). When analyzing supernatants of a cell culture from protease deficient versus wildtype cells, SILAC allows for identifying a set of putative substrates.

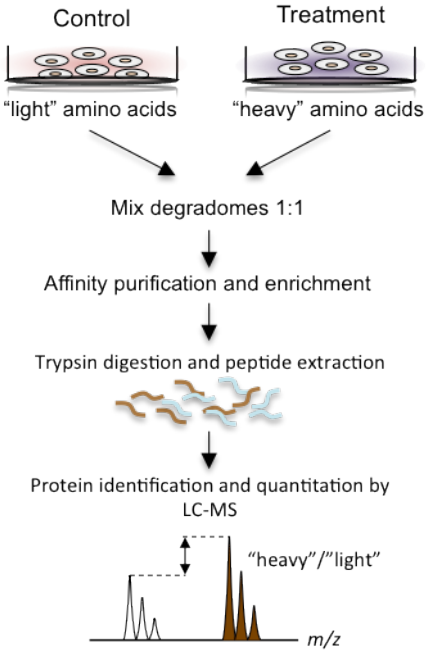

Figure 7. Principles of SILAC labeling. Two population of cells are cultures for at least six doubling times in medium containing either "light" or "heavy" amino acids. Cells or conditioned medium are then combined at 1:1 ratio and after sample purification are dissolved in SDS-PAGE. Protein bands are excised from the gel and digested with trypsin followed by the analysis of LC-MS/MS. Relative quantification is achieved by cal

- MORFOGÉNESIS DEL SISTEMA VASCULAR -

Los vasos sanguíneos se forman bien mediante el proceso de diferenciación a partir de progenitores (vasculogénesis) o a través de la formación coordinada de nuevos capilares a partir de la vasculatura preexistente (angiogénesis). La vasculogénesis, formación *de novo* de los vasos a partir de los precursores de las células endoteliales derivadas del mesodermo (angioblastos), es responsable de la formación del primer sistema vascular en el embrión (Risau 1995; Carmeliet 2003). Sin embargo, crecimiento fisiológico o patológico del la red vascular en el organismo adulto se produce principalmente mediante angiogénesis (Risau 1995, 1997). La angiogénesis es crítica durante el desarrollo y en el adulto aparece a menudo asociada a la respuesta inflamatoria (De Smet et al. 2009).

El crecimiento de una red vascular es un proceso dinámico con multitud de etapas individuales tales como la migración e invasión direccional de las células endoteliales, su proliferación, la anastomosis, la remodelación y regresión vascular, la especificación en arterias, venas y capilares, y el reclutamiento de células murales (pericitos y células del músculo liso). La iniciación del proceso de ramificación capilar requiere la especificación de células endoteliales en tres tipos: las células líder o 'tip' especializadas en la invasión del tejido circundante, las células tallo o 'stalk' encargadas de la elongación del vaso y la formación de la luz capilar, y las células falange o 'phalanx' encargadas de la homeostasis y quiescencia vascular para promover la formación de vasos estables. Además participan las células mieloides, las cuales pueden estimular la ramificación capilar y el establecimiento apropiado de conexiones (anastomosis). Las células endoteliales 'tip' se localizan en el frente del capilar emergente, no forman lumen y son poco proliferativas, además presentan un elevado número de filopodios que se extienden hacia los factores pro-angiogénicos, los cuales inducen la migración direccional de estas células tip (Gerhardt et al. 2003).

La molécula clave en el inicio de la ramificación capilar y su posterior dirección tanto en situaciones fisiológicas como patológicas es el factor de crecimiento endotelial vascular (VEGF, del inglés *Vascular Endotelial Growth Factor*). El VEGF se expresa en múltiples tipos celulares incluidos las células endoteliales, los macrófagos y las células tumorales (Ferrara 1999; Salgado et al. 2001). El efecto de VEGF depende de la presencia de receptores del mismo localizados en las células tip (VEGFR2 y VEGFR3) y 'stalk' (VEGFR1) (Phng and Gerhardt 2009). La activación de estos receptores causa primero un incremento de la permeabilidad vascular así como la activación y migración de las células endoteliales hacia el gradiente de VEGF (de Smet et al. 2009). Además, el VEGF induce la expresión de *Delta-ligand 4* (Dll4), uno de los ligandos de Notch en las células 'tip'. Dll4 a continuación induce la activación de Notch en las células 'stalk' adyacentes lo que

inhibe la expresión de los receptores VEGFR2 y -3 en éstas células (Benedito et al. 2009; Hellstrom et al. 2007; Suchting et al. 2007). Por otro lado las células 'stalk' expresan altos niveles de otro ligando de la familia Notch – Jagged1 (Jag1), que activa más débilmente la vía de Notch en las células 'tip' favoreciendo la ramificación capilar (Benedito et al. 2009). Este equilibrio entre las vías de señalización de la familia Notch y sus dianas (los receptores VEGFR entre otras) mantiene el número correcto de células 'tip' y 'stalk' y define el carácter dinámico de las células endoteliales durante la expansión de la red vascular.

La angiogénesis es crítica durante el desarrollo y en el adulto aparece a menudo asociada a la respuesta inflamatoria (De Smet et al. 2009). Recientemente se ha descrito que factores inflamatorios como el Factor de Necrosis Tumoral alfa (TNFα) puede inducir un fenotipo similar al de las células endoteliales 'tip' (Sainson et al. 2008). La respuesta inflamatoria puede activar el proceso de angiogénesis a través de varios mecanismos: i) el aumento de la permeabilidad vascular y de leucocitos en el tejido inflamado conducen a un aumento local de factores angiogénicos que estimulan la producción de VEGF (Ferrara 1999); ii) el aumento del flujo sanguíneo puede estimular la angiogénesis mediante señales inducidas por el 'estrés de flujo' en el endotelio (Schaper and Scholz 2003); y iii) finalmente, en el tejido inflamado existen condiciones de hipoxia que estimulan también la expresión de factores pro-angiogenicos como VEGF (Taylor and Sivakumar 2005). Habitualmente la angiogénesis asociada al proceso inflamatorio es beneficiosa y necesaria para su resolución, pero en el caso de que la nueva vasculatura persista puede contribuir a la progresión de enfermedades inflamatorias crónicas. Por lo tanto la angiogénesis inflamatoria se considera como un importante patogénico de enfermedades como la psoriasis, la artritis reumatoide, la enfermedad inflamatoria intestinal, la diabetes o el cáncer (Folkman 1995a, 1995b).

- LA FAMILIA DE LAS PROTEASAS MMP -

Para el inicio del proceso de ramificación capilar es fundamental la capacidad de las células endoteliales de invadir el tejido circundante compuesto principalmente por la membrana basal y la matriz extracelular (ECM). La degradación de la ECM es crítica para las primeras etapas de la angiogénesis y las proteasas, en particular, la familia de las metaloproteasas de matriz (MMPs) desempeña un papel importante en este proceso. Las MMPs son capaces de degradar casi cualquier componente de la matriz extracelular así como factores de crecimiento, proteínas de unión a factores de crecimiento e inhibidores de proteasas, lo que les permite modular la migración e invasión celular y por tanto la angiogénesis y la inflamación, entre otros procesos (Zucker et al. 2003). Además, las MMPs pueden aumentar la disponibilidad de moléculas bioactivas y

desencadenar vías de señalización (Page-McCaw et al. 2007), así como alterar el comportamiento de las células afectando la transcripción de genes (Toriseva et al. 2012).

Por su capacidad de remodelar la matriz extracelular, las MMPs participan en el mantenimiento de la homeostasis del organismo, regulando procesos como la cicatrización, la inflamación o la angiogénesis. El análisis de animales deficientes en MMPs concretas ha proporcionado información adicional sobre sus funciones y sustratos.

Varios de los modelos de animales deficientes en MMPs han demostrado defectos asociados a inflamación y angiogénesis. En particular, los ratones deficientes en la proteasa MMP-9 muestran defectos en la angiogénesis del cartílago de huesos largos y en la respuesta angiogénica en el modelo de lesión degenerativa de la retina (Lambert et al. 2003; Vu et al. 1998). Este último se observó también en ratones dobles mutantes para MMP-2 y MMP-9 indicando la redundancia funcional de estas dos proteasas. Aunque en su mayor parte las MMPs favorecen el desarrollo de tumores, los ratones deficientes en MMP-8 constituyen una excepción y muestran la importancia de las MMPs en regular la respuesta inflamatoria e inmune, ya que en ausencia de esta proteasa se observó un aumento de los tumores de la piel (Balbin et al. 2003). Sorprendentemente no hay evidencias de muerte gestacional en ningún mutante de las MMPs, lo que sugiere que las funciones desempeñadas por la MMPs son especialmente importantes durante la angiogénesis postnatal. El posible mecanismo a través de cual las proteasas de matriz contribuyen al proceso de angiogénesis incluye el aumento de su expresión en las células vasculares como células endoteliales y, observado en condiciones tumorales, así como el aumento del procesamiento de la matriz extracelular, en particular colágeno tipo I, que promueve la migración celular. Otros mecanismos incluyen el procesamiento de los factores de señalización como VEGF o PDGF o la regulación de la cobertura perivascular (Bergers et al. 2003; Chantrain et al. 2004; Galvez et al. 2001; Hiratsuka et al. 2002; Huang et al. 2009; Johnson et al. 2004).

Todos los miembros de la familia de las MMPs comparten la misma estructura en varios dominios principales que están compuestos por un péptido señal en el extremo N-terminal, un pro-dominio que las mantiene en forma de zimógeno, seguido de un sitio de corte por furina por el que serán procesadas y activadas. Luego presentan el dominio catalítico, crucial para su actividad proteolítica y el dominio hemopexina que participa en la dimerización y regulación de la migración. Por último, en el extremo C-terminal, puede haber un motivo transmembrana que ancla la proteína a la membrana plasmática y un dominio citosólico que participa en varias funciones como la localización o la transducción de señales (Zucker et al. 2003; Folgueras et al. 2004; Overall et al. 2002). Según esto, se diferencian dos tipos principales de MMPs, las secretadas y las unidas a la membrana (MT-MMPs). Las MT-MMPs se organizan en dos grupos dependiendo de su forma de anclaje a la membrana:

1. las MT-MMPs transmembrana, que contienen un dominio transmembrana y una pequeña cola citosólica (MT1-, MT2-, MT3- y MT5-MMP);
2. y las MT-MMPs ancladas a dominios GPI (MT4- y MT6-MMP), que se unen a la membrana mediante un puente glicosilfosfatidilinositol.

La MMP-23 también se incluye dentro del grupo de las proteasa transmembrana, aunque a diferencia de las demás es una proteína tipo II.

MT1-MMP (MMP-14), fue la primera metaloproteinasa de matriz identificada anclada a la membrana (Sato et al. 2004). Pertenece al grupo de las MT-MMPs transmembrana y se expresa en la gran mayoría de las células. Debido a su alto potencial proteolítico, MT1-MMP está regulada a varios niveles, incluyendo su transcripción, activación de las formas zimógenas y su inhibición por inhibidores tisulares (TIMPs, del inglés *Tissue Inhibitors of Metalloproteinases*). Como otras MMPs, MT1-MMP se produce en forma de zimógeno inactivo con una inserción de cuatro residuos entre el pro-péptido y el dominio catalítico. La activación de la proteasa se lleva a cabo por convertasas de la familia de las furinas y se produce a nivel de retículo endoplasmático antes de que proteasa llegue a la membrana celular (Zucker et al. 2003; Itoh and Seiki 2006; Yana and Weiss 2000).

La MT1-MMP se localiza en diferentes microdominios de la membrana celular, donde se asocia a otras proteínas y esta localización específica define su accesibilidad a los sustratos, así como sus principales funciones. MT1-MMP se encuentra en los siguientes compartimientos en las células endoteliales:

1. **Lamelipodios y filopodios**, así como otras protrusiones de la membrana, donde se es proteolíticamente activa y asociada a caveolina-1 e integrina αvβ3 (Galvez et al. 2010);
2. **Las uniones célula – célula en los dominios de tetraspaninas**, donde la MT1-MMP parece ser proteolíticamente inactiva (Yanez-Mo et al. 2008);
3. **Adhesiones focales,** asociada a otros miembros de las integrinas β1 y proteínas adaptoras como p130Cas o FAK donde MT1-MMP puede regular vías de señalización como la de Rac1 (D'Alessio et al. 2008; Gonzalo and Arroyo 2010; Wang and McNiven 2012);
4. **Podosomas e invadopadios** donde MT1-MMP forma parte de la maquinaria de formación de estas estructuras que son también clave para la invasión celular (Destaing et al. 2011; Frittoli et al. 2011; Nakahara et al. 1997; Poincloux et al. 2009);
5. **Intracelular,** en el retículo endoplasmático/Golgi o en el núcleo, donde se ha demostrado que la MT1-MMP puede regular la función de proteínas tales como FIH1 o impactar en la transcripción de genes como PI3Kσ, respectivamente.

También se ha sugerido que MT1-MMP podría tener actividad proteolítica intracelular y procesar proteínas centrosomales como pericentrin (Golubkov et al. 2005; Shimizu-Hirota et al. 2012).

MT1-MMP es la principal fibrinolisina y colagenasa en células endoteliales, siendo esencial para el desarrollo (Hiraoka et al. 1998). Esto se manifiesta en los defectos vasculares presentes en los ratones deficientes en MT1-MMP, que presentan una vascularización defectuosa en respuesta a FGF en el modelo de córnea así como problemas en la osificación secundaria y en la expansión pulmonar postnatal relacionado con problemas en la vascularización en estos tejidos (Zhou et al. 2000; Holmbeck et al. 1999; Gálvez et al. 2005).

La proteasa MT1-MMP es esencial para la formación de capilares como han demostrado trabajos con animales y células deficientes en MT1-MMP. Además, la expresión de MT1-MMP se ha observado en células 'tip' *in vitro* y *ex vivo* (Yana et al. 2007; Aplin et al. 2009), y modelos matemáticos sugieren que MT1-MMP podría participar en la capacidad invasiva de estas células 'tip' (Kargiannis et al. 2006). MT1-MMP puede contribuir al desarrollo vascular a través de varios mecanismos dependientes o independientes de su actividad catalítica:

1. **Degradación de la lámina basal y las proteínas de la ECM**, es un proceso crítico en la iniciación de la ramificación capilar ya que facilita la migración celular. MT1-MMP también puede generar y/o activar proteínas activadoras o inhibitorias de procesos angiogénicos como trombospondinas, citoquinas solubles o factores de crecimiento (Covington et al. 2006; McQuibban et al. 2002, Ratnikov et al. 2002).
2. **Invasión y migración de las células endoteliales**. En condiciones basales las células endoteliales expresan bajos niveles de MT1-MMP, pero estos niveles se encuentran aumentados durante la migración e invasión en matrices 2D y 3D (Galvez et al. 2001). Además, se ha demostrado que las células 'tip' que se localizan en el frente vascular expresan MT1-MMP (Fisher et al. 2009; Yana et al. 2007).
3. **Activación de genes pro-angiogénicos,** como se ha mencionado anteriormente MT1-MMP puede activar la expresión de algunos genes de forma independiente de su actividad catalítica; unos de ellos es VEGF, el regulador clave del proceso de formación de nuevos vasos (Deryugina et al. 2002[a]; Sounni et al. 2004).
4. **Reclutamiento y activación de células perivasculares** tanto durante el desarrollo de la pared vascular como en respuesta a daño vascular (Filippov et al. 2005).

5. **Regulación de la regresión vascular.** Aplin y coll. han demostrado que la inhibición de la expresión de MT1-MMP interfiere en la regresión de la vasculatura (Aplin at al. 2009).

- ABORDAJE PROTEOMICO PARA EL ANALISIS DE LAS PROTEASAS -

Uno de los abordajes más potentes para caracterizar la función de una proteasa es la identificación de sus sustratos. Actualmente las técnicas de la proteómica cuantitativa permiten caracterizar exhaustivamente la función de una proteasa en una célula, tejido u organismo. Durante los últimos años se ha introducido el concepto del **degradoma** que engloba dos significados: i) el conjunto completo de proteasas e inhibidores secretados en un momento específico por una célula, tejido u organismo y ii) el conjunto de los sustratos de una determinada proteasa en una célula, tejido u organismo (López-Otín and Overall 2002). La identificación de sustratos de MT1-MMP se ha mejorado considerablemente como resultado del uso de técnicas de proteómica como ICAT (Isotope-Coded Affinity Tags) aplicadas a células tumorales (Tam et al. 2004).

Uno de los métodos de proteómica cuantitativa desarrollado recientemente es el marcaje metabólico llamado SILAC (del inglés, *stable-isotope labeling by amino acids in cell culture*), basado en el uso de isótopos no radioactivos de amino ácidos esenciales que se incorporan a todas las proteínas de la célula durante su cultivo. La incorporación de dos isótopos diferentes crea una variación de masa en los amino ácidos, que permite calcular de forma precisa la diferencia en abundancia de una determinada proteína entre dos o más condiciones. En el caso de las proteasas de membrana, la aplicación de esta técnica para el análisis del medio condicional del cultivo derivado de células deficientes en dicha proteasa versus cultivo control permite identificar las proteínas de membrana o secretadas procesadas por la proteasa de interés. En otras palabras, esta técnica permite la identificación del conjunto completo de sustratos procesados por esa proteasa.

- OBJECTIVES -

The analysis of knockout mice performed by our group and others confirmed that MT1-MMP might play an essential role in angiogenesis and inflammation. In order to expand our understanding about MT1-MMP functions in proteolytic events during inflammation-induced angiogenesis we proposed the following aims:

- Set up an *in vitro* model of inflammation-induced endothelial tip cells expressing MT1-MMP;

- Identify and characterize the degradome (collection of substrates) of MT1-MMP in these cells by application of quantitative proteomics to gain insights into its function in inflammatory angiogenesis;

- Validate *in vitro* and *in vivo* processing of putative MT1-MMP substrates in MT1-MMP-deficient endothelial cells;

- Evaluate the possible application of MT1-MMP proteolytic substrates as biomarkers in pathological models of inflammation-driven angiogenesis such as observed in inflammatory bowel diseases.

- MATERIALS AND REAGENTS -

All reagents were of the highest grade commercially available. Tissue-culture plasticware plates were from Falcon (BD Biosciences) or Costar (Corning Incorporated). µ-Slide Angiogenesis were from IBIDI®. Microscope slides and coverslips were purchased from Thermo Fisher Scientific.

Table 2. Cell culture media	
DMEM Ham's F-12 (Dulbecco's modified Eagle's medium)	Lonza, BioWhittaker
IMDM (Iscove's modified Dulbecco's medium)	Lonza, BioWhittaker
Opti-MEM®I Reduced Serum Medium	Lonza, BioWhittaker
M199	Gibco, Invitrogen
DMEM (Dulbecco's modified Eagle's medium)	Sigma-Aldrich
SILAC Advance D-MEM F-12 Flex Medium	Invitrogen

Table 3. Cell culture supplements	
Penicillin (50UI/ml), streptomycin (50 µg/ml) (P/S)	Lonza, BioWhittaker
Fungizone (2,5 µg/ml)	Lonza, BioWhittaker
2 mM L-glutamine	Lonza, BioWhittaker
10 mM HEPES	Lonza, BioWhittaker
Fetal bovine serum (FBS)	Gibco, Invitrogen
Endothelial cell growth factors (ECGFs, 50 µg/ml)	Extracted from bovine cerebrum
10 UI/ml heparine	Mayne
Fibronectin (10 µg/ml)	Sigma
Gelatin (0.1% w/v)	Sigma
Polybrene (8 µg/ml)	Sigma
Type I collagen PureCol™ 10 µg/ml	INAMED Biomaterials
Matrigel® basement membrane matrix	BD Biosciences
Collagenase type I (3,33 mg/ml)	Worthington

Table 4. Reagents and buffers	
Red blood cells lysis buffer - ACK buffer (150mM NH_4Cl; 0.1mM Na_2EDTA; 10mM $KHCO_3$, pH=7.4)	
Dynabeads M-450 sheep anti-rat IgG	Dynal Biotech ASA
WGA-agarose beads	Vector Laboratories
Dextran sodium sulphate (DSS)	Biomedicals
ColoScreen hemoccult	Helena Laboratories
Cell Dissociation Buffer	Gibco

Table 5. Cytokines and ELISA	
Interleukin 3 (IL-3)	PeproTech (Rocky Hill, NJ)
Stem cell factor (SCF)	PeproTech (Rocky Hill, NJ)
Granulocyte macrophage colony-stimulating factor (GM-CSF)	PeproTech (Rocky Hill, NJ)
Macrophage colony-stimulating factor (M-CSF)	PeproTech (Rocky Hill, NJ)
Monocyte chemotactic protein-1 (MCP-1/CCL2)	PeproTech (Rocky Hill, NJ)
Tumor necrosis factor-alpha (TNFα)	PeproTech (Rocky Hill, NJ)
Mouse VEGF DuoSet® ELISA	RnD Systems
Mouse TNFα ELISA	BD Biosciences
Mouse Nidogen-1 (NID1) ELISA kit	Cusabio
Mouse Thrombospondin-1 ELISA kit	Cusabio

Human VEGF DuoSet® ELISA	RnD Systems
Human Thrombospondin-1 DuoSet® ELISA	RnD Systems
Human Nidogen-1 DuoSet® ELISA	RnD Systems
VEGF-A	PeproTech (Rocky Hill, NJ)

Table 6. Antibodies

MT1-MMP (mouse anti m, h)	LEM 2/63, LEM 2/15 (Gálvez, Matías-Román et al. 2001)
MT1-MMP (rabbit anti m, r, h)	Abcam
β actin (mouse anti m, r, h)	Sigma-Aldrich
CD31 (PECAM-1) (hamster anti m, h)	Millipore
ICAM-1 (biotin hamster a m)	BD Biosciences
VCAM-1 (rat anti m)	BD Biosciences
Jagged1 (rabbit anti m)	Cell Signaling
VEGFR2 (rabbit anti m)	Abcam
Delta-ligand 4 (rabbit anti m)	Santa Cruz Biotechnology
Integrin β3 (hamster anti m)	BD Biosciences
CXCR4 (rat anti m)	BD Biosciences
Phalloidin-Texas Red	BD Biosciences
TSP1 (rabbit anti m) clone 7280	ML Iruela-Arispe
TSP1 (mouse anti h)	Thermo Fisher Scientific
NID1 (goat anti m, h)	Santa Cruz Biotechnology
CYR61 (goat anti m, h)	Santa Cruz Biotechnology
SEM3C (goat anti m, h)	Santa Cruz Biotechnology
Isolectin IB4	Sigma
Mac1 (rabbit anti m, h)	Abcam
Collagen IV (rabbit anti m)	AbD Serotec
CD16/32 (rat anti m)	BD Biosciences
ICAM-2	BD Biosciences
CD31 (rabbit anti m, h)	Abcam
NID1 (rat anti m)	Abcam

- ANIMAL MODELS -

Mmp14 knockout mice (MT1-/-)

Generation of mice deficient in MT1-MMP was described elsewhere (Zhou, Apte et al. 2000). Briefly, MT1-MMP-null mice ($MT1^{+/-}$) were generated by gene targeting in embryonic stem cells and bred by heterozygote mating, and heterozygotes were crossed back to the C57BL/6 strain (wildtype, WT). Mice were bred and maintained under specific pathogen-free conditions at the animal unit of the National Centre for Cardiovascular Research (CNIC). Mice were kept at a room temperature and a 12h:12h light/dark cycle and housed at max 5 animals per cage. Mice were fed on a commercial pellet diet and water was available *ad libitum*. All procedures involving animals were conducted in accordance with an institutional Committee's approved protocol for the use of animals in research.

Genotyping was performed by PCR of genomic DNA extracted from tail snips. To confirm the presence of wildtype or null allele the following primers were used respectively, 5'-GCTC ATG AGG CGC CCT CGC-3' and 5'-GGG CAC TTC TGG GAA GCG-3'; 5'-CAC GAG ACT AGT GAG ACG T-3' and 5'-TCA GAA TTA CAC CCC TAA GG-3' (Isogen Life Science). 7-10 day-old mouse pups were used for all experiment involved MT1-MMP-deficient mice.

Induction of colitis in mice

Colitis was induced in 10-14 weeks of age C57BL/6 mice by administration of 1% or 4% (wt/vol) dextran sodium sulphate (DSS) for 7 days applied to mice *ad libitum* as drinking water in a feeding glass bottle. Animals were monitored daily during next 7 days by measuring body weight and colitis score. The baseline colitis score determined at day 0 was scored as 0; weight loss of 1-5% was scored as 1, 5-10% as 2, 10-20% as 3 and more than 20% as 4. For stool consistency normal, well-formed pellet were scored as 0, semi-formed pellet, which not adhere to the anus were qualified as 2 and liquid stool adhering to the anus was scored as 4. Similarly 0 score was assigned for no bleeding, 2 for positive hemoccult (ColoScreen) and 4 for gross rectal bleeding.

After 7 days, mice were sacrificed and serum was collected by cardiac puncture and was used for ELISA measurement of soluble TNFα, VEGF, TSP1 and NID1. The whole colon was removed, cleaned with PBS and sectioned in OCT/paraffin for histological analysis or the whole mount staining. The remaining part of colon was homogenized in 0.05% Tween 20/PBS supplemented with PMSF (1mM) and protease inhibitor cocktail and centrifuges 10 min at 18,000 rpm.

- PATIENT POPULATION -

Patient with active and inactive CD and UC as well as healthy individuals were selected at the Servicio de Aparato Digestivo, Hospital Universitario La Princesa, Madrid, Spain and the study was approved by the institutional committee. The diagnosis of IBD was based on the generally accepted clinical, endoscopic and histopathological criteria. Moreover patients with CD and UC were divided into two groups, with low and high activity based on Mayo index.

- CELL CULTURE -

Primary mouse lung endothelial cells (pMLEC)

Mouse neonates were sacrificed by decapitation and spray down with 70% ethanol. Lungs were excised in the culture hood and placed in a sterile tube containing DMEM-F12 and kept on ice until beginning the cell isolation procedure. After any fat, blood clots and connective tissues were removed, using sterile scissors or scalpel lungs were minced for 5 minutes until the tissues was homogenous. Prepared this way lungs were transferred to a 50 ml tube containing 5 ml of collagenase and incubated in a water bath for 1 hr at 37^{o}C with occasionally swirling. After 1 hr medium was added to stop the digestion and solution was poured 4 times with 21-gauge needle and next passed through a 70 µm cell strainer into a tube containing medium. Cells were pellet by centrifugation and plated into tissue culture flask coated with 10µg/ml fibronectin, 10µg/ml collagen I (Pure Col) and 0.1% gelatin and kept for at least 24 hrs. To produce pure population of endothelial cells obtained cell culture was sorted first to remove macrophages. For that cells were incubated with rat anti-mouse FcγR (CD16/CD32) followed by incubation with sheet anti-rat magnetic Dynabeads and separation on a magnetic holder. Cells were left to grow from 1-3 days and the positive sort was performed. Cells were incubated with antibody solution (rat anti-mouse ICAM-2) and next anti-rat Dynabeads. If needed positive sort was repeated once the cells reached 50% confluence (Oblander, Zhou et al. 2005). Cells were grown in DMEM Ham's F-12 medium supplemented with 20% FBS, L-glutamine, heparin, antibiotics and growth factors.

Immortalized mouse lung endothelial cells (iMLEC)

After selections primary MLEC cells were immortalized using middle T-antigen of polyoma virus by overnight infection with conditioned medium from Gpmt cell line supplemented with 10mM Hepes, 8µg/ml of polybrene and growth factors (25mg/ml). Gpmt cell line producing virus was a kind gift from Dr Reinhard Fässler (Max Planck Institute of Biochemistry, Munich, Germany). MT1-MMP expression and endothelial cell markers for immortalized MLEC were monitored by western blot and flow cytometry. iMLEC were grown in DMEM Ham's F-12 medium supplemented with 10% FBS, L-glutamine, P/S and Hepes and the culture plates were coated with 0.5% gelatin.

Human umbilical vein endothelial cells (HUVECs)

HUVECs from different donors (cultured up to passage 6) were purchased from Lonza or isolated

from freshly harvested umbilical cords as previously described (Gálvez, Matías-Román et al. 2002). Cells were cultured in M199 medium supplemented with 20% fetal bovine serum, 100 U/ml penicillin, 100 µg/ml streptomycin, 2.5 µg/ml fungizone, 10 UI/ml heparin and 50 µg/ml of EC growth supplement extracted from bovine brain.

- EXPERIMENTAL PROCEDURES -

SILAC labelling procedure

MLEC were grown in complete SILAC Advance D-MEM F-12 Flex Medium supplemented with 'light' and 'heavy' amino acids and dialyzed serum to exclude the possibility of incorporating non-labeled amino acids. We used non-labeled lysine and the $^{13}C_6$ form of arginine ('light' conditions) for MT1-MMP null MLEC, and isotopes of lysine ($^{13}C_6$) and arginine ($^{13}C_6$ $^{15}N_4$) for WT MLEC ('heavy' conditions). Cells were cultured for 7 days, corresponding to about 6 doublings, and appropriate amounts of isotopic lysine and arginine were used to optimize isotopic incorporation while minimizing the risk of arginine to proline conversion. For the last 48 h of culture, medium was replaced by serum-free medium, to reduce the serum protein background, and for the last 24 h cells were stimulated with 20 ng/ml TNFα. At the end of the 7 day period, conditioned medium from null and WT cultures was collected and the cells harvested with cold PBS + 10 mM EDTA. Supernatants from null ('light' condition) and WT ('heavy' condition) were pooled 1:1 after bicinchoninic acid protein determination (BCA Protein Assay, Pierce). The pooled media were incubated for 3 h at 4^{o}C with WGA-agarose beads to extract glycoproteins, and the glycoproteins were eluted by incubation with 0.5 M N-acetyl-D-glucosamine. The glycoprotein mixture was concentrated on a 3kDa cut-off centrifugal filter (Amicon Ultra-4, Millipore) to a final volume of 200 µl. Urea was added to a final concentration of 8M, pH 8.5. Proteins were reduced by addition of 50 mM DTT, followed by carbamidomethylation with 125 mM iodoacetamide. Finally, the protein mixture was purified by acetone-trichloroacetic acid precipitation (2D-CleanUp kit, GE Healthcare). The pellet was resuspended in loading buffer, and proteins were separated by 10% SDS-PAGE.

Protein identification and data analysis

After separation of proteins on 10% SDS-PAGE gel, the Coomassie–stained protein bands were excised as 20 slices (**Figure 8**) and each one was subjected to in-gel tryptic digestion using modified porcine trypsin (Promega).

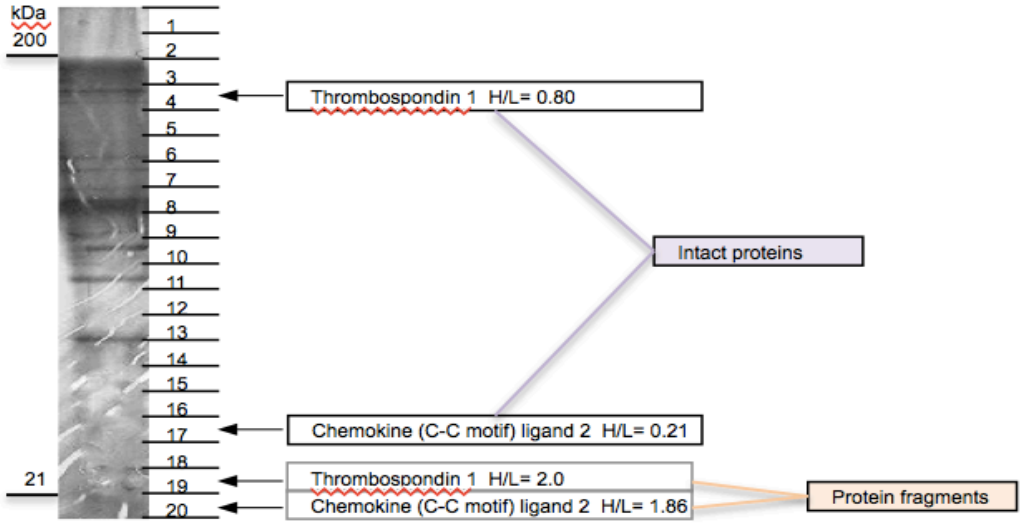

Figure 8. Supernatant protein separation in SDS-PAGE gel after WGA lectin-affinity purification and N-deglycosylation. Supernatant proteins from WT and MT1-/- iMLEC cultures were mixed 1:1. The whole gel lane was divided in 20 horizontal pieces; each band was separately digested with trypsin. In addition to peptide quantitation we obtained information about peptide origin (intact versus protein fragment).

The digests were then dried in a vacuum centrifuge, extracted with formic acid solution and analyzed on an Esquire HCT IT mass spectrometer (Bruker), coupled to a nano-HPLC system (Ultimate, LC Packings). Peptide mixtures were first concentrated on a 300 mm i.d., 1 mm PepMap nanotrapping column and then loaded onto a 75 mm i.d., 15 cm PepMap nanoseparation column (LC Packings). Peptides were then eluted by an acetonitrile (ACN) gradient (0–60% B in 150 min, where B is 80% ACN, 0.1% formic acid in water; flow rate ca. 300 nl/min) through a PicoTip emitter nanospray needle (New-Objective, Woburn) onto the nanospray ionization source of the IT mass spectrometer. MS/MS fragmentation (1.9 s, 100–2800 m/z) was performed on two of the most intense ions, as determined from a 1.2 s MS survey scan (310–1500 m/z), using a dynamic exclusion time of 1.2 min for precursor selection and excluding single-charged ions. Data were processed for protein identification and quantification with Protein Scape 2.1 and WARP-LC 1.2 (Bruker, Bremen), a software platform that integrates processing of LC-MS run data, protein identification through database search of MS/MS spectra, and protein quantification based on the integration of the chromatographic peaks of MS extracted ion chromatograms for each precursor. Amino acid sequences were used to screen the protein databases with dedicated software (Protein Scape). Proteins were identified using Mascot (Matrix Science) search engine and for further protein analysis Protein Knowledgebase UniProtKB (http://www.uniprot.org) and GeneCards database (http://www.genecards.org) were used. MS/MS spectra were searched with a precursor mass tolerance of 1.5 Da, fragment tolerance of 0.5 Da, trypsin specificity with a maximum of 1

missed cleavage, cysteine carbamidomethylation as a fixed modification, and methionine oxidation and the N-terminal and corresponding Lys and Arg SILAC labels as variable modifications. A positive identification criterion was set as an individual Mascot score for each peptide MS/MS spectrum higher than the corresponding homology threshold score. The false positive rate for Mascot protein identification was measured by searching a randomized decoy database and estimated to be under 4%. For protein quantification, H/L ratios were calculated by averaging the measured H/L ratio for the observed peptides, after discarding outliers. For selected proteins of interest, quantitation data obtained from the automated Protein Scape software analysis were manually reviewed.

Bioinformatic data analysis with Babelomics

The Babelomics web tool (http://www.babelomics.org/) is a freely available program suited to analysis of large-scale experiments (microarrays, proteomics) with functional annotation (Medina I 2010). The FatiGO module was used for enrichment analysis of selected proteins (Al-Shahrour, F 2004 Bioinformatics). This functional profiling was performed by comparing two lists of genes, the first being the genes encoding the proteins with an H/L ratio > 1.5 in the SILAC analysis unless otherwise stated, and the second being the rest of the genome.

Overlap analysis

Overlap analysis and generation of Venn diagrams was performed at http://www.pangloss.com/seidel/Protocols/venn4.cgi.

3D endothelial tip-like cell sprouting assay

Matrigel® was thawed overnight on ice at 4°C and all materials were chilled before use. MLEC were plated at confluence in ibidi® angiogenic chambers and left to attach, after which the Matrigel layer was added on top. Medium containing TNFα was added and the chamber was kept at 37 °C for at least 18 h. At the end of incubation, medium was removed and the cells were fixed with freshly prepared 4% PFA for 20 min, followed with permeabilization in 0.3% Triton X-100. Samples were washed with PBS/Triton X-100 and stained for CYR61 as described in Supplemental Information. Samples were examined under a Zeiss LSM700 confocal microscope (Plan-Apochromat 40x1.3 Oil DIC M27) and images were analyzed with ZEN software.

Whole-mount staining

Eyes from 6 to 8 days-old mice (P6-P8) were removed and fixed with 4% PFA overnight at 4°C. Fixed retinas were flat mounted and blocked in 2% BSA/PBS/0.3% Triton X-100 followed by overnight incubation with primary antibodies (anti-CYR61) and isolectin IB4 (Sigma) to visualize vasculature. The next day retinas were extensively washed and incubated with fluorescent-conjugated secondary antibodies.

Part of colon closest to the anus was removed, cleaned and fixed with 4% PFA. Fixed samples were flat-mounted and blocked in 2% BSA/0.3% Triton X-100 in PBS, followed by overnight incubation with primary antibodies (anti-TSP1, -NID1, -MT1-MMP, -CD31). The next day, samples were extensively washed with 0.05% Triton X-100/PBS and incubated with fluorescent-conjugated secondary antibodies. Images were acquired with Zeiss LSM700 confocal microscope (Plan-Apochromat 63X1.4 Oil DIC M27) and analysed with ZEN Software.

Enzyme-Linked Immunosorbent Assay

Soluble levels of VEGF-A, TSP1, NID1 and TNFα were measured in blood serum using enzyme-linked immunosorbent assay (ELISA), according to the manufacturer's instructions. Blood was collected from control individuals and patients with IBD and serum was separated by centrifugation and store at -80°C. Optical density from an average of triplicate readings for each sample and control was measured at 450nm and to correct optical imperfections in the plate the reading was subtracted at 570nm. A four parameter logistic (4-PL) curve-fit was generated using Benchmark Plus microplate spectrophotometer (BIO-RAD) coupled computer software.

Quantitative RT-PCR analysis

For relative quantitation of expression, quantitative real-time PCR analysis was performed using the AB7900 FAST 384 Detection System (Applied Biosystems), according to the manufacturer's instructions. RNA was extracted from confluent and cDNA synthesis was performed with 1 µg of total RNA using Qiagen RNA synthesis kit (RNeasy Plus mini kit, Qiagen). Predesigned qPCR primers for mouse Mmp14, Thbs1, Cyr61, Nid1, Sema3c, Tbp and Hrpt1 were selected from TaqMan Gene Expression Assay database (Applied Biosystems). Relative quantitation of each target gene was performed using comparative threshold multiplex PCR in gene expression relative to the Tbp and Hrpt1. The data were analyzed by qBASE program obtaining the Ct of the amplification products.

Total cellular RNA was purified from cultured HUVEC cells using TRIZOL reagent (Invitrogen), according to the manufacturer's protocol and quantified using a Nanodrop ND-1000 (Thermo Fisher Scientific). cDNA synthesis was performed with 1 µg of total RNA using Qiagen RNA synthesis kit (RNeasy Plus mini kit, Qiagen). cDNAs were subjected to PCR amplification using the following primer pairs for human MT1-MMP: 5'-CGCTACGCCATCCAGGGTCTC-3' and 5'- CGGTCATCATCGGGCAGCACAAAA-3' (Isogen Bioscience). The PCR products were visualized using ethidium bromide in 1% agarose gel.

Transfection of small interfering RNA (siRNA)

SILENCERTM siRNA constructs were purchased from Ambion® (Applied Biosystems). Specific oligonucleotide sequences targeting human MT1-MMP were as follows: 5'-CAUCUGUGACGGGAACUUU- 3' and 5'-GGAAUGAGGAUCUGAAUGG-3' and a non-targeting siRNA control which bears no homology with relevant human genes. For siRNA transfection, cells were seeded in 6-well plates at 2.5 x 10^5 and grown to reach 60-70% confluence. The different amounts of siRNAs and OligofectamineTM Reagent (Invitrogen) were diluted in Opti-MEM® I (Gibco, Invitrogen). The diluted siRNA-liposome complex was added to cells and incubated for 4 h. Following the transfection fresh Opti-MEM® I containing 30% FBS was added and cells were grown for 24h. After that cells were rinsed with fresh M199 medium and cultured with TNF during 24h for analysis.

Western Blotting

For substrate validation by Western Blot analysis cells were cultured in SILAC conditions (see below) unless otherwise stated. Supernatants were taken, cell debris removed and total protein in conditioned medium was incubated with WGA-agarose beads (Vector Laboratories) to enrich medium for glycoproteins, then the protein solution was eluted with 0.5M N-acetyl-D-glucosamine (Sigma) and concentrated by ultracentrifugation (Amicon Ultra-4, 5 kDa cut-off centrifuge tubes, Millipore). Cells were lysed in RIPA buffer containing protease inhibitors. Protein concentration was measured using bicinchoninic acid (BCA) protein assay. In chosen experiments protease inhibitor GM6001 (Chemicon International) was used at concentration 250nM for 24h. Microsomal fraction was obtained by incubation cells with sucrose buffer (20mM Tris-HCl pH 7.4, 0,25M sucrose, 1mM PMSF) after which cells were cracked with 25-guage needle and ultracentrifuged 55000 RPM for 1.5h. Microsome pellet was resuspended in guanidinium chloride (Sigma). Cell lysates, microsomal fraction and conditioned media were resuspended in Laemmli buffer 2x or 4x and loaded on the SDS-PAGE gel and electrophoresis was performed in reduced conditions.

Proteins separated by SDS-PAGE were transferred to nitrocellulose membrane. After blocking non-specific binding sites with 5% skimmed milk (w/v) in PBS containing 0.5% Tween (v/v), the blots were incubated with the primary antibodies overnight at 4°C. Bound primary antibodies were detected using a horseradish peroxidase-conjugated secondary antibody. Signal was detected by chemiluminescence (Amersham, ECL Signal Detection Reagent, GE Healthcare) and relative protein expression was determined by densitometry using ImageJ software.

Fluorescence-activated cell sorting (FACS)

Immortalized MLEC were left untreated or treated with 20 ng/ml of the angiogenic factors VEGF, TNFα, MCP-1, MIP-2 (all from PeproTech), or SDF-1 (R&D Systems). For surface expression analysis, cells were harvested using Cell Dissociation Buffer and stained with rat anti- mouse VCAM-1, biotinylated hamster anti-mouse ICAM-1, hamster anti-mouse PECAM-1, rabbit anti-mouse Jagged-1, rabbit anti-mouse VEGFR2 and rabbit anti-mouse MT1-MMP (HR, Abcam), followed by incubation with appropriate fluorescent-labeled secondary antibodies. Cell surface expression was determined in a flow cytometer (FACScanto; Beckton Dickinson) and data were analyzed with FACSDiva software.

Immunofluorescence staining

For immunofluorescent staining, cells were plated on matrix-coated glass coverslips, then fixed in a solution of 4% PFA for 10 min at room temperature and permeabilized with 0.1% Triton X-100 if needed. Non-specific reactivity was blocked with 2% BSA in PBS fro 30 min. Cells were labelled with primary antibodies (45 min at room temperature) and fluorescently labelled secondary antibodies (45 min at room temperature). Samples were examined under a Zeiss LSM700 confocal microscope (Plan-Apochromat 63x1.4 or 40x1.3 Oil DIC M27) and images were analyzed with ZEN software.

Paraffin-embedded colonic sections of mouse CU and human low and high activity CD and CU were cut into 3-µm slices, deparaffinized then hydrated in alcohol series of decreasing concentration and treated with proteinase K in TE buffer (50mM Tris Base, 1mM EDTA, 0.5% Triton X-100, pH 8.0) for antigen retrieval. Samples were incubated with signal enhancer (Invitrogen) and blocked species-dependent serum. Incubation with a primary antibodies; rabbit anti-mouse TSP1 (provided by Dr M. L. Iruela-Arispe, University of California, Los Angeles, CA, USA), rat anti-mouse NID1, rabbit anti-mouse/human MT1-MMP (HR, Abcam), mouse anti-human TSP1, rabbit anti-human NID1 was performed at a 1:50 dilution at 4°C overnight followed by appropriate fluorescent-label secondary antibody. Intestinal vasculature was evaluated by

immunostaining with rabbit anti mouse/human CD31 (Abcam). Control individuals revealed any neither histopathological nor clinical changes during colonoscopy.

Data analysis and statistics

The protein expression in western blot or semiquantitative PCR images was quantified densitometrically using ImageJ software (NIH, Bethesda, USA) and normalized in respect to the corresponding band of loading control. Graphs were generated using GraphPad Prism 4.0 Software (GraphPad Software, La Jolla, USA). Nonparametric one-way analysis of variance with Tukey's post test was used to compare means of two or more groups. For analysis of two groups within a single experiment Student's t test was applied. All the experiments were performed at least in triplicate. Data are represented as mean value ± SEM. Differences were considered significant when $p<0.05$.

- SETTING UP A MODEL OF INFLAMMATORY ENDOTHELIAL TIP CELLS -

In order to establish *in vitro* model of inflammatory endothelial cells expressing MT1-MMP for shotgun proteomics analysis to understand the MT1-MMP function in the vasculature, we first analyzed its expression by real-time quantitative PCR and western blot in primary ECs in resting conditions or upon inflammatory stimulation with TNFα (**Figure 9**). MT1-MMP mRNA and proteins levels were low in ECs in basal conditions; relative MT1-MMP mRNA and protein levels increased upon stimulation with TNFα. These expression patterns are in accordance with previous observations from our group showing that MT1-MMP was expressed at low levels in peripheral blood human monocytes and upregulated upon their activation by adhesion to matrix components such as fibronectin or to inflammatory endothelial ligands ICAM-1 and VCAM-1 (Matías-Román et al. 2005).

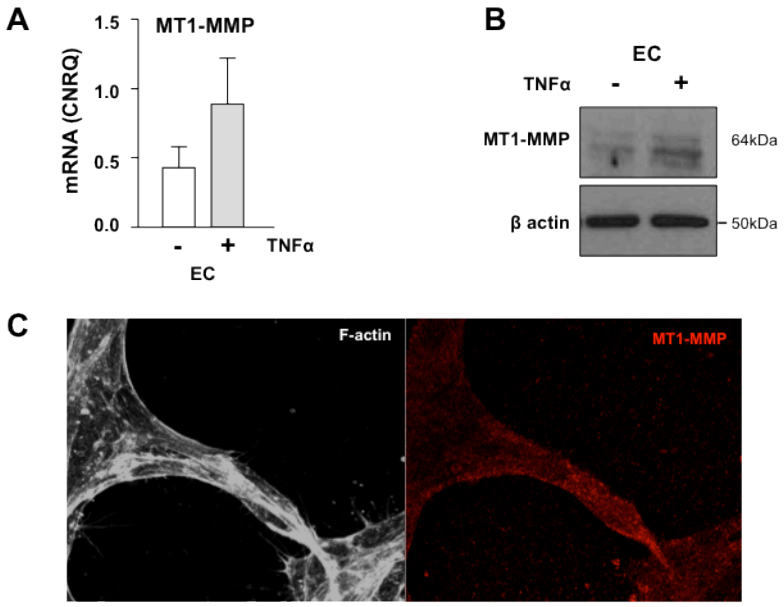

Figure 9. MT1-MMP expression in ECs - key players in vascular remodeling. Quantitavive mRNA (A) and protein levels (B) of MT1-MMP in ECs untreated or treated with overnight with 20 ng/ml TNFα CNRQ: calibrated normalized relative quantity; β actin was used as a loading control; n=3). (C) pMLECs culture in 3D ibidi chamber expressed MT1-MMP after treatment with TNF (20ng/ml).

Mouse lung endothelial cells (MLECs) are useful model to investigate inflammation-induced capillary formation (Gálvez et al. 2005; Genis et al. 2007). Unfortunately only a limited number of endothelial cells can be obtained from neonate mice, meaning an important issue for proteomic analysis. Therefore to ensure sufficient number of cells, primary MLECs (pMLEC) from wildtype (WT) or MT1-MMP null mice were immortalized

by infection with polyoma middle T-antigen (PyV MT) virus, a membrane bound polypeptide transforming the primary cells into a stable cell line by directing the infected cell to enter the cell cycle. Transforming ability of PyV MT is exerted by association with a number of cellular proteins like *src*-family tyrosine kinases, protein phosphatase 2A (PP2A), phosphatidylinositol 3-kinase (PI-3K) and an adaptor protein Shc among others. These interactions in turn stimulate mitogenesis and thus activate cell growth and proliferation via stimulation of Akt and MAP kinases cascades (Cheng et al. 2009; Ichaso and Dilworth 2001).

Immortalized MLEC (iMLEC) maintained endothelial cell morphology and show a stable endothelial cell behavior manifested by monolayer formation and similar response to inflammatory and angiogenic factors. They express typical endothelial cell markers, such as CD31 (PECAM1), and an inflammatory response to TNFα stimulation showed by ICAM-1 and VCAM-1 induction was similar to pMLEC (**Figure 10**).

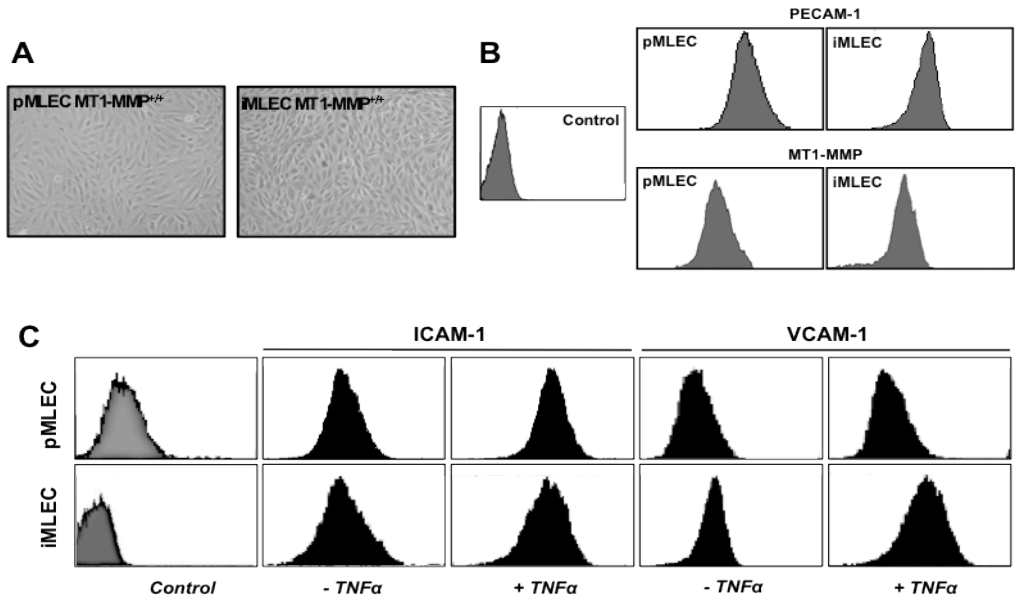

Figure 10. iMLECs respond similarly than pMLECs to TNFα stimulation. (A) pMLECs were immortalized by infection with polyoma middle T virus. Phase contrast images show morphology of pMLECs and iMLECs; (B) levels of PECAM-1 and MT1-MMP in pMLECs and iMLECs assessed by flow cytometry are shown. (C) Histograms show representative flow cytometry analysis of the cell surface expression of ICAM-1 and VCAM-1 in pMLECs and iMLECs stimulated with 20 ng/ml TNFα (n=3).

To establish a model of inflammatory tip cells, we evaluated the effect of some angiogenic and/or inflammatory agents like VEGF and TNFα on the expression of the endothelial tip cell markers Jag1, VEGFR2, Dll4, MT1-MMP, integrin β3, and CXCR4 at different time-points. The expression of these markers was measured 4, 24 and 48h after stimulus, the time window when endothelial cells upon angiogenic stimulus acquired the tip

phenotype and start to sprout (Sainson et al. 2008). Flow cytometry analysis of surface expression showed distinct regulation patterns for each cytokine stimulus (**Figure 11**). The increase of Jag1 surface expression was observed during first hours of stimulation with TNFα, while this induction did not occurred until 48h after pulse of VEGF. The expression of VEGFR2 was low during first hours with all of the stimuli, but with significant tendency to increase in case of TNFα early after stimulation. There were no significant changes in the expression of Dll4 during the treatment in any condition. Even though it was shown that Dll4 significantly changes its expression pattern during sprouting angiogenesis, the oscillation in the expression levels of Jag1/Dll4 might be too short to detect them easily at any time or more probably cells are being primed to induce the tip phenotype but the equilibration mechanism which control tip/stalk balance are not yet active.

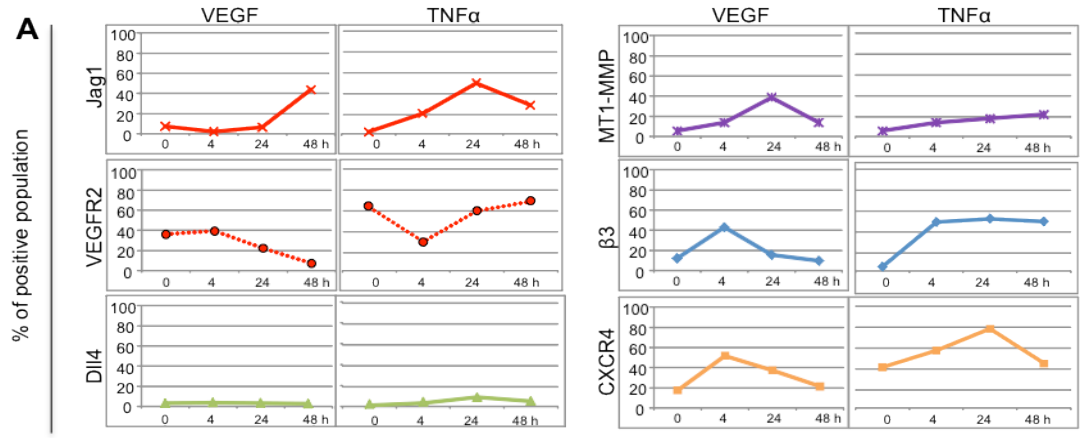

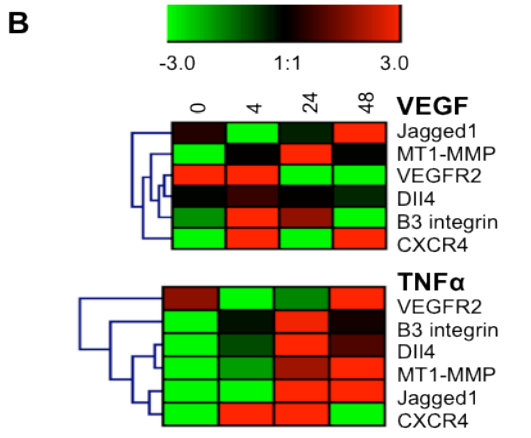

GENE ID	0h	4h	24h	48h
Jag1_**VEGF**	7.53	2.3	6.6	43.93
MT1_VEGF	5.5	13.9	38.73	13.8
VEGFR2_VEGF	36.17	39.33	22.4	7.33
Dll4_VEGF	2	2.76	2.2	1.57
B3_VEGF	12.27	43	15.73	9.9
CXCR4_VEGF	17.57	51.93	37.5	51.53
VEGFR2_**TNFa**	60.7	27.5	57.4	66.5
B3_TNFa	4.2	46.9	50.03	47.4
Dll4_TNFa	1.1	3.33	8.9	5.2
MT1-TNFa	5.4	13.33	17.17	21.0
Jag1_TNFa	1.83	19.6	48.63	27.5
CXCR4_TNFa	39.03	55.07	75.77	42.7

Figure 11. Hierarchical clustering of patterns of induction endothelial tip cells by angiogenic and inflammatory factors. (A) iMLECs were left untreated (0 h) or treated with 20 ng/ml of VEGF or TNFα, and the expression of the tip cell markers VEGFR2, Jag1, Dll4, MT1-MMP, integrin β3 and CXCR4 was analyzed at the cells surface by flow cytometry at 4, 24 and 48 h (n=3). (B) Average percentages of positive population for each marker and condition (right) were analyzed by the high content analysis software Genesis upon normalization of data. Hierarchical schemes obtained for each angiogenic or inflammatory factor are shown (left).

These results confirmed that iMLECs respond to TNFα addition as previously described in primary human ECs (Sainson et al. 2008). In addition, MT1-MMP surface expression was consistently increasing during the whole period of treatment (**Figure 11**), according to previously suggested observation in other cell types (Han et al. 2001). In addition, this particular regulation of MT1-MMP by TNFα suggests its possible implication in specific aspects of angiogenesis, as it has previously been proposed by our group (Gálvez et al. 2005).

To choose the appropriate inflammatory stimulus for inducing endothelial tip cells, we analyzed and compared the expression patterns of the endothelial tip cell markers after stimulation with TNFα and VEGF using hierarchical clustering analysis performed with Genesis (Sturn et al. 2002), a versatile, independent platform Java suite. As shown in **Figure 11**, this global analysis identifies distinct patterns of induction of endothelial tip cells: (1) developmental, induced by VEGF and focused on Dll4 and VEGFR2 regulation (De Smet et al. 2009); (2) inflammatory, induced by TNFα and based on the regulation of Dll4/MT1-MMP and Jag1/CXCR4. This high content analysis provided insights into the molecular heterogeneity of angiogenesis and pointed to TNFα as the prototypic inflammatory inducer of endothelial tip cells (Sainson et al. 2008).

Not only TNFα also induces expression of tip cell markers, but also stimulated endothelial cells to induce tip cell phenotype characterized by formation characteristic membrane protrusions. TNFα-stimulated iMLEC in 2D and pMLEC in 3D were more elongated and exhibited filopodia-like membrane protrusions, respectively, compatible with the morphology of retinal endothelial tip cells (**Figure 12**).

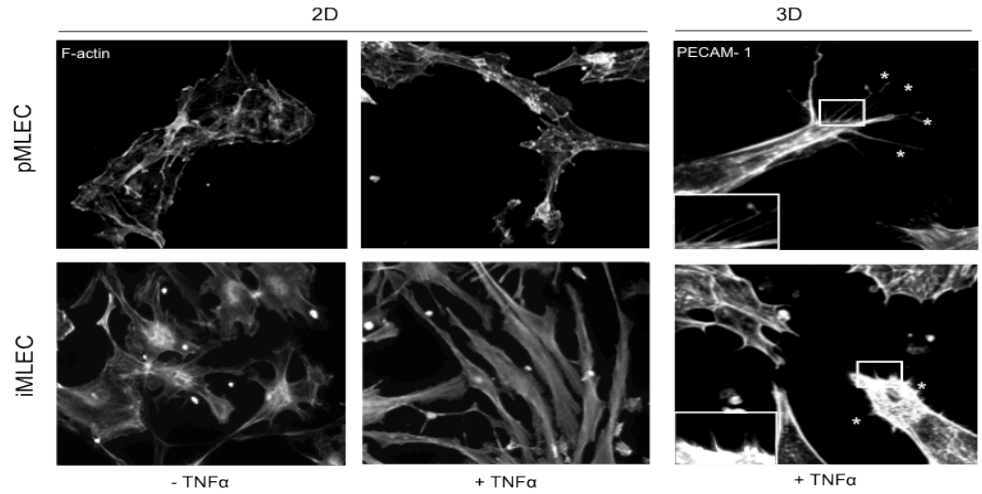

Figure 12. TNFα-stimulated pMLECs and iMLECs showed tip cell phenotype. TNFα-stimulated pMLECs and iMLECs were cultured in 2D or 3D conditions and stained with phalloidin or anti-PECAM-1 antibody; F-actin-based masks and original staining are shown for 2D and 3D conditions, respectively.

Previous studies have shown a positive correlation between vessel sprouting and MT1-MMP expression (Mori et al. 2013; Yana et al. 2007). Moreover mathematical models suggest that MT1-MMP contributes to endothelial tip cell guidance (Karagiannis and Popel 2006), however MT1-MMP gene was not found enriched in the microarray assay performed in retinal tip cells (del Toro et al. 2010; Strasser et al. 2010); low levels of MT1-MMP might have been missed or MT1-MMP might be especially relevant in inflammatory angiogenesis.

Although Dll4 and CXCR4 are the identified tip cell markers in developmental retinal angiogenesis, MT1-MMP is required for inflammation-driven angiogenesis (Gálvez et al. 2005) and Jag1 is the Notch ligand induced in inflammatory tip cells (Sainson et al. 2008). Accordingly TNFα is an early tissue-damage signal for angiogenesis and can induce morphological and molecular changes compatible with induction of endothelial tip cell phenotype (Ligresti et al. 2011; Sainson et al. 2008). Other patterns induced by the chemokines MIP-2 (mouse ortholog of human interleukin-8) or SDF-1 are likely related to their distinct angiogenic properties (Gálvez et al. 2005; Stoll et al. 2011).

The role of TNFα in angiogenesis is controversial due to its reported contrary effect on endothelial cells. It has been shown that TNFα can either block or promote EC migration and proliferation, as well as down- or upregulate VEGFR2 expression and therefore promote or inhibit angiogenesis *in vitro* and *in vivo* (Baluk et al. 2004; Sainson et al. 2008). However, as a major inflammatory mediator can induce expression of adhesion molecules or MMPs, and thus can affect angiogenesis differently at each step.

Endothelial tip cells are crucial to initiate an efficient angiogenic response (De Smet et al. 2009). The molecular fingerprint of these tip cells has started to be elucidated by recent transcriptomics analysis in retinal tip cells; matrix and matrix-related genes as well as secreted proteins such as apelin seemed to be particularly represented (del Toro et al. 2010). We then hypothesized that identification of MT1-MMP collection of substrates in inflammatory tip cells will provide insights into their function.

- A SILAC APPROACH TO CHARACTERIZE MT1-MMP DEGRADOME IN TNFα-INDUCED ENDOTHELIAL TIP CELLS -

Proteolysis by transmembrane proteases mainly impacts other transmembrane or secreted glycoproteins. In particular, transmembrane proteins are present in relatively low abundance and they are often missed in global, broad-spectrum analysis of cell or tissue arrays. MT1-MMP activity might be important from first steps of angiogenic remodeling and

molecules contributing to these initial and probably time-limiting steps might be attractive therapeutic targets for clinical intervention in diseases with pathologic angiogenesis. Therefore comparative analysis of wildtype and MT1-MMP-deficient endothelial tip cells can be useful for identification of molecules specifically regulated by MT1-MMP and contributing to the early angiogenic events.

Having established the model for inflammation-driven endothelial tip cells, we sought to define the MT1-MMP degradome by SILAC. This approach allows identifying and quantifying proteins regulated by MT1-MMP activity. For that wildtype iMLEC were labeled with essential amino acids containing 'heavy' (H) non-radioactive isotopes ($^{13}C_6$ lysine and $^{13}C_6{}^{15}N_4$ arginine), whereas MT1-MMP null iMLEC were labeled with 'light' (L) isotopes (lysine and the $^{13}C_6$ form of arginine) (**Figure 13**). Labeling was accomplished by metabolic incorporation of amino acids implemented in cell culture medium, which was previously dialyzed for removal of any additional lysine and arginine. This metabolic labeling does not affect cell behavior nor physiology and essential amino acids are easily incorporated and replaced in all cell proteins even for protein with low turnover. Approximately five to six cell doublings are needed to incorporate >95% of amino acids and combination of two different amino acids allows mixing differentially labeled cells and so subsequent purification and fractionation steps will not introduce errors in quantification (Mann 2006). To increase the specificity and sensitivity for the extracellular proteins, we have include enrichment for glycoproteins using WGA-lectin beads which can bind oligosaccharides commonly present in secreted and membrane glycoproteins (Guo et al. 2012).

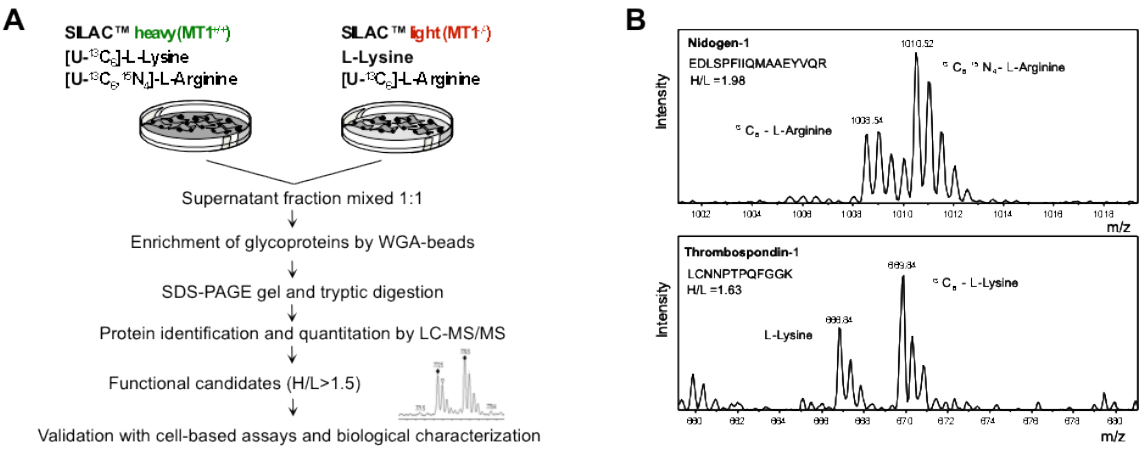

Figure 13. SILAC in TNFα-stimulated immortalized mouse lung endothelial cells (iMLEC). (A) SILAC strategy for comparing the supernatant proteome of WT ($MT1^{+/+}$) and MT1-MMP null ($MT1^{-/-}$) iMLEC stimulated with TNFα (20 ng/ml) for 24 h. (B) Peptide mass spectra for nidogen-1 (NID1) and thrombospondin-1 (TSP1), with relative abundance of heavy and light-labeled forms.

Our particular interest was focused in the proteolytic events; therefore we analyzed in details the culture supernatant from wildtype and MT1-MMP null iMLECs (GLYCOPROTEOME). Corresponding microsomal fraction (PROTEOME) was composed by all mostly plasma membrane and intracellular proteins. After mixing in 1:1 proportion based on protein amount, supernatant glycoproteins were separated by SDS-PAGE, and trypsin-digested gel slices were analyzed by mass spectrometry. 157 proteins in conditioned medium and 797 proteins in microsomal fraction were identified and quantified (relative H/L ratios) (**Table 7** and **Table 8**), with only 28 proteins found in both fractions, suggesting that the presence of putative substrates in the supernatant degradome reflects specific MT1-MMP-dependent processing and not high abundance in inflammation-activated endothelial cells (**Figure 15A**).

Although most of the identified proteins were glycoproteins, a small number of intracellular (nuclear and cytosolic) proteins were also detected likely related to non-specific release of cell proteins by apoptotic cells or to alternative functions of these processed intracellular proteins in the extracellular milieu (Butler et al. 2009). A list of all proteins and their UniProt ID accession is presented in **Table 7** and **8**.

Despite our great efforts to increase protein abundance and to exclude nonspecific intracellular proteins from analysis, the number of identified proteins is not significantly high when compared to other proteomic studies. We can speculate that although our model endothelial cells are immortalized their activity is still far from stable cell lines or cancer cells used in other comparative studies.

Interpretation of H/L ratios in the supernatant glycoproteome is complex and depends mostly on the protein type; a transmembrane protein or a matrix-bound secreted protein shed by MT1-MMP will be more frequent in conditioned medium of WT cells and thus yielding an H/L ratio >1. On the other hand, a secreted protein degraded by MT1-MMP might be more frequent in medium of null cells, giving an H/L ratio <1 (Doucet et al. 2008) (**Figure 14**).

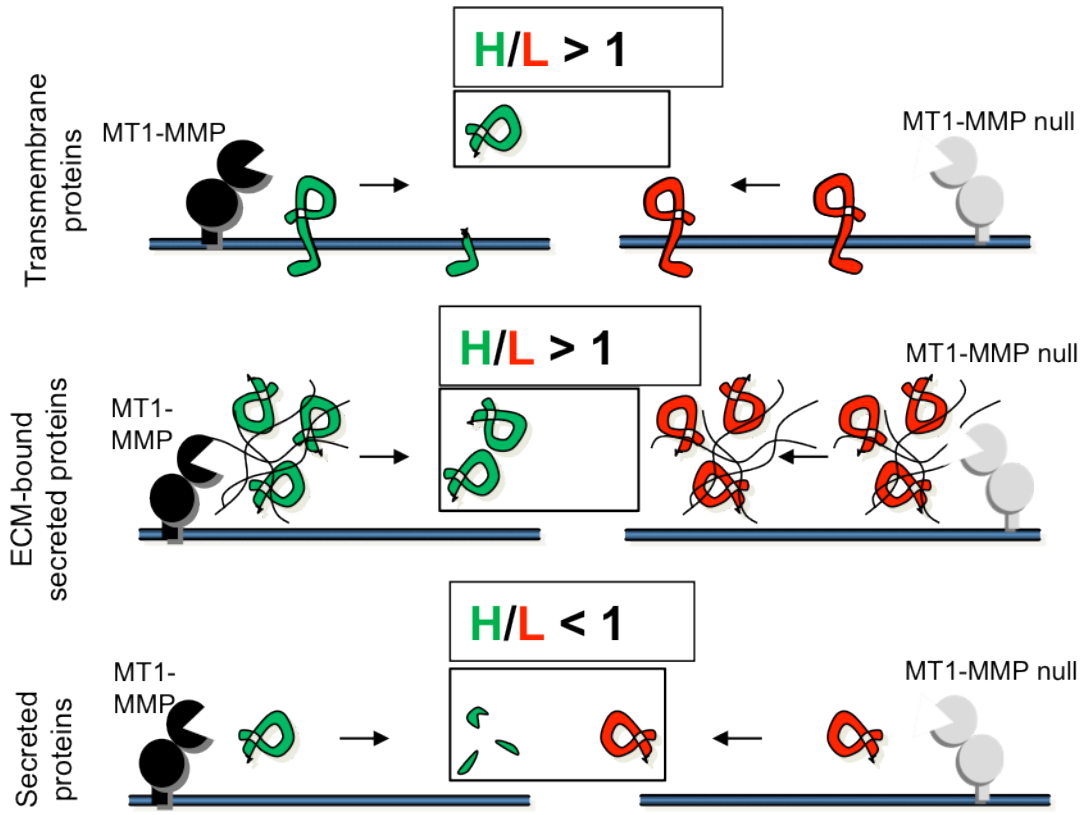

Figure 14. Interpretation of the H/L ratio in SILAC data analysis. Interpretation of the H/L ratio is complex; a transmembrane protein or a matrix-bound secreted protein shed by MT1-MMP will yield an H/L ratio >1 and secreted proteins degraded by MT1-MMP might give H/L ratios < or >1.

816 supernatant and 2765 microsomal peptides with well-defined mass spectra were used to quantify protein ratios between WT (heavy, H) and null (light, L) proteins (**Figure 15C** and **D**). Peptide H/L ratio frequencies show a Gaussian distribution with a peak at log H/L=0, indicating equivalent labeling of WT and MT1-MMP null cells. Since H/L>1 is the more likely outcome for protease action on the supernatant glycoproteome, we defined the MT1-MMP-dependent endothelial DEGRADOME as the set of glycoproteins with an H/L ratio >1.5, taking as a reference well known MT1-MMP substrate collagen type III with H/L=1.67 (**Table 7**). Noteworthy, there were more altered H/L ratios in the supernatant glycoproteome than in the microsomal proteome (31.85% vs 17.82% H/L>1.5) suggesting the proteolytic impact of MT1-MMP in the extracellular compartment (**Figure 15B**).

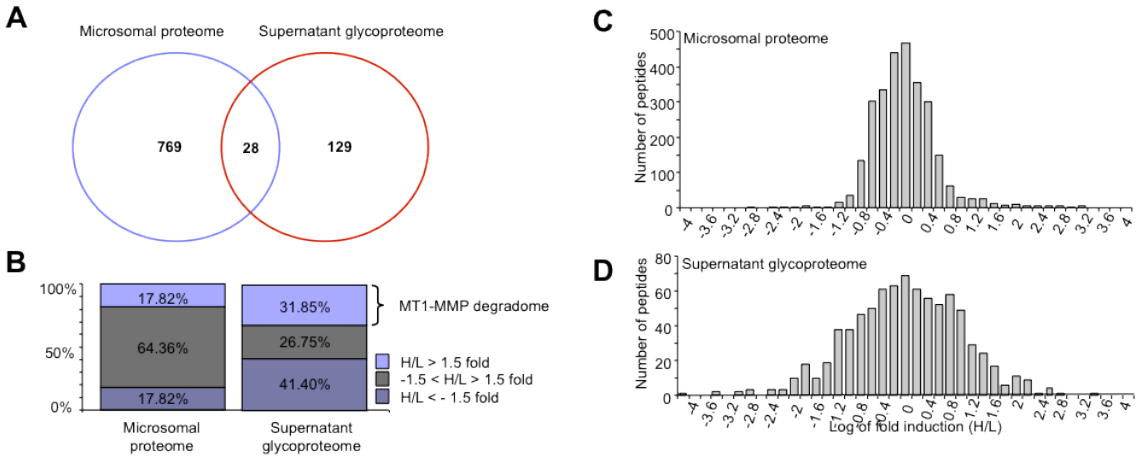

Figure 15. SILAC data analysis. (A) Venn diagram showing proteins identified in both microsomal proteome and supernatant glycoproteome. (B) Histogram shows the percentage of quantified proteins with H/L ratio=1, and < or >1.5-fold change in the microsomal proteome and the supernatant glycoproteome.Normal distribution of H/L ratios of labeled peptides in microsomal proteome (C) and supernatant glycoproteome (D).

This result showed larger variations in the supernatant glycoproteome than in the microsomal proteome in the absence of MT1-MMP, this highlights the power of performing SILAC in culture supernatants for protease analysis, since catalytic activity mostly affects transmembrane and secreted glycoproteins that represent a small fraction of the total proteome (Beck et al. 2011).

- MT1-MMP ENDOTHELIAL DEGRADOME: EXCLUSIVE AND NON-EXCLUSIVE SUBSTRATES -

Functional categorization of the identified proteins based on their generic assigned function (DAVID application (d. W. Huang et al. 2008) and PubMed search defined a group of angiogenesis-related proteins and a smaller group unrelated to angiogenesis (**Table 9**). A literature search showed that while some MT1-MMP degradome proteins are also substrates for other MMPs/ADAMs proteases, most are exclusive substrates of MT1-MMP. Exclusive MT1-MMP substrates included extracellular matrix (ECM)/matricellular proteins (CYR61, FBLN2, SNED1) and non-ECM proteins (PR2C2, SLIT2, EGFR, SFRP1). Among non-exclusive substrates were several ECM proteins such as TSP1 and TSP2, collagen III and IV, fibronectin, fibrillin, laminin, tenascin, and nidogen (**Table 9**).

Table 9. MT1-MMP degradome glycoproteins grouped in relation to their reported function in angiogenesis.

	Protein name		Protein function	Ratio H/L	Processed by MMP / ADAM proteases
Angiogenesis-related	ITPR1	Inositol 1,4,5-trisphosphate receptor type 1	Calcium signaling pathway	18.04	*
	TSP2	Thrombospondin-2	Cell adhesion, ECM-receptor interaction	8.68	ADAMTS1, MMP-2, -9,
	MMP3	Stromelysin-1	Proteolysis	6.04	-
	LYOX	Protein-lysine 6-oxidase	Vasculature development, extracellular matrix organization	5.68	*
	PCOC1	Procollagen C-endopeptidase enhancer 1	Proteolysis	5.53	MMP-2
	TRPM2	Transient receptor potential cation channel subfamily M member 2	Ion transport	5.33	-
	EGFR	Epidermal growth factor receptor	Proliferation, protein interaction	4.60	-
	SODE	Extracellular superoxide dismutase [Cu-Zn]	Oxygen metabolism	4.37	*
	PTX3	Pentraxin-related protein PTX3	Membrane organization, endocytosis	4.20	MT1-MMP
	PR2C2	Prolactin-2C2	Vascular development, cell migration	4.14	-
	IC1	Plasma protease C1 inhibitor	Immune response	3.70	-
	CNTN1	Contactin-1	Cell adhesion	3.67	-
	STC1	Stanniocalcin-1	Cellular ion homeostasis	3.59	MT1-MMP
	SFRP1	Secreted frizzled-related protein 1	Development, differentiation	3.34	-
	TIMP1	Metalloproteinase inhibitor 1	Enzyme inhibitor activity	3.14	MMP-9
	SEM3C	Semaphorin-3C	Vasculature development, axon guidance	2.94	ADAMTS1, ADAMTS13
	CO6A1	Collagen alpha-1(VI) chain	Cell adhesion	2.88	MMP-9, -13
	FBN1	Fibrillin-1	Metal ion binding	2.76	MT1-MMP, MMP-2, -3, -7, -9, -12, -13
	SLIT3	Slit homolog 3 protein	Axon guidance	2.51	-
	LIF	Leukemia inhibitory factor	Receptor interaction, Jak-STAT signaling pathway	2.37	MMP-9
	CERU	Ceruloplasmin	Metal ion binding	2.29	-
	NID1	Nidogen-1	Cell adhesion, binding	2.26	MT1-MMP, ADAMTS1, MMP-15, -19,
	NGAL	Neutrophil gelatinase-associated lipocain	Response to virus	2.11	-
	MMP19	Matrix metalloproteinase-19	Vascular development, differentiation	2.10	-
	CSF1	Macrophage colony-stimulating factor 1	Cytokine-cytokine receptor interaction	2.06	-
	GELS	Gelsolin	Cytoskeleton organization	2.06	MT1-MMP
	TENA	Tenascin	Focal adhesion, ECM-receptor interaction	2.04	MT1-MMP
	FBLN2	Fibulin-2	Cell adhesion, matrix binding	2.04	-
	CO3	Complement C3	Immune response, ECM-receptor interaction	1.96	MT1-MMP
	CCL2	C-C motif chemokine 2	Proliferation. Immune response, chemotaxis	1.86	-
	TIMP3	Metalloproteinase inhibitor 3	Enzyme inhibitory activity	1.80	-
	SLIT2	Slit homolog 2 protein	Axon guidance, cell motion	1.73	-
	TSP1	Thrombospondin-1	Migration, cell adhesion, immune response	1.68	MT1-MMP, ADAMTS1, ADAMTS13
	CYR61	Protein CYR61	Vasculature development, adhesion, proliferation	1.68	MT1-MMP, *
	CO3A1	Collagen alpha-1(III) chain	Vasculature development	1.67	MT1-MMP
	TIMP2	Metalloproteinase inhibitor 2	Enzyme inhibitory activity	1.67	-
	KLRA4	Killer cell lectin-like receptor 4	Cell adhesion, NK mediated cytotoxicity	14.90	-
	KPBB	Phosphorylase b kinase regulatory subunit beta	Calcium signaling pathway	11.58	-
	SNED1	Sushi, nidogen and EGF-like domain-containing protein 1	Cell adhesion	7.05	-
	CPXM1	Probable carboxypeptidase X1	Adhesion, proteolysis	6.12	-
	IGS10	Immunoglobulin superfamily member 10	Receptor signaling	5.85	-
	GDN	Glia-derived nexin	Enzyme inhibitory activity, developmental protein	1.95	-
	AEBP1	Adipocyte enhancer-binding protein 1	Regulation of transcription, cell adhesion	1.77	-
	LOXL3	Lysyl oxidase homolog 3	Oxidoreductase activity	1.73	-

Information about reported protein function was obtained from the DAVID annotation database and PubMed (search keywords: protein or gene name AND angiogenesis, vasculogenesis, endothelial cell migration, endothelial cell adhesion OR endothelial cell proliferation). Reported processing of each protein by MT1-MMP or other MMP/ADAM proteases is indicated. Asterisks (*) mark proteins reported to be processed by other protease families (serine proteases, etc.).

Thus SILAC analysis also provides insights into the question of redundancy versus specificity of substrate cleavage by MMP/ADAM family members in angiogenesis. MT1-MMP shares substrates mainly with ADAMTS1, suggesting molecular and/or functional cooperation or overlap between these proteolytic pathways. Further support for functional overlap between these proteases is that ADAMTS1 is upregulated in the transcriptome of retinal endothelial tip cells (del Toro et al. 2010). Most of the identified MT1-MMP substrates are related directly or indirectly to angiogenesis, supporting the key role of this protease in the process of vessel formation. A few SILAC MT1-MMP substrates were previously identified by iTRAQ/ICAT in tumor cells (Tam et al. 2004) by DIGE in human plasma incubated with the MT1-MMP catalytic domain (Hwang et al. 2004) supporting the robustness of these techniques and pointing to MT1-MMP cleavage of a given substrate in different contexts.

- MT1-MMP ACTIVITY MODULATES KEY BIOLOGICAL PROCESSES IN TNFα-ACTIVATED ENDOTHELIAL CELLS -

Since many of exclusive and non-exclusive putative substrates were known to be involved in angiogenesis and might reflect the essential role of MT1-MMP in this process, we next profiled identified degradome proteins (H/L>1.5) for Gene Ontology (GO) terms (Harris et al. 2004). The degradome protein set was analyzed with the FatiGO (Al-Shahrour et al. 2004) module in the open-source bioinformatics web tool Babelomics (Medina et al. 2010), which compares genes/proteins of interest with the rest of the mouse genome. We analyzed first the Cellular Components terms to assess subcellular location and likely exposure of identified proteins to the protease. The FatiGO analysis indicated that potential MT1-MMP substrates are preferentially located in extracellular and matrix-related compartments (**Figure 16A**).

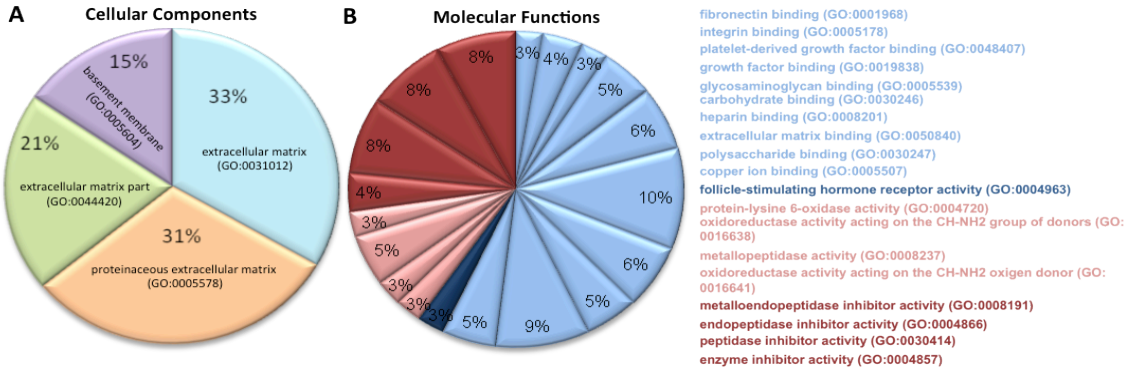

Figure 16. Gene Ontology analysis of MT1-MMP substrates. MT1-MMP putative substrates with an H/L ratio >1.5. were analyzed for GO terms. (A) and (B) Percentages of total identified GO Cellular Components and Molecular Functions terms.

This finding is supported by Kegg (Kanehisa et al. 2004) pathway analysis, which indicated an association of MT1-MMP degradome components with ECM–receptor interactions (**Figure 17**). Accordingly, FatiGO analysis of Molecular Functions GO terms revealed enrichment of matrix and matrix-binding related functions in the MT1-MMP endothelial degradome (**Figure 16B**). Finally, GO analysis of Biological Processes (BPs) showed an enrichment of the MT1-MMP degradome in processes related to cellular adhesion, motility and chemotaxis - key steps in endothelial tip cell function - and to vascular remodeling (**Figure 18**).

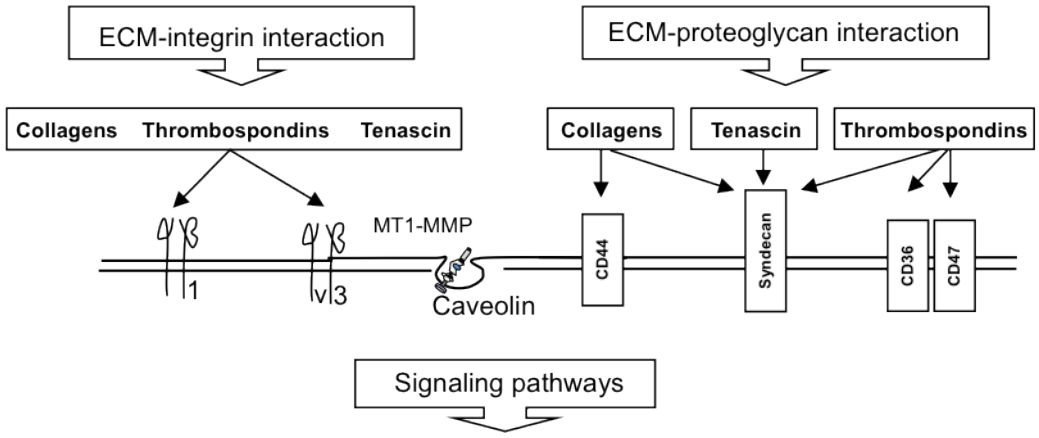

Figure 17. Kegg analysis of the MT1-MMP endothelial degradome. Many proteins in MT1-MMP endothelial degradome can interact with other matrix proteins or cellular receptors, mostly integrins and proteoglycans. The scheme shows information extracted from Kegg analysis that identified the focal adhesion pathway within MT1-MMP degradome. Proteins identified by SILAC as potential substrates for MT1-MMP are highlighted in bold.

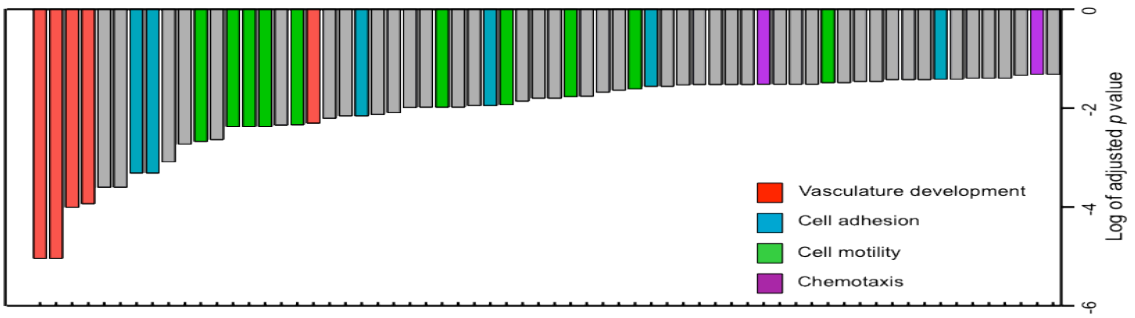

Figure 18. Logarithmic p-values for enrichment in GO Biological Processes. Overlap analysis of identified MT1-MMP substrates included in the four general GO Biological Processes relevant to angiogenesis: cell motility, chemotaxis, cell adhesion, and vasculature development (**Table 10**).

Although we used SILAC to identify transmembrane proteins, most of the identified MT1-MMP substrates in inflammatory endothelial tip cells are ECM proteins in accordance with reported retinal endothelial tip cells transcriptome (del Toro et al. 2010) and reinforcing the idea that matrix and its remodeling are essential during firsts steps of angiogenic growth.

- THE MT1-MMP DEGRADOME REVEALS A COMBINATORIAL PROTEOLYTIC PROGRAM DURING ANGIOGENESIS -

Since several MT1-MMP substrates were common in more that one BP, we performed an overlap analysis with a 4-way Venn diagram for proteins annotated in these particular BPs (**Table 10)**. The functional clustering of selected MT1-MMP substrates included in **Table 10** points to a combinatorial model of processing during inflammatory activation of endothelial cells. In this model MT1-MMP substrates are grouped into specific functional modules linked to GO Biological Processes related to angiogenesis (**Figure 19**). This analysis revealed a proteolytic program of 14 substrates; in which combined rather than single substrate processing by MT1-MMP would control key steps of the angiogenic response (**Figure 19**).

Table 10. Babelomics and FatiGO analysis of GO Biological Processes terms in SILAC-identified supernatant glycoproteins (proteins with H/L ratio >1.5, rest of proteins, blue bars) versus the rest of genome.

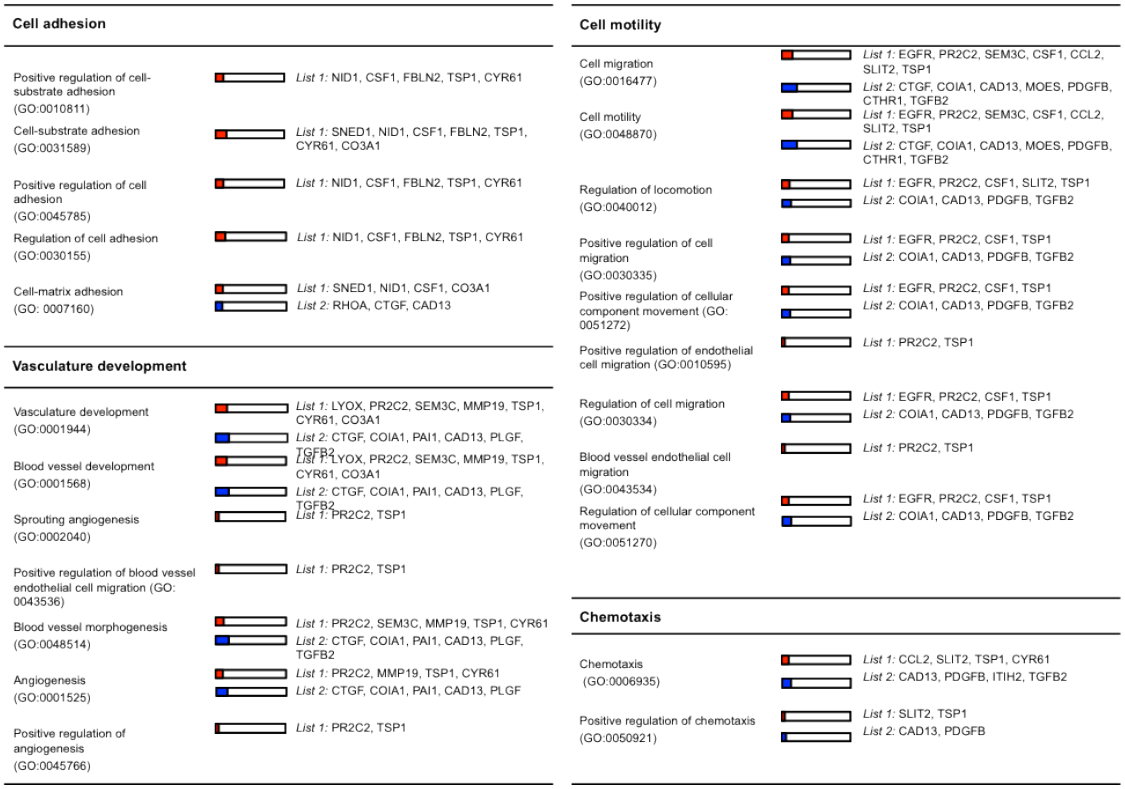

TSP1 seems to be critical for the MT1-MMP response since it is present in most of the functional modules. TSP1 can also be processed by other proteases such as ADAMTS1 (Lee et al. 2006), which also is present in the MT1-MMP degradome and is upregulated in the transcriptome of WT pMLEC activated with the inflammatory chemokine MCP-1 suggesting that these two proteases and TSP1 cooperate during angiogenesis. Other identified substrates such as MMP19, CO3A1 and LYOX are also upregulated in the transcriptome of MCP-1–activated WT MLEC, suggesting that their relative abundance in the supernatant of WT MLEC might be related to regulation of their transcription or processing by MT1-MMP.

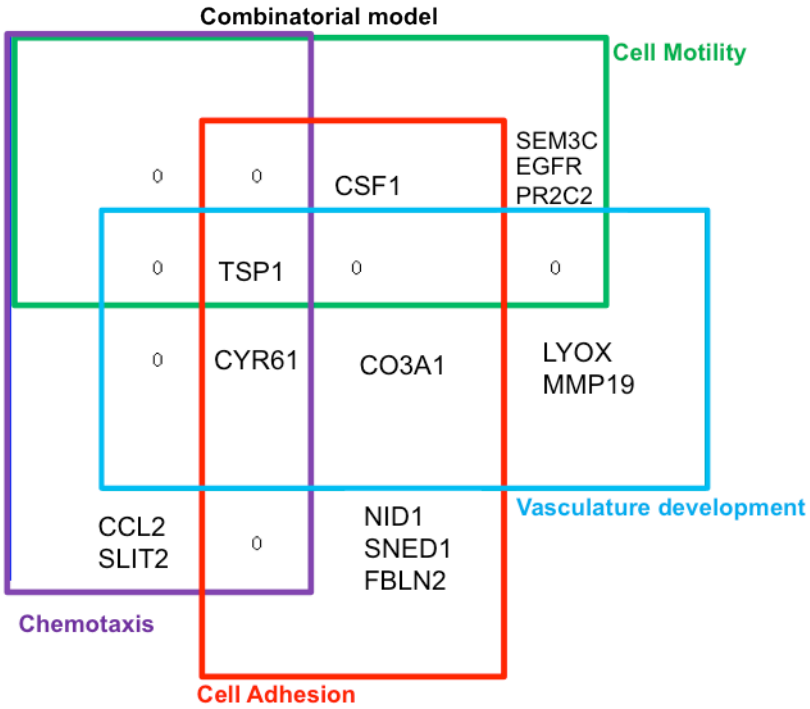

Figure 19. MT1-MMP combinatorial program in TNFα-activated endothelial cells. Venn diagram showing substrates shared between BPs, indicating combinatorial rather than single processing of substrates. Colored lines demark the four GO Biological Processes.

In this combinatorial model TSP1 is a master regulator of all four BPs and its processing in combination with MT1-MMP-mediated cleavage of other substrates would lead preferentially to specific downstream outcomes; for example, co-processing with NID1 would affect endothelial cell adhesion, while processing with PR2C2 or SLIT2 would affect motility. CYR61 processing together with TSP1, CCL2 and SLIT2 determines chemotaxis. Additional processing of TSP1 with other substrates in the modules, such as SNED1, FBLN2, EGFR, CSF1, CCL2 or SEM3C, would further modulate these biological processes, leading finally to angiogenesis and vessel morphogenesis (**Figure 19**). Interestingly, some of these proteins, such as SNED1, were not previously identified as related to angiogenesis (**Table 9**). In the proposed model, modules can cross-combine: while the processing of some MT1-MMP substrates is linked to defined functions (such as CCL2 or SLIT2 to cell motility and chemotaxis), the processing of substrates with broader roles will affect multiple functions; for example, CYR61, which could contribute to cell adhesion, chemotaxis or vascular development depending on the accompanying substrates. This systems biology analysis indicates the existence of finely-tuned and orchestrated rather than random proteolysis during the angiogenic response. Overlap analysis also showed that

endothelial cell adhesion and vasculature development are molecularly closer and that cell motility is the most unique in the combination of processed substrates.

One of the most novel aspects of our study involves the identification of a combinatorial proteolytic program of MT1-MMP in endothelial tip cells, which suggest a modular organization where substrates are grouped into functional modules linked to Biological Processes related to angiogenesis. There is also a hierarchical organization of these substrates since some of them are present in several functional modules. The common component of key GO modules related to angiogenesis is TSP1, identifying this multi-domain matrix glycoprotein as a master regulator of biological processes including adhesion, motility, chemotaxis and morphogenesis, and potentially explaining the tight regulation and coordinated processing by MT1-MMP and ADAMTS1 (Lee et al. 2006). The outcome of angiogenesis will then depend on combined rather than individual processing of substrates, whose fragments might act in a competitive, synergic or sequential manner to angiogenic response. In this regard, several of the identified substrates share structural domains and are therefore able to interact with similar matrix proteins or cell receptors. For instance, key substrates such as TSP1 and CYR61, can directly or indirectly bind integrin αvβ3, an adhesion receptor expressed on ECs (del Toro et al. 2010; Galvez et al. 2002).

- VALIDATION OF MT1-MMP SUBSTRATE PROCESSING *IN VITRO*: TSP1, CYR61, NID1 AND SEM3C -

Several candidate proteins that were identified by SILAC and are being enriched in four main BPs were selected and validated *in silico* to confirm that these proteins contain putative MT1-MMP cleavage sequence (Arg – nonPro – X_{polar} – X_{Hy}) at positions that predict the peptides identified by SILAC. For further validation TSP1, CYR61, NID1 and SEM3C were chosen within each of the 4 main BPs of Venn organization. *In silico* analysis confirmed that all four selected substrates contain putative MT1-MMP cleavage sequence at distinct positions (Kridel et al. 2002) that coincide with distribution of peptides identified by SILAC (**Figure 20**).

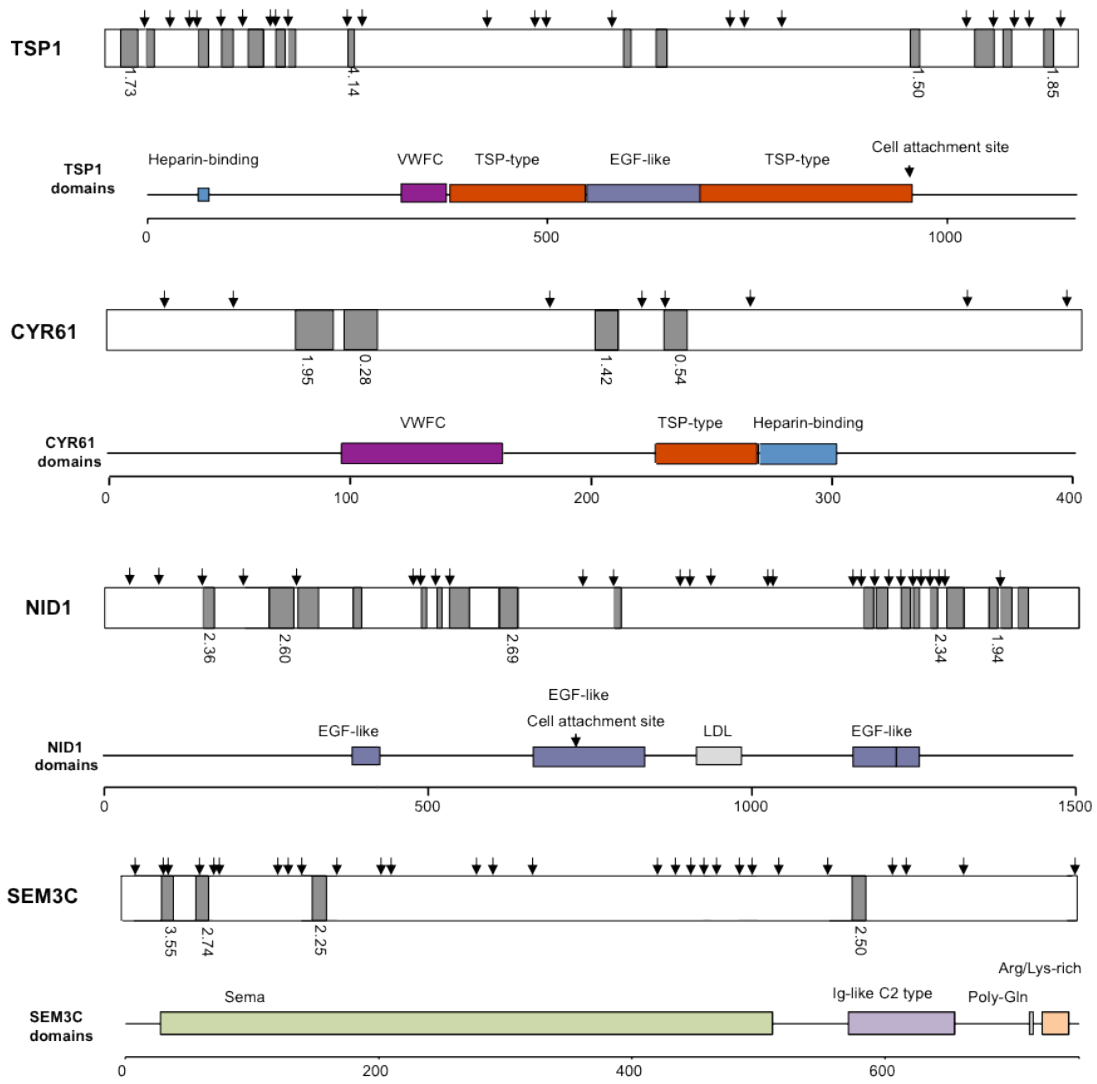

Figure 20. Proteolytic maps and domain structures of TSP1, CYR61, NID1 and SEM3C. Arrows mark potential MT1-MMP cleavage sites beginning with R and gray-shaded areas indicate SILAC-identified tryptic peptides. Examples of H/L ratios >1.5 are also indicated; (source http://www.uniprot.org/).

Based on SILAC analysis performed in culture supernatant (CSUP) and the ability of the identified proteins (TSP1, CYR61, NID1 and SEM3C) to bind to ECM and/or the basement membrane, we next hypothesized that the absence of MT1-MMP might affect cleavage of these proteins from the ECM and therefore their release to the supernatant. No major differences were observed in mRNA and protein levels of TSP1, CYR61, NID1 (undetectable in total lysate) and SEM3C in total lysates of WT and MT1-MMP-null pMLECs treated with TNFα (24h), pointing to similar expression level and abundance of these substrates (**Figure 21A and B**). Lower soluble TSP1, NID1 and SEM3C levels were detected in culture supernatants of MT1-MMP-null pMLECs, indicating that MT1-MMP proteolytic action releases these proteins or its fragments from the ECM; consistent with cleavage of NID1 at the N or C terminus, the molecular weight of NID1 in supernatants from WT pMLECs was slightly smaller (**Figure 21B**). Higher levels of CYR61 were, however, found in medium from MT1-MMP-deficient cells, correlating with a more complex SILAC peptide profile and pointing to an active processing of the intact secreted form of CYR61 by MT1-MMP. Since decreased cleavage of these proteins from ECM could result in accumulation of intact proteins in cells and ECM, we verified distribution of these proteins in 2D cultures by immunofluorescence. Impaired processing in the absence of MT1-MMP led to accumulation of TSP1, CYR61, NID1 and SEM3C in pericellular clusters in contact with the matrix and/or adhesion sites in MT1-MMP-null pMLECs (**Figure 21C**).

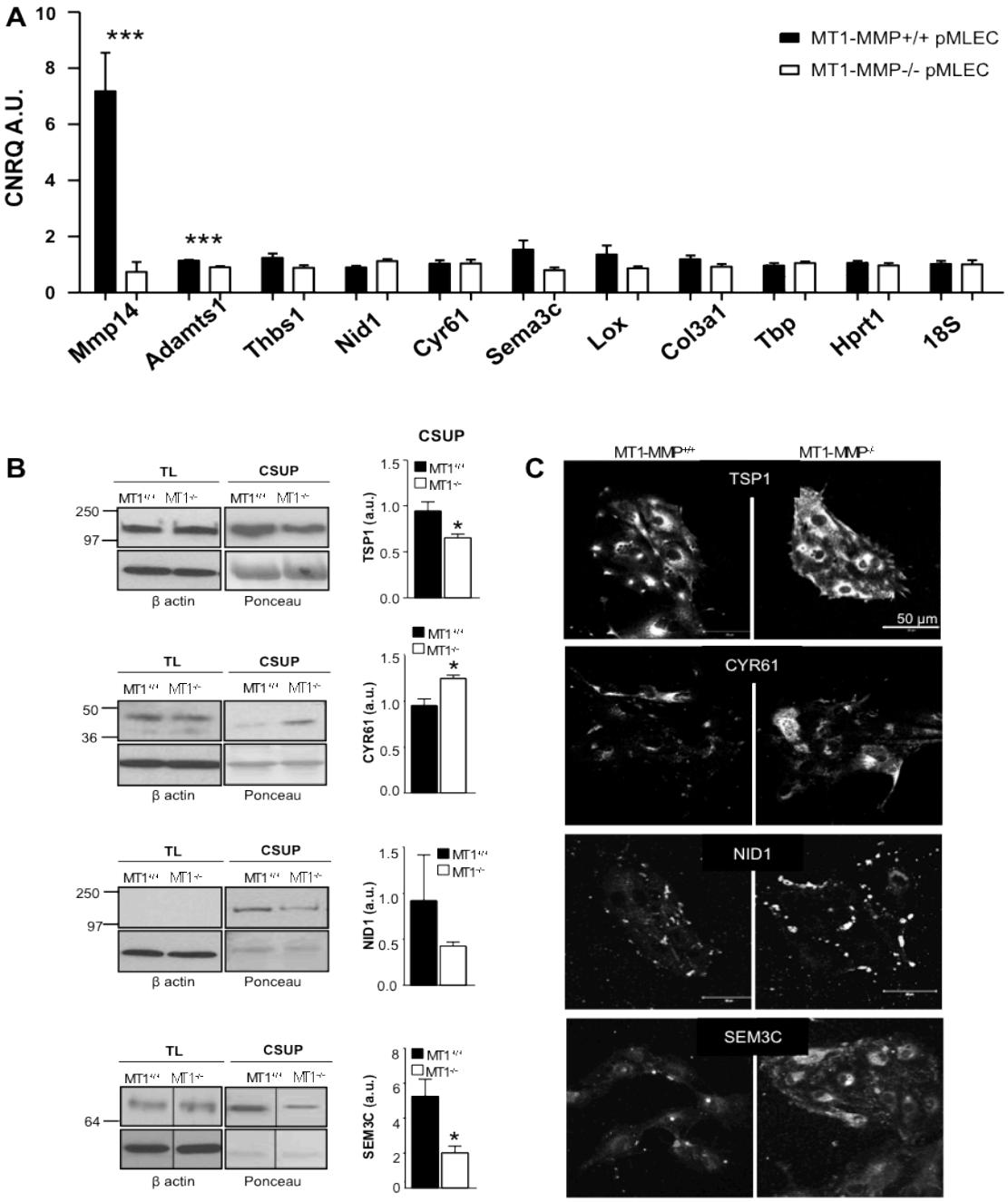

Figure 21. Impaired processing of TSP1, CYR61, NID1 and SEM3C in MT1-MMP null pMLEC. (A) Quantitative mRNA levels of selected MT1-MMP substrates. (B) Immunoblots show detection of TSP1, CYR61, NID1 and SEM3C in total lysates (TL) and culture supernatants (CSUP) of TNFα-stimulated WT ($MT1^{+/+}$) and null ($MT1^{-/-}$) pMLEC; bar charts show densitometric quantification of proteins in supernatants (n=3) (left). (C) Confocal microscopy analysis was performed in TNFα-stimulated WT and MT1-MMP null pMLEC immunostained for TSP1, CYR61, NID1 or SEM3C; representative maximal projections are shown (n=5) (right).

- ALTERED MT1-MMP-DEPENDENT PROCESSING OF SELECTED SUBSTRATES IN 3D ANGIOGENIC MODEL AND IN *IN VIVO* MODEL OF RETINAL DEVELOPMENT -

TSP1, CYR61, NID1 and SEM3C have been related to angiogenesis and vascular development (Esselens et al. 2010; Ho et al. 2008; Iruela-Arispe et al. 2004; S. Kubota and Takigawa 2007) and we therefore analyzed the effect of MT1-MMP-mediated processing of these substrates in models better mimicking vascular development, such as 3D-Matrigel pMLEC cultures and retina postnatal vascularization. Although no major differences were observed in TSP1, CYR61, NID1, and SEM3C signal along endothelial cell 3D-tubes, enrichment and/or pericellular clusters of these substrates, especially of CYR61 and NID1, were observed along the endothelial tip cells formed by MT1-MMP-null pMLEC compared with WT (**Figure 22**).

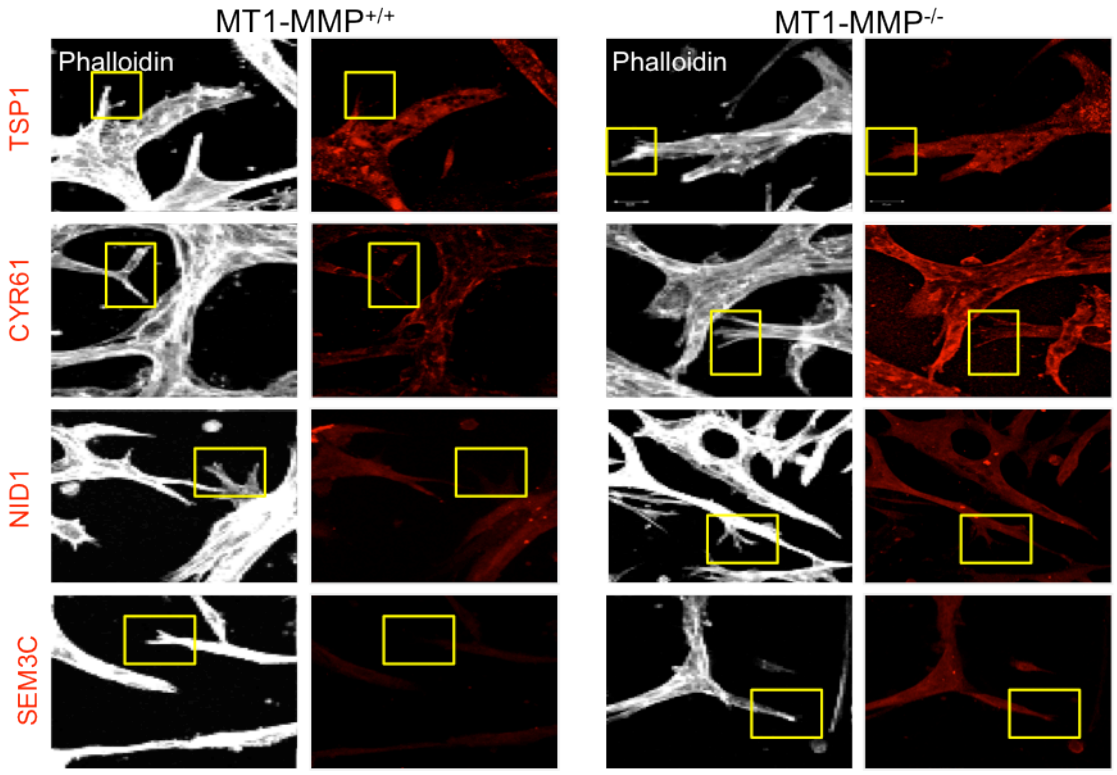

Figure 22. Impaired processing of TSP1, CYR61, NID1 and SEM3C in 3D Ibidi model. Confocal immunofluorescence of TSP1, CYR61, NID1 and SEM3C (red) and F-actin (white) in TNFα-stimulated WT and null pMLEC grown in Ibidi chambers covered by 3D-Matrigel; representative maximal projections are shown (n=5).

Accordingly, we observed accumulation of CYR61 and NID1 along the filopodia of endothelial tip cells at the vascular front of retinas from MT1-MMP null neonates in contrast to the restricted distribution of CYR61 and NID1 to the posterior pole of retinal tip cells in wildtype (**Figure 23**); this points to an active role of MT1-MMP in CYR61 and NID1 processing during vascular sprouting also *in vivo*. SEM3C and TSP1 were undetectable in the vasculature of mouse neonate retinas.

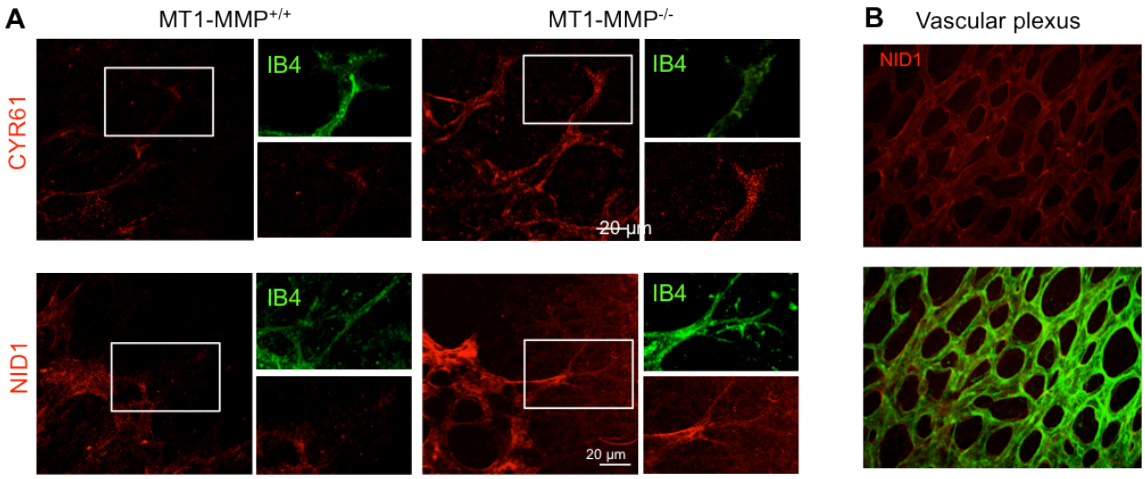

Figure 23. Accumulation of CYR61 and NID1 in endothelial tip cells of retinas from MT1-MMP null mouse neonates. Whole mount confocal immunofluorescence of isolectin B4 (green) and CYR61 and NID1 (red) in retnas of P6 WT (MT1-MMP$^{+/+}$) and null (MT1-MMP$^{-/-}$) mice; representative maximal projections are shown (n=4).

We focused on validation of MT1-MMP processing of selected substrates involved in the four main BPs, cell motility, chemotaxis, cell adhesion and vasculature development (TSP1, CYR61, NID1 and SEM3C) whose cleavage would likely occur within the same time-frame cooperating in driving cellular responses leading to inflammatory capillary sprouting. However, it will be interesting to explore in the future whether MT1-MMP processing of other identified proteins such as PR2C2, CCL2 and CSF1 might also modulate their angiogenic properties in different scenarios. Conversely, as we demonstrated in TNF□-stimulated MT1-MMP null pMLECs, in the absence of MT1-MMP simultaneous accumulation of these substrates in ECs might contribute to defective angiogenesis.

- VALIDATION OF SELECTED MT1-MMP SUBSTRATES IN HUMAN PRIMARY ENDOTHELIAL CELLS -

We next investigated whether the MT1-MMP proteolytic program identified in mouse ECs could be extendable to the human model. To this purpose, MT1-MMP expression was interfered by two independent siRNA oligonucleotides in human endothelial cells (HUVEC); the efficiency of MT1- MMP interference was higher than 70% assessed by RT-PCR and western blot (**Figure 24**). TSP1, CYR61, NID1 and SEM3C levels in total lysates from negative siRNA and MT1-MMP-interfered HUVEC were similar. Lower levels of TSP1, CYR61, and NID1 were however found in supernatants from MT1-MMP-interfered compared with negative siRNA-interfered HUVEC pointing to decreased processing of these substrates in cells with reduced levels of MT1-MMP (**Figure 25A)**. No differences could be detected in supernatant levels of SEM3C.

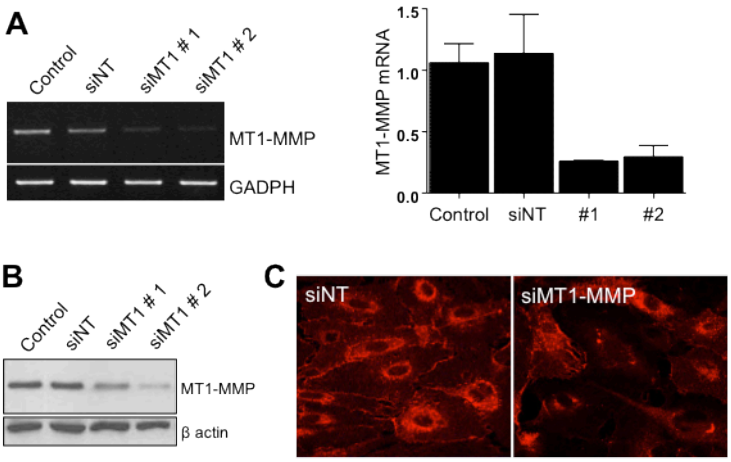

Figure 24. MT1-MMP-interfered human ECs. (A) MT1-MMP expression was interfered by siRNA transfection of two different MT1-MMP siRNA oligonucleotides (MT1#1 and MT1#2) or a negative siRNA (siNT) in HUVEC; MT1-MMP mRNA and (B) protein levels were assessed by RT-PCR and western-blot, respectively. (C) Representative images of MT1-MMP staining in control (siNT) and interfered HUVECs (siMT1-MMP).

In a complementary approach we compared substrate subcellular distribution in MT1-MMP-interfered HUVEC. As shown in **Figure 25B**, the subcellular distribution of TSP1, CYR61, NID1 and SEM3C was changed in HUVEC with reduced expression of MT1-MMP; in particular, CYR61 and SEM3C appeared more intense and NID1 formed pericellular clusters in HUVEC with lower expression of MT1-MMP.

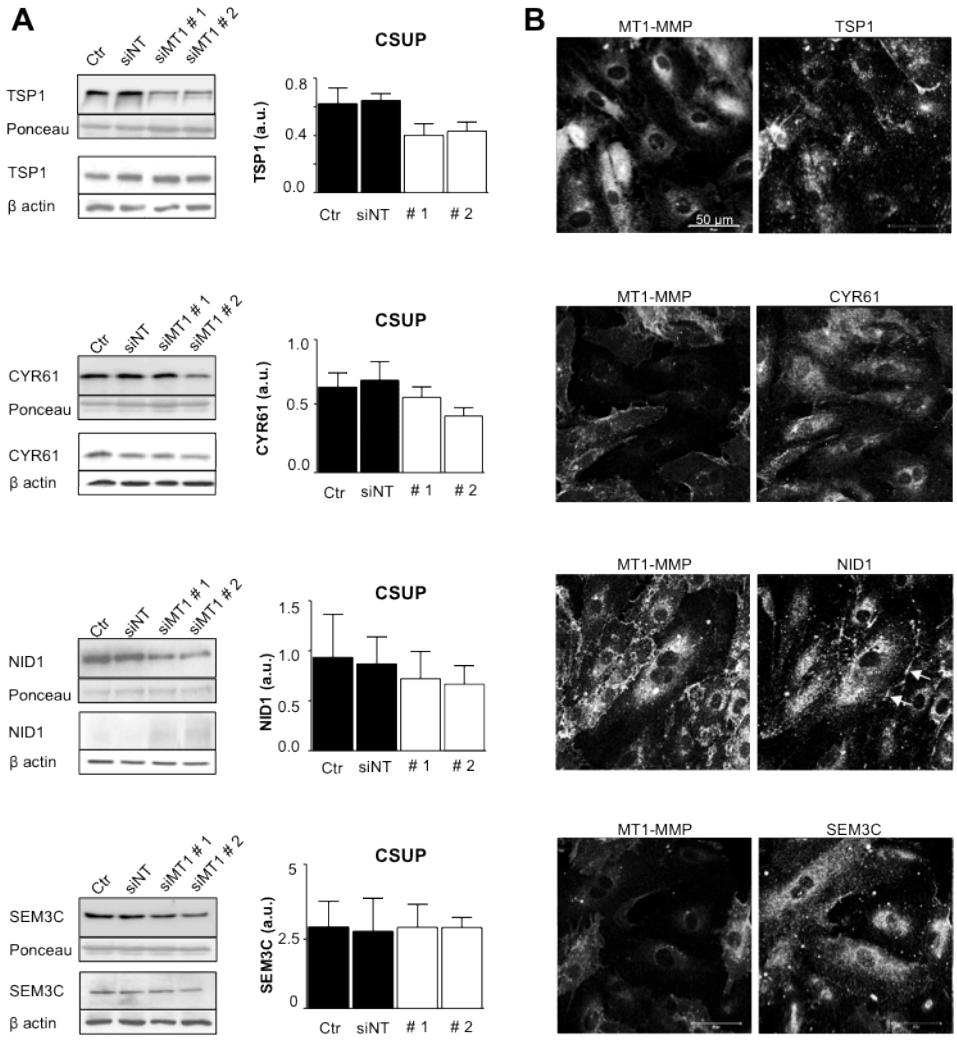

Figure 25. Impaired processing of TSP1, CYR61, NID1 and SEM3C in MT1-MMP-interfered human ECs. (A) Immunoblots show detection of TSP1, CYR61, NID1 and SEM3C in culture supernatants (CSUP) of TNF -stimulated HUVEC transfected with negative siRNA (siNT) or two different MT1-MMP-siRNA (MT1#1 and MT1#2); bar charts show densitometric quantification of proteins in supernatants (n=4-6). (B) Confocal microscopy analysis was performed in TNFα-stimulated MT1-MMP-siRNA HUVEC immunostained for MT1-MMP and TSP1, CYR61, NID1 or SEM3C; representative maximal projections are shown (n=4); arrows point to NID1 pericellular deposits.

Present data support that the combinatorial program driven by MT1-MMP identified in mouse cells is also acting in human ECs since decreasing MT1-MMP expression impacts on the processing and subcellular distribution of TSP1, CYR61, NID1 and SEM3C in HUVEC; milder effects were however observed likely related to the experimental approach and maybe to a different repertoire of proteases expressed by human ECs.

TSP1 and NID1, key components of the combinatorial MT1-MMP proteolytic program, have been described in other cellular models as substrates of MT1-MMP (Butler et al. 2008; d'Ortho et al. 1997). The multidomain structure of matricellular proteins contributes to their pleiotropic functions in angiogenesis. Thus, TSP1 effects on angiogenesis largely depend on whether it is soluble or matrix-bound basement membrane localized TSP1 in mature or quiescent vascular beds might provide stabilizing signals, whereas excess soluble TSP1 during angiogenesis can suppress capillary sprouting (Iruela-Arispe et al. 2004). TSP1 can be cleaved by ADAMTS1, releasing a soluble C-terminal monomer and leaving a matrix-bound N-terminal trimeric fragment (Lee et al. 2006). During inflammatory angiogenesis, MT1-MMP could further modulate the angiogenic properties of TSP1 either by cooperating with ADAMTS1 or by acting at a different cleavage site, perhaps affecting interactions with receptors such as integrin αvβ3, CD36 or CD47 (Li et al. 2002). Recently described pathways include TSP1 scavenger receptor CD36 expressed in endothelial cells that may promote both pro- and antiangiogenic signals depending on interaction with different Src family kinases; thus CD36-Fyn complex will inhibit angiogenesis while CD36-Syk interaction can promote VEGF-A-induced endothelial cell migration and phosphorylation of VEGFR-2 priming angiogenic switch (Kazerounian et al. 2011). Accumulation of TSP1 clusters in TNFα-stimulated MT1-MMP null ECs indicates that MT1-MMP is required for TSP1 processing events that are not compensated for ADAMTS1. Increased pericellular TSP1 deposits might contribute to the reduced angiogenesis reported in MT1-MMP null cells (Galvez et al. 2005; Oblander et al. 2005).

CYR61/CCN1, a member of the CNN family of matricellular proteins, promotes endothelial cell adhesion, migration and proliferation (S. Kubota and Takigawa 2007). CYR61 seems to be an exclusive substrate of MT1-MMP within the metalloproteinase family (Butler et al. 2008). CYR61 knockout is embryonically lethal due to vascular defects (Kubota 2007), and a dual role for this protein has been recently described in physiological and pathological vascularization in retina (Hasan et al. 2011). In our analysis, CYR61 accumulated at the periphery of MT1-MMP-deficient ECs and around endothelial null retinas, pointing to a key role for MT1-MMP in CYR61 processing *in vitro* and *in vivo*. The main effect of MT1-MMP cleavage of CYR61 might be to modulate its binding to integrins α6β1 and αvβ3 (Leu et al. 2004) or as recently reported for its cleavage by serine proteases to modulate its interactions with growth factors (Guillon-Munos et al. 2011). Therefore loss of MT1-MMP processing of CYR61 might mimic the effect of CYR61 knockout, contributing to vascular defects observed in MT1-MMP null retinas.

Likewise, pericellular deposits of NID1, a protein normally associated to laminin and fibulin at the basement membrane (Ho et al. 2008) might confer basement membrane-like 'quiescence' signals hindering endothelial cell active sprouting. NID1 has been reported to be cleaved by ADAMTS1 (downstream of the N-terminal domain) and MT1-MMP, likely at a different site (Canals et al. 2006; d'Ortho et al. 1997). Although NID1 was undetectable in total lysates, levels of soluble NID1 were also significantly increased in culture supernatants from WT pMLECs, suggesting MT1-MMP-dependent release of NID1 from the basement membrane. The effect of NID1 proteolytic processing is unknown. NID1 contributes to basement membrane stability, and therefore the increased NID1 levels observed in MT1-MMP null ECs might confer basement membrane-like 'quiescence' signals, thus hindering the angiogenic response by impeding ECs engagement in active sprouting.

Finally, since SEM3C processing by ADAMTS1 can contribute to tumor cell migration (Esselens et al. 2010) and therefore we can imagine that MT1-MMP-processing of SEM3C might impact on EC migration required for capillary sprouting; in the absence of this processing impaired migration might lead to defective angiogenesis. In sum, TSP1, CYR61, NID1 and SEM3C can modulate endothelial cell adhesive and migratory behavior through complementary mechanisms including binding to integrins; the synergistic or competitive action of these accumulated substrates in the absence of MT1-MMP would impair migration and adhesion, yielding a more quiescent endothelial state and defective angiogenesis (**Figure 26**).

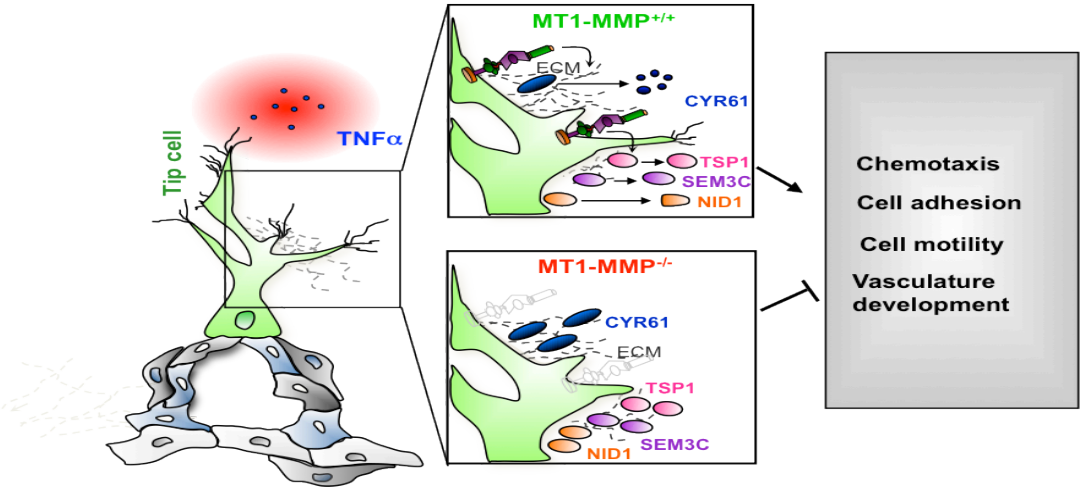

Figure 26. MT1-MMP combined substrate processing in inflammatory angiogenesis. Combined processing of TSP1, CYR61, NID1, SEM3C and other substrates by MT1-MMP has a major impact on the regulation of endothelial cell adhesion and motility, and chemotaxis ultimately leading to vasculature development. This proteolytic program is activated by inflammatory stimuli such as TNF. The absence of MT1-MMP in stimulated endothelial cells results in impaired processing and accumulation of the identified substrates dampening the capillary sprouting process and favoring quiescence of the vasculature.

- MT1-MMP IS UPREGULATED IN A MODEL OF DSS-INDUCED EXPERIMENTAL MOUSE COLITIS –

Since angiogenesis is often linked to acute and chronic inflammatory responses, the role of inflammatory angiogenesis has recently focused attention in many chronic inflammatory disorders. To analyse the potential relevance of the identified MT1-MMP substrates in inflammatory angiogenesis we sought for a model of chronic inflammatory disease that fits two conditions: (1) involvement of inflammatory angiogenesis and (2) expression of MT1-MMP in ECs. Inflammation followed by angiogenesis is considered as an integral part of the pathology in inflammatory bowel disease (IBD) with its two major types: Crohn's disease and ulcerative colitis. Upregulation of proangiogenic factors and increased vessel density have become a well-recognized markers of disease progression (Di Sabatino et al. 2004; Kanazawa et al. 2001). We analyzed the functional role of some of the identified proteins as biomarkers of inflammation-driven angiogenesis by employing the human and experimental mouse model of ulcerative colitis.

DSS treatment induced colitis in mice that mimics IBD observed in human patients. C57BL76 mice were treated with different doses of DSS during 7 days to induce progressive intestinal disease. As shown in **Figure 27A**, treatment with 1% and 4% of DSS induced moderate and severe IBD, respectively. Significant body weight loss was observed after 6 (moderate) and 3 (severe) days of consecutive administration with DSS, persisting and worsens until day 7 when animals were sacrificed. Daily assessment of colitis score represented by weight loss, stool consistency and bleeding resulted in a significant body weight loss and maximal colitis activity (total clinical score, **Figure 27B**) at the end of the treatment. Macroscopic analysis of the colons at day 7 showed considered colon retraction in case of severe colitis (**Figure 27C**) and remarkable epithelial tissue mucosa and crypt destruction (**Figure 27D**).

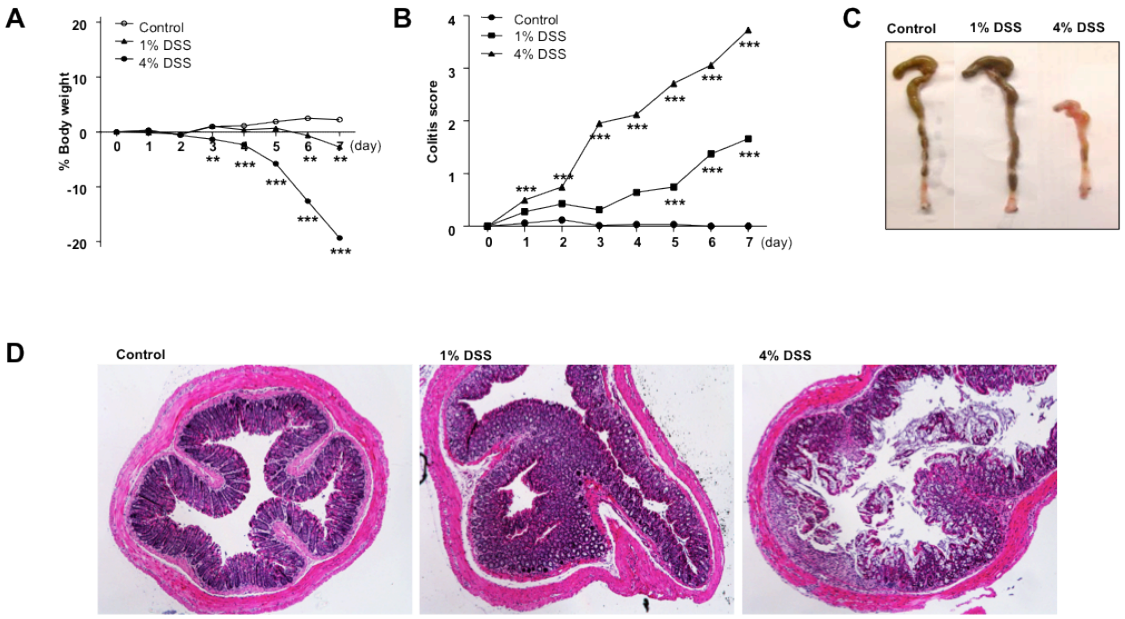

Figure 27. DSS treatment induces colitis in mice that mimics IBD observed in human patients. (A) 1% and 4%DSS induced moderate and severe IBD, respectively. (B) Daily assessment of colitis score represented by weight loss, stool consistency and bleeding resulted in a significant body weight loss and colitis activity at the end of the treatment. (C) Macroscopic and (D) histochemical analysis at day 7 showed considered colon retraction and mucosa destruction, respectively.

Serum levels of the pro-inflammatory cytokine TNFα were upregulated in this model in a DSS-dose response manner being significant in severely affected mice (**Figure 28A**). Consistent with previous reports of increased VEGF-A levels in UC and CD (Di Sabatino et al. 2004; Kanazawa et al. 2001) we observed increased serum levels of the proangiogenic growth factor VEGF-A that were significant in the severe condition (**Figure 28B**). Since TNFα enhances the expression of cell adhesion molecules and thus might promote tissue infiltration with inflammatory cells, we expectedly observed that according to the inflammatory cytokine increased secretion; administration of DSS induced an increased infiltration of Mac1 positive inflammatory cells into the mucosa (**Figure 28C**).

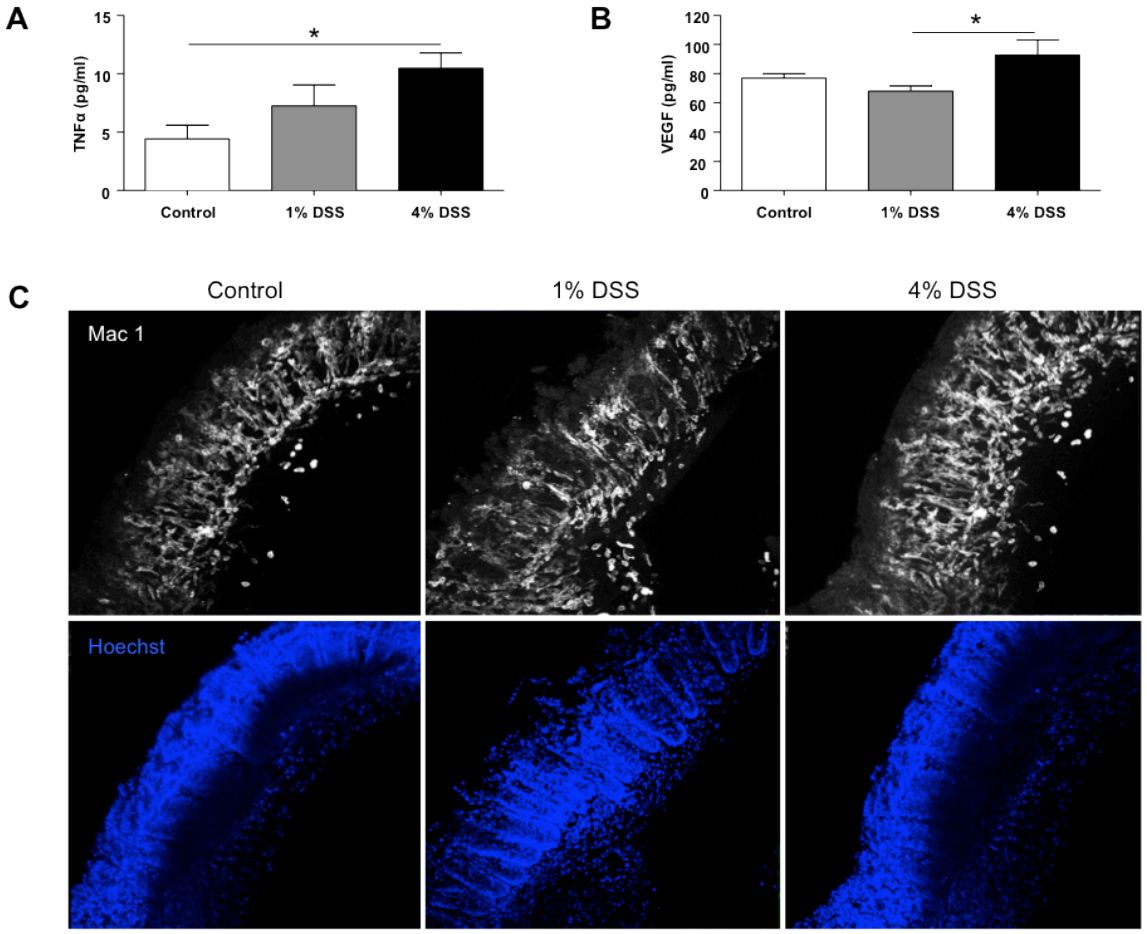

Figure 28. Effect of DSS on proinflammatory and proangiogenic cytokines. (A) Serum levels of the proinflammatory cytokine TNFα were upregulated in a DSS-dose dependent manner. Moreover there was a significant increase of the proangiogenic growth factor VEGF in severe condition (B), as a result increased infiltration of inflammatory cells (Mac1+) was observed in DSS-treated animals (C) suggesting an active inflammation and angiogenesis; * $p < 0.05$.

We next checked the vasculature morphogenesis occurring in DDS-induced model of experimental colitis. According to the whole-mount staining of anti-CD31 (an endothelial marker), administration of DSS induced increased new vessel growth both in 1 and 4 % DSS treatment. Nonetheless, angiogenesis in IBD does not simply mean increase in vessel density; vessels formed during inflammation are different from those formed during normal neovascularization. These vessels are immature, tortuous, lacking investment in supporting cells (pericytes/VSMCs), leakier and more sensitive to growth factors (Cromer et al. 2011). As result, new vasculature formed in IBD maintains and actively promotes disease severity.

In fact, both in moderate and severe condition vasculature was altered with apparent blind-ended new sprouts, increased in small capillaries and a denser vascular meshwork

compared with organized polygonal vascular plexus observed in control animals (**Figure 29A**). Collagen IV staining endothelial basement membrane confirmed that control vasculature was more stable/mature than the one from 1 and 4% DSS treatment that only was Col IV positive at the external part of intestine and new sprouts that were raising above stable vasculature were CD31+/Col IV- (**Figure 29B and C**). This suggest that angiogenesis, the formation of new vessels from preexisting capillaries, was particularly active starting in moderate disease and later in severe condition.

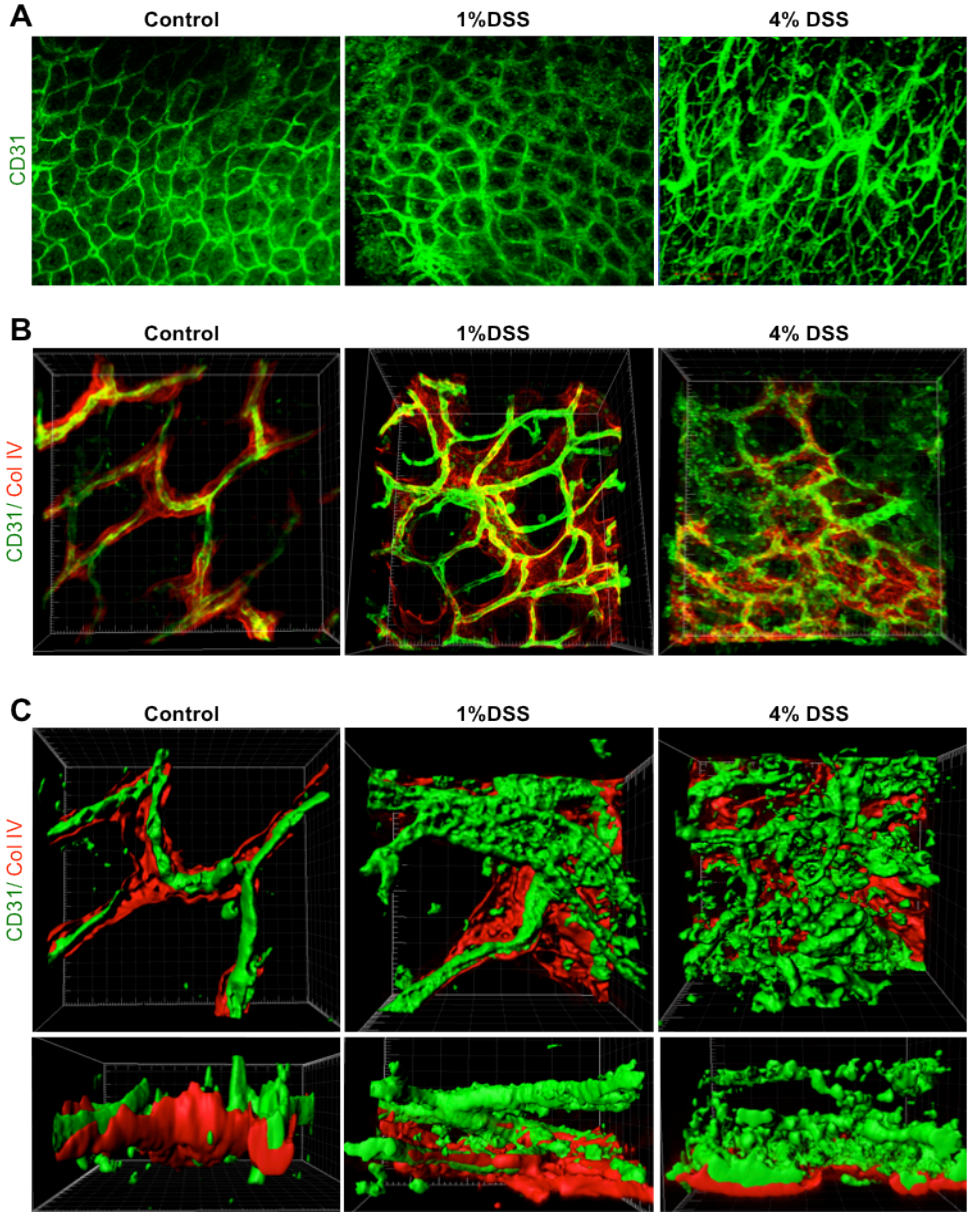

Figure 29. DSS treatment induces increased vessel density. (A) CD31 (green) staining of instestinal vasculature showed denser and disorganized meshwork in moderate and severe colitis. (B) and (C) ColIV (red) positive vessel were mostly observed in control animals, while newly formed sprouts raised above stable vasculature in moderate and severe colitis.

We next investigated whether MT1-MMP is upregulated during DSS-induced colits. For that we quantitated by western blot in homogenates of colonic tissues the expression of the protease MT1-MMP in control and DSS-treated mice; as shown in **Figure 30A and B**, total expression of MT1-MP was significantly upregulated upon treatment with 1% to 4% DSS. This MT1-MMP expression was localized in both epithelial and endothelial cells (**Figure 30C**) and confirmed our previous results demonstrating that TNFα activated and upregulated expression of MT1-MMP in endothelial cells (Koziol et al. 2012b).

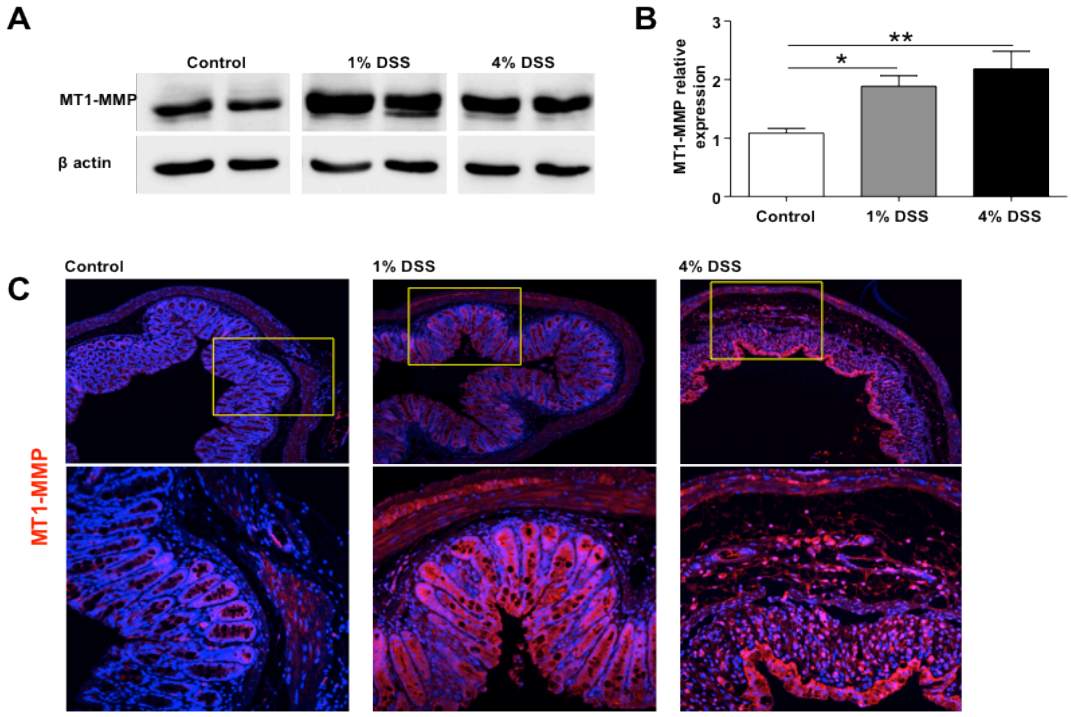

Figure 30. Regulation of MT1-MMP expression along DSS-induced experimental mouse colitis. (A and B). Total expression of MT1-MMP was upregulated upon treatment with 1% to 4% DSS as analysed by western-blot. (C) MT1-MMP localizes mostly in epithelium in control condition as well as in vessels in 1% and 4% DSS and in infiltrating leukocytes in 4% DSS-treated mice.

- MT1-MMP SUBSTRATES AS BIOMARKERS OF INFLAMMATORY ANGIOGENESIS -

As shown in the **Figure 30** TNFα-activated ECs MT1-MMP can process several substrates thus impacting on the angiogenic process. We aimed at analyzing the expression pattern of two of these MT1-MMP identified substrates, TSP1 and NID1, in the vasculature of control or mice affected by colitis. Since TSP1 and NID1 are proteins normally present at the ECM, their processing by MT1-MMP might generate soluble fragments able to reach the

bloodstream thus serving as biomarkers of the activity of the intestinal inflammatory disease. To test this hypothesis we quantitated the soluble levels of TSP1 and NID1 in the serum of control or diseased mice. As shown in **Figure 31A and B** soluble serum levels of both TSP1 and NID1 tend to be higher starting in 1%-treated mice compared with controls and reaching maximum in 4% DSS-treated mice. These data point to release of TSP1 and NID1 to the bloodstream in severe disease likely by MT1-MMP at the new vessels of DSS-treated mice.

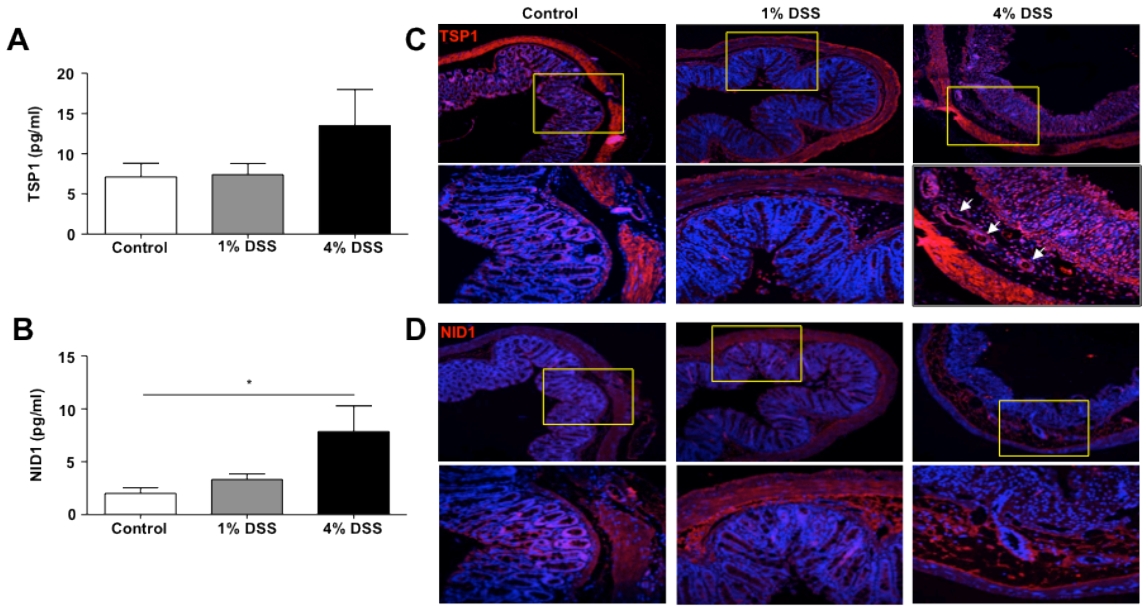

Figure 31. Regulation of the expression of MT1-MMP substrates TSP1 and NID1 along DSS-induced experimental mouse colitis. Serum levels of TSP1 and NID1 increased in severe colitis (A and B). (C) TSP1 was slightly expressed in epithelial cells and in the submucosa of all mouse groups; in addition, TSP1 was also expressed in some vessels of 1% and 4% DSS-treated mice (white arrows) and in the abundant infiltrate in 4% DSS-treated mice. (D) NID1 was mainly located at the submucosa and in vessels in 4% DSS-treated mice.

MT1-MMP was expressed in epithelial cells in control and 1% or 4% DSS-treated mice. Interestingly, MT1-MMP was found co-localizing with CD31 in vessels observed in 1 and 4% DSS-treated mice and in the inflammatory infiltrate. We next analyzed TSP1 and NID1 to address whether the pattern of these substrates change along severity of colitis in correlation with the observed changes in MT1-MMP pattern. TSP1 was slightly expressed in epithelial cells and in the submucosa of all mouse groups; in addition, TSP1 was also expressed in some vessels of 1% and 4% DSS-treated mice (**Figure 31C**, white arrows) and in the abundant infiltrate in 4% DSS-treated mice. NID1 was mainly located at the submucosa and in vessels in 4% DSS-treated mice, but also found in vessels (**Figure 31D**).

- SERUM LEVELS OF MT1-MMP SUBSTRATES TSP1 AND NID1 ARE ELEVATED IN HUMAN PATIENTS AFFECTED BY ACTIVE ULCERATIVE COLITIS OR CROHN'S DISEASE -

Patients with UC and CD were divided into two groups, with low and high disease activity based on clinical score. In patients with high UC and CD activity, we found VEGF-A levels in serum higher as compared to low activity individuals (**Figure 32A and D**). This increased VEGF concentration in serum correlates positively with clinical activity of UC and CD. We also observed altered levels of MT1-MMP substrates, TSP1 and NID1 in serum from patients with active UC and CD thus can indicate the origin of these soluble forms from the inflamed intestine. VEGF produced excessively by intestinal epithelium may induce loosening of endothelial tight junction and in consequence vessel leakage and passage of intestinal fluid to the bloodstream. Nevertheless, in contrast to previously observed in mouse colitis model, we observed increased TSP1 (**Figure 32B and E**) and NID1 (**Figure 32C and F**) levels in conditions with low disease activity compared to high activity.

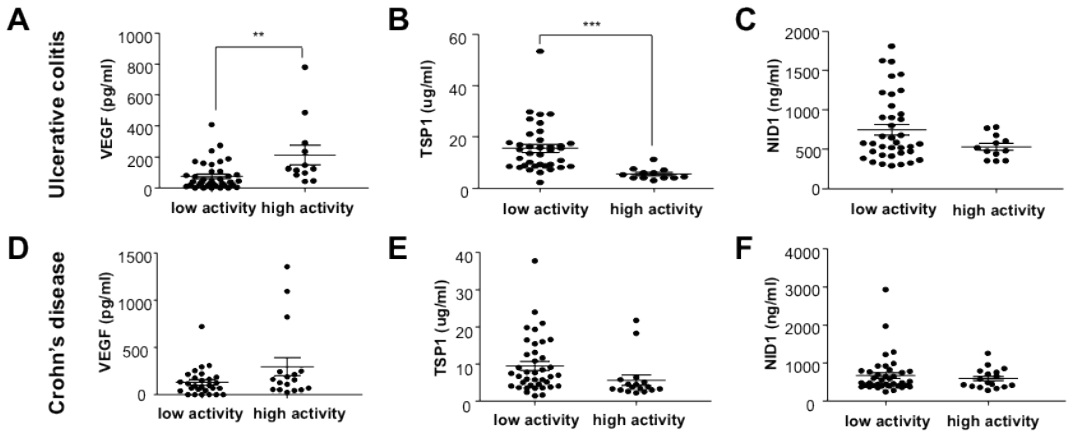

Figure 32. Levels of TSP1 and NID1 in serum from patients with ulcerative colitis (UC) or Crohn's disease (CD). Samples of serum from patients suffering ulcerative colitis or Crohn's disease were analysed by ELISA and we observed increased levels of soluble TSP1 and NID1 in low active compared to high active disease. VEGF was found elevated in patients with highly active IBD.

The feasible mechanism for these findings is that the most active TSP1 and NID1 processing takes place during first steps of sprouting angiogenesis, but it is not so striking during followed vessels maturation and stability as it occurs in advanced disease progression. That would concur with some clinical studies, which showed that decrease in TSP1 expression in human colorectal carcinomas (Maeda et al. 2001; Miao et al. 2001). The function of TSP1 is still controversial. Treatment with DSS induced a more severe colitis in TSP1-/- mice (Punekar et al. 2008) and treatment with its mimetic peptide ABT-510 was

showed to be protective against colon cancer angiogenesis (Allegrini et al. 2004; Punekar et al. 2008). The TSP1 ability to bind integrins may additionally impact new vessel formation. Danese and coll. showed that blokage of the murine endothelial αvβ3 by ATN161 effectively decreases both inflammation and angiogenesis in model of IL-10-/- colitis mice (Danese et al. 2005). In conclusion, TSP1 seems to play an important pathological function in inflammation and angiogenesis acting by multiple pathways. The study of signalling mechanisms may be useful to elucidate the impact of TSP1 and therapeutic strategies for pathological angiogenesis.

Little is known about the implication of NID1 in IBD and in inflammatory-angiogenesis disorders in general. We can speculate that since NID1 is among others responsible for basement membrane stability, its role in IBD confine to a microenvironment factor that controls endothelial barrier function.

Dysfunctional immune response is known to be causative factor in IBD and experimental colitis as well as other chronic inflammatory diseases. During inflammation activated cell signalling leads to increased expression of cytokines, MMPs and adhesion molecules on the endothelium surface what facilitates blood vessel extravasation and leukocyte recruitment to the inflammation site. Once on the tissue they release a range of inflammation and angiogenic mediators initiating chronic inflammation and activating endothelium to sprouting angiogenesis.

We proposed a cell model system that applies *in vivo* during inflammatory angiogenic disorders such as IBD, in which protease MT1-MMP activated by inflammatory stimulus TNF a is actively processing several pericellular substrates and thus impacting early angiogenic responses related to new vessel formation (**Figure 33**). Profiling of these MT1-MMP-processed substrates in plasma could be used as a surrogate marker of angiogenic activity in chronic inflammatory disorders and identifying patients who might benefit from antiangiogenic therapies.

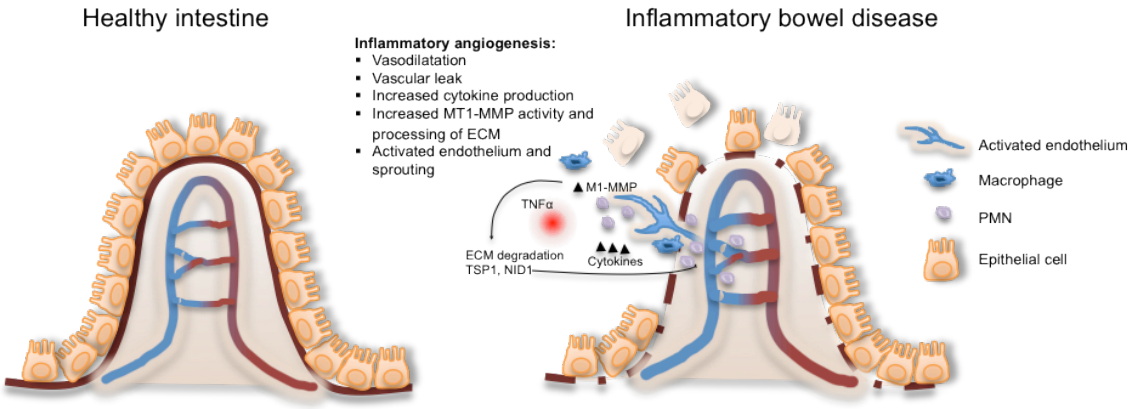

Figure 33. Schematic illustration of healthy and IBD-affected intestinal tissue. Inflammation triggers a change in the endothelium of the intestinal vasculature in response to the cytokines, chemokines and growth factors released by immune cells leading to increased angiogenesis. Protease MT1-MMP can promote this process by processing of ECM molecules such as TSP1 and NID1.

- GENERAL DISCUSSION -

Matrix metalloproteases have been collectively quoted as able to degrade all components of extracellular matrix and thus being main enzymes responsible for matrix and basement membrane remodeling, supporting cell migration, inflammation, tumor progression and neovascularization.

Persistent and aberrant angiogenesis is a hallmark of chronic inflammatory disorders such as psoriasis, rheumatoid arthritis, atherosclerosis or inflammatory bowel disease, thus it has been proposed as a therapeutic target for these conditions and MT1-MMP was found upregulated in several animal and human disorders.

Over 70 pharmaceutical companies were involved in large MMP inhibitor programs that reached phase III clinical trials. However, most of them failed to show their therapeutic benefits due to negative side effects, and unexpected advantage in cancer metastasis (Coussens et al. 2002). This was further supported by report on MMP-8 knockout mice which contrary to other MMP-deficient animals strongly increased the evidence of skin tumors (Balbín et al. 2003). This suggests more complex roles of MMPs in angiogenesis and need to develop more advanced tools to define better their implication in particular cell-dependent processes.

We have established a valid cell model system for studying the mechanistic link between proteolysis and biological responses in the context of inflammation-activated ECs. SILAC-based proteomics identified the supernatant glycoproteome as the main protein set targeted by the protease MT1-MMP. Combination of SILAC with bioinformatics revealed

that the main contribution of MT1-MMP to inflammatory angiogenesis is a combinatorial processing of defined substrates impacting early and rapid responses such as motility, chemotaxis and adhesion finally leading to new vessel formation. This model can be applied to animal and human disorders, thus profiling of MT1-MMP-processed substrates in plasma could be used as a surrogate marker of angiogenic activity in chronic inflammatory disease such as rheumatoid arthritis, inflammatory bowel disease, psoriasis and atherosclerosis, potentially identifying patients who might benefit of anti-angiogenic therapies.

Table 7. List of all supernatant proteins identified by SILAC and LC-MS/MS analysis in WT and MT1-MMP-deficient endothelial cells.

Accession	Protein	H/L	#Cmpds	# quant	SD (H/L)	% CV
ITPR1_MOUSE	Inositol 1,4,5-trisphosphate receptor type 1 OS=Mus musculus GN=Itpr1 PE=1 SV=1	**18.04**	8	2	9.68	53.66
KLRA4_MOUSE	Killer cell lectin-like receptor 4 OS=Mus musculus GN=Klra4 PE=2 SV=2	**14.90**	1	1	0.00	0.00
KPBB_MOUSE	Phosphorylase b kinase regulatory subunit beta OS=Mus musculus GN=Phkb PE=1 SV=1	**11.58**	1	1	0.00	0.00
TSP2_MOUSE	Thrombospondin-2 OS=Mus musculus GN=Thbs2 PE=2 SV=1	**8.68**	9	8	2.73	31.49
PRGR_MOUSE	Progesterone receptor OS=Mus musculus GN=Pgr PE=2 SV=1	**7.42**	2	1	0.00	0.00
PRPK_MOUSE	TP53-regulating kinase OS=Mus musculus GN=Tp53rk PE=2 SV=1	**7.32**	1	1	0.00	0.00
SNED1_MOUSE	Sushi, nidogen and EGF-like domain-containing protein 1 OS=Mus musculus GN=Sned1 PE=2 SV=2	**7.05**	1	1	0.00	0.00
CPXM1_MOUSE	Probable carboxypeptidase X1 OS=Mus musculus GN=Cpxm1 PE=2 SV=1	**6.12**	5	5	1.46	23.83
MMP3_MOUSE	Stromelysin-1 OS=Mus musculus GN=Mmp3 PE=2 SV=2	**6.04**	42	13	2.18	36.08
CDYL_MOUSE	Chromodomain Y-like protein OS=Mus musculus GN=Cdyl PE=1 SV=1	**6.02**	1	1	0.00	0.00
IGS10_MOUSE	Immunoglobulin superfamily member 10 OS=Mus musculus GN=Igsf10 PE=2 SV=2	**5.85**	3	3	1.09	18.55
LYOX_MOUSE	Protein-lysine 6-oxidase OS=Mus musculus GN=Lox PE=2 SV=1	**5.68**	1	1	0.00	0.00
PCOC1_MOUSE	Procollagen C-endopeptidase enhancer 1 OS=Mus musculus GN=Pcolce PE=1 SV=2	**5.53**	2	2	1.80	32.61
TRPM2_MOUSE	Transient receptor potential cation channel subfamily M member 2 OS=Mus musculus GN=Trpm2 PE=2 SV=1	**5.33**	1	1	0.00	0.00
EGFR_MOUSE	Epidermal growth factor receptor OS=Mus musculus GN=Egfr PE=1 SV=1	**4.60**	1	1	0.00	0.00
SODE_MOUSE	Extracellular superoxide dismutase [Cu-Zn] OS=Mus musculus GN=Sod3 PE=1 SV=1	**4.37**	1	1	0.00	0.00
PTX3_MOUSE	Pentraxin-related protein PTX3 OS=Mus musculus GN=Ptx3 PE=1 SV=2	**4.20**	8	6	0.56	13.33
SPA3N_MOUSE	Serine protease inhibitor A3N OS=Mus musculus GN=Serpina3n PE=1 SV=1	**4.19**	4	4	0.58	13.74
PR2C2_MOUSE	Prolactin-2C2 OS=Mus musculus GN=Prl2c2 PE=2 SV=1	**4.14**	1	1	0.00	0.00
IC1_MOUSE	Plasma protease C1 inhibitor OS=Mus musculus GN=Serping1 PE=1 SV=2	**3.70**	21	12	1.26	34.01
CNTN1_MOUSE	Contactin-1 OS=Mus musculus GN=Cntn1 PE=1 SV=1	**3.67**	1	1	0.00	0.00
CLCN5_MOUSE	Chloride channel protein 5 OS=Mus musculus GN=Clcn5 PE=2 SV=1	**3.61**	10	2	0.31	8.45
STC1_MOUSE	Stanniocalcin-1 OS=Mus musculus GN=Stc1 PE=2 SV=1	**3.59**	1	1	0.00	0.00
SFRP1_MOUSE	Secreted frizzled-related protein 1 OS=Mus musculus GN=Sfrp1 PE=1 SV=2	**3.34**	1	1	0.00	0.00
TIMP1_MOUSE	Metalloproteinase inhibitor 1 OS=Mus musculus GN=Timp1 PE=2 SV=2	**3.14**	3	3	0.17	5.29
SEM3C_MOUSE	Semaphorin-3C OS=Mus musculus GN=Sema3c PE=2 SV=1	**2.94**	8	5	0.57	19.23
CO6A1_MOUSE	Collagen alpha-1(VI) chain OS=Mus musculus GN=Col6a1 PE=2 SV=1	**2.88**	3	3	0.71	24.82
FBN1_MOUSE	Fibrillin-1 OS=Mus musculus GN=Fbn1 PE=1 SV=1	**2.76**	5	4	0.81	29.35
SLIT3_MOUSE	Slit homolog 3 protein OS=Mus musculus GN=Slit3 PE=2 SV=1	**2.51**	4	4	0.49	19.40
LIF_MOUSE	Leukemia inhibitory factor OS=Mus musculus GN=Lif PE=1 SV=1	**2.37**	1	1	0.00	0.00
CERU_MOUSE	Ceruloplasmin OS=Mus musculus GN=Cp PE=1 SV=2	**2.29**	11	9	0.45	19.58
NID1_MOUSE	Nidogen-1 OS=Mus musculus GN=Nid1 PE=1 SV=1	**2.26**	189	56	0.34	15.06
NGAL_MOUSE	Neutrophil gelatinase-associated lipocalin OS=Mus musculus GN=Lcn2 PE=1 SV=1	**2.11**	5	3	0.12	5.79
MMP19_MOUSE	Matrix metalloproteinase-19 OS=Mus musculus GN=Mmp19 PE=2 SV=1	**2.10**	1	1	0.00	0.00

Accession	Protein	H/L	#Cmpds	# quant	SD (H/L)	% CV
GSTP1_MOUSE	Glutathione S-transferase P 1 OS=Mus musculus GN=Gstp1 PE=1 SV=2	**1.95**	1	1	0.00	0.00
GDN_MOUSE	Glia-derived nexin OS=Mus musculus GN=Serpine2 PE=2 SV=2	**1.93**	3	3	0.38	19.52
CCL2_MOUSE	C-C motif chemokine 2 OS=Mus musculus GN=Ccl2 PE=1 SV=1	**1.86**	99	15	0.63	33.88
TIMP3_MOUSE	Metalloproteinase inhibitor 3 OS=Mus musculus GN=Timp3 PE=2 SV=1	**1.80**	2	2	0.32	17.84
AEBP1_MOUSE	Adipocyte enhancer-binding protein 1 OS=Mus musculus GN=Aebp1 PE=1 SV=1	**1.77**	16	8	0.59	33.34
LOXL3_MOUSE	Lysyl oxidase homolog 3 OS=Mus musculus GN=Loxl3 PE=2 SV=1	**1.73**	1	1	0.00	0.00
SLIT2_MOUSE	Slit homolog 2 protein OS=Mus musculus GN=Slit2 PE=2 SV=1	**1.73**	3	3	0.38	21.94
TSP1_MOUSE	Thrombospondin-1 OS=Mus musculus GN=Thbs1 PE=1 SV=1	**1.68**	227	52	0.66	39.44
CYR61_MOUSE	Protein CYR61 OS=Mus musculus GN=Cyr61 PE=1 SV=1	**1.68**	4	2	0.27	15.93
CO3A1_MOUSE	Collagen alpha-1(III) chain OS=Mus musculus GN=Col3a1 PE=2 SV=4	**1.67**	1	1	0.00	0.00
TIMP2_MOUSE	Metalloproteinase inhibitor 2 OS=Mus musculus GN=Timp2 PE=1 SV=2	**1.67**	5	4	0.22	13.44
CATL1_MOUSE	Cathepsin L1 OS=Mus musculus GN=Ctsl1 PE=1 SV=2	**1.43**	1	1	0.00	0.00
WWC2_MOUSE	Protein WWC2 OS=Mus musculus GN=Wwc2 PE=2 SV=1	**1.42**	1	1	0.00	0.00
QSOX1_MOUSE	Sulfhydryl oxidase 1 OS=Mus musculus GN=Qsox1 PE=2 SV=1	**1.31**	2	2	0.51	38.64
LG3BP_MOUSE	Galectin-3-binding protein OS=Mus musculus GN=Lgals3bp PE=1 SV=1	**1.31**	10	8	0.46	35.26
PNPH_MOUSE	Purine nucleoside phosphorylase OS=Mus musculus GN=Np PE=1 SV=2	**1.30**	2	2	0.11	8.57
FSTL1_MOUSE	Follistatin-related protein 1 OS=Mus musculus GN=Fstl1 PE=1 SV=1	**1.30**	26	10	0.60	46.14
B4GT1_MOUSE	Beta-1,4-galactosyltransferase 1 OS=Mus musculus GN=B4galt1 PE=2 SV=1	**1.28**	1	1	0.00	0.00
ASPG_MOUSE	N(4)-(beta-N-acetylglucosaminyl)-L-asparaginase OS=Mus musculus GN=Aga PE=2 SV=1	**1.27**	1	1	0.00	0.00
CO4A1_MOUSE	Collagen alpha-1(IV) chain OS=Mus musculus GN=Col4a1 PE=2 SV=4	**1.27**	1	1	0.00	0.00
TPA_MOUSE	Tissue-type plasminogen activator OS=Mus musculus GN=Plat PE=1 SV=3	**1.25**	1	1	0.00	0.00
HGFA_MOUSE	Hepatocyte growth factor activator OS=Mus musculus GN=Hgfac PE=1 SV=1	**1.22**	2	1	0.00	0.00
FBLN3_MOUSE	EGF-containing fibulin-like extracellular matrix protein 1 OS=Mus musculus GN=Efemp1 PE=2 SV=1	**1.21**	10	4	0.42	34.72
BMP1_MOUSE	Bone morphogenetic protein 1 OS=Mus musculus GN=Bmp1 PE=2 SV=1	**1.15**	4	3	0.18	16.01
SEM3F_MOUSE	Semaphorin-3F OS=Mus musculus GN=Sema3f PE=2 SV=1	**1.12**	1	1	0.00	0.00
SERPH_MOUSE	Serpin H1 OS=Mus musculus GN=Serpinh1 PE=1 SV=2	**1.09**	2	2	0.16	15.07
LUM_MOUSE	Lumican OS=Mus musculus GN=Lum PE=1 SV=2	**1.04**	2	2	0.22	20.86
AGRIN_MOUSE	Agrin OS=Mus musculus GN=Agrn PE=2 SV=1	**1.00**	2	1	0.00	0.00
SAP_MOUSE	Sulfated glycoprotein 1 OS=Mus musculus GN=Psap PE=1 SV=2	**0.99**	5	3	0.12	12.27
LTBP2_MOUSE	Latent-transforming growth factor beta-binding protein 2 OS=Mus musculus GN=Ltbp2 PE=1 SV=2	**0.99**	8	7	0.25	24.89
CADH5_MOUSE	Cadherin-5 OS=Mus musculus GN=Cdh5 PE=2 SV=2	**0.95**	9	6	0.21	22.43
EF2_MOUSE	Elongation factor 2 OS=Mus musculus GN=Eef2 PE=1 SV=2	**0.92**	1	1	0.00	0.00
LAMC1_MOUSE	Laminin subunit gamma-1 OS=Mus musculus GN=Lamc1 PE=1 SV=2	**0.89**	13	7	0.27	30.42
EMIL1_MOUSE	EMILIN-1 OS=Mus musculus GN=Emilin1 PE=1 SV=1	**0.88**	1	1	0.00	0.00
CATB_MOUSE	Cathepsin B OS=Mus musculus GN=Ctsb PE=1 SV=2	**0.86**	1	1	0.00	0.00
LAMB1_MOUSE	Laminin subunit beta-1 OS=Mus musculus GN=Lamb1-1 PE=1 SV=2	**0.85**	18	8	0.34	40.44
PEBP1_MOUSE	Phosphatidylethanolamine-binding protein 1 OS=Mus musculus GN=Pebp1 PE=1 SV=3	**0.84**	3	3	0.17	19.56
ECM1_MOUSE	Extracellular matrix protein 1 OS=Mus musculus GN=Ecm1 PE=1 SV=1	**0.83**	2	2	0.12	14.29
PGBM_MOUSE	Basement membrane-specific heparan sulfate proteoglycan core protein OS=Mus musculus GN=Hspg2PE=1SV=1	**0.83**	17	15	0.28	33.34
PGS1_MOUSE	Biglycan OS=Mus musculus GN=Bgn PE=2 SV=1	**0.83**	16	8	0.38	45.91
LOXL2_MOUSE	Lysyl oxidase homolog 2 OS=Mus musculus GN=Loxl2 PE=2 SV=2	**0.83**	2	2	0.01	0.90

Accession	Protein	H/L	#Cmpds	# quant	SD (H/L)	% CV
FBLN5_MOUSE	Fibulin-5 OS=Mus musculus GN=Fbln5 PE=2 SV=1	**0.79**	1	1	0.00	0.00
WDR19_MOUSE	WD repeat-containing protein 19 OS=Mus musculus GN=Wdr19 PE=2 SV=1	**0.77**	2	2	0.00	0.00
CLUS_MOUSE	Clusterin OS=Mus musculus GN=Clu PE=1 SV=1	**0.77**	34	16	0.17	22.11
CFAH_MOUSE	Complement factor H OS=Mus musculus GN=Cfh PE=1 SV=1	**0.74**	15	12	0.15	20.33
PGS2_MOUSE	Decorin OS=Mus musculus GN=Dcn PE=2 SV=1	**0.74**	62	22	0.21	28.73
FINC_MOUSE	Fibronectin OS=Mus musculus GN=Fn1 PE=1 SV=3	**0.73**	405	106	0.34	47.50
LAMA4_MOUSE	Laminin subunit alpha-4 OS=Mus musculus GN=Lama4 PE=1 SV=2	**0.72**	21	10	0.33	46.38
ESTD_MOUSE	S-formylglutathione hydrolase OS=Mus musculus GN=Esd PE=2 SV=1	**0.72**	1	1	0.00	0.00
HS90B_MOUSE	Heat shock protein HSP 90-beta OS=Mus musculus GN=Hsp90ab1 PE=1 SV=2	**0.70**	3	3	0.03	4.60
PGAM1_MOUSE	Phosphoglycerate mutase 1 OS=Mus musculus GN=Pgam1 PE=1 SV=3	**0.68**	5	4	0.36	53.10
ATS1_MOUSE	A disintegrin and metalloproteinase with thrombospondin motifs 1 OS=Mus musculus GN=Adamts1 PE=1 SV=3	**0.67**	1	1	0.00	0.00
CCD80_MOUSE	Coiled-coil domain-containing protein 80 OS=Mus musculus GN=Ccdc80 PE=1 SV=2	**0.67**	10	7	0.35	52.40
VCAM1_MOUSE	Vascular cell adhesion protein 1 OS=Mus musculus GN=Vcam1 PE=1 SV=1	**0.66**	2	2	0.31	46.07
A4_MOUSE	Amyloid beta A4 protein OS=Mus musculus GN=App PE=1 SV=3	**0.66**	2	2	0.05	7.87
K2C4_MOUSE	Keratin, type II cytoskeletal 4 OS=Mus musculus GN=Krt4 PE=1 SV=2	**0.66**	1	1	0.00	0.00
ANGP2_MOUSE	Angiopoietin-2 OS=Mus musculus GN=Angpt2 PE=2 SV=2	**0.64**	36	14	0.35	54.74
HA11_MOUSE	H-2 class I histocompatibility antigen, D-B alpha chain OS=Mus musculus GN=H2-D1 PE=1 SV=2	**0.63**	21	7	0.33	52.97
ICAM1_MOUSE	Intercellular adhesion molecule 1 OS=Mus musculus GN=Icam1 PE=1 SV=1	**0.60**	4	2	0.11	18.52
ACTS_MOUSE	Actin, alpha skeletal muscle OS=Mus musculus GN=Acta1 PE=1 SV=1	**0.60**	8	6	0.09	14.85
CXL16_MOUSE	C-X-C motif chemokine 16 OS=Mus musculus GN=Cxcl16 PE=1 SV=2	**0.60**	2	2	0.19	32.50
FSCN1_MOUSE	Fascin OS=Mus musculus GN=Fscn1 PE=1 SV=4	**0.60**	1	1	0.00	0.00
MA2B1_MOUSE	Lysosomal alpha-mannosidase OS=Mus musculus GN=Man2b1 PE=2 SV=3	**0.60**	1	1	0.00	0.00
UBR4_MOUSE	E3 ubiquitin-protein ligase UBR4 OS=Mus musculus GN=Ubr4 PE=1 SV=1	**0.58**	1	1	0.00	0.00
G6PI_MOUSE	Glucose-6-phosphate isomerase OS=Mus musculus GN=Gpi PE=1 SV=4	**0.56**	3	3	0.22	39.27
ACMSD_MOUSE	2-amino-3-carboxymuconate-6-semialdehyde decarboxylase OS=Mus musculus GN=Acmsd PE=1 SV=2	**0.55**	1	1	0.00	0.00
ACTB_MOUSE	Actin, cytoplasmic 1 OS=Mus musculus GN=Actb PE=1 SV=1	**0.55**	17	11	0.11	19.63
PXDN_MOUSE	Peroxidasin homolog OS=Mus musculus GN=Pxdn PE=2 SV=1	**0.55**	25	14	0.27	49.27
CO4A2_MOUSE	Collagen alpha-2(IV) chain OS=Mus musculus GN=Col4a2 PE=2 SV=4	**0.54**	18	10	0.33	60.02
PRDX1_MOUSE	Peroxiredoxin-1 OS=Mus musculus GN=Prdx1 PE=1 SV=1	**0.54**	14	10	0.24	43.94
CLH_MOUSE	Clathrin heavy chain 1 OS=Mus musculus GN=Cltc PE=1 SV=3	**0.51**	2	2	0.08	15.94
CD018_MOUSE	Uncharacterized protein C4orf18 homolog OS=Mus musculus PE=2 SV=1	**0.51**	2	2	0.00	0.00
CHSS1_MOUSE	Chondroitin sulfate synthase 1 OS=Mus musculus GN=Chsy1 PE=2 SV=2	**0.49**	1	1	0.00	0.00
SPRC_MOUSE	SPARC OS=Mus musculus GN=Sparc PE=1 SV=1	**0.49**	11	7	0.20	40.81
MANBA_MOUSE	Beta-mannosidase OS=Mus musculus GN=Manba PE=2 SV=1	**0.48**	4	4	0.19	39.43
RHOA_MOUSE	Transforming protein RhoA OS=Mus musculus GN=Rhoa PE=1 SV=1	**0.48**	1	1	0.00	0.00
MUC18_MOUSE	Cell surface glycoprotein MUC18 OS=Mus musculus GN=Mcam PE=2 SV=1	**0.41**	2	2	0.13	30.91
FAM3C_MOUSE	Protein FAM3C OS=Mus musculus GN=Fam3c PE=1 SV=1	**0.39**	1	1	0.00	0.00
MMRN2_MOUSE	Multimerin-2 OS=Mus musculus GN=Mmrn2 PE=2 SV=1	**0.37**	1	1	0.00	0.00
HA1Q_MOUSE	H-2 class I histocompatibility antigen, K-Q alpha chain (Fragment) OS=Mus musculus GN=H2-K1 PE=2 SV=1	**0.37**	16	4	0.05	14.11
PGK1_MOUSE	Phosphoglycerate kinase 1 OS=Mus musculus GN=Pgk1 PE=1 SV=4	**0.37**	4	2	0.08	22.45
TBA1A_MOUSE	Tubulin alpha-1A chain OS=Mus musculus GN=Tuba1a PE=1 SV=1	**0.35**	2	2	0.16	44.68

Accession	Protein	H/L	#Cmpds	# quant	SD (H/L)	% CV
TLL1_MOUSE	Tolloid-like protein 1 OS=Mus musculus GN=Tll1 PE=1 SV=1	**0.34**	3	3	0.12	36.03
CTGF_MOUSE	Connective tissue growth factor OS=Mus musculus GN=Ctgf PE=2 SV=2	**0.34**	2	2	0.05	15.56
COIA1_MOUSE	Collagen alpha-1(XVIII) chain OS=Mus musculus GN=Col18a1 PE=1 SV=4	**0.34**	12	8	0.17	48.47
PAI1_MOUSE	Plasminogen activator inhibitor 1 OS=Mus musculus GN=Serpine1 PE=1 SV=1	**0.34**	29	12	0.11	33.95
LAMP1_MOUSE	Lysosome-associated membrane glycoprotein 1 OS=Mus musculus GN=Lamp1 PE=1 SV=2	**0.31**	1	1	0.00	0.00
CCL2_MOUSE_L	C-C motif chemokine 2 OS=Mus musculus GN=Ccl2 PE=1 SV=1	**0.31**	24	5	0.03	11.13
CAD13_MOUSE	Cadherin-13 OS=Mus musculus GN=Cdh13 PE=2 SV=1	**0.29**	8	4	0.12	39.28
GDIB_MOUSE	Rab GDP dissociation inhibitor beta OS=Mus musculus GN=Gdi2 PE=1 SV=1	**0.28**	1	1	0.00	0.00
CAPZB_MOUSE	F-actin-capping protein subunit beta OS=Mus musculus GN=Capzb PE=1 SV=3	**0.27**	2	2	0.07	27.78
CBPE_MOUSE	Carboxypeptidase E OS=Mus musculus GN=Cpe PE=1 SV=2	**0.27**	4	2	0.00	0.00
COEA1_MOUSE	Collagen alpha-1(XIV) chain OS=Mus musculus GN=Col14a1 PE=2 SV=2	**0.27**	1	1	0.00	0.00
K2C73_MOUSE	Keratin, type II cytoskeletal 73 OS=Mus musculus GN=Krt73 PE=1 SV=1	**0.27**	10	1	0.00	0.00
PLGF_MOUSE	Placenta growth factor OS=Mus musculus GN=Pgf PE=1 SV=1	**0.25**	4	2	0.13	51.52
C1QR1_MOUSE	Complement component C1q receptor OS=Mus musculus GN=Cd93 PE=1 SV=1	**0.24**	1	1	0.00	0.00
MOES_MOUSE	Moesin OS=Mus musculus GN=Msn PE=1 SV=3	**0.24**	1	1	0.00	0.00
ELMO1_MOUSE	Engulfment and cell motility protein 1 OS=Mus musculus GN=Elmo1 PE=1 SV=2	**0.23**	81	3	0.08	34.70
PDGFB_MOUSE	Platelet-derived growth factor subunit B OS=Mus musculus GN=Pdgfb PE=2 SV=1	**0.23**	8	4	0.13	54.84
SP3_MOUSE	Transcription factor Sp3 OS=Mus musculus GN=Sp3 PE=2 SV=2	**0.23**	84	6	0.10	44.78
A2MP_MOUSE	Alpha-2-macroglobulin-P OS=Mus musculus GN=A2mp PE=2 SV=1	**0.23**	19	5	0.05	23.32
P5I13_MOUSE	Tumor protein p53-inducible protein 13 OS=Mus musculus GN=Tp53i13 PE=3 SV=1	**0.21**	6	3	0.04	16.44
K2C74_MOUSE	Keratin, type II cytoskeletal 74 OS=Mus musculus GN=Krt74 PE=2 SV=1	**0.20**	91	10	0.09	43.73
CTHR1_MOUSE	Collagen triple helix repeat-containing protein 1 OS=Mus musculus GN=Cthrc1 PE=2 SV=1	**0.19**	4	2	0.03	15.38
ITIH2_MOUSE	Inter-alpha-trypsin inhibitor heavy chain H2 OS=Mus musculus GN=Itih2 PE=1 SV=1	**0.19**	4	2	0.03	15.38
IBP3_MOUSE	Insulin-like growth factor-binding protein 3 OS=Mus musculus GN=Igfbp3 PE=2 SV=1	**0.19**	13	5	0.06	34.02
VIME_MOUSE	Vimentin OS=Mus musculus GN=Vim PE=1 SV=3	**0.19**	4	4	0.04	20.00
TGFB2_MOUSE	Transforming growth factor beta-2 OS=Mus musculus GN=Tgfb2 PE=2 SV=1	**0.16**	1	1	0.00	0.00
A2M_MOUSE	Alpha-2-macroglobulin OS=Mus musculus GN=A2m PE=1 SV=2	**0.16**	6	3	0.13	78.20
CTL2A_MOUSE	Protein CTLA-2-alpha OS=Mus musculus GN=Ctla2a PE=2 SV=2	**0.15**	3	3	0.06	37.42
NRCAM_MOUSE	Neuronal cell adhesion molecule OS=Mus musculus GN=Nrcam PE=1 SV=2	**0.15**	1	1	0.00	0.00
LYVE1_MOUSE	Lymphatic vessel endothelial hyaluronic acid receptor 1 OS=Mus musculus GN=Lyve1 PE=1 SV=1	**0.14**	12	5	0.04	28.41
RAB3A_MOUSE	Ras-related protein Rab-3A OS=Mus musculus GN=Rab3a PE=1 SV=1	**0.13**	2	2	0.01	11.11
EPCR_MOUSE	Endothelial protein C receptor OS=Mus musculus GN=Procr PE=2 SV=2	**0.13**	5	3	0.01	5.44
TLR3_MOUSE	Toll-like receptor 3 OS=Mus musculus GN=Tlr3 PE=1 SV=2	**0.07**	4	2	0.03	40.00
SOX14_MOUSE	Transcription factor SOX-14 OS=Mus musculus GN=Sox14 PE=2 SV=2	**0.06**	4	2	0.00	0.00
HIF1A_MOUSE	Hypoxia-inducible factor 1 alpha OS=Mus musculus GN=Hif1a PE=1 SV=3	**0.06**	1	1	0.00	0.00
ATRIP_MOUSE	ATR-interacting protein OS=Mus musculus GN=Atrip PE=2 SV=1	**0.04**	4	2	0.01	20.00

Table 8. List of all microsomal proteins identified by SILAC and LC-MS/MS analysis in WT and MT1-MMP-deficient endothelial cells.

Accession	Protein	H/L	#Cmpds	# quant	SD (H/L)	% CV
ARH_MOUSE	Low density lipoprotein receptor adapter protein 1 OS=Mus musculus GN=Ldlrap1 PE=1 SV=2	**93.66**	1	1	0.00	0.00
DNAI1_MOUSE	Dynein intermediate chain 1, axonemal OS=Mus musculus GN=Dnai1 PE=2 SV=1	**29.05**	4	2	8.47	29.16
AIDA_MOUSE	Axin interactor, dorsalization associated protein OS=Mus musculus GN=Aida PE=1 SV=1	**24.36**	1	1	0.00	0.00
ERCC3_MOUSE	TFIIH basal transcription factor complex helicase XPB subunit OS=Mus musculus GN=Ercc3 PE=2 SV=1	**22.63**	1	1	0.00	0.00
ECHM_MOUSE	Enoyl-CoA hydratase, mitochondrial OS=Mus musculus GN=Echs1 PE=1 SV=1	**18.76**	1	1	0.00	0.00
PR15B_MOUSE	Protein phosphatase 1 regulatory subunit 15B OS=Mus musculus GN=Ppp1r15b PE=1 SV=1	**15.88**	1	1	0.00	0.00
UBP36_MOUSE	Ubiquitin carboxyl-terminal hydrolase 36 OS=Mus musculus GN=Usp36 PE=2 SV=1	**15.88**	3	2	6.96	43.81
SOS2_MOUSE	Son of sevenless homolog 2 OS=Mus musculus GN=Sos2 PE=1 SV=2	**13.80**	2	2	8.47	61.36
RRP44_MOUSE	Exosome complex exonuclease RRP44 OS=Mus musculus GN=Dis3 PE=2 SV=4	**13.16**	1	1	0.00	0.00
ZMAT1_MOUSE	Zinc finger matrin-type protein 1 OS=Mus musculus GN=Zmat1 PE=2 SV=2	**13.14**	1	1	0.00	0.00
K1219_MOUSE	Protein KIAA1219 OS=Mus musculus GN=Kiaa1219 PE=1 SV=2	**12.37**	1	1	0.00	0.00
CTDSL_MOUSE	CTD small phosphatase-like protein OS=Mus musculus GN=Ctdspl PE=2 SV=2	**10.16**	2	1	0.00	0.00
PPID_MOUSE	40 kDa peptidyl-prolyl cis-trans isomerase OS=Mus musculus GN=Ppid PE=1 SV=3	**9.71**	1	1	0.00	0.00
RPGR1_MOUSE	X-linked retinitis pigmentosa GTPase regulator-interacting protein 1 OS=Mus musculus GN=Rpgrip1 PE=1 SV=1	**9.24**	1	1	0.00	0.00
SGPP1_MOUSE	Sphingosine-1-phosphate phosphatase 1 OS=Mus musculus GN=Sgpp1 PE=1 SV=1	**8.79**	1	1	0.00	0.00
F164A_MOUSE	UPF0418 protein FAM164A OS=Mus musculus GN=Fam164a PE=2 SV=1	**8.54**	2	2	7.48	87.61
CP110_MOUSE	Centriolin OS=Mus musculus GN=Cep110 PE=1 SV=2	**8.05**	1	1	0.00	0.00
STXB2_MOUSE	Syntaxin-binding protein 2 OS=Mus musculus GN=Stxbp2 PE=2 SV=1	**7.85**	1	1	0.00	0.00
IF2B3_MOUSE	Insulin-like growth factor 2 mRNA-binding protein 3 OS=Mus musculus GN=Igf2bp3 PE=1 SV=1	**7.64**	2	1	0.00	0.00
SDPR_MOUSE	Serum deprivation-response protein OS=Mus musculus GN=Sdpr PE=1 SV=3	**7.27**	1	1	0.00	0.00
DHRS7_MOUSE	Dehydrogenase/reductase SDR family member 7 OS=Mus musculus GN=Dhrs7 PE=2 SV=2	**7.24**	2	2	6.15	84.98
REEP5_MOUSE	Receptor expression-enhancing protein 5 OS=Mus musculus GN=Reep5 PE=1 SV=1	**6.38**	1	1	0.00	0.00
BT3L4_MOUSE	Transcription factor BTF3 homolog 4 OS=Mus musculus GN=Btf3l4 PE=2 SV=1	**6.35**	1	1	0.00	0.00
GCP60_MOUSE	Golgi resident protein GCP60 OS=Mus musculus GN=Acbd3 PE=1 SV=3	**6.29**	2	2	5.47	86.97
CLD23_MOUSE	Claudin-23 OS=Mus musculus GN=Cldn23 PE=2 SV=1	**6.09**	1	1	0.00	0.00
H4_MOUSE	Histone H4 OS=Mus musculus GN=Hist1h4a PE=1 SV=2	**5.67**	11	5	5.22	92.11
P66B_MOUSE	Transcriptional repressor p66-beta OS=Mus musculus GN=Gatad2b PE=1 SV=1	**5.44**	1	1	0.00	0.00
SYIC_MOUSE	Isoleucyl-tRNA synthetase, cytoplasmic OS=Mus musculus GN=Iars PE=2 SV=1	**5.38**	6	4	5.67	105.42
GSK3B_MOUSE	Glycogen synthase kinase-3 beta OS=Mus musculus GN=Gsk3b PE=1 SV=2	**5.24**	1	1	0.00	0.00
CTU1_MOUSE	Cytoplasmic tRNA 2-thiolation protein 1 OS=Mus musculus GN=Atpbd3 PE=2 SV=1	**4.99**	1	1	0.00	0.00
FAT3_MOUSE	Protocadherin Fat 3 OS=Mus musculus GN=Fat3 PE=1 SV=2	**4.98**	1	1	0.00	0.00
AB48R_MOUSE	Apolipoprotein B-100 receptor OS=Mus musculus GN=Apob48r PE=2 SV=1	**4.96**	1	1	0.00	0.00
LCA5_MOUSE	Lebercilin OS=Mus musculus GN=Lca5 PE=2 SV=1	**4.89**	2	2	4.28	87.50
NARG1_MOUSE	NMDA receptor-regulated protein 1 OS=Mus musculus GN=Narg1 PE=1 SV=1	**4.87**	2	2	2.03	41.59
TMED9_MOUSE	Transmembrane emp24 domain-containing protein 9 OS=Mus musculus GN=Tmed9 PE=2 SV=2	**4.86**	13	6	6.60	135.79
SYCC_MOUSE	Cysteinyl-tRNA synthetase, cytoplasmic OS=Mus musculus GN=Cars PE=1 SV=2	**4.78**	1	1	0.00	0.00
UACA_MOUSE	Uveal autoantigen with coiled-coil domains and ankyrin repeats OS=Mus musculus GN=Uaca PE=1 SV=2	**4.71**	1	1	0.00	0.00
SPT41_MOUSE	Transcription elongation factor SPT4 1 OS=Mus musculus GN=Supt4h1 PE=2 SV=1	**4.65**	1	1	0.00	0.00

Accession	Protein	H/L	#Cmpds	# quant	SD (H/L)	% CV
GOGA4_MOUSE	Golgin subfamily A member 4 OS=Mus musculus GN=Golga4 PE=1 SV=2	**4.56**	26	6	5.86	128.63
ANGL2_MOUSE	Angiopoietin-related protein 2 OS=Mus musculus GN=Angptl2 PE=2 SV=1	**4.48**	1	1	0.00	0.00
LYSM3_MOUSE	LysM and putative peptidoglycan-binding domain-containing protein 3 OS=Mus musculus GN=Lysmd3 PE=2 SV=1	**4.29**	1	1	0.00	0.00
ATRX_MOUSE	Transcriptional regulator ATRX OS=Mus musculus GN=Atrx PE=1 SV=2	**4.26**	1	1	0.00	0.00
BAG1_MOUSE	BAG family molecular chaperone regulator 1 OS=Mus musculus GN=Bag1 PE=1 SV=3	**4.17**	1	1	0.00	0.00
SCAP_MOUSE	Sterol regulatory element-binding protein cleavage-activating protein OS=Mus musculus GN=Scap PE=1 SV=1	**3.81**	1	1	0.00	0.00
MSPD2_MOUSE	Motile sperm domain-containing protein 2 OS=Mus musculus GN=Mospd2 PE=1 SV=2	**3.78**	1	1	0.00	0.00
SHQ1_MOUSE	Protein SHQ1 homolog OS=Mus musculus GN=Shq1 PE=2 SV=2	**3.75**	1	1	0.00	0.00
ESYT3_MOUSE	Extended synaptotagmin-3 OS=Mus musculus GN=Fam62c PE=2 SV=2	**3.71**	1	1	0.00	0.00
TF2H1_MOUSE	General transcription factor IIH subunit 1 OS=Mus musculus GN=Gtf2h1 PE=2 SV=2	**3.71**	1	1	0.00	0.00
COGA1_MOUSE	Collagen alpha-1(XVI) chain OS=Mus musculus GN=Col16a1 PE=2 SV=2	**3.70**	1	1	0.00	0.00
FA59B_MOUSE	Protein FAM59B OS=Mus musculus GN=Fam59b PE=2 SV=2	**3.70**	1	1	0.00	0.00
ANS4B_MOUSE	Ankyrin repeat and SAM domain-containing protein 4B OS=Mus musculus GN=Anks4b PE=1 SV=1	**3.55**	1	1	0.00	0.00
MCCB_MOUSE	Methylcrotonoyl-CoA carboxylase beta chain, mitochondrial OS=Mus musculus GN=Mccc2 PE=2 SV=1	**3.47**	1	1	0.00	0.00
CAD13_MOUSE	Cadherin-13 OS=Mus musculus GN=Cdh13 PE=2 SV=1	**3.46**	1	1	0.00	0.00
BCORL_MOUSE	BCoR-like protein 1 OS=Mus musculus GN=Bcorl1 PE=2 SV=1	**3.43**	1	1	0.00	0.00
K1C10_MOUSE	Keratin, type I cytoskeletal 10 OS=Mus musculus GN=Krt10 PE=1 SV=3	**3.39**	19	3	2.45	72.29
F16A2_MOUSE	UPF0518 protein FAM160A2 OS=Mus musculus GN=Fam160a2 PE=2 SV=2	**3.35**	1	1	0.00	0.00
EPHA1_MOUSE	Ephrin type-A receptor 1 OS=Mus musculus GN=Epha1 PE=1 SV=2	**3.29**	1	1	0.00	0.00
DNA2L_MOUSE	DNA2-like helicase OS=Mus musculus GN=Dna2 PE=2 SV=2	**3.13**	1	1	0.00	0.00
FBXL2_MOUSE	F-box/LRR-repeat protein 2 OS=Mus musculus GN=Fbxl2 PE=2 SV=1	**3.13**	1	1	0.00	0.00
PSB4_MOUSE	Proteasome subunit beta type-4 OS=Mus musculus GN=Psmb4 PE=1 SV=1	**3.11**	1	1	0.00	0.00
PYC_MOUSE	Pyruvate carboxylase, mitochondrial OS=Mus musculus GN=Pc PE=1 SV=1	**3.05**	1	1	0.00	0.00
RL18_MOUSE	60S ribosomal protein L18 OS=Mus musculus GN=Rpl18 PE=2 SV=3	**2.99**	4	4	3.88	129.58
ENAH_MOUSE	Protein enabled homolog OS=Mus musculus GN=Enah PE=1 SV=2	**2.97**	1	1	0.00	0.00
TSP1_MOUSE	Thrombospondin-1 OS=Mus musculus GN=Thbs1 PE=1 SV=1	**2.85**	1	1	0.00	0.00
CO4A2_MOUSE	Collagen alpha-2(IV) chain OS=Mus musculus GN=Col4a2 PE=2 SV=4	**2.80**	1	1	0.00	0.00
SCAM2_MOUSE	Secretory carrier-associated membrane protein 2 OS=Mus musculus GN=Scamp2 PE=2 SV=1	**2.79**	1	1	0.00	0.00
EPN4_MOUSE	Clathrin interactor 1 OS=Mus musculus GN=Clint1 PE=1 SV=2	**2.55**	2	2	1.74	68.42
NUCB2_MOUSE	Nucleobindin-2 OS=Mus musculus GN=Nucb2 PE=1 SV=2	**2.54**	2	2	1.47	57.77
STIP1_MOUSE	Stress-induced-phosphoprotein 1 OS=Mus musculus GN=Stip1 PE=1 SV=1	**2.52**	1	1	0.00	0.00
FA50B_MOUSE	Protein FAM50B OS=Mus musculus GN=Fam50b PE=2 SV=1	**2.50**	1	1	0.00	0.00
SGIP1_MOUSE	SH3-containing GRB2-like protein 3-interacting protein 1 OS=Mus musculus GN=Sgip1 PE=1 SV=1	**2.50**	1	1	0.00	0.00
C1TC_MOUSE	C-1-tetrahydrofolate synthase, cytoplasmic OS=Mus musculus GN=Mthfd1 PE=1 SV=3	**2.49**	1	1	0.00	0.00
DHRS1_MOUSE	Dehydrogenase/reductase SDR family member 1 OS=Mus musculus GN=Dhrs1 PE=2 SV=1	**2.47**	2	1	0.00	0.00
KIF17_MOUSE	Kinesin-like protein KIF17 OS=Mus musculus GN=Kif17 PE=1 SV=1	**2.44**	1	1	0.00	0.00
NDUV1_MOUSE	NADH dehydrogenase [ubiquinone] flavoprotein 1, mitochondrial OS=Mus musculus GN=Ndufv1 PE=1 SV=1	**2.43**	2	2	1.40	57.67
TMX1_MOUSE	Thioredoxin-related transmembrane protein 1 OS=Mus musculus GN=Tmx1 PE=1 SV=1	**2.43**	1	1	0.00	0.00
PEX14_MOUSE	Peroxisomal membrane protein PEX14 OS=Mus musculus GN=Pex14 PE=1 SV=1	**2.41**	2	2	0.72	29.63
MET10_MOUSE	Putative methyltransferase METT10D OS=Mus musculus GN=Mett10d PE=1 SV=1	**2.41**	1	1	0.00	0.00
RRAS2_MOUSE	Ras-related protein R-Ras2 OS=Mus musculus GN=Rras2 PE=1 SV=1	**2.38**	2	2	0.63	26.65

Accession	Protein	H/L	#Cmpds	# quant	SD (H/L)	% CV
SHIP2_MOUSE	Phosphatidylinositol-3,4,5-trisphosphate 5-phosphatase 2 OS=Mus musculus GN=Inppl1 PE=1 SV=1	**2.37**	1	1	0.00	0.00
SEPT8_MOUSE	Septin-8 OS=Mus musculus GN=Sept8 PE=1 SV=4	**2.37**	2	2	0.97	40.88
WBP2_MOUSE	WW domain-binding protein 2 OS=Mus musculus GN=Wbp2 PE=1 SV=1	**2.37**	2	1	0.00	0.00
PDRG1_MOUSE	p53 and DNA damage-regulated protein 1 OS=Mus musculus GN=Pdrg1 PE=2 SV=1	**2.34**	1	1	0.00	0.00
UBP2L_MOUSE	Ubiquitin-associated protein 2-like OS=Mus musculus GN=Ubap2l PE=1 SV=1	**2.31**	3	2	1.22	52.90
T176A_MOUSE	Transmembrane protein 176A OS=Mus musculus GN=Tmem176a PE=2 SV=2	**2.29**	2	1	0.00	0.00
FGD6_MOUSE	FYVE, RhoGEF and PH domain-containing protein 6 OS=Mus musculus GN=Fgd6 PE=1 SV=2	**2.21**	1	1	0.00	0.00
KIF12_MOUSE	Kinesin-like protein KIF12 OS=Mus musculus GN=Kif12 PE=2 SV=1	**2.18**	1	1	0.00	0.00
HES6_MOUSE	Transcription cofactor HES-6 OS=Mus musculus GN=Hes6 PE=1 SV=1	**2.16**	1	1	0.00	0.00
HELQ_MOUSE	Helicase POLQ-like OS=Mus musculus GN=Helq PE=2 SV=2	**2.15**	1	1	0.00	0.00
H15_MOUSE	Histone H1.5 OS=Mus musculus GN=Hist1h1b PE=1 SV=2	**2.13**	1	1	0.00	0.00
T4S1_MOUSE	Transmembrane 4 L6 family member 1 OS=Mus musculus GN=Tm4sf1 PE=1 SV=1	**2.06**	2	1	0.00	0.00
SURF4_MOUSE	Surfeit locus protein 4 OS=Mus musculus GN=Surf4 PE=2 SV=1	**2.04**	2	2	0.01	0.73
NDUS7_MOUSE	NADH dehydrogenase [ubiquinone] iron-sulfur protein 7, mitochondrial OS=Mus musculus GN=Ndufs7 PE=1 SV=1	**2.03**	1	1	0.00	0.00
GAB2_MOUSE	GRB2-associated-binding protein 2 OS=Mus musculus GN=Gab2 PE=1 SV=2	**2.02**	4	2	1.66	82.29
NIBAN_MOUSE	Protein Niban OS=Mus musculus GN=Niban PE=2 SV=2	**2.01**	1	1	0.00	0.00
CL070_MOUSE	Uncharacterized protein C12orf70 homolog OS=Mus musculus PE=2 SV=1	**2.01**	1	1	0.00	0.00
SCOT1_MOUSE	Succinyl-CoA:3-ketoacid-coenzyme A transferase 1, mitochondrial OS=Mus musculus GN=Oxct1 PE=1 SV=1	**1.98**	2	2	1.27	63.91
CL035_MOUSE	Uncharacterized protein C12orf35 homolog OS=Mus musculus GN=Kiaa1551 PE=2 SV=2	**1.98**	1	1	0.00	0.00
MA7D3_MOUSE	MAP7 domain-containing protein 3 OS=Mus musculus GN=Map7d3 PE=2 SV=1	**1.97**	1	1	0.00	0.00
TREX1_MOUSE	Three prime repair exonuclease 1 OS=Mus musculus GN=Trex1 PE=1 SV=2	**1.97**	1	1	0.00	0.00
SEC20_MOUSE	Vesicle transport protein SEC20 OS=Mus musculus GN=Bnip1 PE=2 SV=1	**1.97**	1	1	0.00	0.00
SFI1_MOUSE	Protein SFI1 homolog OS=Mus musculus GN=Sfi1 PE=2 SV=1	**1.94**	1	1	0.00	0.00
VP26A_MOUSE	Vacuolar protein sorting-associated protein 26A OS=Mus musculus GN=Vps26a PE=2 SV=1	**1.94**	1	1	0.00	0.00
KCNH3_MOUSE	Potassium voltage-gated channel subfamily H member 3 OS=Mus musculus GN=Kcnh3 PE=2 SV=1	**1.92**	1	1	0.00	0.00
AKCL2_MOUSE	1,5-anhydro-D-fructose reductase OS=Mus musculus GN=Akr1e1 PE=1 SV=1	**1.91**	1	1	0.00	0.00
CREG1_MOUSE	Protein CREG1 OS=Mus musculus GN=Creg1 PE=2 SV=1	**1.91**	1	1	0.00	0.00
ASPH_MOUSE	Aspartyl/asparaginyl beta-hydroxylase OS=Mus musculus GN=Asph PE=2 SV=1	**1.86**	2	2	0.91	48.80
MLKL_MOUSE	Mixed lineage kinase domain-like protein OS=Mus musculus GN=Mlkl PE=2 SV=1	**1.83**	2	2	0.63	34.15
RCN2_MOUSE	Reticulocalbin-2 OS=Mus musculus GN=Rcn2 PE=2 SV=1	**1.83**	1	1	0.00	0.00
FITM1_MOUSE	Fat storage-inducing transmembrane protein 1 OS=Mus musculus GN=Fitm1 PE=1 SV=1	**1.82**	1	1	0.00	0.00
ACADM_MOUSE	Medium-chain specific acyl-CoA dehydrogenase, mitochondrial OS=Mus musculus GN=Acadm PE=1 SV=1	**1.82**	1	1	0.00	0.00
DLG1_MOUSE	Disks large homolog 1 OS=Mus musculus GN=Dlg1 PE=1 SV=1	**1.80**	1	1	0.00	0.00
IF4B_MOUSE	Eukaryotic translation initiation factor 4B OS=Mus musculus GN=Eif4b PE=1 SV=1	**1.80**	1	1	0.00	0.00
ARD1_MOUSE	GTP-binding protein ARD-1 OS=Mus musculus GN=Trim23 PE=2 SV=1	**1.79**	1	1	0.00	0.00
FUMH_MOUSE	Fumarate hydratase, mitochondrial OS=Mus musculus GN=Fh PE=1 SV=2	**1.79**	3	2	0.64	35.83
DNJB4_MOUSE	DnaJ homolog subfamily B member 4 OS=Mus musculus GN=Dnajb4 PE=2 SV=1	**1.77**	2	2	0.64	36.13
BST2_MOUSE	Bone marrow stromal antigen 2 OS=Mus musculus GN=Bst2 PE=1 SV=1	**1.77**	6	4	0.74	41.75
NU188_MOUSE	Nucleoporin NUP188 homolog OS=Mus musculus GN=Nup188 PE=1 SV=2	**1.76**	1	1	0.00	0.00
JHD2C_MOUSE	Probable JmjC domain-containing histone demethylation protein 2C OS=Mus musculus GN=Jmjd1c PE=1 SV=2	**1.74**	1	1	0.00	0.00
VMA5A_MOUSE	von Willebrand factor A domain-containing protein 5A OS=Mus musculus GN=Vwa5a PE=1 SV=2	**1.74**	2	2	0.37	21.03

Accession	Protein	H/L	#Cmpds	# quant	SD (H/L)	% CV
LMNB1_MOUSE	Lamin-B1 OS=Mus musculus GN=Lmnb1 PE=1 SV=3	**1.73**	3	2	0.69	39.66
RAB18_MOUSE	Ras-related protein Rab-18 OS=Mus musculus GN=Rab18 PE=2 SV=2	**1.72**	3	3	1.51	87.73
EIF1_MOUSE	Eukaryotic translation initiation factor 1 OS=Mus musculus GN=Eif1 PE=2 SV=2	**1.70**	1	1	0.00	0.00
ACADL_MOUSE	Long-chain specific acyl-CoA dehydrogenase, mitochondrial OS=Mus musculus GN=Acadl PE=2 SV=2	**1.70**	3	2	1.36	79.82
PAWR_MOUSE	PRKC apoptosis WT1 regulator protein OS=Mus musculus GN=Pawr PE=1 SV=2	**1.70**	1	1	0.00	0.00
CATA_MOUSE	Catalase OS=Mus musculus GN=Cat PE=1 SV=3	**1.68**	2	1	0.00	0.00
DJC10_MOUSE	DnaJ homolog subfamily C member 10 OS=Mus musculus GN=Dnajc10 PE=1 SV=1	**1.68**	1	1	0.00	0.00
PDLI5_MOUSE	PDZ and LIM domain protein 5 OS=Mus musculus GN=Pdlim5 PE=1 SV=3	**1.66**	4	3	1.17	70.08
SYFA_MOUSE	Phenylalanyl-tRNA synthetase alpha chain OS=Mus musculus GN=Farsa PE=2 SV=1	**1.66**	2	2	0.93	56.05
ANXA6_MOUSE	Annexin A6 OS=Mus musculus GN=Anxa6 PE=1 SV=2	**1.66**	4	4	0.81	48.81
FSCN1_MOUSE	Fascin OS=Mus musculus GN=Fscn1 PE=1 SV=4	**1.66**	4	4	0.70	42.14
YA046_MOUSE	Uncharacterized protein ENSP00000361571 homolog OS=Mus musculus PE=2 SV=2	**1.65**	1	1	0.00	0.00
PTBP1_MOUSE	Polypyrimidine tract-binding protein 1 OS=Mus musculus GN=Ptbp1 PE=1 SV=2	**1.65**	2	2	0.72	43.89
CLAP1_MOUSE	CLIP-associating protein 1 OS=Mus musculus GN=Clasp1 PE=1 SV=2	**1.62**	1	1	0.00	0.00
DCTN2_MOUSE	Dynactin subunit 2 OS=Mus musculus GN=Dctn2 PE=1 SV=3	**1.62**	1	1	0.00	0.00
PDLI7_MOUSE	PDZ and LIM domain protein 7 OS=Mus musculus GN=Pdlim7 PE=2 SV=1	**1.61**	1	1	0.00	0.00
KAD7_MOUSE	Putative adenylate kinase 7 OS=Mus musculus GN=Ak7 PE=2 SV=1	**1.61**	1	1	0.00	0.00
KINH_MOUSE	Kinesin-1 heavy chain OS=Mus musculus GN=Kif5b PE=1 SV=2	**1.61**	7	6	0.78	48.81
DNJC3_MOUSE	DnaJ homolog subfamily C member 3 OS=Mus musculus GN=Dnajc3 PE=1 SV=1	**1.56**	1	1	0.00	0.00
PB1_MOUSE	Protein polybromo-1 OS=Mus musculus GN=Pbrm1 PE=1 SV=3	**1.56**	1	1	0.00	0.00
2AAA_MOUSE	Serine/threonine-protein phosphatase 2A 65 kDa regulatory subunit A alpha isoform OS=Mus musculus GN=Ppp2r1a PE=1 SV=3	**1.56**	1	1	0.00	0.00
MAK10_MOUSE	Protein MAK10 homolog OS=Mus musculus GN=Mak10 PE=1 SV=1	**1.52**	1	1	0.00	0.00
UBR4_MOUSE	E3 ubiquitin-protein ligase UBR4 OS=Mus musculus GN=Ubr4 PE=1 SV=1	**1.50**	1	1	0.00	0.00
PCKGM_MOUSE	Phosphoenolpyruvate carboxykinase [GTP], mitochondrial OS=Mus musculus GN=Pck2 PE=2 SV=1	**1.50**	2	2	0.21	13.86
HA11_MOUSE	H-2 class I histocompatibility antigen, D-B alpha chain OS=Mus musculus GN=H2-D1 PE=1 SV=2	**1.50**	7	5	1.15	77.16
ALPK2_MOUSE	Alpha-protein kinase 2 OS=Mus musculus GN=Alpk2 PE=2 SV=2	**1.49**	1	1	0.00	0.00
AGAP1_MOUSE	Arf-GAP, GTPase, ANK repeat and PH domain-containing protein 1 OS=Mus musculus GN=Agap1 PE=2 SV=1	**1.49**	1	1	0.00	0.00
DOCK6_MOUSE	Dedicator of cytokinesis protein 6 OS=Mus musculus GN=Dock6 PE=1 SV=3	**1.49**	1	1	0.00	0.00
DNMT1_MOUSE	DNA (cytosine-5)-methyltransferase 1 OS=Mus musculus GN=Dnmt1 PE=1 SV=5	**1.49**	1	1	0.00	0.00
FANCI_MOUSE	Fanconi anemia group I protein homolog OS=Mus musculus GN=Fanci PE=1 SV=2	**1.49**	1	1	0.00	0.00
TSC1_MOUSE	Hamartin OS=Mus musculus GN=Tsc1 PE=1 SV=1	**1.49**	1	1	0.00	0.00
ODPA_MOUSE	Pyruvate dehydrogenase E1 component subunit alpha, somatic form, mitochondrial OS=Mus musculus GN=Pdha1 PE=1 SV=1	**1.49**	1	1	0.00	0.00
SMKTR_MOUSE	Sperm motility kinase Tcr mutant form OS=Mus musculus GN=Smoktcr PE=2 SV=1	**1.49**	1	1	0.00	0.00
UD17C_MOUSE	UDP-glucuronosyltransferase 1-7C OS=Mus musculus GN=Ugt1a7c PE=2 SV=1	**1.47**	13	5	0.80	54.66
METK2_MOUSE	S-adenosylmethionine synthetase isoform type-2 OS=Mus musculus GN=Mat2a PE=2 SV=2	**1.46**	1	1	0.00	0.00
RS2_MOUSE	40S ribosomal protein S2 OS=Mus musculus GN=Rps2 PE=1 SV=3	**1.46**	8	7	2.14	146.96
MYH14_MOUSE	Myosin-14 OS=Mus musculus GN=Myh14 PE=1 SV=1	**1.45**	17	9	1.03	71.04
FA13C_MOUSE	Protein FAM13C1 OS=Mus musculus GN=Fam13c1 PE=2 SV=1	**1.45**	1	1	0.00	0.00
SGOL1_MOUSE	Shugoshin-like 1 OS=Mus musculus GN=Sgol1 PE=2 SV=1	**1.45**	1	1	0.00	0.00
ZN608_MOUSE	Zinc finger protein 608 OS=Mus musculus GN=Znf608 PE=2 SV=1	**1.45**	1	1	0.00	0.00

Accession	Protein	H/L	#Cmpds	# quant	SD (H/L)	% CV
AP2A1_MOUSE	AP-2 complex subunit alpha-1 OS=Mus musculus GN=Ap2a1 PE=1 SV=1	**1.44**	3	3	0.47	32.45
AP2A2_MOUSE	AP-2 complex subunit alpha-2 OS=Mus musculus GN=Ap2a2 PE=1 SV=1	**1.44**	2	2	0.31	21.24
RSSA_MOUSE	40S ribosomal protein SA OS=Mus musculus GN=Rpsa PE=1 SV=4	**1.43**	1	1	0.00	0.00
TFP11_MOUSE	Tuftelin-interacting protein 11 OS=Mus musculus GN=Tfip11 PE=1 SV=1	**1.42**	2	2	0.84	59.16
PSMD1_MOUSE	26S proteasome non-ATPase regulatory subunit 1 OS=Mus musculus GN=Psmd1 PE=1 SV=1	**1.42**	3	2	0.51	36.13
NICA_MOUSE	Nicastrin OS=Mus musculus GN=Ncstn PE=1 SV=2	**1.42**	1	1	0.00	0.00
HYEP_MOUSE	Epoxide hydrolase 1 OS=Mus musculus GN=Ephx1 PE=1 SV=1	**1.40**	13	12	0.41	29.41
PSA1_MOUSE	Proteasome subunit alpha type-1 OS=Mus musculus GN=Psma1 PE=1 SV=1	**1.40**	1	1	0.00	0.00
SVIL_MOUSE	Supervillin OS=Mus musculus GN=Svil PE=1 SV=1	**1.40**	1	1	0.00	0.00
MYH11_MOUSE	Myosin-11 OS=Mus musculus GN=Myh11 PE=1 SV=1	**1.40**	27	15	1.02	73.11
HCD2_MOUSE	3-hydroxyacyl-CoA dehydrogenase type-2 OS=Mus musculus GN=Hsd17b10 PE=1 SV=4	**1.39**	2	1	0.00	0.00
MED17_MOUSE	Mediator of RNA polymerase II transcription subunit 17 OS=Mus musculus GN=Med17 PE=1 SV=1	**1.39**	1	1	0.00	0.00
PGAM5_MOUSE	Phosphoglycerate mutase family member 5 OS=Mus musculus GN=Pgam5 PE=2 SV=1	**1.39**	1	1	0.00	0.00
TR150_MOUSE	Thyroid hormone receptor-associated protein 3 OS=Mus musculus GN=Thrap3 PE=1 SV=1	**1.39**	1	1	0.00	0.00
EF1D_MOUSE	Elongation factor 1-delta OS=Mus musculus GN=Eef1d PE=1 SV=3	**1.38**	5	5	0.26	18.71
GVIN1_MOUSE	Interferon-induced very large GTPase 1 OS=Mus musculus GN=Gvin1 PE=1 SV=1	**1.38**	2	2	0.02	1.62
GLU2B_MOUSE	Glucosidase 2 subunit beta OS=Mus musculus GN=Prkcsh PE=1 SV=1	**1.37**	5	4	0.65	47.54
H12_MOUSE	Histone H1.2 OS=Mus musculus GN=Hist1h1c PE=1 SV=2	**1.37**	5	3	1.27	93.00
LYRIC_MOUSE	Protein LYRIC OS=Mus musculus GN=Mtdh PE=1 SV=1	**1.37**	2	2	0.03	2.17
MOV10_MOUSE	Putative helicase MOV-10 OS=Mus musculus GN=Mov10 PE=1 SV=2	**1.37**	1	1	0.00	0.00
AT2A1_MOUSE	Sarcoplasmic/endoplasmic reticulum calcium ATPase 1 OS=Mus musculus GN=Atp2a1 PE=2 SV=1	**1.36**	2	2	0.27	19.78
GIMA4_MOUSE	GTPase IMAP family member 4 OS=Mus musculus GN=Gimap4 PE=2 SV=1	**1.34**	1	1	0.00	0.00
MESD_MOUSE	LDLR chaperone MESD OS=Mus musculus GN=Mesdc2 PE=1 SV=1	**1.34**	1	1	0.00	0.00
LIMS1_MOUSE	LIM and senescent cell antigen-like-containing domain protein 1 OS=Mus musculus GN=Lims1 PE=1 SV=3	**1.34**	2	2	0.12	8.89
GBB1_MOUSE	Guanine nucleotide-binding protein G(I)/G(S)/G(T) subunit beta-1 OS=Mus musculus GN=Gnb1 PE=1 SV=3	**1.34**	3	3	0.38	28.42
P3H2_MOUSE	Prolyl 3-hydroxylase 2 OS=Mus musculus GN=Leprel1 PE=2 SV=1	**1.33**	1	1	0.00	0.00
PTN14_MOUSE	Tyrosine-protein phosphatase non-receptor type 14 OS=Mus musculus GN=Ptpn14 PE=1 SV=1	**1.33**	1	1	0.00	0.00
CHCH3_MOUSE	Coiled-coil-helix-coiled-coil-helix domain-containing protein 3, mitochondrial OS=Mus musculus GN=Chchd3 PE=1 SV=1	**1.32**	5	5	0.72	54.78
MVP_MOUSE	Major vault protein OS=Mus musculus GN=Mvp PE=2 SV=3	**1.32**	4	4	0.42	31.86
PSD12_MOUSE	26S proteasome non-ATPase regulatory subunit 12 OS=Mus musculus GN=Psmd12 PE=2 SV=3	**1.31**	1	1	0.00	0.00
YX017_MOUSE	Uncharacterized protein ENSP00000358542 homolog OS=Mus musculus PE=2 SV=1	**1.31**	1	1	0.00	0.00
HNRH2_MOUSE	Heterogeneous nuclear ribonucleoprotein H2 OS=Mus musculus GN=Hnrnph2 PE=1 SV=1	**1.30**	3	2	0.11	8.57
H14_MOUSE	Histone H1.4 OS=Mus musculus GN=Hist1h1e PE=1 SV=2	**1.30**	5	3	1.33	101.93
AFAD_MOUSE	Afadin OS=Mus musculus GN=Mllt4 PE=1 SV=3	**1.30**	1	1	0.00	0.00
CDIPT_MOUSE	CDP-diacylglycerol--inositol 3-phosphatidyltransferase OS=Mus musculus GN=Cdipt PE=1 SV=1	**1.30**	1	1	0.00	0.00
DC1L1_MOUSE	Cytoplasmic dynein 1 light intermediate chain 1 OS=Mus musculus GN=Dync1li1 PE=1 SV=1	**1.30**	2	2	0.31	24.14
LEMD2_MOUSE	LEM domain-containing protein 2 OS=Mus musculus GN=Lemd2 PE=1 SV=1	**1.30**	1	1	0.00	0.00
DYHC1_MOUSE	Cytoplasmic dynein 1 heavy chain 1 OS=Mus musculus GN=Dync1h1 PE=1 SV=1	**1.29**	12	10	0.39	30.55
HNRPG_MOUSE	Heterogeneous nuclear ribonucleoprotein G OS=Mus musculus GN=Rbmx PE=2 SV=1	**1.29**	4	3	0.23	17.78
ALDOA_MOUSE	Fructose-bisphosphate aldolase A OS=Mus musculus GN=Aldoa PE=1 SV=2	**1.29**	11	7	0.76	58.64
RALY_MOUSE	RNA-binding protein Raly OS=Mus musculus GN=Raly PE=1 SV=2	**1.29**	2	2	0.20	15.61

Accession	Protein	H/L	#Cmpds	# quant	SD (H/L)	% CV
DJB10_MOUSE	DnaJ homolog subfamily B member 10 OS=Mus musculus GN=Dnajb10 PE=2 SV=2	**1.28**	1	1	0.00	0.00
FR1L4_MOUSE	Fer-1-like protein 4 OS=Mus musculus GN=Fer1l4 PE=2 SV=2	**1.28**	1	1	0.00	0.00
HMOX2_MOUSE	Heme oxygenase 2 OS=Mus musculus GN=Hmox2 PE=2 SV=1	**1.28**	1	1	0.00	0.00
PLOD3_MOUSE	Procollagen-lysine,2-oxoglutarate 5-dioxygenase 3 OS=Mus musculus GN=Plod3 PE=2 SV=1	**1.28**	1	1	0.00	0.00
RAB5C_MOUSE	Ras-related protein Rab-5C OS=Mus musculus GN=Rab5c PE=1 SV=2	**1.28**	6	3	0.21	16.07
NCPR_MOUSE	NADPH--cytochrome P450 reductase OS=Mus musculus GN=Por PE=1 SV=2	**1.27**	2	2	0.29	22.81
MK01_MOUSE	Mitogen-activated protein kinase 1 OS=Mus musculus GN=Mapk1 PE=1 SV=3	**1.27**	2	2	0.44	34.50
SFXN1_MOUSE	Sideroflexin-1 OS=Mus musculus GN=Sfxn1 PE=1 SV=3	**1.27**	2	2	0.23	18.13
KAD3_MOUSE	GTP:AMP phosphotransferase mitochondrial OS=Mus musculus GN=Ak3 PE=1 SV=3	**1.27**	3	3	0.83	65.63
ODP2_MOUSE	Dihydrolipoyllysine-residue acetyltransferase component of pyruvate dehydrogenase complex, mitochondrial OS=Mus musculus GN=Dlat PE=1 SV=2	**1.27**	2	2	0.22	17.65
SNX2_MOUSE	Sorting nexin-2 OS=Mus musculus GN=Snx2 PE=1 SV=2	**1.27**	2	2	0.51	40.00
FKB10_MOUSE	FK506-binding protein 10 OS=Mus musculus GN=Fkbp10 PE=1 SV=1	**1.26**	9	8	0.35	27.73
IRGM_MOUSE	Immunity-related GTPase family M protein OS=Mus musculus GN=Irgm PE=1 SV=1	**1.26**	2	2	0.11	8.88
IMMT_MOUSE	Mitochondrial inner membrane protein OS=Mus musculus GN=Immt PE=1 SV=1	**1.26**	8	6	0.35	28.07
PRS8_MOUSE	26S protease regulatory subunit 8 OS=Mus musculus GN=Psmc5 PE=1 SV=1	**1.25**	2	2	0.07	5.95
ADDA_MOUSE	Alpha-adducin OS=Mus musculus GN=Add1 PE=1 SV=2	**1.25**	1	1	0.00	0.00
AOFA_MOUSE	Amine oxidase [flavin-containing] A OS=Mus musculus GN=Maoa PE=1 SV=2	**1.25**	5	4	0.31	24.64
NFKB2_MOUSE	Nuclear factor NF-kappa-B p100 subunit OS=Mus musculus GN=Nfkb2 PE=1 SV=1	**1.25**	1	1	0.00	0.00
GSTM1_MOUSE	Glutathione S-transferase Mu 1 OS=Mus musculus GN=Gstm1 PE=1 SV=2	**1.24**	2	2	0.32	25.75
F120A_MOUSE	Constitutive coactivator of PPAR-gamma-like protein 1 OS=Mus musculus GN=FAM120A PE=1 SV=2	**1.24**	3	3	0.30	24.04
ARF4_MOUSE	ADP-ribosylation factor 4 OS=Mus musculus GN=Arf4 PE=2 SV=2	**1.24**	1	1	0.00	0.00
ANXA3_MOUSE	Annexin A3 OS=Mus musculus GN=Anxa3 PE=2 SV=3	**1.24**	2	2	0.10	8.43
ATAD1_MOUSE	ATPase family AAA domain-containing protein 1 OS=Mus musculus GN=Atad1 PE=1 SV=1	**1.24**	1	1	0.00	0.00
SNX18_MOUSE	Sorting nexin-18 OS=Mus musculus GN=Snx18 PE=2 SV=1	**1.24**	1	1	0.00	0.00
DDAH1_MOUSE	N(G),N(G)-dimethylarginine dimethylaminohydrolase 1 OS=Mus musculus GN=Ddah1 PE=1 SV=3	**1.23**	2	2	0.45	36.97
P3H1_MOUSE	Prolyl 3-hydroxylase 1 OS=Mus musculus GN=Lepre1 PE=2 SV=2	**1.23**	5	4	0.43	35.47
QCR1_MOUSE	Cytochrome b-c1 complex subunit 1, mitochondrial OS=Mus musculus GN=Uqcrc1 PE=1 SV=1	**1.22**	1	1	0.00	0.00
FKBP8_MOUSE	FK506-binding protein 8 OS=Mus musculus GN=Fkbp8 PE=1 SV=2	**1.22**	2	1	0.00	0.00
GT251_MOUSE	Glycosyltransferase 25 family member 1 OS=Mus musculus GN=Glt25d1 PE=2 SV=2	**1.22**	1	1	0.00	0.00
MTCH2_MOUSE	Mitochondrial carrier homolog 2 OS=Mus musculus GN=Mtch2 PE=1 SV=1	**1.22**	2	2	0.33	26.83
MAOM_MOUSE	NAD-dependent malic enzyme, mitochondrial OS=Mus musculus GN=Me2 PE=2 SV=1	**1.22**	1	1	0.00	0.00
OAT_MOUSE	Ornithine aminotransferase, mitochondrial OS=Mus musculus GN=Oat PE=1 SV=1	**1.22**	1	1	0.00	0.00
THOC4_MOUSE	THO complex subunit 4 OS=Mus musculus GN=Thoc4 PE=1 SV=3	**1.22**	2	2	0.00	0.00
LMNA_MOUSE	Lamin-A/C OS=Mus musculus GN=Lmna PE=1 SV=2	**1.22**	16	9	0.34	28.06
AT1A1_MOUSE	Sodium/potassium-transporting ATPase subunit alpha-1 OS=Mus musculus GN=Atp1a1 PE=1 SV=1	**1.22**	4	4	0.47	38.39
CTRO_MOUSE	Citron Rho-interacting kinase OS=Mus musculus GN=Cit PE=1 SV=3	**1.21**	2	2	0.34	27.61
FINC_MOUSE	Fibronectin OS=Mus musculus GN=Fn1 PE=1 SV=3	**1.21**	34	20	1.00	82.40
CS060_MOUSE	Uncharacterized protein C19orf60 homolog OS=Mus musculus PE=2 SV=1	**1.21**	1	1	0.00	0.00
ANXA2_MOUSE	Annexin A2 OS=Mus musculus GN=Anxa2 PE=1 SV=2	**1.20**	4	3	0.42	35.01
SND1_MOUSE	Staphylococcal nuclease domain-containing protein 1 OS=Mus musculus GN=Snd1 PE=1 SV=1	**1.20**	2	2	0.10	8.07
CS063_MOUSE	UPF0510 protein C19orf63 homolog OS=Mus musculus PE=2 SV=2	**1.20**	2	2	0.29	24.22

Accession	Protein	H/L	#Cmpds	# quant	SD (H/L)	% CV
CALR_MOUSE	Calreticulin OS=Mus musculus GN=Calr PE=1 SV=1	**1.20**	16	9	1.68	139.79
HNRPK_MOUSE	Heterogeneous nuclear ribonucleoprotein K OS=Mus musculus GN=Hnrnpk PE=1 SV=1	**1.19**	11	11	0.51	42.67
PRS10_MOUSE	26S protease regulatory subunit S10B OS=Mus musculus GN=Psmc6 PE=1 SV=1	**1.19**	1	1	0.00	0.00
IL6RB_MOUSE	Interleukin-6 receptor subunit beta OS=Mus musculus GN=Il6st PE=1 SV=1	**1.19**	2	2	0.21	17.50
MPPA_MOUSE	Mitochondrial-processing peptidase subunit alpha OS=Mus musculus GN=Pmpca PE=1 SV=1	**1.19**	2	2	0.57	47.50
NIPS1_MOUSE	Protein NipSnap homolog 1 OS=Mus musculus GN=Nipsnap1 PE=1 SV=1	**1.19**	1	1	0.00	0.00
ERO1A_MOUSE	ERO1-like protein alpha OS=Mus musculus GN=Ero1l PE=1 SV=2	**1.19**	3	3	0.74	61.96
LMAN1_MOUSE	Protein ERGIC-53 OS=Mus musculus GN=Lman1 PE=2 SV=1	**1.19**	8	6	1.25	105.24
ENOB_MOUSE	Beta-enolase OS=Mus musculus GN=Eno3 PE=1 SV=3	**1.18**	3	3	0.66	55.96
STOM_MOUSE	Erythrocyte band 7 integral membrane protein OS=Mus musculus GN=Stom PE=1 SV=3	**1.18**	1	1	0.00	0.00
HNRPQ_MOUSE	Heterogeneous nuclear ribonucleoprotein Q OS=Mus musculus GN=Syncrip PE=1 SV=2	**1.18**	1	1	0.00	0.00
STX7_MOUSE	Syntaxin-7 OS=Mus musculus GN=Stx7 PE=1 SV=3	**1.18**	1	1	0.00	0.00
VPS35_MOUSE	Vacuolar protein sorting-associated protein 35 OS=Mus musculus GN=Vps35 PE=1 SV=1	**1.18**	1	1	0.00	0.00
GSTM2_MOUSE	Glutathione S-transferase Mu 2 OS=Mus musculus GN=Gstm2 PE=1 SV=2	**1.18**	2	2	0.25	21.52
DDX3X_MOUSE	ATP-dependent RNA helicase DDX3X OS=Mus musculus GN=Ddx3x PE=1 SV=3	**1.17**	4	4	0.28	24.12
GANAB_MOUSE	Neutral alpha-glucosidase AB OS=Mus musculus GN=Ganab PE=1 SV=1	**1.17**	10	10	0.35	30.42
MPCP_MOUSE	Phosphate carrier protein, mitochondrial OS=Mus musculus GN=Slc25a3 PE=1 SV=1	**1.16**	47	11	0.43	37.28
CHM1A_MOUSE	Charged multivesicular body protein 1a OS=Mus musculus GN=Chmp1a PE=1 SV=1	**1.16**	1	1	0.00	0.00
EIF3F_MOUSE	Eukaryotic translation initiation factor 3 subunit F OS=Mus musculus GN=Eif3f PE=1 SV=1	**1.16**	1	1	0.00	0.00
ROA2_MOUSE	Heterogeneous nuclear ribonucleoproteins A2/B1 OS=Mus musculus GN=Hnrnpa2b1 PE=1 SV=2	**1.16**	1	1	0.00	0.00
K22E_MOUSE	Keratin, type II cytoskeletal 2 epidermal OS=Mus musculus GN=Krt2 PE=1 SV=1	**1.16**	6	3	0.40	34.32
DJB11_MOUSE	DnaJ homolog subfamily B member 11 OS=Mus musculus GN=Dnajb11 PE=1 SV=1	**1.16**	3	3	0.17	14.58
MUC18_MOUSE	Cell surface glycoprotein MUC18 OS=Mus musculus GN=Mcam PE=2 SV=1	**1.15**	2	2	0.35	30.32
ETFD_MOUSE	Electron transfer flavoprotein-ubiquinone oxidoreductase, mitochondrial OS=Mus musculus GN=Etfdh PE=1 SV=1	**1.15**	3	3	0.14	12.33
UBIQ_MOUSE	Ubiquitin OS=Mus musculus GN=Rps27a PE=1 SV=1	**1.15**	4	3	0.27	23.16
PCBP1_MOUSE	Poly(rC)-binding protein 1 OS=Mus musculus GN=Pcbp1 PE=1 SV=1	**1.15**	8	6	0.46	40.25
SPTA2_MOUSE	Spectrin alpha chain, brain OS=Mus musculus GN=Sptan1 PE=1 SV=4	**1.15**	21	19	0.62	53.84
PSMD2_MOUSE	26S proteasome non-ATPase regulatory subunit 2 OS=Mus musculus GN=Psmd2 PE=1 SV=1	**1.15**	1	1	0.00	0.00
GSH0_MOUSE	Glutamate--cysteine ligase regulatory subunit OS=Mus musculus GN=Gclm PE=2 SV=1	**1.15**	1	1	0.00	0.00
KSR2_MOUSE	Kinase suppressor of Ras 2 OS=Mus musculus GN=Ksr2 PE=2 SV=2	**1.15**	1	1	0.00	0.00
MOL1B_MOUSE	Mps one binder kinase activator-like 1B OS=Mus musculus GN=Mobkl1b PE=2 SV=3	**1.15**	1	1	0.00	0.00
UAP56_MOUSE	Spliceosome RNA helicase Bat1 OS=Mus musculus GN=Bat1 PE=1 SV=1	**1.15**	1	1	0.00	0.00
SF3A1_MOUSE	Splicing factor 3 subunit 1 OS=Mus musculus GN=Sf3a1 PE=1 SV=1	**1.15**	2	1	0.00	0.00
SR140_MOUSE	U2-associated protein SR140 OS=Mus musculus GN=Sr140 PE=2 SV=2	**1.15**	1	1	0.00	0.00
NEDD4_MOUSE	E3 ubiquitin-protein ligase NEDD4 OS=Mus musculus GN=Nedd4 PE=1 SV=3	**1.14**	2	2	0.50	43.79
SPTB2_MOUSE	Spectrin beta chain, brain 1 OS=Mus musculus GN=Sptbn1 PE=1 SV=2	**1.13**	15	13	0.28	24.46
VINC_MOUSE	Vinculin OS=Mus musculus GN=Vcl PE=1 SV=4	**1.13**	14	10	0.35	30.54
CO4A1_MOUSE	Collagen alpha-1(IV) chain OS=Mus musculus GN=Col4a1 PE=2 SV=4	**1.13**	1	1	0.00	0.00
TGM2_MOUSE	Protein-glutamine gamma-glutamyltransferase 2 OS=Mus musculus GN=Tgm2 PE=1 SV=4	**1.13**	1	1	0.00	0.00
RAB5A_MOUSE	Ras-related protein Rab-5A OS=Mus musculus GN=Rab5a PE=1 SV=1	**1.13**	3	2	0.43	38.16
STAT3_MOUSE	Signal transducer and activator of transcription 3 OS=Mus musculus GN=Stat3 PE=1 SV=2	**1.13**	2	2	0.30	26.32

Accession	Protein	H/L	#Cmpds	# quant	SD (H/L)	% CV
FLNC_MOUSE	Filamin-C OS=Mus musculus GN=Flnc PE=1 SV=3	**1.13**	5	5	0.41	36.39
DYHC2_MOUSE	Cytoplasmic dynein 2 heavy chain 1 OS=Mus musculus GN=Dync2h1 PE=1 SV=1	**1.12**	2	2	0.34	29.80
RTN4_MOUSE	Reticulon-4 OS=Mus musculus GN=Rtn4 PE=1 SV=2	**1.12**	42	12	0.25	22.49
PGAM1_MOUSE	Phosphoglycerate mutase 1 OS=Mus musculus GN=Pgam1 PE=1 SV=3	**1.12**	5	5	0.62	55.25
CBR2_MOUSE	Carbonyl reductase [NADPH] 2 OS=Mus musculus GN=Cbr2 PE=1 SV=1	**1.12**	2	2	0.13	12.00
GDF5_MOUSE	Growth/differentiation factor 5 OS=Mus musculus GN=Gdf5 PE=2 SV=1	**1.12**	1	1	0.00	0.00
LPPRC_MOUSE	Leucine-rich PPR motif-containing protein, mitochondrial OS=Mus musculus GN=Lrpprc PE=1 SV=2	**1.12**	1	1	0.00	0.00
LSM12_MOUSE	Protein LSM12 homolog OS=Mus musculus GN=Lsm12 PE=1 SV=1	**1.12**	1	1	0.00	0.00
EWS_MOUSE	RNA-binding protein EWS OS=Mus musculus GN=Ewsr1 PE=1 SV=1	**1.12**	2	2	0.46	41.33
HS71L_MOUSE	Heat shock 70 kDa protein 1L OS=Mus musculus GN=Hspa1l PE=2 SV=4	**1.11**	22	7	0.72	64.75
MDHM_MOUSE	Malate dehydrogenase, mitochondrial OS=Mus musculus GN=Mdh2 PE=1 SV=3	**1.11**	18	10	1.26	112.76
G3BP1_MOUSE	Ras GTPase-activating protein-binding protein 1 OS=Mus musculus GN=G3bp1 PE=1 SV=1	**1.11**	2	2	0.28	24.83
COPD_MOUSE	Coatomer subunit delta OS=Mus musculus GN=Arcn1 PE=2 SV=1	**1.11**	2	2	0.47	42.28
NIPS2_MOUSE	Protein NipSnap homolog 2 OS=Mus musculus GN=Gbas PE=2 SV=1	**1.11**	3	3	0.71	64.26
SGPL1_MOUSE	Sphingosine-1-phosphate lyase 1 OS=Mus musculus GN=Sgpl1 PE=2 SV=1	**1.11**	8	7	0.30	27.08
TBB5_MOUSE	Tubulin beta-5 chain OS=Mus musculus GN=Tubb5 PE=1 SV=1	**1.11**	28	13	0.52	47.29
G6PE_MOUSE	GDH/6PGL endoplasmic bifunctional protein OS=Mus musculus GN=H6pd PE=2 SV=1	**1.10**	8	7	0.68	61.35
LEG9_MOUSE	Galectin-9 OS=Mus musculus GN=Lgals9 PE=1 SV=1	**1.10**	2	2	0.21	18.92
CDC37_MOUSE	Hsp90 co-chaperone Cdc37 OS=Mus musculus GN=Cdc37 PE=2 SV=1	**1.10**	1	1	0.00	0.00
CLH_MOUSE	Clathrin heavy chain 1 OS=Mus musculus GN=Cltc PE=1 SV=3	**1.10**	12	6	0.27	24.11
RL4_MOUSE	60S ribosomal protein L4 OS=Mus musculus GN=Rpl4 PE=1 SV=3	**1.10**	5	5	0.49	44.76
VATA_MOUSE	V-type proton ATPase catalytic subunit A OS=Mus musculus GN=Atp6v1a PE=1 SV=2	**1.10**	3	3	0.06	5.24
IMB1_MOUSE	Importin subunit beta-1 OS=Mus musculus GN=Kpnb1 PE=1 SV=1	**1.10**	5	3	0.27	24.32
NDUS1_MOUSE	NADH-ubiquinone oxidoreductase 75 kDa subunit, mitochondrial OS=Mus musculus GN=Ndufs1 PE=1 SV=1	**1.10**	2	2	0.07	6.12
CAND1_MOUSE	Cullin-associated NEDD8-dissociated protein 1 OS=Mus musculus GN=Cand1 PE=2 SV=2	**1.10**	2	2	0.04	3.40
ACON_MOUSE	Aconitate hydratase, mitochondrial OS=Mus musculus GN=Aco2 PE=1 SV=1	**1.09**	5	5	0.52	47.68
TOM70_MOUSE	Mitochondrial import receptor subunit TOM70 OS=Mus musculus GN=Tomm70a PE=1 SV=1	**1.09**	3	3	0.17	15.16
CO3_MOUSE	Complement C3 OS=Mus musculus GN=C3 PE=1 SV=2	**1.09**	6	5	0.54	49.53
NDUA9_MOUSE	NADH dehydrogenase [ubiquinone] 1 alpha subcomplex subunit 9, mitochondrial OS=Mus musculus GN=Ndufa9 PE=1 SV=1	**1.09**	4	4	0.28	25.68
RAB21_MOUSE	Ras-related protein Rab-21 OS=Mus musculus GN=Rab21 PE=1 SV=4	**1.09**	2	2	0.16	15.07
TTC35_MOUSE	Tetratricopeptide repeat protein 35 OS=Mus musculus GN=Ttc35 PE=2 SV=1	**1.08**	6	4	0.37	33.76
DHSA_MOUSE	Succinate dehydrogenase [ubiquinone] flavoprotein subunit, mitochondrial OS=Mus musculus GN=Sdha PE=1 SV=1	**1.08**	6	4	0.23	21.11
HS12A_MOUSE	Heat shock 70 kDa protein 12A OS=Mus musculus GN=Hspa12a PE=1 SV=1	**1.08**	2	2	0.42	39.31
GNAI2_MOUSE	Guanine nucleotide-binding protein G(i), alpha-2 subunit OS=Mus musculus GN=Gnai2 PE=1 SV=4	**1.07**	12	7	0.51	47.09
CTND1_MOUSE	Catenin delta-1 OS=Mus musculus GN=Ctnnd1 PE=1 SV=2	**1.07**	3	2	0.04	4.17
PCCA_MOUSE	Propionyl-CoA carboxylase alpha chain, mitochondrial OS=Mus musculus GN=Pcca PE=2 SV=2	**1.07**	1	1	0.00	0.00
YIF1B_MOUSE	Protein YIF1B OS=Mus musculus GN=Yif1b PE=2 SV=2	**1.07**	1	1	0.00	0.00
TMM43_MOUSE	Transmembrane protein 43 OS=Mus musculus GN=Tmem43 PE=1 SV=1	**1.07**	1	1	0.00	0.00
CH041_MOUSE	Uncharacterized protein C8orf41 homolog OS=Mus musculus PE=2 SV=1	**1.07**	1	1	0.00	0.00
RSU1_MOUSE	Ras suppressor protein 1 OS=Mus musculus GN=Rsu1 PE=2 SV=3	**1.06**	2	2	0.43	40.85

Accession	Protein	H/L	#Cmpds	# quant	SD (H/L)	% CV
LMAN2_MOUSE	Vesicular integral-membrane protein VIP36 OS=Mus musculus GN=Lman2 PE=2 SV=1	**1.06**	3	2	0.61	57.75
VATB2_MOUSE	V-type proton ATPase subunit B, brain isoform OS=Mus musculus GN=Atp6v1b2 PE=1 SV=1	**1.06**	7	6	0.24	22.73
AP2B1_MOUSE	AP-2 complex subunit beta-1 OS=Mus musculus GN=Ap2b1 PE=1 SV=1	**1.06**	1	1	0.00	0.00
ABCD3_MOUSE	ATP-binding cassette sub-family D member 3 OS=Mus musculus GN=Abcd3 PE=1 SV=1	**1.06**	1	1	0.00	0.00
IF4G1_MOUSE	Eukaryotic translation initiation factor 4 gamma 1 OS=Mus musculus GN=Eif4g1 PE=1 SV=1	**1.06**	1	1	0.00	0.00
LYN_MOUSE	Tyrosine-protein kinase Lyn OS=Mus musculus GN=Lyn PE=1 SV=4	**1.06**	1	1	0.00	0.00
GBB2_MOUSE	Guanine nucleotide-binding protein G(I)/G(S)/G(T) subunit beta-2 OS=Mus musculus GN=Gnb2 PE=1 SV=3	**1.05**	3	3	0.44	41.62
SEP11_MOUSE	Septin-11 OS=Mus musculus GN=Sept11 PE=1 SV=4	**1.05**	3	3	0.34	32.05
TCPH_MOUSE	T-complex protein 1 subunit eta OS=Mus musculus GN=Cct7 PE=1 SV=1	**1.05**	4	4	0.38	36.24
TPD54_MOUSE	Tumor protein D54 OS=Mus musculus GN=Tpd52l2 PE=1 SV=1	**1.05**	2	2	0.23	21.99
1433F_MOUSE	14-3-3 protein eta OS=Mus musculus GN=Ywhah PE=1 SV=2	**1.05**	8	6	0.35	33.53
RAI14_MOUSE	Ankycorbin OS=Mus musculus GN=Rai14 PE=1 SV=1	**1.05**	6	4	0.27	25.33
TCPA2_MOUSE	T-complex protein 1 subunit alpha B OS=Mus musculus GN=Cct1 PE=1 SV=3	**1.05**	5	4	0.33	31.39
RU17_MOUSE	U1 small nuclear ribonucleoprotein 70 kDa OS=Mus musculus GN=Snrnp70 PE=1 SV=2	**1.05**	4	4	0.48	45.73
GBP5_MOUSE	Guanylate-binding protein 5 OS=Mus musculus GN=Gbp5 PE=2 SV=1	**1.04**	5	4	0.09	8.81
PRS4_MOUSE	26S protease regulatory subunit 4 OS=Mus musculus GN=Psmc1 PE=1 SV=1	**1.04**	4	4	0.43	41.03
B2L13_MOUSE	Bcl-2-like 13 protein OS=Mus musculus GN=Bcl2l13 PE=1 SV=1	**1.04**	1	1	0.00	0.00
FKBP9_MOUSE	FK506-binding protein 9 OS=Mus musculus GN=Fkbp9 PE=1 SV=1	**1.04**	1	1	0.00	0.00
HMOX1_MOUSE	Heme oxygenase 1 OS=Mus musculus GN=Hmox1 PE=2 SV=1	**1.04**	2	2	0.01	1.43
DHSB_MOUSE	Succinate dehydrogenase [ubiquinone] iron-sulfur subunit, mitochondrial OS=Mus musculus GN=Sdhb PE=1 SV=1	**1.04**	1	1	0.00	0.00
TOIP1_MOUSE	Torsin-1A-interacting protein 1 OS=Mus musculus GN=Tor1aip1 PE=1 SV=1	**1.04**	1	1	0.00	0.00
UBP5_MOUSE	Ubiquitin carboxyl-terminal hydrolase 5 OS=Mus musculus GN=Usp5 PE=1 SV=1	**1.04**	1	1	0.00	0.00
P4HA1_MOUSE	Prolyl 4-hydroxylase subunit alpha-1 OS=Mus musculus GN=P4ha1 PE=2 SV=2	**1.04**	10	9	1.06	102.18
TPM3_MOUSE	Tropomyosin alpha-3 chain OS=Mus musculus GN=Tpm3 PE=1 SV=2	**1.04**	12	9	0.58	55.67
CAP1_MOUSE	Adenylyl cyclase-associated protein 1 OS=Mus musculus GN=Cap1 PE=1 SV=3	**1.04**	2	2	0.02	2.16
GRP78_MOUSE	78 kDa glucose-regulated protein OS=Mus musculus GN=Hspa5 PE=1 SV=3	**1.03**	71	23	0.87	83.97
PLS1_MOUSE	Phospholipid scramblase 1 OS=Mus musculus GN=Plscr1 PE=2 SV=1	**1.03**	4	3	0.43	41.89
SYVC_MOUSE	Valyl-tRNA synthetase OS=Mus musculus GN=Vars PE=2 SV=1	**1.03**	3	3	0.11	10.56
6PGL_MOUSE	6-phosphogluconolactonase OS=Mus musculus GN=Pgls PE=2 SV=1	**1.03**	1	1	0.00	0.00
ASM3B_MOUSE	Acid sphingomyelinase-like phosphodiesterase 3b OS=Mus musculus GN=Smpdl3b PE=2 SV=1	**1.03**	1	1	0.00	0.00
NDRG1_MOUSE	Protein NDRG1 OS=Mus musculus GN=Ndrg1 PE=1 SV=1	**1.03**	1	1	0.00	0.00
SRPR_MOUSE	Signal recognition particle receptor subunit alpha OS=Mus musculus GN=Srpr PE=1 SV=1	**1.03**	1	1	0.00	0.00
NUCB1_MOUSE	Nucleobindin-1 OS=Mus musculus GN=Nucb1 PE=1 SV=2	**1.02**	7	6	0.19	18.91
PCYOX_MOUSE	Prenylcysteine oxidase OS=Mus musculus GN=Pcyox1 PE=1 SV=1	**1.02**	4	3	0.23	22.10
APOOL_MOUSE	Apolipoprotein O-like OS=Mus musculus GN=Apool PE=2 SV=1	**1.02**	2	2	0.07	6.57
MYPT1_MOUSE	Protein phosphatase 1 regulatory subunit 12A OS=Mus musculus GN=Ppp1r12a PE=1 SV=1	**1.02**	2	2	0.26	25.55
EF1A1_MOUSE	Elongation factor 1-alpha 1 OS=Mus musculus GN=Eef1a1 PE=1 SV=3	**1.02**	18	10	0.36	35.36
UGGG1_MOUSE	UDP-glucose:glycoprotein glucosyltransferase 1 OS=Mus musculus GN=Ugcgl1 PE=1 SV=3	**1.02**	4	4	0.25	24.50
SRC8_MOUSE	Src substrate cortactin OS=Mus musculus GN=Cttn PE=1 SV=1	**1.01**	1	1	0.00	0.00
SFPQ_MOUSE	Splicing factor, proline- and glutamine-rich OS=Mus musculus GN=Sfpq PE=1 SV=1	**1.01**	11	5	0.39	38.30
KTN1_MOUSE	Kinectin OS=Mus musculus GN=Ktn1 PE=1 SV=1	**1.01**	11	9	0.19	19.13

Accession	Protein	H/L	#Cmpds	# quant	SD (H/L)	% CV
PGRC2_MOUSE	Membrane-associated progesterone receptor component 2 OS=Mus musculus GN=Pgrmc2 PE=1 SV=2	**1.01**	4	3	0.37	36.86
VA0D1_MOUSE	V-type proton ATPase subunit d 1 OS=Mus musculus GN=Atp6v0d1 PE=1 SV=2	**1.01**	4	3	0.74	73.80
ACTN4_MOUSE	Alpha-actinin-4 OS=Mus musculus GN=Actn4 PE=1 SV=1	**1.00**	25	14	0.32	31.42
DHE3_MOUSE	Glutamate dehydrogenase 1, mitochondrial OS=Mus musculus GN=Glud1 PE=1 SV=1	**1.00**	7	5	0.29	28.78
MPRIP_MOUSE	Myosin phosphatase Rho-interacting protein OS=Mus musculus GN=Mprip PE=1 SV=2	**1.00**	5	4	0.20	20.02
PLCD1_MOUSE	1-phosphatidylinositol-4,5-bisphosphate phosphodiesterase delta-1 OS=Mus musculus GN=Plcd1 PE=2 SV=1	**1.00**	1	1	0.00	0.00
LYPA1_MOUSE	Acyl-protein thioesterase 1 OS=Mus musculus GN=Lypla1 PE=1 SV=1	**1.00**	1	1	0.00	0.00
IMPA1_MOUSE	Inositol monophosphatase OS=Mus musculus GN=Impa1 PE=2 SV=1	**1.00**	1	1	0.00	0.00
ILK_MOUSE	Integrin-linked protein kinase OS=Mus musculus GN=Ilk PE=1 SV=2	**1.00**	1	1	0.00	0.00
K1C14_MOUSE	Keratin, type I cytoskeletal 14 OS=Mus musculus GN=Krt14 PE=1 SV=2	**1.00**	1	1	0.00	0.00
P4HA2_MOUSE	Prolyl 4-hydroxylase subunit alpha-2 OS=Mus musculus GN=P4ha2 PE=2 SV=1	**1.00**	1	1	0.00	0.00
PP2BA_MOUSE	Serine/threonine-protein phosphatase 2B catalytic subunit alpha isoform OS=Mus musculus GN=Ppp3ca PE=1 SV=1	**1.00**	1	1	0.00	0.00
GLOD4_MOUSE	Glyoxalase domain-containing protein 4 OS=Mus musculus GN=Glod4 PE=2 SV=1	**1.00**	2	2	0.48	47.76
LXN_MOUSE	Latexin OS=Mus musculus GN=Lxn PE=1 SV=2	**1.00**	2	2	0.19	19.40
PSA5_MOUSE	Proteasome subunit alpha type-5 OS=Mus musculus GN=Psma5 PE=1 SV=1	**1.00**	2	2	0.33	32.84
TCPG_MOUSE	T-complex protein 1 subunit gamma OS=Mus musculus GN=Cct3 PE=1 SV=1	**1.00**	4	4	0.30	29.89
LETM1_MOUSE	LETM1 and EF-hand domain-containing protein 1, mitochondrial OS=Mus musculus GN=Letm1 PE=2 SV=1	**0.99**	3	3	0.26	26.45
MLEC_MOUSE	Malectin OS=Mus musculus GN=Mlec PE=2 SV=2	**0.99**	5	3	0.18	17.93
TERA_MOUSE	Transitional endoplasmic reticulum ATPase OS=Mus musculus GN=Vcp PE=1 SV=4	**0.99**	13	7	0.40	40.32
GOLI4_MOUSE	Golgi integral membrane protein 4 OS=Mus musculus GN=Golim4 PE=1 SV=1	**0.99**	2	2	0.39	39.85
CERU_MOUSE	Ceruloplasmin OS=Mus musculus GN=Cp PE=1 SV=2	**0.99**	3	3	0.15	14.89
ACSF2_MOUSE	Acyl-CoA synthetase family member 2, mitochondrial OS=Mus musculus GN=Acsf2 PE=2 SV=1	**0.98**	1	1	0.00	0.00
KAD2_MOUSE	Adenylate kinase 2, mitochondrial OS=Mus musculus GN=Ak2 PE=1 SV=5	**0.98**	3	3	0.28	28.77
MA2A1_MOUSE	Alpha-mannosidase 2 OS=Mus musculus GN=Man2a1 PE=1 SV=1	**0.98**	2	2	0.63	63.64
NPM_MOUSE	Nucleophosmin OS=Mus musculus GN=Npm1 PE=1 SV=1	**0.98**	1	1	0.00	0.00
CTNA1_MOUSE	Catenin alpha-1 OS=Mus musculus GN=Ctnna1 PE=1 SV=1	**0.98**	13	12	0.24	24.46
PGAM2_MOUSE	Phosphoglycerate mutase 2 OS=Mus musculus GN=Pgam2 PE=1 SV=3	**0.98**	5	5	0.70	71.22
ANXA1_MOUSE	Annexin A1 OS=Mus musculus GN=Anxa1 PE=1 SV=2	**0.98**	5	5	0.26	26.62
NONO_MOUSE	Non-POU domain-containing octamer-binding protein OS=Mus musculus GN=Nono PE=1 SV=3	**0.98**	5	5	0.24	24.63
MCAT_MOUSE	Mitochondrial carnitine/acylcarnitine carrier protein OS=Mus musculus GN=Slc25a20 PE=1 SV=1	**0.98**	2	2	0.10	9.92
ATPB_MOUSE	ATP synthase subunit beta, mitochondrial OS=Mus musculus GN=Atp5b PE=1 SV=2	**0.97**	34	20	0.35	36.23
PLEC1_MOUSE	Plectin-1 OS=Mus musculus GN=Plec1 PE=1 SV=2	**0.97**	47	40	0.31	31.65
MUTA_MOUSE	Methylmalonyl-CoA mutase, mitochondrial OS=Mus musculus GN=Mut PE=2 SV=1	**0.97**	1	1	0.00	0.00
DIC_MOUSE	Mitochondrial dicarboxylate carrier OS=Mus musculus GN=Slc25a10 PE=2 SV=2	**0.97**	1	1	0.00	0.00
SSRD_MOUSE	Translocon-associated protein subunit delta OS=Mus musculus GN=Ssr4 PE=2 SV=1	**0.97**	1	1	0.00	0.00
TBA4A_MOUSE	Tubulin alpha-4A chain OS=Mus musculus GN=Tuba4a PE=1 SV=1	**0.97**	13	6	0.44	45.72
CN159_MOUSE	UPF0317 protein C14orf159 homolog, mitochondrial OS=Mus musculus PE=2 SV=1	**0.97**	1	1	0.00	0.00
CHM4B_MOUSE	Charged multivesicular body protein 4b OS=Mus musculus GN=Chmp4b PE=2 SV=2	**0.97**	4	4	0.21	21.84
COPA_MOUSE	Coatomer subunit alpha OS=Mus musculus GN=Copa PE=1 SV=1	**0.97**	6	5	0.21	21.47
FLOT1_MOUSE	Flotillin-1 OS=Mus musculus GN=Flot1 PE=1 SV=1	**0.97**	2	2	0.10	10.77
MYO1C_MOUSE	Myosin-Ic OS=Mus musculus GN=Myo1c PE=1 SV=2	**0.97**	14	10	0.22	22.24

Accession	Protein	H/L	#Cmpds	# quant	SD (H/L)	% CV
CTNB1_MOUSE	Catenin beta-1 OS=Mus musculus GN=Ctnnb1 PE=1 SV=1	**0.97**	13	9	0.29	30.35
SERPH_MOUSE	Serpin H1 OS=Mus musculus GN=Serpinh1 PE=1 SV=2	**0.96**	25	16	0.76	79.06
IDHP_MOUSE	Isocitrate dehydrogenase [NADP], mitochondrial OS=Mus musculus GN=Idh2 PE=1 SV=3	**0.96**	6	6	0.32	32.92
ACTN1_MOUSE	Alpha-actinin-1 OS=Mus musculus GN=Actn1 PE=2 SV=1	**0.96**	14	11	0.23	23.55
UBA1_MOUSE	Ubiquitin-like modifier-activating enzyme 1 OS=Mus musculus GN=Uba1 PE=1 SV=1	**0.96**	6	5	0.13	14.05
RAB14_MOUSE	Ras-related protein Rab-14 OS=Mus musculus GN=Rab14 PE=1 SV=3	**0.96**	11	5	0.33	34.25
FLNB_MOUSE	Filamin-B OS=Mus musculus GN=Flnb PE=2 SV=2	**0.96**	35	30	0.36	37.52
CAPZB_MOUSE	F-actin-capping protein subunit beta OS=Mus musculus GN=Capzb PE=1 SV=3	**0.96**	4	4	0.36	37.33
LAP2B_MOUSE	Lamina-associated polypeptide 2, isoforms beta/delta/epsilon/gamma OS=Mus musculus GN=Tmpo PE=1 SV=3	**0.96**	9	5	0.20	20.46
ANXA7_MOUSE	Annexin A7 OS=Mus musculus GN=Anxa7 PE=2 SV=1	**0.95**	1	1	0.00	0.00
MEST_MOUSE	Mesoderm-specific transcript protein OS=Mus musculus GN=Mest PE=2 SV=1	**0.95**	2	2	0.16	17.19
PTN1_MOUSE	Tyrosine-protein phosphatase non-receptor type 1 OS=Mus musculus GN=Ptpn1 PE=1 SV=2	**0.95**	1	1	0.00	0.00
AIFM1_MOUSE	Apoptosis-inducing factor 1, mitochondrial OS=Mus musculus GN=Aifm1 PE=1 SV=1	**0.95**	3	3	0.08	7.97
RS3_MOUSE	40S ribosomal protein S3 OS=Mus musculus GN=Rps3 PE=1 SV=1	**0.95**	10	6	0.33	34.61
G3P_MOUSE	Glyceraldehyde-3-phosphate dehydrogenase OS=Mus musculus GN=Gapdh PE=1 SV=2	**0.95**	13	12	0.62	65.09
SYEP_MOUSE	Bifunctional aminoacyl-tRNA synthetase OS=Mus musculus GN=Eprs PE=2 SV=3	**0.95**	3	3	0.22	23.10
EF1A2_MOUSE	Elongation factor 1-alpha 2 OS=Mus musculus GN=Eef1a2 PE=1 SV=1	**0.95**	10	6	0.38	40.20
TBB2C_MOUSE	Tubulin beta-2C chain OS=Mus musculus GN=Tubb2c PE=1 SV=1	**0.94**	31	14	0.44	47.03
MTX2_MOUSE	Metaxin-2 OS=Mus musculus GN=Mtx2 PE=1 SV=1	**0.94**	1	1	0.00	0.00
RRAS_MOUSE	Ras-related protein R-Ras OS=Mus musculus GN=Rras PE=2 SV=1	**0.94**	1	1	0.00	0.00
GDPD1_MOUSE	Glycerophosphodiester phosphodiesterase domain-containing protein 1 OS=Mus musculus GN=Gdpd1 PE=2 SV=1	**0.94**	2	2	0.34	36.51
EHD1_MOUSE	EH domain-containing protein 1 OS=Mus musculus GN=Ehd1 PE=1 SV=1	**0.94**	5	5	0.19	19.82
RHOA_MOUSE	Transforming protein RhoA OS=Mus musculus GN=Rhoa PE=1 SV=1	**0.94**	6	5	0.08	8.51
PDIA4_MOUSE	Protein disulfide-isomerase A4 OS=Mus musculus GN=Pdia4 PE=1 SV=2	**0.94**	16	13	0.59	63.40
SC22B_MOUSE	Vesicle-trafficking protein SEC22b OS=Mus musculus GN=Sec22b PE=1 SV=3	**0.93**	10	7	0.40	43.31
E41L3_MOUSE	Band 4.1-like protein 3 OS=Mus musculus GN=Epb41l3 PE=1 SV=1	**0.92**	3	3	0.05	5.74
CLPT1_MOUSE	Cleft lip and palate transmembrane protein 1 homolog OS=Mus musculus GN=Clptm1 PE=1 SV=1	**0.92**	1	1	0.00	0.00
FIGN_MOUSE	Fidgetin OS=Mus musculus GN=Fign PE=2 SV=1	**0.92**	1	1	0.00	0.00
ITAV_MOUSE	Integrin alpha-V OS=Mus musculus GN=Itgav PE=2 SV=1	**0.92**	3	2	0.07	8.06
NUCL_MOUSE	Nucleolin OS=Mus musculus GN=Ncl PE=1 SV=2	**0.92**	1	1	0.00	0.00
PRDX6_MOUSE	Peroxiredoxin-6 OS=Mus musculus GN=Prdx6 PE=1 SV=3	**0.92**	3	3	0.23	24.39
SFXN3_MOUSE	Sideroflexin-3 OS=Mus musculus GN=Sfxn3 PE=1 SV=1	**0.92**	1	1	0.00	0.00
CA077_MOUSE	Uncharacterized protein C1orf77 homolog OS=Mus musculus GN=MNCb-1706 PE=2 SV=2	**0.92**	1	1	0.00	0.00
CALU_MOUSE	Calumenin OS=Mus musculus GN=Calu PE=1 SV=1	**0.92**	8	6	0.52	56.70
MYH10_MOUSE	Myosin-10 OS=Mus musculus GN=Myh10 PE=1 SV=2	**0.92**	60	36	0.40	43.39
CH60_MOUSE	60 kDa heat shock protein, mitochondrial OS=Mus musculus GN=Hspd1 PE=1 SV=1	**0.92**	16	11	0.44	48.42
RAB12_MOUSE	Ras-related protein Rab-12 OS=Mus musculus GN=Rab12 PE=1 SV=3	**0.92**	10	4	0.26	28.46
EFTU_MOUSE	Elongation factor Tu, mitochondrial OS=Mus musculus GN=Tufm PE=1 SV=1	**0.91**	3	3	0.20	22.17
PHB_MOUSE	Prohibitin OS=Mus musculus GN=Phb PE=1 SV=1	**0.91**	9	6	0.37	40.28
IQGA1_MOUSE	Ras GTPase-activating-like protein IQGAP1 OS=Mus musculus GN=Iqgap1 PE=1 SV=1	**0.91**	6	6	0.27	29.70
PABP1_MOUSE	Polyadenylate-binding protein 1 OS=Mus musculus GN=Pabpc1 PE=1 SV=1	**0.91**	4	4	0.23	25.84

Accession	Protein	H/L	#Cmpds	# quant	SD (H/L)	% CV
ACADS_MOUSE	Short-chain specific acyl-CoA dehydrogenase, mitochondrial OS=Mus musculus GN=Acads PE=2 SV=1	**0.91**	2	2	0.25	27.87
ECH1_MOUSE	Delta(3,5)-Delta(2,4)-dienoyl-CoA isomerase, mitochondrial OS=Mus musculus GN=Ech1 PE=2 SV=1	**0.91**	1	1	0.00	0.00
CT007_MOUSE	Probable methyltransferase C20orf7 homolog, mitochondrial OS=Mus musculus PE=2 SV=1	**0.91**	1	1	0.00	0.00
SEPT2_MOUSE	Septin-2 OS=Mus musculus GN=Sept2 PE=1 SV=2	**0.91**	1	1	0.00	0.00
TM55A_MOUSE	Transmembrane protein 55A OS=Mus musculus GN=Tmem55a PE=1 SV=1	**0.91**	1	1	0.00	0.00
TLN1_MOUSE	Talin-1 OS=Mus musculus GN=Tln1 PE=1 SV=1	**0.91**	27	18	0.22	24.29
TAGL2_MOUSE	Transgelin-2 OS=Mus musculus GN=Tagln2 PE=1 SV=4	**0.91**	5	5	0.28	30.53
CAPG_MOUSE	Macrophage-capping protein OS=Mus musculus GN=Capg PE=1 SV=2	**0.90**	3	2	0.23	25.62
FUS_MOUSE	RNA-binding protein FUS OS=Mus musculus GN=Fus PE=2 SV=1	**0.90**	2	2	0.25	27.27
EMD_MOUSE	Emerin OS=Mus musculus GN=Emd PE=1 SV=1	**0.90**	2	2	0.19	20.66
RAB6A_MOUSE	Ras-related protein Rab-6A OS=Mus musculus GN=Rab6a PE=1 SV=4	**0.90**	15	9	0.23	25.70
SNRPA_MOUSE	U1 small nuclear ribonucleoprotein A OS=Mus musculus GN=Snrpa PE=2 SV=3	**0.90**	6	4	0.14	15.67
PYRG1_MOUSE	CTP synthase 1 OS=Mus musculus GN=Ctps PE=1 SV=2	**0.89**	1	1	0.00	0.00
HNRPM_MOUSE	Heterogeneous nuclear ribonucleoprotein M OS=Mus musculus GN=Hnrnpm PE=1 SV=3	**0.89**	1	1	0.00	0.00
HYOU1_MOUSE	Hypoxia up-regulated protein 1 OS=Mus musculus GN=Hyou1 PE=1 SV=1	**0.89**	9	7	0.40	44.28
MYO6_MOUSE	Myosin-VI OS=Mus musculus GN=Myo6 PE=1 SV=1	**0.89**	1	1	0.00	0.00
PTH2_MOUSE	Peptidyl-tRNA hydrolase 2, mitochondrial OS=Mus musculus GN=Ptrh2 PE=2 SV=1	**0.89**	1	1	0.00	0.00
PKHO2_MOUSE	Pleckstrin homology domain-containing family O member 2 OS=Mus musculus GN=Plekho2 PE=1 SV=1	**0.89**	1	1	0.00	0.00
TCPQ_MOUSE	T-complex protein 1 subunit theta OS=Mus musculus GN=Cct8 PE=1 SV=3	**0.89**	2	2	0.04	5.00
FLNA_MOUSE	Filamin-A OS=Mus musculus GN=Flna PE=1 SV=4	**0.89**	48	31	0.30	33.64
RRBP1_MOUSE	Ribosome-binding protein 1 OS=Mus musculus GN=Rrbp1 PE=2 SV=2	**0.89**	20	16	0.48	54.13
STT3A_MOUSE	Dolichyl-diphosphooligosaccharide--protein glycosyltransferase subunit STT3A OS=Mus musculus GN=Stt3a PE=1 SV=1	**0.89**	2	2	0.34	37.82
HSP7C_MOUSE	Heat shock cognate 71 kDa protein OS=Mus musculus GN=Hspa8 PE=1 SV=1	**0.89**	40	21	0.29	33.16
PHB2_MOUSE	Prohibitin-2 OS=Mus musculus GN=Phb2 PE=1 SV=1	**0.89**	8	7	0.34	38.23
SYDC_MOUSE	Aspartyl-tRNA synthetase, cytoplasmic OS=Mus musculus GN=Dars PE=2 SV=1	**0.88**	4	4	0.09	10.15
MYH9_MOUSE	Myosin-9 OS=Mus musculus GN=Myh9 PE=1 SV=4	**0.88**	119	75	0.49	55.81
ACADV_MOUSE	Very long-chain specific acyl-CoA dehydrogenase, mitochondrial OS=Mus musculus GN=Acadvl PE=1 SV=3	**0.88**	5	5	0.15	16.77
GNAQ_MOUSE	Guanine nucleotide-binding protein G(q) subunit alpha OS=Mus musculus GN=Gnaq PE=1 SV=4	**0.88**	8	7	0.31	35.33
ETFB_MOUSE	Electron transfer flavoprotein subunit beta OS=Mus musculus GN=Etfb PE=1 SV=3	**0.88**	6	5	0.44	49.98
HA1B_MOUSE	H-2 class I histocompatibility antigen, K-B alpha chain OS=Mus musculus GN=H2-K1 PE=1 SV=1	**0.88**	7	5	0.36	40.58
RTN3_MOUSE	Reticulon-3 OS=Mus musculus GN=Rtn3 PE=1 SV=2	**0.88**	4	2	0.37	42.37
HS90B_MOUSE	Heat shock protein HSP 90-beta OS=Mus musculus GN=Hsp90ab1 PE=1 SV=2	**0.87**	30	21	0.32	36.90
GNA11_MOUSE	Guanine nucleotide-binding protein subunit alpha-11 OS=Mus musculus GN=Gna11 PE=1 SV=1	**0.87**	8	6	0.39	44.93
SC23A_MOUSE	Protein transport protein Sec23A OS=Mus musculus GN=Sec23a PE=1 SV=2	**0.87**	3	3	0.40	46.56
CO3A1_MOUSE	Collagen alpha-1(III) chain OS=Mus musculus GN=Col3a1 PE=2 SV=4	**0.86**	1	1	0.00	0.00
PSA2_MOUSE	Proteasome subunit alpha type-2 OS=Mus musculus GN=Psma2 PE=1 SV=2	**0.86**	1	1	0.00	0.00
RAB34_MOUSE	Ras-related protein Rab-34 OS=Mus musculus GN=Rab34 PE=1 SV=2	**0.86**	1	1	0.00	0.00
SF3A2_MOUSE	Splicing factor 3A subunit 2 OS=Mus musculus GN=Sf3a2 PE=2 SV=2	**0.86**	1	1	0.00	0.00
U2AF1_MOUSE	Splicing factor U2AF 35 kDa subunit OS=Mus musculus GN=U2af1 PE=2 SV=4	**0.86**	1	1	0.00	0.00
TXND5_MOUSE	Thioredoxin domain-containing protein 5 OS=Mus musculus GN=Txndc5 PE=1 SV=2	**0.86**	1	1	0.00	0.00
RPN1_MOUSE	Dolichyl-diphosphooligosaccharide--protein glycosyltransferase subunit 1 OS=Mus musculus GN=Rpn1 PE=2	**0.86**	13	9	0.26	30.60

Accession	Protein	H/L	#Cmpds	# quant	SD (H/L)	% CV
	SV=1					
LDHA_MOUSE	L-lactate dehydrogenase A chain OS=Mus musculus GN=Ldha PE=1 SV=3	**0.86**	3	3	0.03	3.56
ITB1_MOUSE	Integrin beta-1 OS=Mus musculus GN=Itgb1 PE=1 SV=1	**0.85**	9	6	0.12	14.51
RS18_MOUSE	40S ribosomal protein S18 OS=Mus musculus GN=Rps18 PE=2 SV=3	**0.85**	2	2	0.22	26.32
DBNL_MOUSE	Drebrin-like protein OS=Mus musculus GN=Dbnl PE=1 SV=2	**0.85**	1	1	0.00	0.00
PALM_MOUSE	Paralemmin OS=Mus musculus GN=Palm PE=1 SV=1	**0.85**	1	1	0.00	0.00
P5CR2_MOUSE	Pyrroline-5-carboxylate reductase 2 OS=Mus musculus GN=Pycr2 PE=2 SV=1	**0.85**	2	2	0.07	8.77
ATPA_MOUSE	ATP synthase subunit alpha, mitochondrial OS=Mus musculus GN=Atp5a1 PE=1 SV=1	**0.85**	28	17	0.38	45.32
VAT1_MOUSE	Synaptic vesicle membrane protein VAT-1 homolog OS=Mus musculus GN=Vat1 PE=2 SV=3	**0.84**	5	5	0.14	16.14
D3D2_MOUSE	3,2-trans-enoyl-CoA isomerase, mitochondrial OS=Mus musculus GN=Dci PE=2 SV=1	**0.84**	2	2	0.32	38.05
JAM1_MOUSE	Junctional adhesion molecule A OS=Mus musculus GN=F11r PE=1 SV=1	**0.84**	3	2	0.04	4.42
TPM4_MOUSE	Tropomyosin alpha-4 chain OS=Mus musculus GN=Tpm4 PE=2 SV=3	**0.84**	12	10	0.26	31.06
RAB5B_MOUSE	Ras-related protein Rab-5B OS=Mus musculus GN=Rab5b PE=1 SV=1	**0.84**	8	4	0.43	51.04
AATM_MOUSE	Aspartate aminotransferase, mitochondrial OS=Mus musculus GN=Got2 PE=1 SV=1	**0.84**	5	5	0.28	33.94
VIME_MOUSE	Vimentin OS=Mus musculus GN=Vim PE=1 SV=3	**0.84**	54	33	0.30	36.41
RL10A_MOUSE	60S ribosomal protein L10a OS=Mus musculus GN=Rpl10a PE=1 SV=3	**0.83**	2	1	0.00	0.00
DLDH_MOUSE	Dihydrolipoyl dehydrogenase, mitochondrial OS=Mus musculus GN=Dld PE=1 SV=2	**0.83**	3	2	0.25	30.36
DREB_MOUSE	Drebrin OS=Mus musculus GN=Dbn1 PE=1 SV=4	**0.83**	1	1	0.00	0.00
AL3A2_MOUSE	Fatty aldehyde dehydrogenase OS=Mus musculus GN=Aldh3a2 PE=2 SV=1	**0.83**	2	2	0.06	7.14
PGRC1_MOUSE	Membrane-associated progesterone receptor component 1 OS=Mus musculus GN=Pgrmc1 PE=1 SV=4	**0.83**	3	3	0.16	19.62
TIM50_MOUSE	Mitochondrial import inner membrane translocase subunit TIM50 OS=Mus musculus GN=Timm50 PE=1 SV=1	**0.83**	1	1	0.00	0.00
SCPDH_MOUSE	Probable saccharopine dehydrogenase OS=Mus musculus GN=Sccpdh PE=2 SV=1	**0.83**	1	1	0.00	0.00
VAPB_MOUSE	Vesicle-associated membrane protein-associated protein B OS=Mus musculus GN=Vapb PE=2 SV=3	**0.83**	5	4	0.40	48.33
HA1K_MOUSE	H-2 class I histocompatibility antigen, K-K alpha chain OS=Mus musculus GN=H2-K1 PE=1 SV=1	**0.83**	7	5	0.35	41.39
RAB10_MOUSE	Ras-related protein Rab-10 OS=Mus musculus GN=Rab10 PE=1 SV=1	**0.83**	15	7	0.32	37.77
LAMP1_MOUSE	Lysosome-associated membrane glycoprotein 1 OS=Mus musculus GN=Lamp1 PE=1 SV=2	**0.83**	10	5	0.23	27.38
VNN1_MOUSE	Pantetheinase OS=Mus musculus GN=Vnn1 PE=1 SV=2	**0.83**	5	4	0.38	45.37
CISY_MOUSE	Citrate synthase, mitochondrial OS=Mus musculus GN=Cs PE=1 SV=1	**0.83**	4	4	0.26	31.31
ACTC_MOUSE	Actin, alpha cardiac muscle 1 OS=Mus musculus GN=Actc1 PE=1 SV=1	**0.83**	83	22	0.42	51.08
SQRD_MOUSE	Sulfide:quinone oxidoreductase, mitochondrial OS=Mus musculus GN=Sqrdl PE=2 SV=2	**0.83**	4	4	0.26	31.32
PDIA6_MOUSE	Protein disulfide-isomerase A6 OS=Mus musculus GN=Pdia6 PE=1 SV=3	**0.83**	19	10	0.32	38.91
ENPL_MOUSE	Endoplasmin OS=Mus musculus GN=Hsp90b1 PE=1 SV=2	**0.82**	40	24	0.30	36.79
RAC1_MOUSE	Ras-related C3 botulinum toxin substrate 1 OS=Mus musculus GN=Rac1 PE=1 SV=1	**0.82**	3	3	0.18	21.50
SPCS2_MOUSE	Signal peptidase complex subunit 2 OS=Mus musculus GN=Spcs2 PE=2 SV=1	**0.82**	4	3	0.11	13.39
VTI1B_MOUSE	Vesicle transport through interaction with t-SNAREs homolog 1B OS=Mus musculus GN=Vti1b PE=1 SV=1	**0.82**	3	3	0.13	15.92
E41L2_MOUSE	Band 4.1-like protein 2 OS=Mus musculus GN=Epb41l2 PE=1 SV=1	**0.82**	3	3	0.13	15.64
CMC1_MOUSE	Calcium-binding mitochondrial carrier protein Aralar1 OS=Mus musculus GN=Slc25a12 PE=1 SV=1	**0.82**	3	3	0.18	22.17
MYL6_MOUSE	Myosin light polypeptide 6 OS=Mus musculus GN=Myl6 PE=1 SV=3	**0.82**	2	2	0.18	21.82
HS90A_MOUSE	Heat shock protein HSP 90-alpha OS=Mus musculus GN=Hsp90aa1 PE=1 SV=4	**0.82**	20	14	0.31	38.30
THIL_MOUSE	Acetyl-CoA acetyltransferase, mitochondrial OS=Mus musculus GN=Acat1 PE=1 SV=1	**0.81**	6	6	0.39	48.47
RBBP4_MOUSE	Histone-binding protein RBBP4 OS=Mus musculus GN=Rbbp4 PE=1 SV=4	**0.81**	2	2	0.37	44.95

Accession	Protein	H/L	#Cmpds	# quant	SD (H/L)	% CV
SNP23_MOUSE	Synaptosomal-associated protein 23 OS=Mus musculus GN=Snap23 PE=1 SV=1	**0.81**	2	2	0.02	2.75
RCN1_MOUSE	Reticulocalbin-1 OS=Mus musculus GN=Rcn1 PE=1 SV=1	**0.81**	2	2	0.05	6.42
RHOG_MOUSE	Rho-related GTP-binding protein RhoG OS=Mus musculus GN=Rhog PE=2 SV=1	**0.81**	3	3	0.19	23.00
CAPR1_MOUSE	Caprin-1 OS=Mus musculus GN=Caprin1 PE=1 SV=2	**0.81**	4	4	0.33	40.71
ADT2_MOUSE	ADP/ATP translocase 2 OS=Mus musculus GN=Slc25a5 PE=1 SV=3	**0.81**	41	14	0.22	27.36
VCAM1_MOUSE	Vascular cell adhesion protein 1 OS=Mus musculus GN=Vcam1 PE=1 SV=1	**0.81**	50	22	0.22	27.71
MCM8_MOUSE	DNA replication licensing factor MCM8 OS=Mus musculus GN=Mcm8 PE=2 SV=3	**0.80**	1	1	0.00	0.00
RICH2_MOUSE	Rho GTPase-activating protein RICH2 OS=Mus musculus GN=Rich2 PE=2 SV=1	**0.80**	1	1	0.00	0.00
RMTL1_MOUSE	RNA methyltransferase-like protein 1 OS=Mus musculus GN=Rnmtl1 PE=2 SV=1	**0.80**	1	1	0.00	0.00
PRDX3_MOUSE	Thioredoxin-dependent peroxide reductase, mitochondrial OS=Mus musculus GN=Prdx3 PE=1 SV=1	**0.80**	3	3	0.43	53.95
RL8_MOUSE	60S ribosomal protein L8 OS=Mus musculus GN=Rpl8 PE=2 SV=2	**0.80**	4	4	0.11	13.25
RL10L_MOUSE	60S ribosomal protein L10-like OS=Mus musculus GN=Rpl10l PE=2 SV=1	**0.80**	5	5	0.18	22.19
1433T_MOUSE	14-3-3 protein theta OS=Mus musculus GN=Ywhaq PE=1 SV=1	**0.80**	6	4	0.16	19.63
SEC62_MOUSE	Translocation protein SEC62 OS=Mus musculus GN=Sec62 PE=1 SV=1	**0.80**	2	2	0.34	42.06
ICAM1_MOUSE	Intercellular adhesion molecule 1 OS=Mus musculus GN=Icam1 PE=1 SV=1	**0.80**	40	15	0.16	19.87
1433B_MOUSE	14-3-3 protein beta/alpha OS=Mus musculus GN=Ywhab PE=1 SV=3	**0.80**	7	5	0.31	38.57
ACTG_MOUSE	Actin, cytoplasmic 2 OS=Mus musculus GN=Actg1 PE=1 SV=1	**0.79**	107	25	0.39	49.27
ECHA_MOUSE	Trifunctional enzyme subunit alpha, mitochondrial OS=Mus musculus GN=Hadha PE=1 SV=1	**0.79**	9	8	0.24	30.71
ALDR_MOUSE	Aldose reductase OS=Mus musculus GN=Akr1b1 PE=1 SV=3	**0.79**	1	1	0.00	0.00
IF2A_MOUSE	Eukaryotic translation initiation factor 2 subunit 1 OS=Mus musculus GN=Eif2s1 PE=1 SV=3	**0.79**	1	1	0.00	0.00
IF4E2_MOUSE	Eukaryotic translation initiation factor 4E type 2 OS=Mus musculus GN=Eif4e2 PE=1 SV=1	**0.79**	1	1	0.00	0.00
ROCK2_MOUSE	Rho-associated protein kinase 2 OS=Mus musculus GN=Rock2 PE=2 SV=1	**0.79**	1	1	0.00	0.00
TIAM1_MOUSE	T-lymphoma invasion and metastasis-inducing protein 1 OS=Mus musculus GN=Tiam1 PE=1 SV=1	**0.79**	1	1	0.00	0.00
RAB35_MOUSE	Ras-related protein Rab-35 OS=Mus musculus GN=Rab35 PE=1 SV=1	**0.78**	12	5	0.25	32.01
OST48_MOUSE	Dolichyl-diphosphooligosaccharide--protein glycosyltransferase 48 kDa subunit OS=Mus musculus GN=Ddost PE=1 SV=1	**0.78**	3	2	0.02	2.86
K2C5_MOUSE	Keratin, type II cytoskeletal 5 OS=Mus musculus GN=Krt5 PE=1 SV=1	**0.78**	11	2	0.38	48.57
1433G_MOUSE	14-3-3 protein gamma OS=Mus musculus GN=Ywhag PE=1 SV=2	**0.78**	8	6	0.21	26.46
TCPZ_MOUSE	T-complex protein 1 subunit zeta OS=Mus musculus GN=Cct6a PE=1 SV=3	**0.78**	2	2	0.10	12.38
RAB1A_MOUSE	Ras-related protein Rab-1A OS=Mus musculus GN=Rab1A PE=1 SV=3	**0.78**	15	8	0.21	27.43
RAB7A_MOUSE	Ras-related protein Rab-7a OS=Mus musculus GN=Rab7a PE=1 SV=2	**0.78**	11	10	0.17	21.26
RB11A_MOUSE	Ras-related protein Rab-11A OS=Mus musculus GN=Rab11a PE=1 SV=3	**0.78**	7	7	0.22	27.84
ARP2_MOUSE	Actin-related protein 2 OS=Mus musculus GN=Actr2 PE=1 SV=1	**0.77**	1	1	0.00	0.00
CD44_MOUSE	CD44 antigen OS=Mus musculus GN=Cd44 PE=1 SV=3	**0.77**	2	2	0.00	0.00
CD81_MOUSE	CD81 antigen OS=Mus musculus GN=Cd81 PE=1 SV=1	**0.77**	1	1	0.00	0.00
CLIC4_MOUSE	Chloride intracellular channel protein 4 OS=Mus musculus GN=Clic4 PE=1 SV=3	**0.77**	2	2	0.01	1.92
SSRB_MOUSE	Translocon-associated protein subunit beta OS=Mus musculus GN=Ssr2 PE=1 SV=1	**0.77**	1	1	0.00	0.00
COMT_MOUSE	Catechol O-methyltransferase OS=Mus musculus GN=Comt PE=1 SV=1	**0.77**	2	2	0.16	21.15
PCCB_MOUSE	Propionyl-CoA carboxylase beta chain, mitochondrial OS=Mus musculus GN=Pccb PE=1 SV=1	**0.77**	3	3	0.36	46.39
ODPB_MOUSE	Pyruvate dehydrogenase E1 component subunit beta, mitochondrial OS=Mus musculus GN=Pdhb PE=1 SV=1	**0.77**	6	5	0.60	77.12
NB5R3_MOUSE	NADH-cytochrome b5 reductase 3 OS=Mus musculus GN=Cyb5r3 PE=1 SV=3	**0.77**	18	10	0.25	32.77
ETFA_MOUSE	Electron transfer flavoprotein subunit alpha, mitochondrial OS=Mus musculus GN=Etfa PE=1 SV=2	**0.77**	8	5	0.29	37.86

Accession	Protein	H/L	#Cmpds	# quant	SD (H/L)	% CV
PLOD2_MOUSE	Procollagen-lysine,2-oxoglutarate 5-dioxygenase 2 OS=Mus musculus GN=Plod2 PE=2 SV=1	**0.77**	5	5	0.47	60.55
GNAS2_MOUSE	Guanine nucleotide-binding protein G(s) subunit alpha isoforms short OS=Mus musculus GN=Gnas PE=1 SV=1	**0.77**	6	2	0.17	22.33
PLST_MOUSE	Plastin-3 OS=Mus musculus GN=Pls3 PE=1 SV=3	**0.77**	5	5	0.31	40.26
CP1B1_MOUSE	Cytochrome P450 1B1 OS=Mus musculus GN=Cyp1b1 PE=2 SV=2	**0.76**	6	4	0.32	42.51
ADT1_MOUSE	ADP/ATP translocase 1 OS=Mus musculus GN=Slc25a4 PE=1 SV=4	**0.76**	21	12	0.26	34.78
RL7_MOUSE	60S ribosomal protein L7 OS=Mus musculus GN=Rpl7 PE=1 SV=2	**0.76**	3	3	0.12	15.27
CTHR1_MOUSE	Collagen triple helix repeat-containing protein 1 OS=Mus musculus GN=Cthrc1 PE=2 SV=1	**0.76**	1	1	0.00	0.00
RPN2_MOUSE	Dolichyl-diphosphooligosaccharide--protein glycosyltransferase subunit 2 OS=Mus musculus GN=Rpn2 PE=2 SV=1	**0.76**	5	3	0.21	27.91
H2AJ_MOUSE	Histone H2A.J OS=Mus musculus GN=H2afj PE=2 SV=1	**0.76**	1	1	0.00	0.00
ILF2_MOUSE	Interleukin enhancer-binding factor 2 OS=Mus musculus GN=Ilf2 PE=1 SV=1	**0.76**	1	1	0.00	0.00
MOSC2_MOUSE	MOSC domain-containing protein 2, mitochondrial OS=Mus musculus GN=Mosc2 PE=1 SV=1	**0.76**	1	1	0.00	0.00
YBOX1_MOUSE	Nuclease-sensitive element-binding protein 1 OS=Mus musculus GN=Ybx1 PE=1 SV=3	**0.76**	1	1	0.00	0.00
SFRS7_MOUSE	Splicing factor, arginine/serine-rich 7 OS=Mus musculus GN=Sfrs7 PE=1 SV=1	**0.76**	2	1	0.00	0.00
KPYM_MOUSE	Pyruvate kinase isozymes M1/M2 OS=Mus musculus GN=Pkm2 PE=1 SV=4	**0.76**	10	9	0.30	39.61
CNN2_MOUSE	Calponin-2 OS=Mus musculus GN=Cnn2 PE=2 SV=1	**0.76**	6	6	0.23	29.91
SC31A_MOUSE	Protein transport protein Sec31A OS=Mus musculus GN=Sec31a PE=1 SV=2	**0.75**	3	3	0.29	37.87
TBA1C_MOUSE	Tubulin alpha-1C chain OS=Mus musculus GN=Tuba1c PE=1 SV=1	**0.75**	21	7	0.11	14.21
ALDH2_MOUSE	Aldehyde dehydrogenase, mitochondrial OS=Mus musculus GN=Aldh2 PE=1 SV=1	**0.75**	9	7	0.23	30.00
1433E_MOUSE	14-3-3 protein epsilon OS=Mus musculus GN=Ywhae PE=1 SV=1	**0.75**	3	2	0.03	4.00
CMTD1_MOUSE	Catechol-O-methyltransferase domain-containing protein 1 OS=Mus musculus GN=Comtd1 PE=2 SV=1	**0.75**	1	1	0.00	0.00
ODO2_MOUSE	Dihydrolipoyllysine-residue succinyltransferase component of 2-oxoglutarate dehydrogenase complex, mitochondrial OS=Mus musculus GN=Dlst PE=1 SV=1	**0.75**	4	4	0.17	22.18
ERGI3_MOUSE	Endoplasmic reticulum-Golgi intermediate compartment protein 3 OS=Mus musculus GN=Ergic3 PE=2 SV=1	**0.75**	1	1	0.00	0.00
HNRPL_MOUSE	Heterogeneous nuclear ribonucleoprotein L OS=Mus musculus GN=Hnrnpl PE=1 SV=2	**0.75**	1	1	0.00	0.00
MYO1D_MOUSE	Myosin-Id OS=Mus musculus GN=Myo1d PE=1 SV=1	**0.75**	1	1	0.00	0.00
CLPP_MOUSE	Putative ATP-dependent Clp protease proteolytic subunit, mitochondrial OS=Mus musculus GN=Clpp PE=2 SV=1	**0.75**	1	1	0.00	0.00
SMC1B_MOUSE	Structural maintenance of chromosomes protein 1B OS=Mus musculus GN=Smc1b PE=1 SV=1	**0.75**	1	1	0.00	0.00
TCPD_MOUSE	T-complex protein 1 subunit delta OS=Mus musculus GN=Cct4 PE=1 SV=3	**0.75**	2	2	0.12	16.00
T176B_MOUSE	Transmembrane protein 176B OS=Mus musculus GN=Tmem176b PE=1 SV=1	**0.75**	1	1	0.00	0.00
NDUS3_MOUSE	NADH dehydrogenase [ubiquinone] iron-sulfur protein 3, mitochondrial OS=Mus musculus GN=Ndufs3 PE=1 SV=2	**0.74**	4	3	0.23	30.59
RAB8B_MOUSE	Ras-related protein Rab-8B OS=Mus musculus GN=Rab8b PE=1 SV=1	**0.74**	6	3	0.07	9.05
SCFD1_MOUSE	Sec1 family domain-containing protein 1 OS=Mus musculus GN=Scfd1 PE=2 SV=1	**0.74**	3	3	0.16	21.71
ATPG_MOUSE	ATP synthase subunit gamma, mitochondrial OS=Mus musculus GN=Atp5c1 PE=1 SV=1	**0.74**	8	5	0.33	44.51
GRPE1_MOUSE	GrpE protein homolog 1, mitochondrial OS=Mus musculus GN=Grpel1 PE=2 SV=1	**0.74**	2	2	0.07	9.09
SFRS3_MOUSE	Splicing factor, arginine/serine-rich 3 OS=Mus musculus GN=Sfrs3 PE=2 SV=1	**0.74**	2	2	0.07	9.09
RL15_MOUSE	60S ribosomal protein L15 OS=Mus musculus GN=Rpl15 PE=2 SV=4	**0.74**	2	2	0.01	1.01
MPRD_MOUSE	Cation-dependent mannose-6-phosphate receptor OS=Mus musculus GN=M6pr PE=2 SV=1	**0.74**	3	2	0.17	23.23
ECHB_MOUSE	Trifunctional enzyme subunit beta, mitochondrial OS=Mus musculus GN=Hadhb PE=1 SV=1	**0.73**	5	4	0.23	31.66
EF2_MOUSE	Elongation factor 2 OS=Mus musculus GN=Eef2 PE=1 SV=2	**0.73**	5	5	0.22	29.58
RS3A_MOUSE	40S ribosomal protein S3a OS=Mus musculus GN=Rps3a PE=1 SV=3	**0.73**	5	5	0.32	43.28
MOES_MOUSE	Moesin OS=Mus musculus GN=Msn PE=1 SV=3	**0.73**	28	24	0.33	45.69

Accession	Protein	H/L	#Cmpds	# quant	SD (H/L)	% CV
GRP75_MOUSE	Stress-70 protein, mitochondrial OS=Mus musculus GN=Hspa9 PE=1 SV=2	**0.73**	19	15	0.24	32.94
IF4A1_MOUSE	Eukaryotic initiation factor 4A-I OS=Mus musculus GN=Eif4a1 PE=2 SV=1	**0.73**	3	3	0.24	33.20
LONM_MOUSE	Lon protease homolog, mitochondrial OS=Mus musculus GN=Lonp1 PE=1 SV=2	**0.73**	1	1	0.00	0.00
NDUBA_MOUSE	NADH dehydrogenase [ubiquinone] 1 beta subcomplex subunit 10 OS=Mus musculus GN=Ndufb10 PE=1 SV=3	**0.73**	1	1	0.00	0.00
GDIB_MOUSE	Rab GDP dissociation inhibitor beta OS=Mus musculus GN=Gdi2 PE=1 SV=1	**0.73**	1	1	0.00	0.00
STX12_MOUSE	Syntaxin-12 OS=Mus musculus GN=Stx12 PE=2 SV=1	**0.73**	1	1	0.00	0.00
CAZA1_MOUSE	F-actin-capping protein subunit alpha-1 OS=Mus musculus GN=Capza1 PE=1 SV=4	**0.73**	3	3	0.27	36.96
QCR2_MOUSE	Cytochrome b-c1 complex subunit 2, mitochondrial OS=Mus musculus GN=Uqcrc2 PE=1 SV=1	**0.72**	5	5	0.17	23.95
H2B1C_MOUSE	Histone H2B type 1-C/E/G OS=Mus musculus GN=Hist1h2bc PE=1 SV=3	**0.72**	2	2	0.54	75.00
ACDSB_MOUSE	Short/branched chain specific acyl-CoA dehydrogenase, mitochondrial OS=Mus musculus GN=Acadsb PE=1 SV=1	**0.72**	2	2	0.21	29.17
3HIDH_MOUSE	3-hydroxyisobutyrate dehydrogenase, mitochondrial OS=Mus musculus GN=Hibadh PE=2 SV=1	**0.72**	1	1	0.00	0.00
AKA12_MOUSE	A-kinase anchor protein 12 OS=Mus musculus GN=Akap12 PE=1 SV=1	**0.72**	1	1	0.00	0.00
API5_MOUSE	Apoptosis inhibitor 5 OS=Mus musculus GN=Api5 PE=2 SV=1	**0.72**	1	1	0.00	0.00
CCD18_MOUSE	Coiled-coil domain-containing protein 18 OS=Mus musculus GN=Ccdc18 PE=2 SV=1	**0.72**	1	1	0.00	0.00
CC90B_MOUSE	Coiled-coil domain-containing protein 90B, mitochondrial OS=Mus musculus GN=Ccdc90b PE=2 SV=1	**0.72**	1	1	0.00	0.00
GHITM_MOUSE	Growth hormone-inducible transmembrane protein OS=Mus musculus GN=Ghitm PE=2 SV=1	**0.72**	1	1	0.00	0.00
H33_MOUSE	Histone H3.3 OS=Mus musculus GN=H3f3a PE=1 SV=2	**0.72**	1	1	0.00	0.00
S45A4_MOUSE	Solute carrier family 45 member 4 OS=Mus musculus GN=Slc45a4 PE=2 SV=1	**0.72**	3	1	0.00	0.00
VAPA_MOUSE	Vesicle-associated membrane protein-associated protein A OS=Mus musculus GN=Vapa PE=1 SV=2	**0.72**	6	5	0.18	24.72
CX4NB_MOUSE	Neighbor of COX4 OS=Mus musculus GN=Cox4nb PE=1 SV=1	**0.71**	5	4	0.45	63.32
SRPRB_MOUSE	Signal recognition particle receptor subunit beta OS=Mus musculus GN=Srprb PE=1 SV=1	**0.71**	3	3	0.07	9.81
VDAC1_MOUSE	Voltage-dependent anion-selective channel protein 1 OS=Mus musculus GN=Vdac1 PE=1 SV=3	**0.71**	12	9	0.33	46.51
CARKD_MOUSE	Carbohydrate kinase domain-containing protein OS=Mus musculus GN=Carkd PE=1 SV=1	**0.70**	1	1	0.00	0.00
CP2B9_MOUSE	Cytochrome P450 2B9 OS=Mus musculus GN=Cyp2b9 PE=2 SV=1	**0.70**	1	1	0.00	0.00
AL4A1_MOUSE	Delta-1-pyrroline-5-carboxylate dehydrogenase, mitochondrial OS=Mus musculus GN=Aldh4a1 PE=1 SV=2	**0.70**	2	2	0.24	34.04
SPAT5_MOUSE	Spermatogenesis-associated protein 5 OS=Mus musculus GN=Spata5 PE=2 SV=2	**0.70**	1	1	0.00	0.00
CJ118_MOUSE	Uncharacterized protein C10orf118 homolog OS=Mus musculus GN=Otg1 PE=2 SV=2	**0.70**	1	1	0.00	0.00
PDIA3_MOUSE	Protein disulfide-isomerase A3 OS=Mus musculus GN=Pdia3 PE=1 SV=2	**0.70**	37	30	0.27	39.15
IDH3A_MOUSE	Isocitrate dehydrogenase [NAD] subunit alpha, mitochondrial OS=Mus musculus GN=Idh3a PE=1 SV=1	**0.70**	3	3	0.22	31.56
RL6_MOUSE	60S ribosomal protein L6 OS=Mus musculus GN=Rpl6 PE=1 SV=3	**0.69**	5	5	0.36	51.48
FERM2_MOUSE	Fermitin family homolog 2 OS=Mus musculus GN=Fermt2 PE=2 SV=1	**0.69**	2	2	0.07	9.68
LAMP2_MOUSE	Lysosome-associated membrane glycoprotein 2 OS=Mus musculus GN=Lamp2 PE=2 SV=1	**0.69**	2	2	0.16	22.58
RL26_MOUSE	60S ribosomal protein L26 OS=Mus musculus GN=Rpl26 PE=2 SV=1	**0.69**	1	1	0.00	0.00
ATLA3_MOUSE	Atlastin-3 OS=Mus musculus GN=Atl3 PE=2 SV=1	**0.69**	2	2	0.03	4.35
MGST1_MOUSE	Microsomal glutathione S-transferase 1 OS=Mus musculus GN=Mgst1 PE=1 SV=3	**0.69**	1	1	0.00	0.00
OLF8_MOUSE	Olfactory receptor 8 OS=Mus musculus GN=Olfr8 PE=2 SV=2	**0.69**	1	1	0.00	0.00
PGRP4_MOUSE	Peptidoglycan recognition protein I-beta OS=Mus musculus GN=Pglyrp4 PE=2 SV=1	**0.69**	1	1	0.00	0.00
PPWD1_MOUSE	Peptidylprolyl isomerase domain and WD repeat-containing protein 1 OS=Mus musculus GN=Ppwd1 PE=2 SV=1	**0.69**	1	1	0.00	0.00
PRR18_MOUSE	Proline-rich protein 18 OS=Mus musculus GN=Prr18 PE=2 SV=2	**0.69**	1	1	0.00	0.00
TCPE_MOUSE	T-complex protein 1 subunit epsilon OS=Mus musculus GN=Cct5 PE=1 SV=1	**0.69**	1	1	0.00	0.00
MARCS_MOUSE	Myristoylated alanine-rich C-kinase substrate OS=Mus musculus GN=Marcks PE=1 SV=2	**0.68**	39	12	0.25	36.71

Accession	Protein	H/L	#Cmpds	# quant	SD (H/L)	% CV
ENOA_MOUSE	Alpha-enolase OS=Mus musculus GN=Eno1 PE=1 SV=3	**0.68**	18	14	0.24	35.52
1433Z_MOUSE	14-3-3 protein zeta/delta OS=Mus musculus GN=Ywhaz PE=1 SV=1	**0.68**	8	5	0.09	13.26
RL12_MOUSE	60S ribosomal protein L12 OS=Mus musculus GN=Rpl12 PE=1 SV=2	**0.67**	1	1	0.00	0.00
ML12B_MOUSE	Myosin regulatory light chain 12B OS=Mus musculus GN=Myl12b PE=1 SV=2	**0.67**	2	2	0.07	11.11
TPIS_MOUSE	Triosephosphate isomerase OS=Mus musculus GN=Tpi1 PE=1 SV=3	**0.67**	2	2	0.18	26.67
RLA0_MOUSE	60S acidic ribosomal protein P0 OS=Mus musculus GN=Rplp0 PE=1 SV=3	**0.66**	8	7	0.18	26.52
RL19_MOUSE	60S ribosomal protein L19 OS=Mus musculus GN=Rpl19 PE=1 SV=1	**0.66**	4	2	0.01	1.12
EF1G_MOUSE	Elongation factor 1-gamma OS=Mus musculus GN=Eef1g PE=1 SV=3	**0.66**	2	2	0.02	3.37
RL18A_MOUSE	60S ribosomal protein L18a OS=Mus musculus GN=Rpl18a PE=2 SV=1	**0.66**	5	4	0.14	22.09
EDC4_MOUSE	Enhancer of mRNA-decapping protein 4 OS=Mus musculus GN=Edc4 PE=1 SV=2	**0.66**	2	2	0.22	34.09
GLCM_MOUSE	Glucosylceramidase OS=Mus musculus GN=Gba PE=1 SV=1	**0.66**	3	2	0.06	9.09
CD47_MOUSE	Leukocyte surface antigen CD47 OS=Mus musculus GN=Cd47 PE=1 SV=2	**0.66**	1	1	0.00	0.00
NQO1_MOUSE	NAD(P)H dehydrogenase [quinone] 1 OS=Mus musculus GN=Nqo1 PE=1 SV=3	**0.66**	2	2	0.03	4.55
VDAC2_MOUSE	Voltage-dependent anion-selective channel protein 2 OS=Mus musculus GN=Vdac2 PE=1 SV=2	**0.65**	10	6	0.15	23.06
RS9_MOUSE	40S ribosomal protein S9 OS=Mus musculus GN=Rps9 PE=2 SV=3	**0.65**	4	4	0.11	16.35
RL13A_MOUSE	60S ribosomal protein L13a OS=Mus musculus GN=Rpl13a PE=1 SV=4	**0.65**	3	2	0.13	19.54
CALX_MOUSE	Calnexin OS=Mus musculus GN=Canx PE=1 SV=1	**0.65**	17	15	0.22	33.91
PAIRB_MOUSE	Plasminogen activator inhibitor 1 RNA-binding protein OS=Mus musculus GN=Serbp1 PE=1 SV=2	**0.64**	13	7	0.18	27.88
LRC59_MOUSE	Leucine-rich repeat-containing protein 59 OS=Mus musculus GN=Lrrc59 PE=2 SV=1	**0.64**	4	4	0.06	9.72
PRDX1_MOUSE	Peroxiredoxin-1 OS=Mus musculus GN=Prdx1 PE=1 SV=1	**0.64**	21	11	0.15	23.80
CAV1_MOUSE	Caveolin-1 OS=Mus musculus GN=Cav1 PE=1 SV=1	**0.64**	3	2	0.22	34.88
CD14_MOUSE	Monocyte differentiation antigen CD14 OS=Mus musculus GN=Cd14 PE=1 SV=1	**0.64**	6	5	0.32	49.81
PIMT_MOUSE	Protein-L-isoaspartate(D-aspartate) O-methyltransferase OS=Mus musculus GN=Pcmt1 PE=1 SV=3	**0.64**	1	1	0.00	0.00
TOM40_MOUSE	Mitochondrial import receptor subunit TOM40 homolog OS=Mus musculus GN=Tomm40 PE=1 SV=3	**0.63**	2	2	0.17	27.06
DDAH2_MOUSE	N(G),N(G)-dimethylarginine dimethylaminohydrolase 2 OS=Mus musculus GN=Ddah2 PE=1 SV=1	**0.63**	2	2	0.14	22.35
STML2_MOUSE	Stomatin-like protein 2 OS=Mus musculus GN=Stoml2 PE=1 SV=1	**0.63**	4	3	0.09	14.73
SYNPO_MOUSE	Synaptopodin OS=Mus musculus GN=Synpo PE=1 SV=2	**0.63**	13	5	0.16	25.85
RS7_MOUSE	40S ribosomal protein S7 OS=Mus musculus GN=Rps7 PE=2 SV=1	**0.63**	1	1	0.00	0.00
SIA8F_MOUSE	Alpha-2,8-sialyltransferase 8F OS=Mus musculus GN=St8sia6 PE=1 SV=1	**0.63**	1	1	0.00	0.00
CBR4_MOUSE	Carbonyl reductase 4 OS=Mus musculus GN=Cbr4 PE=2 SV=2	**0.63**	1	1	0.00	0.00
CPSF5_MOUSE	Cleavage and polyadenylation specificity factor subunit 5 OS=Mus musculus GN=Nudt21 PE=2 SV=1	**0.63**	1	1	0.00	0.00
GORS2_MOUSE	Golgi reassembly-stacking protein 2 OS=Mus musculus GN=Gorasp2 PE=1 SV=3	**0.63**	2	2	0.04	7.14
OX2G_MOUSE	OX-2 membrane glycoprotein OS=Mus musculus GN=Cd200 PE=1 SV=1	**0.63**	11	5	0.16	25.24
SCUB3_MOUSE	Signal peptide, CUB and EGF-like domain-containing protein 3 OS=Mus musculus GN=Scube3 PE=1 SV=1	**0.63**	1	1	0.00	0.00
CKAP4_MOUSE	Cytoskeleton-associated protein 4 OS=Mus musculus GN=Ckap4 PE=2 SV=2	**0.62**	22	16	0.24	39.22
ERLN2_MOUSE	Erlin-2 OS=Mus musculus GN=Erlin2 PE=1 SV=1	**0.62**	4	4	0.35	56.08
RL11_MOUSE	60S ribosomal protein L11 OS=Mus musculus GN=Rpl11 PE=1 SV=4	**0.61**	1	1	0.00	0.00
BASI_MOUSE	Basigin OS=Mus musculus GN=Bsg PE=1 SV=2	**0.61**	5	3	0.31	50.50
ENTP1_MOUSE	Ectonucleoside triphosphate diphosphohydrolase 1 OS=Mus musculus GN=Entpd1 PE=2 SV=1	**0.61**	4	4	0.13	21.61
EIF3H_MOUSE	Eukaryotic translation initiation factor 3 subunit H OS=Mus musculus GN=Eif3h PE=1 SV=1	**0.61**	2	2	0.15	24.39
FAM3C_MOUSE	Protein FAM3C OS=Mus musculus GN=Fam3c PE=1 SV=1	**0.61**	7	5	0.12	19.57

Accession	Protein	H/L	#Cmpds	# quant	SD (H/L)	% CV
ATP5H_MOUSE	ATP synthase subunit d, mitochondrial OS=Mus musculus GN=Atp5h PE=1 SV=3	**0.61**	3	3	0.32	52.41
PPIB_MOUSE	Peptidyl-prolyl cis-trans isomerase B OS=Mus musculus GN=Ppib PE=2 SV=2	**0.61**	4	3	0.22	35.48
TADBP_MOUSE	TAR DNA-binding protein 43 OS=Mus musculus GN=Tardbp PE=1 SV=1	**0.61**	3	3	0.04	7.05
RUVB1_MOUSE	RuvB-like 1 OS=Mus musculus GN=Ruvbl1 PE=1 SV=1	**0.60**	2	2	0.11	18.52
H2AY_MOUSE	Core histone macro-H2A.1 OS=Mus musculus GN=H2afy PE=1 SV=3	**0.60**	3	3	0.23	37.46
ARC1B_MOUSE	Actin-related protein 2/3 complex subunit 1B OS=Mus musculus GN=Arpc1b PE=2 SV=3	**0.60**	3	2	0.13	22.50
ERP29_MOUSE	Endoplasmic reticulum protein ERp29 OS=Mus musculus GN=Erp29 PE=1 SV=2	**0.59**	5	5	0.11	18.69
ODO1_MOUSE	2-oxoglutarate dehydrogenase E1 component, mitochondrial OS=Mus musculus GN=Ogdh PE=1 SV=3	**0.58**	1	1	0.00	0.00
ERD22_MOUSE	ER lumen protein retaining receptor 2 OS=Mus musculus GN=Kdelr2 PE=2 SV=1	**0.58**	1	1	0.00	0.00
MEN1_MOUSE	Menin OS=Mus musculus GN=Men1 PE=2 SV=1	**0.58**	1	1	0.00	0.00
RALA_MOUSE	Ras-related protein Ral-A OS=Mus musculus GN=Rala PE=1 SV=1	**0.58**	2	2	0.00	0.00
ATPO_MOUSE	ATP synthase subunit O, mitochondrial OS=Mus musculus GN=Atp5o PE=1 SV=1	**0.58**	4	3	0.11	19.16
RL3_MOUSE	60S ribosomal protein L3 OS=Mus musculus GN=Rpl3 PE=2 SV=2	**0.57**	6	6	0.25	43.17
RL13_MOUSE	60S ribosomal protein L13 OS=Mus musculus GN=Rpl13 PE=2 SV=3	**0.57**	13	10	0.26	45.75
MRP_MOUSE	MARCKS-related protein OS=Mus musculus GN=Marcksl1 PE=1 SV=2	**0.57**	7	3	0.29	50.82
M2OM_MOUSE	Mitochondrial 2-oxoglutarate/malate carrier protein OS=Mus musculus GN=Slc25a11 PE=1 SV=3	**0.57**	4	3	0.11	18.61
DECR_MOUSE	2,4-dienoyl-CoA reductase, mitochondrial OS=Mus musculus GN=Decr1 PE=1 SV=1	**0.57**	4	4	0.10	17.94
PDLI1_MOUSE	PDZ and LIM domain protein 1 OS=Mus musculus GN=Pdlim1 PE=2 SV=4	**0.57**	1	1	0.00	0.00
TMEDA_MOUSE	Transmembrane emp24 domain-containing protein 10 OS=Mus musculus GN=Tmed10 PE=2 SV=1	**0.57**	6	4	0.17	29.83
RS8_MOUSE	40S ribosomal protein S8 OS=Mus musculus GN=Rps8 PE=1 SV=2	**0.56**	8	7	0.23	41.16
PDIA1_MOUSE	Protein disulfide-isomerase OS=Mus musculus GN=P4hb PE=1 SV=1	**0.56**	27	20	0.15	27.51
RS4X_MOUSE	40S ribosomal protein S4, X isoform OS=Mus musculus GN=Rps4x PE=2 SV=2	**0.56**	5	4	0.19	34.24
CYB5B_MOUSE	Cytochrome b5 type B OS=Mus musculus GN=Cyb5b PE=1 SV=1	**0.55**	1	1	0.00	0.00
DHB12_MOUSE	Estradiol 17-beta-dehydrogenase 12 OS=Mus musculus GN=Hsd17b12 PE=2 SV=1	**0.55**	1	1	0.00	0.00
GDIR1_MOUSE	Rho GDP-dissociation inhibitor 1 OS=Mus musculus GN=Arhgdia PE=1 SV=3	**0.55**	1	1	0.00	0.00
AT5F1_MOUSE	ATP synthase subunit b, mitochondrial OS=Mus musculus GN=Atp5f1 PE=1 SV=1	**0.55**	9	7	0.13	23.46
BAP31_MOUSE	B-cell receptor-associated protein 31 OS=Mus musculus GN=Bcap31 PE=1 SV=3	**0.54**	9	6	0.02	4.10
RL21_MOUSE	60S ribosomal protein L21 OS=Mus musculus GN=Rpl21 PE=2 SV=3	**0.54**	1	1	0.00	0.00
VDAC3_MOUSE	Voltage-dependent anion-selective channel protein 3 OS=Mus musculus GN=Vdac3 PE=1 SV=1	**0.53**	10	4	0.02	4.23
LYPA2_MOUSE	Acyl-protein thioesterase 2 OS=Mus musculus GN=Lypla2 PE=1 SV=1	**0.52**	1	1	0.00	0.00
EF1B_MOUSE	Elongation factor 1-beta OS=Mus musculus GN=Eef1b PE=1 SV=5	**0.52**	1	1	0.00	0.00
LAMA2_MOUSE	Laminin subunit alpha-2 OS=Mus musculus GN=Lama2 PE=1 SV=1	**0.52**	1	1	0.00	0.00
SAE1_MOUSE	SUMO-activating enzyme subunit 1 OS=Mus musculus GN=Sae1 PE=2 SV=1	**0.52**	1	1	0.00	0.00
RL24_MOUSE	60S ribosomal protein L24 OS=Mus musculus GN=Rpl24 PE=2 SV=2	**0.52**	3	3	0.03	5.93
ES1_MOUSE	ES1 protein homolog, mitochondrial OS=Mus musculus GN=D10Jhu81e PE=1 SV=1	**0.51**	2	2	0.02	4.35
FHL1_MOUSE	Four and a half LIM domains protein 1 OS=Mus musculus GN=Fhl1 PE=2 SV=3	**0.51**	2	1	0.00	0.00
MLL4_MOUSE	Histone-lysine N-methyltransferase MLL4 OS=Mus musculus GN=Wbp7 PE=1 SV=2	**0.51**	1	1	0.00	0.00
PPIC_MOUSE	Peptidyl-prolyl cis-trans isomerase C OS=Mus musculus GN=Ppic PE=1 SV=1	**0.51**	3	2	0.00	0.00
KRT82_MOUSE	Keratin, type II cuticular Hb2 OS=Mus musculus GN=Krt82 PE=2 SV=1	**0.50**	2	2	0.01	1.49
RAB2A_MOUSE	Ras-related protein Rab-2A OS=Mus musculus GN=Rab2a PE=1 SV=1	**0.50**	2	2	0.04	7.46
SODM_MOUSE	Superoxide dismutase [Mn], mitochondrial OS=Mus musculus GN=Sod2 PE=1 SV=3	**0.49**	6	5	0.14	28.54

Accession	Protein	H/L	#Cmpds	# quant	SD (H/L)	% CV
ASAH1_MOUSE	Acid ceramidase OS=Mus musculus GN=Asah1 PE=2 SV=1	**0.49**	1	1	0.00	0.00
CD63_MOUSE	CD63 antigen OS=Mus musculus GN=Cd63 PE=2 SV=2	**0.49**	1	1	0.00	0.00
FUBP2_MOUSE	Far upstream element-binding protein 2 OS=Mus musculus GN=Khsrp PE=1 SV=1	**0.49**	1	1	0.00	0.00
GPDM_MOUSE	Glycerol-3-phosphate dehydrogenase, mitochondrial OS=Mus musculus GN=Gpd2 PE=1 SV=2	**0.49**	1	1	0.00	0.00
FA81A_MOUSE	Protein FAM81A OS=Mus musculus GN=Fam81a PE=2 SV=2	**0.49**	1	1	0.00	0.00
RS6_MOUSE	40S ribosomal protein S6 OS=Mus musculus GN=Rps6 PE=1 SV=1	**0.49**	3	3	0.11	21.43
TMED4_MOUSE	Transmembrane emp24 domain-containing protein 4 OS=Mus musculus GN=Tmed4 PE=2 SV=1	**0.48**	6	3	0.36	76.08
THIKA_MOUSE	3-ketoacyl-CoA thiolase A, peroxisomal OS=Mus musculus GN=Acaa1a PE=2 SV=1	**0.48**	1	1	0.00	0.00
SYIM_MOUSE	Isoleucyl-tRNA synthetase, mitochondrial OS=Mus musculus GN=Iars2 PE=2 SV=1	**0.48**	1	1	0.00	0.00
MINT_MOUSE	Msx2-interacting protein OS=Mus musculus GN=Spen PE=1 SV=2	**0.48**	1	1	0.00	0.00
PRDX4_MOUSE	Peroxiredoxin-4 OS=Mus musculus GN=Prdx4 PE=1 SV=1	**0.48**	2	2	0.06	12.50
PTRF_MOUSE	Polymerase I and transcript release factor OS=Mus musculus GN=Ptrf PE=1 SV=1	**0.48**	1	1	0.00	0.00
RIF1_MOUSE	Telomere-associated protein RIF1 OS=Mus musculus GN=Rif1 PE=1 SV=2	**0.48**	1	1	0.00	0.00
TPPC3_MOUSE	Trafficking protein particle complex subunit 3 OS=Mus musculus GN=Trappc3 PE=1 SV=1	**0.48**	1	1	0.00	0.00
SSRA_MOUSE	Translocon-associated protein subunit alpha OS=Mus musculus GN=Ssr1 PE=1 SV=1	**0.48**	4	2	0.04	9.38
RAN_MOUSE	GTP-binding nuclear protein Ran OS=Mus musculus GN=Ran PE=1 SV=3	**0.47**	5	3	0.08	16.78
RL7A_MOUSE	60S ribosomal protein L7a OS=Mus musculus GN=Rpl7a PE=2 SV=2	**0.47**	6	3	0.01	3.01
COF1_MOUSE	Cofilin-1 OS=Mus musculus GN=Cfl1 PE=1 SV=3	**0.46**	1	1	0.00	0.00
XRP2_MOUSE	Protein XRP2 OS=Mus musculus GN=Rp2 PE=2 SV=3	**0.46**	1	1	0.00	0.00
DYN3_MOUSE	Dynamin-3 OS=Mus musculus GN=Dnm3 PE=1 SV=1	**0.45**	1	1	0.00	0.00
FKB11_MOUSE	FK506-binding protein 11 OS=Mus musculus GN=Fkbp11 PE=2 SV=1	**0.45**	3	2	0.16	36.67
K2C8_MOUSE	Keratin, type II cytoskeletal 8 OS=Mus musculus GN=Krt8 PE=1 SV=4	**0.43**	22	5	0.06	14.30
CB078_MOUSE	Uncharacterized protein C2orf78 homolog OS=Mus musculus PE=2 SV=1	**0.43**	1	1	0.00	0.00
H10_MOUSE	Histone H1.0 OS=Mus musculus GN=H1f0 PE=2 SV=4	**0.42**	2	1	0.00	0.00
CEBPZ_MOUSE	CCAAT/enhancer-binding protein zeta OS=Mus musculus GN=Cebpz PE=2 SV=2	**0.40**	1	1	0.00	0.00
CNDG2_MOUSE	Condensin-2 complex subunit G2 OS=Mus musculus GN=Ncapg2 PE=2 SV=1	**0.40**	1	1	0.00	0.00
FAK1_MOUSE	Focal adhesion kinase 1 OS=Mus musculus GN=Ptk2 PE=1 SV=3	**0.40**	1	1	0.00	0.00
K2C79_MOUSE	Keratin, type II cytoskeletal 79 OS=Mus musculus GN=Krt79 PE=2 SV=2	**0.40**	8	1	0.00	0.00
RL17_MOUSE	60S ribosomal protein L17 OS=Mus musculus GN=Rpl17 PE=2 SV=3	**0.39**	2	2	0.04	9.43
RS25_MOUSE	40S ribosomal protein S25 OS=Mus musculus GN=Rps25 PE=2 SV=1	**0.39**	1	1	0.00	0.00
BCL7C_MOUSE	B-cell CLL/lymphoma 7 protein family member C OS=Mus musculus GN=Bcl7c PE=1 SV=1	**0.39**	1	1	0.00	0.00
SUCB2_MOUSE	Succinyl-CoA ligase [GDP-forming] subunit beta, mitochondrial OS=Mus musculus GN=Suclg2 PE=2 SV=3	**0.39**	2	1	0.00	0.00
TMM19_MOUSE	Transmembrane protein 19 OS=Mus musculus GN=Tmem19 PE=2 SV=1	**0.39**	1	1	0.00	0.00
K0090_MOUSE	Uncharacterized protein KIAA0090 OS=Mus musculus GN=Kiaa0090 PE=2 SV=1	**0.39**	1	1	0.00	0.00
KAP2_MOUSE	cAMP-dependent protein kinase type II-alpha regulatory subunit OS=Mus musculus GN=Prkar2a PE=1 SV=2	**0.39**	2	2	0.33	84.62
RS5_MOUSE	40S ribosomal protein S5 OS=Mus musculus GN=Rps5 PE=2 SV=3	**0.37**	1	1	0.00	0.00
IQEC1_MOUSE	IQ motif and SEC7 domain-containing protein 1 OS=Mus musculus GN=Iqsec1 PE=1 SV=2	**0.37**	1	1	0.00	0.00
RL29_MOUSE	60S ribosomal protein L29 OS=Mus musculus GN=Rpl29 PE=2 SV=2	**0.36**	2	2	0.00	0.00
AA3R_MOUSE	Adenosine A3 receptor OS=Mus musculus GN=Adora3 PE=2 SV=2	**0.36**	1	1	0.00	0.00
LRRC7_MOUSE	Leucine-rich repeat-containing protein 7 OS=Mus musculus GN=Lrrc7 PE=1 SV=2	**0.36**	1	1	0.00	0.00
RABE1_MOUSE	Rab GTPase-binding effector protein 1 OS=Mus musculus GN=Rabep1 PE=1 SV=1	**0.36**	1	1	0.00	0.00

Accession	Protein	H/L	#Cmpds	# quant	SD (H/L)	% CV
CYTIP_MOUSE	Cytohesin-interacting protein OS=Mus musculus GN=Cytip PE=2 SV=1	**0.34**	1	1	0.00	0.00
GASP1_MOUSE	G-protein coupled receptor-associated sorting protein 1 OS=Mus musculus GN=Gprasp1 PE=2 SV=1	**0.34**	1	1	0.00	0.00
SCRB2_MOUSE	Lysosome membrane protein 2 OS=Mus musculus GN=Scarb2 PE=1 SV=3	**0.33**	1	1	0.00	0.00
MYO1B_MOUSE	Myosin-Ib OS=Mus musculus GN=Myo1b PE=2 SV=2	**0.33**	1	1	0.00	0.00
ZYX_MOUSE	Zyxin OS=Mus musculus GN=Zyx PE=1 SV=1	**0.33**	1	1	0.00	0.00
EIF3D_MOUSE	Eukaryotic translation initiation factor 3 subunit D OS=Mus musculus GN=Eif3d PE=1 SV=2	**0.31**	1	1	0.00	0.00
RASF6_MOUSE	Ras association domain-containing protein 6 OS=Mus musculus GN=Rassf6 PE=2 SV=1	**0.30**	1	1	0.00	0.00
CSRP2_MOUSE	Cysteine and glycine-rich protein 2 OS=Mus musculus GN=Csrp2 PE=2 SV=3	**0.28**	1	1	0.00	0.00
RPGP2_MOUSE	Rap1 GTPase-activating protein 2 OS=Mus musculus GN=Garnl4 PE=1 SV=1	**0.25**	1	1	0.00	0.00
TRI67_MOUSE	Tripartite motif-containing protein 67 OS=Mus musculus GN=Trim67 PE=2 SV=1	**0.25**	1	1	0.00	0.00
TITIN_MOUSE	Titin OS=Mus musculus GN=Ttn PE=1 SV=1	**0.22**	1	1	0.00	0.00
MYO5B_MOUSE	Myosin-Vb OS=Mus musculus GN=Myo5b PE=2 SV=2	**0.18**	1	1	0.00	0.00
K1C15_MOUSE	Keratin, type I cytoskeletal 15 OS=Mus musculus GN=Krt15 PE=1 SV=2	**0.16**	3	1	0.00	0.00
K1C19_MOUSE	Keratin, type I cytoskeletal 19 OS=Mus musculus GN=Krt19 PE=2 SV=1	**0.16**	3	1	0.00	0.00
ZN276_MOUSE	Zinc finger protein 276 OS=Mus musculus GN=Znf276 PE=1 SV=3	**0.16**	1	1	0.00	0.00
XRN2_MOUSE	5'-3' exoribonuclease 2 OS=Mus musculus GN=Xrn2 PE=1 SV=1	**0.13**	1	1	0.00	0.00
POLK_MOUSE	DNA polymerase kappa OS=Mus musculus GN=Polk PE=1 SV=1	**0.13**	1	1	0.00	0.00
MAD1_MOUSE	MAD protein OS=Mus musculus GN=Mxd1 PE=1 SV=2	**0.12**	1	1	0.00	0.00
DACT2_MOUSE	Dapper homolog 2 OS=Mus musculus GN=Dact2 PE=2 SV=2	**0.10**	2	1	0.00	0.00
RPGF5_MOUSE	Rap guanine nucleotide exchange factor 5 OS=Mus musculus GN=Rapgef5 PE=2 SV=2	**0.10**	1	1	0.00	0.00
DAPLE_MOUSE	Protein Daple OS=Mus musculus GN=Ccdc88c PE=1 SV=1	**0.09**	1	1	0.00	0.00
TIF1A_MOUSE	Transcription intermediary factor 1-alpha OS=Mus musculus GN=Trim24 PE=1 SV=1	**0.09**	2	1	0.00	0.00
TNR6B_MOUSE	Trinucleotide repeat-containing gene 6B protein OS=Mus musculus GN=Tnrc6b PE=2 SV=2	**0.06**	2	1	0.00	0.00
SYT17_MOUSE	Synaptotagmin-17 OS=Mus musculus GN=Syt17 PE=2 SV=1	**0.04**	1	1	0.00	0.00

- CONCLUSIONS -

1st. TNFα can induce a tip cell phenotype in mouse endothelial cells, characterized by elongation and filopodia extension, as well as expression of the endothelial tip cell markers Jag1 and CXCR4 and increased MT1-MMP expression.

2nd. Quantitative proteomics (SILAC) performed in TNFα-activated immortalized mouse endothelial cells (wildtype versus MT1-MMP-deficient) has identified the MT1-MMP substrates in inflammation-activated endothelial tip cells: TSP1, NID1, CYR61 and SEM3C.

3rd. Bioinformatics analysis points to MT1-MMP combinatorial proteolytic programme, where processing of various MT1-MMP substrates instead of their individual processing determines the biological decisions in activated endothelial cells such as adhesion, motility, chemotaxis and vessel morphogenesis. In this combined programme matricelular protein TSP1 is a master regulator and contributes to all mentioned processes.

4th. The absence of MT1-MMP results in impaired processing and abnormal accumulation of TSP1, CYR61, NID1 and SEM3C in endothelial cells *in vitro* and *in vivo*.

5th. In an experimental animal model of DSS-induced colitis, levels of the angiogenic cytokine VEGF and inflammatory cytokine TNFα positively correlate with disease progression, leading to formation of new vessels and accumulation of inflammatory cells, respectively.

6th. MT1-MMP expression is upregulated in colon in animals treated with DSS and it is localized in epithelial cells in control conditions and in vessels and infiltrating inflammatory cells after DSS treatment.

7th. Soluble levels of MT1-MMP substrates TSP1 and NID in serum increase along DSS-induced mouse experimental colitis suggesting their release from the extracellular matrix likely by MT1-MMP-dependent processing. The expression pattern of TSP1 and NID1 in colon changes along disease progression being upregulated in vessels and inflammatory cells in severe condition.

8th. Soluble levels of TSP1 and NID1 are higher in serum from patients affected with ulcerative colitis or Crohn's disease with low disease activity supporting the potential use of these MT1-MMP substrates as biomarkers in chronic inflammatory disorders.

- CONCLUSIONES -

1º. La citoquina inflamatoria TNFα induce el fenotipo 'tip' (líder) en células endoteliales de ratón, caracterizado por la morfología alargada y por la expresión de los marcadores Jag1 y CXCR4 y de la proteasa MT1-MMP.

2º. El ensayo de proteómica cuantitativa SILAC realizado en células endoteliales de ratón inmortalizadas (genotipo silvestre versus deficientes en MT1-MMP) y activadas con TNFα ha identificado la colección de sustratos de MT1-MMP en células endoteliales 'tip' inflamatorias. Estos sustratos incluye las proteínas TSP1, NID1, CYR61 y SEM3C.

3º. El análisis bioinformático de los datos proteómicos ha desvelado un programa proteolítico combinatorial, en el cual el procesamiento combinado de varios sustratos por MT1-MMP en vez del procesamiento de sustratos individuales es el que determina las decisiones biológicas de las células endoteliales activadas tales como quimiotaxis, motilidad y adhesión celular, y desarrollo vascular. En este programa combinatorial el procesamiento de la proteína matricelular TSP1 es esencial y contribuye a todos los procesos biológicos mencionados.

4º. La ausencia de MT1-MMP disminuye el procesamiento y conlleva a la acumulación anómala de TSP1, CYR61, NID1 y SEM3C en células endoteliales *in vitro* e *in vivo*.

5º. En el modelo animal experimental de colitis inducida por DSS, los niveles séricos de la citoquina inflamatoria TNFα y del factor angiogénico VEGF-A correlacionan positivamente con la progresión de enfermedad y con la acumulación de células inflamatorias y la formación de nuevos vasos, respectivamente.

6º. La expresión de MT1-MMP aumenta en el colon de ratones tratados con DSS localizándose en células epiteliales en condiciones basales y en vasos y en células del infiltrado inflamatorio tras el tratamiento con DSS.

7º. Los niveles séricos de los sustratos de MT1-MMP TSP1 y NID1 aumentan con la colitis inducida por DSS, sugiriendo su liberación desde la matriz extracelular por la acción proteolítica de MT1-MMP. La distribución tisular en colon de TSP1 y NID1 también cambia a lo largo de la progresión de la enfermedad, aumentando en vasos y células inflamatorias en condiciones severas.

8º. Los niveles solubles de TSP1 y NID1 están aumentados en los sueros de los pacientes afectados por colitis ulcerosa o enfermedad de Crohn de baja actividad apoyando el uso potencial de estos sustratos de MT1-MMP como biomarcadores en enfermedades inflamatorias crónicas

Adams, J. C. (2004), 'Functions of the conserved thrombospondin carboxy-terminal cassette in cell-extracellular matrix interactions and signaling', *Int J Biochem Cell Biol,* 36 (6), 1102-14.

Adams, R. H. and Eichmann, A. (2010), 'Axon guidance molecules in vascular patterning', *Cold Spring Harb Perspect Biol,* 2 (5), a001875.

Al-Shahrour, F., Diaz-Uriarte, R., and Dopazo, J. (2004), 'FatiGO: a web tool for finding significant associations of Gene Ontology terms with groups of genes', *Bioinformatics,* 20 (4), 578-80.

Alfranca, A., et al. (2008), 'PGE2 induces angiogenesis via MT1-MMP-mediated activation of the TGFbeta/Alk5 signaling pathway', *Blood,* 112 (4), 1120-8.

Allegrini, G., et al. (2004), 'Thrombospondin-1 plus irinotecan: a novel antiangiogenic-chemotherapeutic combination that inhibits the growth of advanced human colon tumor xenografts in mice', *Cancer Chemother Pharmacol,* 53 (3), 261-6.

Anilkumar, N., et al. (2005), 'Palmitoylation at Cys574 is essential for MT1-MMP to promote cell migration', *FASEB J,* 19 (10), 1326-8.

Aplin, A. C., et al. (2009), 'Vascular regression and survival are differentially regulated by MT1-MMP and TIMPs in the aortic ring model of angiogenesis', *Am J Physiol Cell Physiol,* 297 (2), C471-80.

Apte, S. S., et al. (1997), 'The matrix metalloproteinase-14 (MMP-14) gene is structurally distinct from other MMP genes and is co-expressed with the TIMP-2 gene during mouse embryogenesis', *J Biol Chem,* 272 (41), 25511-7.

Armulik, A., Abramsson, A., and Betsholtz, C. (2005), 'Endothelial/pericyte interactions', *Circ Res,* 97 (6), 512-23.

Baciu, P. C., et al. (2003), 'Membrane type-1 matrix metalloproteinase (MT1-MMP) processing of pro-alphav integrin regulates cross-talk between alphavbeta3 and alpha2beta1 integrins in breast carcinoma cells', *Exp Cell Res,* 291 (1), 167-75.

Baker, A. H., Edwards, D. R., and Murphy, G. (2002), 'Metalloproteinase inhibitors: biological actions and therapeutic opportunities', *J Cell Sci,* 115 (Pt 19), 3719-27.

Balbín, M., et al. (2003), 'Loss of collagenase-2 confers increased skin tumor susceptibility to male mice', *Nat Genet,* 35 (3), 252-7.

Baluk, P., et al. (2004), 'Regulated angiogenesis and vascular regression in mice overexpressing vascular endothelial growth factor in airways', *Am J Pathol,* 165 (4), 1071-85.

Basile, J. R., et al. (2006), 'Semaphorin 4D provides a link between axon guidance processes and tumor-induced angiogenesis', *Proc Natl Acad Sci U S A,* 103 (24), 9017-22.

Beck, M., et al. (2011), 'The quantitative proteome of a human cell line', *Mol Syst Biol,* 7, 549.

Belkin, A. M., et al. (2001), 'Matrix-dependent proteolysis of surface transglutaminase by membrane-type metalloproteinase regulates cancer cell adhesion and locomotion', *J Biol Chem,* 276 (21), 18415-22.

Belotti, D., et al. (2003), 'Matrix metalloproteinases (MMP9 and MMP2) induce the release of vascular endothelial growth factor (VEGF) by ovarian carcinoma cells: implications for ascites formation', *Cancer Res,* 63 (17), 5224-9.

Benedito, R., et al. (2009), 'The notch ligands Dll4 and Jagged1 have opposing effects on angiogenesis', *Cell,* 137 (6), 1124-35.

Bergers, G., et al. (2000), 'Matrix metalloproteinase-9 triggers the angiogenic switch during carcinogenesis', *Nat Cell Biol,* 2 (10), 737-44.

Betsholtz, C., Lindblom, P., and Gerhardt, H. (2005), 'Role of pericytes in vascular morphogenesis', *EXS,* (94), 115-25.

Biswas, C., et al. (1995), 'The human tumor cell-derived collagenase stimulatory factor (renamed EMMPRIN) is a member of the immunoglobulin superfamily', *Cancer Res,* 55 (2), 434-9.

Borden, P. and Heller, R. A. (1997), 'Transcriptional control of matrix metalloproteinases and the tissue inhibitors of matrix metalloproteinases', *Crit Rev Eukaryot Gene Expr,* 7 (1-2), 159-78.

Butler, G. S., et al. (2008), 'Pharmacoproteomics of a metalloproteinase hydroxamate inhibitor in breast cancer cells: dynamics of membrane type 1 matrix metalloproteinase-mediated membrane protein shedding', *Mol Cell Biol,* 28 (15), 4896-914.

Butler, G. S., et al. (2009), 'Membrane protease degradomics: proteomic identification and quantification of cell surface protease substrates', *Methods Mol Biol,* 528, 159-76.

Canals, F., et al. (2006), 'Identification of substrates of the extracellular protease ADAMTS1 by DIGE proteomic analysis', *Proteomics,* 6 Suppl 1, S28-35.

Carmeliet, P. (2003), 'Angiogenesis in health and disease', *Nat Med,* 9 (6), 653-60.

Caterina, J. J., et al. (2002), 'Enamelysin (matrix metalloproteinase 20)-deficient mice display an amelogenesis imperfecta phenotype', *J Biol Chem,* 277 (51), 49598-604.

Cauwe, B., Van den Steen, P. E., and Opdenakker, G. (2007), 'The biochemical, biological, and pathological kaleidoscope of cell surface substrates processed by matrix metalloproteinases', *Crit Rev Biochem Mol Biol,* 42 (3), 113-85.

Chantrain, C. F., et al. (2004), 'Stromal matrix metalloproteinase-9 regulates the vascular architecture in neuroblastoma by promoting pericyte recruitment', *Cancer Res,* 64 (5), 1675-86.

Cheng, J., et al. (2009), 'Cellular transformation by Simian Virus 40 and Murine Polyoma Virus T antigens', *Semin Cancer Biol,* 19 (4), 218-28.

Chun, T. H., et al. (2004), 'MT1-MMP-dependent neovessel formation within the confines of the three-dimensional extracellular matrix', *J Cell Biol,* 167 (4), 757-67.

Colnot, C., et al. (2003), 'Altered fracture repair in the absence of MMP9', *Development,* 130 (17), 4123-33.

Cornelius, L. A., et al. (1998), 'Matrix metalloproteinases generate angiostatin: effects on neovascularization', *J Immunol,* 161 (12), 6845-52.

Coussens, L. M., Fingleton, B., and Matrisian, L. M. (2002), 'Matrix metalloproteinase inhibitors and cancer: trials and tribulations', *Science,* 295 (5564), 2387-92.

Covington, M. D., Burghardt, R. C., and Parrish, A. R. (2006), 'Ischemia-induced cleavage of cadherins in NRK cells requires MT1-MMP (MMP-14)', *Am J Physiol Renal Physiol,* 290 (1), F43-51.

Crawford, Y. and Ferrara, N. (2009), 'Tumor and stromal pathways mediating refractoriness/resistance to anti-angiogenic therapies', *Trends Pharmacol Sci,* 30 (12), 624-30.

Cromer, W. E., et al. (2011), 'Role of the endothelium in inflammatory bowel diseases', *World J Gastroenterol,* 17 (5), 578-93.

Curran, S., et al. (2004), 'Matrix metalloproteinase/tissue inhibitors of matrix metalloproteinase phenotype identifies poor prognosis colorectal cancers', *Clin Cancer Res,* 10 (24), 8229-34.

D'Alessio, S., et al. (2008), 'Tissue inhibitor of metalloproteinases-2 binding to membrane-type 1 matrix metalloproteinase induces MAPK activation and cell growth by a non-proteolytic mechanism', *J Biol Chem,* 283 (1), 87-99.

D'Haese, A., et al. (2000), 'In vivo neutrophil recruitment by granulocyte chemotactic protein-2 is assisted by gelatinase B/MMP-9 in the mouse', *J Interferon Cytokine Res,* 20 (7), 667-74.

d'Ortho, M. P., et al. (1997), 'Membrane-type matrix metalloproteinases 1 and 2 exhibit broad-spectrum proteolytic capacities comparable to many matrix metalloproteinases', *Eur J Biochem,* 250 (3), 751-7.

Danese, S., De la Rue, S. A., and Gasbarrini, A. (2005), 'Antibody to alpha4beta7 integrin for ulcerative colitis', *N Engl J Med,* 353 (11), 1180-1; author reply 80-1.

De Smet, F., et al. (2009), 'Mechanisms of vessel branching: filopodia on endothelial tip cells lead the way', *Arterioscler Thromb Vasc Biol,* 29 (5), 639-49.

del Toro, R., et al. (2010), 'Identification and functional analysis of endothelial tip cell-enriched genes', *Blood,* 116 (19), 4025-33.

Denekamp, J. (1984), 'Vascular endothelium as the vulnerable element in tumours', *Acta Radiol Oncol,* 23 (4), 217-25.

Deryugina, E. I., Soroceanu, L., and Strongin, A. Y. (2002a), 'Up-regulation of vascular endothelial growth factor by membrane-type 1 matrix metalloproteinase stimulates human glioma xenograft growth and angiogenesis', *Cancer Res,* 62 (2), 580-8.

Deryugina, E. I., et al. (2002b), 'Processing of integrin alpha(v) subunit by membrane type 1 matrix metalloproteinase stimulates migration of breast carcinoma cells on vitronectin and enhances tyrosine phosphorylation of focal adhesion kinase', *J Biol Chem,* 277 (12), 9749-56.

Destaing, O., et al. (2011), 'Invadosome regulation by adhesion signaling', *Curr Opin Cell Biol,* 23 (5), 597-606.

Di Sabatino, A., et al. (2004), 'Serum bFGF and VEGF correlate respectively with bowel wall thickness and intramural blood flow in Crohn's disease', *Inflamm Bowel Dis,* 10 (5), 573-7.

Doucet, A., et al. (2008), 'Metadegradomics: toward in vivo quantitative degradomics of proteolytic post-translational modifications of the cancer proteome', *Mol Cell Proteomics,* 7 (10), 1925-51.

Duffy, M. J., et al. (2000), 'Metalloproteinases: role in breast carcinogenesis, invasion and metastasis', *Breast Cancer Res,* 2 (4), 252-7.

Egawa, N., et al. (2006), 'Membrane type 1 matrix metalloproteinase (MT1-MMP/MMP-14) cleaves and releases a 22-kDa extracellular matrix metalloproteinase inducer (EMMPRIN) fragment from tumor cells', *J Biol Chem,* 281 (49), 37576-85.

Egeblad, M. and Werb, Z. (2002), 'New functions for the matrix metalloproteinases in cancer progression', *Nat Rev Cancer,* 2 (3), 161-74.

Eilken, H. M. and Adams, R. H. (2010), 'Dynamics of endothelial cell behavior in sprouting angiogenesis', *Curr Opin Cell Biol,* 22 (5), 617-25.

Endo, K., et al. (2003), 'Cleavage of syndecan-1 by membrane type matrix metalloproteinase-1 stimulates cell migration', *J Biol Chem,* 278 (42), 40764-70.

Esselens, C., et al. (2010), 'The cleavage of semaphorin 3C induced by ADAMTS1 promotes cell migration', *J Biol Chem,* 285 (4), 2463-73.

Evans, B. R., et al. (2012), 'Mutation of membrane type-1 metalloproteinase, MT1-MMP, causes the multicentric osteolysis and arthritis disease Winchester syndrome', *Am J Hum Genet,* 91 (3), 572-6.

Fantin, A., et al. (2010), 'Tissue macrophages act as cellular chaperones for vascular anastomosis downstream of VEGF-mediated endothelial tip cell induction', *Blood,* 116 (5), 829-40.

Ferrara, N. (1999), 'Role of vascular endothelial growth factor in the regulation of angiogenesis', *Kidney Int,* 56 (3), 794-814.

Filippov, S., et al. (2005), 'MT1-matrix metalloproteinase directs arterial wall invasion and neointima formation by vascular smooth muscle cells', *J Exp Med,* 202 (5), 663-71.

Fisher, K. E., et al. (2009), 'MT1-MMP- and Cdc42-dependent signaling co-regulate cell invasion and tunnel formation in 3D collagen matrices', *J Cell Sci,* 122 (Pt 24), 4558-69.

Folgueras, A. R., et al. (2004), 'Matrix metalloproteinases in cancer: from new functions to improved inhibition strategies', *Int J Dev Biol,* 48 (5-6), 411-24.

Folkman, J. (1995a), 'Angiogenesis in cancer, vascular, rheumatoid and other disease', *Nat Med,* 1 (1), 27-31.

Folkman, J. (1995b), 'Seminars in Medicine of the Beth Israel Hospital, Boston. Clinical applications of research on angiogenesis', *N Engl J Med,* 333 (26), 1757-63.

Forget, M. A., Desrosiers, R. R., and Béliveau, R. (1999), 'Physiological roles of matrix metalloproteinases: implications for tumor growth and metastasis', *Can J Physiol Pharmacol,* 77 (7), 465-80.

Frittoli, E., et al. (2011), 'Secretory and endo/exocytic trafficking in invadopodia formation: the MT1-MMP paradigm', *Eur J Cell Biol,* 90 (2-3), 108-14.

Galvez, B. G., et al. (2001), 'Membrane type 1-matrix metalloproteinase is activated during migration of human endothelial cells and modulates endothelial motility and matrix remodeling', *J Biol Chem,* 276 (40), 37491-500.

Galvez, B. G., et al. (2002), 'ECM regulates MT1-MMP localization with beta1 or alphavbeta3 integrins at distinct cell compartments modulating its internalization and activity on human endothelial cells', *J Cell Biol,* 159 (3), 509-21.

Galvez, B. G., et al. (2004), 'Caveolae are a novel pathway for membrane-type 1 matrix metalloproteinase traffic in human endothelial cells', *Mol Biol Cell,* 15 (2), 678-87.

Galvez, B. G., et al. (2005), 'Membrane type 1-matrix metalloproteinase is regulated by chemokines monocyte-chemoattractant protein-1/ccl2 and interleukin-8/CXCL8 in endothelial cells during angiogenesis', *J Biol Chem,* 280 (2), 1292-8.

Gálvez, B. G., et al. (2005), 'Membrane type 1-matrix metalloproteinase is regulated by chemokines monocyte-chemoattractant protein-1/ccl2 and interleukin-8/CXCL8 in endothelial cells during angiogenesis', *J Biol Chem,* 280 (2), 1292-8.

Genis, L., et al. (2007), 'Functional interplay between endothelial nitric oxide synthase and membrane type 1 matrix metalloproteinase in migrating endothelial cells', *Blood,* 110 (8), 2916-23.

Gerhardt, H., et al. (2003), 'VEGF guides angiogenic sprouting utilizing endothelial tip cell filopodia', *J Cell Biol,* 161 (6), 1163-77.

Geudens, I. and Gerhardt, H. (2011), 'Coordinating cell behaviour during blood vessel formation', *Development,* 138 (21), 4569-83.

Gingras, D. and Béliveau, R. (2010), 'Emerging concepts in the regulation of membrane-type 1 matrix metalloproteinase activity', *Biochim Biophys Acta,* 1803 (1), 142-50.

Golubkov, V. S., et al. (2005), 'Centrosomal pericentrin is a direct cleavage target of membrane type-1 matrix metalloproteinase in humans but not in mice: potential implications for tumorigenesis', *J Biol Chem,* 280 (51), 42237-41.

Gonzalo, P. and Arroyo, A. G. (2010), 'MT1-MMP: A novel component of the macrophage cell fusion machinery', *Commun Integr Biol,* 3 (3), 256-9.

Gonzalo, P., et al. (2010), 'MT1-MMP is required for myeloid cell fusion via regulation of Rac1 signaling', *Dev Cell,* 18 (1), 77-89.

GROSS, J. and LAPIERE, C. M. (1962), 'Collagenolytic activity in amphibian tissues: a tissue culture assay', *Proc Natl Acad Sci U S A,* 48, 1014-22.

Guillon-Munos, A., et al. (2011), 'Kallikrein-related peptidase 12 hydrolyzes matricellular proteins of the CCN family and modifies interactions of CCN1 and CCN5 with growth factors', *J Biol Chem,* 286 (29), 25505-18.

Guo, L., et al. (2012), 'Shedding of kidney injury molecule-1 by membrane-type 1 matrix metalloproteinase', *J Biochem,* 152 (5), 425-32.

Haas, T. L., et al. (1999), 'Egr-1 mediates extracellular matrix-driven transcription of membrane type 1 matrix metalloproteinase in endothelium', *J Biol Chem,* 274 (32), 22679-85.

Hamano, Y., et al. (2003), 'Physiological levels of tumstatin, a fragment of collagen IV alpha3 chain, are generated by MMP-9 proteolysis and suppress angiogenesis via alphaV beta3 integrin', *Cancer Cell,* 3 (6), 589-601.

Han, Y. P., et al. (2001), 'TNF-alpha stimulates activation of pro-MMP2 in human skin through NF-(kappa)B mediated induction of MT1-MMP', *J Cell Sci,* 114 (Pt 1), 131-39.

Harris, M. A., et al. (2004), 'The Gene Ontology (GO) database and informatics resource', *Nucleic Acids Res,* 32 (Database issue), D258-61.

Hasan, A., et al. (2011), 'The matricellular protein cysteine-rich protein 61 (CCN1/Cyr61) enhances physiological adaptation of retinal vessels and reduces pathological neovascularization associated with ischemic retinopathy', *J Biol Chem,* 286 (11), 9542-54.

Hellström, M., et al. (2007), 'Dll4 signalling through Notch1 regulates formation of tip cells during angiogenesis', *Nature,* 445 (7129), 776-80.

Hikita, A., et al. (2006), 'Negative regulation of osteoclastogenesis by ectodomain shedding of receptor activator of NF-kappaB ligand', *J Biol Chem,* 281 (48), 36846-55.

Hiller, O., et al. (2000), 'Matrix metalloproteinases collagenase-2, macrophage elastase, collagenase-3, and membrane type 1-matrix metalloproteinase impair clotting by degradation of fibrinogen and factor XII', *J Biol Chem,* 275 (42), 33008-13.

Hiraoka, N., et al. (1998), 'Matrix metalloproteinases regulate neovascularization by acting as pericellular fibrinolysins', *Cell,* 95 (3), 365-77.

Hiratsuka, S., et al. (2002), 'MMP9 induction by vascular endothelial growth factor receptor-1 is involved in lung-specific metastasis', *Cancer Cell,* 2 (4), 289-300.

Ho, M. S., et al. (2008), 'Nidogens-Extracellular matrix linker molecules', *Microsc Res Tech,* 71 (5), 387-95.

Holmbeck, K., et al. (2003), 'MT1-MMP-dependent, apoptotic remodeling of unmineralized cartilage: a critical process in skeletal growth', *J Cell Biol,* 163 (3), 661-71.

Holmbeck, K., et al. (2005), 'The metalloproteinase MT1-MMP is required for normal development and maintenance of osteocyte processes in bone', *J Cell Sci,* 118 (Pt 1), 147-56.

Holmbeck, K., et al. (1999), 'MT1-MMP-deficient mice develop dwarfism, osteopenia, arthritis, and connective tissue disease due to inadequate collagen turnover', *Cell,* 99 (1), 81-92.

Holopainen, J. M., et al. (2003), 'Activation of matrix metalloproteinase-8 by membrane type 1-MMP and their expression in human tears after photorefractive keratectomy', *Invest Ophthalmol Vis Sci,* 44 (6), 2550-6.

Hotary, K. B., et al. (2002), 'Matrix metalloproteinases (MMPs) regulate fibrin-invasive activity via MT1-MMP-dependent and -independent processes', *J Exp Med,* 195 (3), 295-308.

Huang, da W, et al. (2008), 'DAVID gene ID conversion tool', *Bioinformation,* 2 (10), 428-30.

Huang, P. H., et al. (2009), 'Matrix metalloproteinase-9 is essential for ischemia-induced neovascularization by modulating bone marrow-derived endothelial progenitor cells', *Arterioscler Thromb Vasc Biol,* 29 (8), 1179-84.

Hwang, I. K., et al. (2004), 'A proteomic approach to identify substrates of matrix metalloproteinase-14 in human plasma', *Biochim Biophys Acta,* 1702 (1), 79-87.

Ichaso, N. and Dilworth, S. M. (2001), 'Cell transformation by the middle T-antigen of polyoma virus', *Oncogene,* 20 (54), 7908-16.

Inada, M., et al. (2004), 'Critical roles for collagenase-3 (Mmp13) in development of growth plate cartilage and in endochondral ossification', *Proc Natl Acad Sci U S A,* 101 (49), 17192-7.

Iruela-Arispe, M. L., Luque, A., and Lee, N. (2004), 'Thrombospondin modules and angiogenesis', *Int J Biochem Cell Biol,* 36 (6), 1070-8.

Itoh, Y. and Nagase, H. (2002), 'Matrix metalloproteinases in cancer', *Essays Biochem,* 38, 21-36.

Itoh, Y. and Seiki, M. (2006), 'MT1-MMP: a potent modifier of pericellular microenvironment', *J Cell Physiol,* 206 (1), 1-8.

Itoh, Y., et al. (1999), 'Membrane type 4 matrix metalloproteinase (MT4-MMP, MMP-17) is a glycosylphosphatidylinositol-anchored proteinase', *J Biol Chem,* 274 (48), 34260-6.

Jakobsson, L., et al. (2010), 'Endothelial cells dynamically compete for the tip cell position during angiogenic sprouting', *Nat Cell Biol,* 12 (10), 943-53.

Johnson, C., et al. (2004), 'Matrix metalloproteinase-9 is required for adequate angiogenic revascularization of ischemic tissues: potential role in capillary branching', *Circ Res,* 94 (2), 262-8.

Kadono, Y., et al. (1998), 'Membrane type 1-matrix metalloproteinase is involved in the formation of hepatocyte growth factor/scatter factor-induced branching tubules in madin-darby canine kidney epithelial cells', *Biochem Biophys Res Commun,* 251 (3), 681-7.

Kanazawa, S., et al. (2001), 'VEGF, basic-FGF, and TGF-beta in Crohn's disease and ulcerative colitis: a novel mechanism of chronic intestinal inflammation', *Am J Gastroenterol,* 96 (3), 822-8.

Kanehisa, M., et al. (2004), 'The KEGG resource for deciphering the genome', *Nucleic Acids Res,* 32 (Database issue), D277-80.

Karagiannis, E. D. and Popel, A. S. (2006), 'Distinct modes of collagen type I proteolysis by matrix metalloproteinase (MMP) 2 and membrane type I MMP during the migration of a tip endothelial cell: insights from a computational model', *J Theor Biol,* 238 (1), 124-45.

Karsdal, M. A., et al. (2002), 'Matrix metalloproteinase-dependent activation of latent transforming growth factor-beta controls the conversion of osteoblasts into osteocytes by blocking osteoblast apoptosis', *J Biol Chem,* 277 (46), 44061-7.

Kazerounian, S., et al. (2011), 'Priming of the vascular endothelial growth factor signaling pathway by thrombospondin-1, CD36, and spleen tyrosine kinase', *Blood,* 117 (17), 4658-66.

Kennedy, A. M., et al. (2005), 'MMP13 mutation causes spondyloepimetaphyseal dysplasia, Missouri type (SEMD(MO)', *J Clin Invest,* 115 (10), 2832-42.

Kheradmand, F., Rishi, K., and Werb, Z. (2002), 'Signaling through the EGF receptor controls lung morphogenesis in part by regulating MT1-MMP-mediated activation of gelatinase A/MMP2', *J Cell Sci,* 115 (Pt 4), 839-48.

Kim, J. W., et al. (2005), 'MMP-20 mutation in autosomal recessive pigmented hypomaturation amelogenesis imperfecta', *J Med Genet,* 42 (3), 271-5.

Kojima, S., et al. (2000), 'Membrane-type 6 matrix metalloproteinase (MT6-MMP, MMP-25) is the second glycosyl-phosphatidyl inositol (GPI)-anchored MMP', *FEBS Lett,* 480 (2-3), 142-6.

Koshikawa, N., et al. (2000), 'Role of cell surface metalloprotease MT1-MMP in epithelial cell migration over laminin-5', *J Cell Biol,* 148 (3), 615-24.

Koziol, A., et al. (2012a), 'Site-specific cellular functions of MT1-MMP', *Eur J Cell Biol,* 91 (11-12), 889-95.

Koziol, A., et al. (2012b), 'The protease MT1-MMP drives a combinatorial proteolytic program in activated endothelial cells', *FASEB J,* 26 (11), 4481-94.

Kridel, S. J., et al. (2002), 'A unique substrate binding mode discriminates membrane type-1 matrix metalloproteinase from other matrix metalloproteinases', *J Biol Chem,* 277 (26), 23788-93.

Kubota, S. and Takigawa, M. (2007), 'CCN family proteins and angiogenesis: from embryo to adulthood', *Angiogenesis,* 10 (1), 1-11.

Kubota, Y., et al. (2009), 'M-CSF inhibition selectively targets pathological angiogenesis and lymphangiogenesis', *J Exp Med,* 206 (5), 1089-102.

Kumagai, K., et al. (1999), 'Inhibition of matrix metalloproteinases prevents allergen-induced airway inflammation in a murine model of asthma', *J Immunol,* 162 (7), 4212-9.

Lambert, V., et al. (2003), 'MMP-2 and MMP-9 synergize in promoting choroidal neovascularization', *FASEB J,* 17 (15), 2290-2.

Lee, N. V., et al. (2006), 'ADAMTS1 mediates the release of antiangiogenic polypeptides from TSP1 and 2', *EMBO J,* 25 (22), 5270-83.

Lehti, K., et al. (2000), 'Regulation of membrane-type-1 matrix metalloproteinase activity by its cytoplasmic domain', *J Biol Chem,* 275 (20), 15006-13.

Lehti, K., et al. (2002), 'Oligomerization through hemopexin and cytoplasmic domains regulates the activity and turnover of membrane-type 1 matrix metalloproteinase', *J Biol Chem,* 277 (10), 8440-8.

Lehti, K., et al. (2005), 'An MT1-MMP-PDGF receptor-beta axis regulates mural cell investment of the microvasculature', *Genes Dev,* 19 (8), 979-91.

Leu, S. J., et al. (2004), 'Targeted mutagenesis of the angiogenic protein CCN1 (CYR61). Selective inactivation of integrin alpha6beta1-heparan sulfate proteoglycan coreceptor-mediated cellular functions', *J Biol Chem,* 279 (42), 44177-87.

Li, Q., et al. (2002), 'Matrilysin shedding of syndecan-1 regulates chemokine mobilization and transepithelial efflux of neutrophils in acute lung injury', *Cell,* 111 (5), 635-46.

Ligresti, G., et al. (2011), 'Macrophage-derived tumor necrosis factor-alpha is an early component of the molecular cascade leading to angiogenesis in response to aortic injury', *Arterioscler Thromb Vasc Biol,* 31 (5), 1151-9.

López-Otín, C. and Overall, C. M. (2002), 'Protease degradomics: a new challenge for proteomics', *Nat Rev Mol Cell Biol,* 3 (7), 509-19.

Luttun, A., et al. (2002), 'Revascularization of ischemic tissues by PlGF treatment, and inhibition of tumor angiogenesis, arthritis and atherosclerosis by anti-Flt1', *Nat Med,* 8 (8), 831-40.

Maeda, K., et al. (2001), 'Expression of thrombospondin-1 inversely correlated with tumor vascularity and hematogenous metastasis in colon cancer', *Oncol Rep,* 8 (4), 763-6.

Mann, M. (2006), 'Functional and quantitative proteomics using SILAC', *Nat Rev Mol Cell Biol,* 7 (12), 952-8.

Martignetti, J. A., et al. (2001), 'Mutation of the matrix metalloproteinase 2 gene (MMP2) causes a multicentric osteolysis and arthritis syndrome', *Nat Genet,* 28 (3), 261-5.

Matías-Román, S., et al. (2005), 'Membrane type 1-matrix metalloproteinase is involved in migration of human monocytes and is regulated through their interaction with fibronectin or endothelium', *Blood,* 105 (10), 3956-64.

Mazzone, M., et al. (2009), 'Heterozygous deficiency of PHD2 restores tumor oxygenation and inhibits metastasis via endothelial normalization', *Cell,* 136 (5), 839-51.

McQuibban, G. A., et al. (2002), 'Matrix metalloproteinase processing of monocyte chemoattractant proteins generates CC chemokine receptor antagonists with anti-inflammatory properties in vivo', *Blood,* 100 (4), 1160-7.

McQuibban, G. A., et al. (2001), 'Matrix metalloproteinase activity inactivates the CXC chemokine stromal cell-derived factor-1', *J Biol Chem,* 276 (47), 43503-8.

Medina, I., et al. (2010), 'Babelomics: an integrative platform for the analysis of transcriptomics, proteomics and genomic data with advanced functional profiling', *Nucleic Acids Res,* 38 Suppl, W210-3.

Miao, W. M., et al. (2001), 'Thrombospondin-1 type 1 repeat recombinant proteins inhibit tumor growth through transforming growth factor-beta-dependent and -independent mechanisms', *Cancer Res,* 61 (21), 7830-9.

Miyamori, H., et al. (2001), 'Claudin promotes activation of pro-matrix metalloproteinase-2 mediated by membrane-type matrix metalloproteinases', *J Biol Chem,* 276 (30), 28204-11.

Mori, H., et al. (2013), 'Transmembrane/cytoplasmic, rather than catalytic, domains of Mmp14 signal to MAPK activation and mammary branching morphogenesis via binding to integrin β1', *Development,* 140 (2), 343-52.

Müllberg, J., et al. (2000), 'The importance of shedding of membrane proteins for cytokine biology', *Eur Cytokine Netw,* 11 (1), 27-38.

Nagase, H. (1997), 'Activation mechanisms of matrix metalloproteinases', *Biol Chem,* 378 (3-4), 151-60.

Nagase, H. and Woessner, J. F. (1999), 'Matrix metalloproteinases', *J Biol Chem,* 274 (31), 21491-4.

Nagase, H., Visse, R., and Murphy, G. (2006), 'Structure and function of matrix metalloproteinases and TIMPs', *Cardiovasc Res,* 69 (3), 562-73.

Nakahara, H., et al. (1997), 'Transmembrane/cytoplasmic domain-mediated membrane type 1-matrix metalloprotease docking to invadopodia is required for cell invasion', *Proc Natl Acad Sci U S A,* 94 (15), 7959-64.

Nishida, C., et al. (2012), 'MT1-MMP plays a critical role in hematopoiesis by regulating HIF-mediated chemokine/cytokine gene transcription within niche cells', *Blood,* 119 (23), 5405-16.

Nyalendo, C., et al. (2007), 'Src-dependent phosphorylation of membrane type I matrix metalloproteinase on cytoplasmic tyrosine 573: role in endothelial and tumor cell migration', *J Biol Chem,* 282 (21), 15690-9.

Oblander, S. A., et al. (2005), 'Distinctive functions of membrane type 1 matrix-metalloprotease (MT1-MMP or MMP-14) in lung and submandibular gland development are independent of its role in pro-MMP-2 activation', *Dev Biol,* 277 (1), 255-69.

Oh, J., et al. (2001), 'The membrane-anchored MMP inhibitor RECK is a key regulator of extracellular matrix integrity and angiogenesis', *Cell,* 107 (6), 789-800.

Ohuchi, E., et al. (1997), 'Membrane type 1 matrix metalloproteinase digests interstitial collagens and other extracellular matrix macromolecules', *J Biol Chem,* 272 (4), 2446-51.

Okada, A., et al. (1997), 'Expression of matrix metalloproteinases during rat skin wound healing: evidence that membrane type-1 matrix metalloproteinase is a stromal activator of pro-gelatinase A', *J Cell Biol,* 137 (1), 67-77.

Ong, S. E., et al. (2002), 'Stable isotope labeling by amino acids in cell culture, SILAC, as a simple and accurate approach to expression proteomics', *Mol Cell Proteomics,* 1 (5), 376-86.

Overall, C. M. (2002), 'Molecular determinants of metalloproteinase substrate specificity: matrix metalloproteinase substrate binding domains, modules, and exosites', *Mol Biotechnol,* 22 (1), 51-86.

Overall, C. M., McQuibban, G. A., and Clark-Lewis, I. (2002), 'Discovery of chemokine substrates for matrix metalloproteinases by exosite scanning: a new tool for degradomics', *Biol Chem,* 383 (7-8), 1059-66.

Page-McCaw, A., Ewald, A. J., and Werb, Z. (2007), 'Matrix metalloproteinases and the regulation of tissue remodelling', *Nat Rev Mol Cell Biol,* 8 (3), 221-33.

Pepper, M. S., et al. (1996), 'Angiogenesis-regulating cytokines: activities and interactions', *Curr Top Microbiol Immunol,* 213 (Pt 2), 31-67.

Phng, L. K. and Gerhardt, H. (2009), 'Angiogenesis: a team effort coordinated by notch', *Dev Cell,* 16 (2), 196-208.

Pipp, F., et al. (2003), 'VEGFR-1-selective VEGF homologue PlGF is arteriogenic: evidence for a monocyte-mediated mechanism', *Circ Res,* 92 (4), 378-85.

Poincloux, R., Lizarraga, F., and Chavrier, P. (2009), 'Matrix invasion by tumour cells: a focus on MT1-MMP trafficking to invadopodia', *J Cell Sci,* 122 (Pt 17), 3015-24.

Potente, M., Gerhardt, H., and Carmeliet, P. (2011), 'Basic and therapeutic aspects of angiogenesis', *Cell,* 146 (6), 873-87.

Puente, X. S., et al. (2003), 'Human and mouse proteases: a comparative genomic approach', *Nat Rev Genet,* 4 (7), 544-58.

Punekar, S., et al. (2008), 'Thrombospondin 1 and its mimetic peptide ABT-510 decrease angiogenesis and inflammation in a murine model of inflammatory bowel disease', *Pathobiology,* 75 (1), 9-21.

Rajavashisth, T. B., et al. (1999), 'Inflammatory cytokines and oxidized low density lipoproteins increase endothelial cell expression of membrane type 1-matrix metalloproteinase', *J Biol Chem,* 274 (17), 11924-9.

Ratnikov, B. I., et al. (2002), 'An alternative processing of integrin alpha(v) subunit in tumor cells by membrane type-1 matrix metalloproteinase', *J Biol Chem,* 277 (9), 7377-85.

Rawlings, N. D., Morton, F. R., and Barrett, A. J. (2006), 'MEROPS: the peptidase database', *Nucleic Acids Res,* 34 (Database issue), D270-2.

Risau, W. (1995), 'Differentiation of endothelium', *FASEB J,* 9 (10), 926-33.

Risau, W. (1997), 'Mechanisms of angiogenesis', *Nature,* 386 (6626), 671-4.

Roca, C. and Adams, R. H. (2007), 'Regulation of vascular morphogenesis by Notch signaling', *Genes Dev,* 21 (20), 2511-24.

Rocha, S. F. and Adams, R. H. (2009), 'Molecular differentiation and specialization of vascular beds', *Angiogenesis,* 12 (2), 139-47.

Rodriguez-Manzaneque, J. C., et al. (2001), 'Thrombospondin-1 suppresses spontaneous tumor growth and inhibits activation of matrix metalloproteinase-9 and mobilization of vascular endothelial growth factor', *Proc Natl Acad Sci U S A,* 98 (22), 12485-90.

Rozanov, D. V., et al. (2004), 'Aberrant, persistent inclusion into lipid rafts limits the tumorigenic function of membrane type-1 matrix metalloproteinase in malignant cells', *Exp Cell Res,* 293 (1), 81-95.

Rozanov, D. V., et al. (2001), 'Mutation analysis of membrane type-1 matrix metalloproteinase (MT1-MMP). The role of the cytoplasmic tail Cys(574), the active site Glu(240), and furin cleavage motifs in oligomerization, processing, and self-proteolysis of MT1-MMP expressed in breast carcinoma cells', *J Biol Chem,* 276 (28), 25705-14.

Rymo, S. F., et al. (2011), 'A two-way communication between microglial cells and angiogenic sprouts regulates angiogenesis in aortic ring cultures', *PLoS One,* 6 (1), e15846.

Sainson, R. C., et al. (2008), 'TNF primes endothelial cells for angiogenic sprouting by inducing a tip cell phenotype', *Blood,* 111 (10), 4997-5007.

Salgado, R., et al. (2001), 'Platelets and vascular endothelial growth factor (VEGF): a morphological and functional study', *Angiogenesis,* 4 (1), 37-43.

Sato, H., et al. (1994), 'A matrix metalloproteinase expressed on the surface of invasive tumour cells', *Nature,* 370 (6484), 61-5.

Schaper, W. and Scholz, D. (2003), 'Factors regulating arteriogenesis', *Arterioscler Thromb Vasc Biol,* 23 (7), 1143-51.

Schlöndorff, J. and Blobel, C. P. (1999), 'Metalloprotease-disintegrins: modular proteins capable of promoting cell-cell interactions and triggering signals by protein-ectodomain shedding', *J Cell Sci,* 112 (Pt 21), 3603-17.

Shimizu-Hirota, R., et al. (2012), 'MT1-MMP regulates the PI3Kdelta.Mi-2/NuRD-dependent control of macrophage immune function', *Genes Dev,* 26 (4), 395-413.

Siefert, S. A. and Sarkar, R. (2012), 'Matrix metalloproteinases in vascular physiology and disease', *Vascular,* 20 (4), 210-6.

Sounni, N. E., et al. (2002), 'MT1-MMP expression promotes tumor growth and angiogenesis through an up-regulation of vascular endothelial growth factor expression', *FASEB J,* 16 (6), 555-64.

Sounni, N. E., et al. (2004), 'Up-regulation of vascular endothelial growth factor-A by active membrane-type 1 matrix metalloproteinase through activation of Src-tyrosine kinases', *J Biol Chem,* 279 (14), 13564-74.

Stamenkovic, I. (2000), 'Matrix metalloproteinases in tumor invasion and metastasis', *Semin Cancer Biol,* 10 (6), 415-33.

Sternlicht, M. D. and Werb, Z. (2001), 'How matrix metalloproteinases regulate cell behavior', *Annu Rev Cell Dev Biol,* 17, 463-516.

Stickens, D., et al. (2004), 'Altered endochondral bone development in matrix metalloproteinase 13-deficient mice', *Development,* 131 (23), 5883-95.

Stoll, S. J., et al. (2011), 'The transcription factor HOXC9 regulates endothelial cell quiescence and vascular morphogenesis in zebrafish via inhibition of interleukin 8', *Circ Res,* 108 (11), 1367-77.

Stone, J., et al. (1995), 'Development of retinal vasculature is mediated by hypoxia-induced vascular endothelial growth factor (VEGF) expression by neuroglia', *J Neurosci,* 15 (7 Pt 1), 4738-47.

Strasser, G. A., Kaminker, J. S., and Tessier-Lavigne, M. (2010), 'Microarray analysis of retinal endothelial tip cells identifies CXCR4 as a mediator of tip cell morphology and branching', *Blood,* 115 (24), 5102-10.

Stratman, A. N., et al. (2009), 'Endothelial cell lumen and vascular guidance tunnel formation requires MT1-MMP-dependent proteolysis in 3-dimensional collagen matrices', *Blood,* 114 (2), 237-47.

Strongin, A. Y., et al. (1995), 'Mechanism of cell surface activation of 72-kDa type IV collagenase. Isolation of the activated form of the membrane metalloprotease', *J Biol Chem,* 270 (10), 5331-8.

Sturn, A., Quackenbush, J., and Trajanoski, Z. (2002), 'Genesis: cluster analysis of microarray data', *Bioinformatics,* 18 (1), 207-8.

Suchting, S., et al. (2007), 'The Notch ligand Delta-like 4 negatively regulates endothelial tip cell formation and vessel branching', *Proc Natl Acad Sci U S A,* 104 (9), 3225-30.

Tam, E. M., et al. (2004), 'Membrane protease proteomics: Isotope-coded affinity tag MS identification of undescribed MT1-matrix metalloproteinase substrates', *Proc Natl Acad Sci U S A,* 101 (18), 6917-22.

Tanaka, S. S., et al. (1997), 'Cell-cell contact down-regulates expression of membrane type metalloproteinase-1 (MT1-MMP) in a mouse mammary gland epithelial cell line', *Zoolog Sci,* 14 (1), 95-9.

Tanney, D. C., et al. (1998), 'Regulated expression of matrix metalloproteinases and TIMP in nephrogenesis', *Dev Dyn,* 213 (1), 121-9.

Taraboletti, G., et al. (2002), 'Shedding of the matrix metalloproteinases MMP-2, MMP-9, and MT1-MMP as membrane vesicle-associated components by endothelial cells', *Am J Pathol,* 160 (2), 673-80.

Taylor, P. C. and Sivakumar, B. (2005), 'Hypoxia and angiogenesis in rheumatoid arthritis', *Curr Opin Rheumatol,* 17 (3), 293-8.

Tomita, T., et al. (2000), 'Granulocyte-macrophage colony-stimulating factor upregulates matrix metalloproteinase-2 (MMP-2) and membrane type-1 MMP (MT1-MMP) in human head and neck cancer cells', *Cancer Lett,* 156 (1), 83-91.

Toriseva, M., et al. (2012), 'MMP-13 regulates growth of wound granulation tissue and modulates gene expression signatures involved in inflammation, proteolysis, and cell viability', *PLoS One,* 7 (8), e42596.

Uekita, T., et al. (2001), 'Cytoplasmic tail-dependent internalization of membrane-type 1 matrix metalloproteinase is important for its invasion-promoting activity', *J Cell Biol,* 155 (7), 1345-56.

Van den Steen, P. E., et al. (2000), 'Neutrophil gelatinase B potentiates interleukin-8 tenfold by aminoterminal processing, whereas it degrades CTAP-III, PF-4, and GRO-alpha and leaves RANTES and MCP-2 intact', *Blood,* 96 (8), 2673-81.

Van Wart, H. E. and Birkedal-Hansen, H. (1990), 'The cysteine switch: a principle of regulation of metalloproteinase activity with potential applicability to the entire matrix metalloproteinase gene family', *Proc Natl Acad Sci U S A,* 87 (14), 5578-82.

Visse, R. and Nagase, H. (2003), 'Matrix metalloproteinases and tissue inhibitors of metalloproteinases: structure, function, and biochemistry', *Circ Res,* 92 (8), 827-39.

Vu, T. H., et al. (1998), 'MMP-9/gelatinase B is a key regulator of growth plate angiogenesis and apoptosis of hypertrophic chondrocytes', *Cell,* 93 (3), 411-22.

Wang, Y. and McNiven, M. A. (2012), 'Invasive matrix degradation at focal adhesions occurs via protease recruitment by a FAK-p130Cas complex', *J Cell Biol,* 196 (3), 375-85.

Westermarck, J. and Kähäri, V. M. (1999), 'Regulation of matrix metalloproteinase expression in tumor invasion', *FASEB J,* 13 (8), 781-92.

Wilson, C. L., et al. (1999), 'Regulation of intestinal alpha-defensin activation by the metalloproteinase matrilysin in innate host defense', *Science,* 286 (5437), 113-7.

Wiseman, B. S., et al. (2003), 'Site-specific inductive and inhibitory activities of MMP-2 and MMP-3 orchestrate mammary gland branching morphogenesis', *J Cell Biol,* 162 (6), 1123-33.

Yana, I. and Weiss, S. J. (2000), 'Regulation of membrane type-1 matrix metalloproteinase activation by proprotein convertases', *Mol Biol Cell,* 11 (7), 2387-401.

Yana, I., et al. (2007), 'Crosstalk between neovessels and mural cells directs the site-specific expression of MT1-MMP to endothelial tip cells', *J Cell Sci,* 120 (Pt 9), 1607-14.

Yanez-Mo, M., et al. (2008), 'MT1-MMP collagenolytic activity is regulated through association with tetraspanin CD151 in primary endothelial cells', *Blood,* 112 (8), 3217-26.

Yu, Q. and Stamenkovic, I. (2000), 'Cell surface-localized matrix metalloproteinase-9 proteolytically activates TGF-beta and promotes tumor invasion and angiogenesis', *Genes Dev,* 14 (2), 163-76.

Zhang, J., et al. (2000), 'Progesterone inhibits activation of latent matrix metalloproteinase (MMP)-2 by membrane-type 1 MMP: enzymes coordinately expressed in human endometrium', *Biol Reprod,* 62 (1), 85-94.

Zhou, Z., et al. (2000), 'Impaired endochondral ossification and angiogenesis in mice deficient in membrane-type matrix metalloproteinase I', *Proc Natl Acad Sci U S A,* 97 (8), 4052-7.

Zucker, S., et al. (2003), 'Membrane type-matrix metalloproteinases (MT-MMP)', *Curr Top Dev Biol,* 54, 1-74.

European Journal of Cell Biology 91 (2012) 889–895

Contents lists available at SciVerse ScienceDirect

European Journal of Cell Biology

journal homepage: www.elsevier.com/locate/ejcb

Review

Site-specific cellular functions of MT1-MMP

Agnieszka Koziol[1], Mara Martín-Alonso[1], Cristina Clemente, Pilar Gonzalo, Alicia G. Arroyo*

Vascular Biology and Inflammation Department, Centro Nacional de Investigaciones Cardiovasculares (CNIC), 28029 Madrid, Spain

ARTICLE INFO

Article history:
Received 6 June 2012
Received in revised form 18 July 2012
Accepted 19 July 2012

Keywords:
MT1-MMP
Subcellular location
Cell migration
Cell metabolism
Hypoxia
Chromatin remodeling
Macrophages
Inflammation
Endothelial cells
Angiogenesis

ABSTRACT

The response to environmental cues such as inflammatory stimuli requires coordinated cellular functions. Certain proteins have functions on both sides of the plasma membrane to allow coordination between the extracellular and intracellular milieus. The membrane-anchored matrix metalloproteinase MT1-MMP is well positioned to sense and modify the extracellular environment by processing matrix components, transmembrane proteins and soluble factors. Recent findings show, however, that MT1-MMP also plays unexpected intracellular roles in macrophages through its location at the plasma membrane, the Golgi or the nucleus, impacting cell motility, metabolism and gene transcription. MT1-MMP is thus an example of the evolutionary diversification of protein function, allowing optimal coordination between extracellular stimuli and cellular responses. It remains to be determined whether these new MT1-MMP functions are specific to macrophages, professional phagocytes involved in inflammation, or are present in other inflammation-responsive cells. In this review, we will summarize these site-specific MT1-MMP functions in macrophages and comment on the possible conservation of these functions in endothelial cells.

Introduction

Cells explore their microenvironment to sense cues that activate appropriate adaptive responses. Different evolutionary mechanisms have expanded the functional repertoire of certain proteins to allow coordination between their functions on both sides of the plasma membrane, the extracellular and intracellular milieus. These mechanisms include unconventional secretion of proteins with dual topology, such as syntaxin 2, HGMB1 and tissue transglutaminase, and interdependence of function and location for membrane-anchored proteins, such as β-catenin, which was the first individual protein shown to have distinct but linked functions related to its subcellular compartmentalization (Radisky et al., 2009).

Matrix metalloproteinases (MMPs) can sense and induce environmental modifications since they are secreted enzymes able to degrade a battery of extracellular matrix (ECM) components (Page-McCaw et al., 2007). A subfamily of MMPs is anchored to the membrane instead of being secreted, and this fact positions these MT-MMPs as prime candidates to coordinate extracellular cues with cellular responses. MT1-MMP is especially suited for pericellular proteolysis through its ability to process ECM components, transmembrane proteins and soluble factors (Itoh and Seiki, 2006). Moreover, it has been proposed that MT1-MMP might also be involved in processing of intracellular substrates such as pericentrin, pro-αv integrin and focal adhesion kinase (Golubkov et al., 2005; Ratnikov et al., 2002; Shofuda et al., 2004) (Fig. 1). Accordingly, as with other MMPs, recent proteomics approaches have identified intracellular proteins as possible MT1-MMP substrates; for example, HGMB1 (one of the unconventional dual topology proteins just mentioned), DJ-1, hsp90α, and γ-enolase, although it is not clear if processing would occur in the extracellular or intracellular compartments (Butler et al., 2008; Cauwe and Opdenakker, 2010) (Fig. 1). These findings indicate that under certain circumstances MT1-MMP might unexpectedly be proteolytically active inside cells, through as-yet unclear mechanisms. Regulated compartmentalization of MT1-MMP is essential for this diversity of proteolytic actions; in this regard, the presence of MT1-MMP at caveolae/lipid raft domains – apart from their role in its internalization – often dictates protease location and function in different cell contexts (Frittoli et al., 2011; Poincloux et al., 2009). As an example, forced location of MT1-MMP to lipid rafts by deletion of its cytosolic tail limited its access and processing of E-cadherin and thereby tumor cell locomotion and growth (Rozanov et al., 2004). Moreover, MT1-MMP co-localizes and co-traffics with caveolin-1 to invadopodia, actin-rich invasive protrusions, resulting in matrix degradation in several tumor cell types (Grass et al., 2012; Yamaguchi et al., 2009).

* Corresponding author at: Matrix Metalloproteinases Lab, Centro Nacional de Investigaciones Cardiovasculares (CNIC), Melchor Fernández Almagro 3, 28029 Madrid, Spain. Tel.: +34 91 4531200x1159; fax: +34 91 4531265.
E-mail address: agarroyo@cnic.es (A.G. Arroyo).
[1] These authors contributed equally to this work.

0171-9335/$ – see front matter © 2012 Elsevier GmbH. All rights reserved.
http://dx.doi.org/10.1016/j.ejcb.2012.07.003

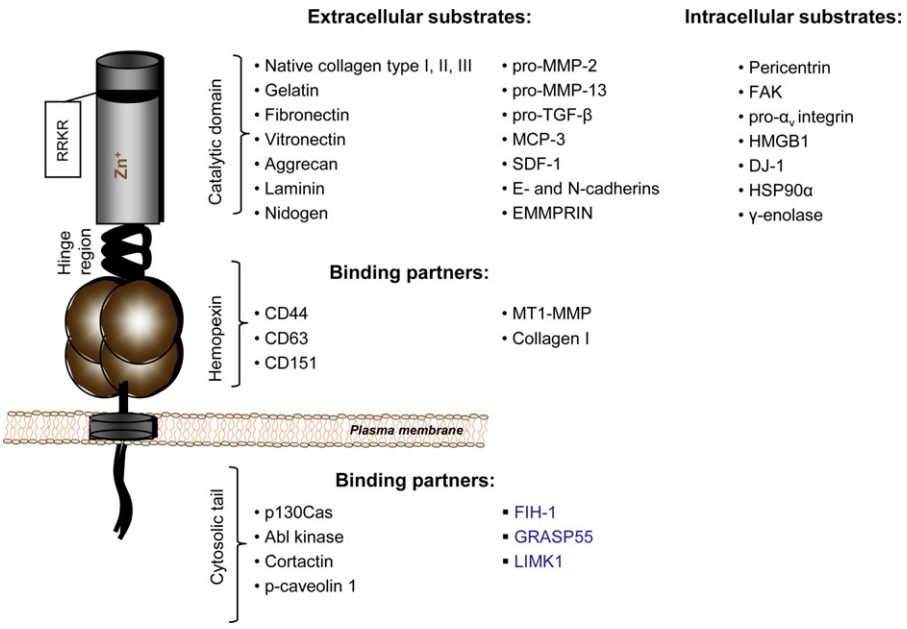

Fig. 1. Extracellular and intracellular substrates and partners of MT1-MMP. The domain structure of MT1-MMP is shown together with lists of selected extracellular and intracellular substrates and binding partners associated with each domain. Intracellular binding partners that interact with MT1-MMP at the Golgi apparatus are indicated in blue text.

But in addition to its proteolytic activities, MT1-MMP can also modulate intracellular responses through molecular interactions of its cytosolic tail leading to induction of signaling pathways such as ERK (Gingras and Beliveau, 2010). Most identified molecular partners interact with the MT1-MMP cytosolic tail at the plasma membrane; however, associations at other cell compartments such as the Golgi have been reported (Fig. 1) (Artym et al., 2006; Cauwe et al., 2007; Gingras et al., 2008; Gonzalo et al., 2010; Labrecque et al., 2004; Roghi et al., 2010; Sakamoto and Seiki, 2010; Smith-Pearson et al., 2010; Tapia et al., 2011).

This information suggests that the compartmentalization of MT1-MMP is linked to proteolytic-dependent and proteolytic-independent functions, through which it can coordinate extracellular cues with cellular responses. We will summarize recent data about new functions of MT1-MMP in macrophages linked to its location at the plasma membrane, the Golgi and the nucleus and discuss the possible conservation of these functions in endothelial cells, another cell type relevant to inflammation.

Site-specific functions of MT1-MMP in macrophages

Macrophages, which derive from myeloid progenitors/monocytes, are phagocytes with a high phenotypic plasticity associated with their essential role in inflammation. MT1-MMP is expressed and active at the plasma membrane of monocyte/macrophages (Matias-Roman et al., 2005), and also of hematopoietic progenitors whose G-CSF-induced mobilization involves enhanced MT1-MMP location at lipid rafts (Shirvaikar et al., 2010). Moreover, MT1-MMP is a component of the podosome machinery in macrophages and of the sealing zone of osteoclasts (macrophage-derived cells), and is involved in matrix degradation at these specialized membrane protrusions (Nusblat et al., 2011). Recent data from our group and others have, however, challenged this paradigm, and shown that MT1-MMP can also exert non-catalytic functions at the macrophage plasma membrane, and more importantly has unexpected functions at other cell compartments, including the Golgi/trans-Golgi network (TGN) and the nucleus.

We showed that the absence of MT1-MMP results in a defect in the fusion of macrophages to form multinucleate osteoclasts and giant cells, and that this defect is related to deficient motility and membrane protrusive activity of MT1-MMP null bone marrow-derived myeloid progenitors/macrophages (Gonzalo et al., 2010). Interestingly, normal progenitor motility and fusion was rescued by re-expression of a catalytically dead mutant, pointing to a proteolysis-independent mechanism. Further analysis showed that MT1-MMP associates with the adapter protein p130Cas at the plasma membrane, promoting optimal recruitment and activity of the small GTPase Rac1 (Gonzalo et al., 2010). Association with p130Cas involves MT1-MMP cytosolic tail Tyr^{573} which had previously been proposed to be phosphorylated by Src kinase (Nyalendo et al., 2007). This study established that the MT1-MMP/p130Cas/Rac1 molecular complex thus coordinates proper macrophage cell motility, migration and fusion both in vitro and in vivo (Fig. 2).

In an independent study, Seiki's group reported that, unlike macrophage invasion (which requires MT1-MMP catalytic activity), migration of mouse bone marrow-derived macrophages is also dependent on the MT1-MMP cytosolic tail (Sakamoto and Seiki, 2009). Macrophages are metabolically unusual in that, to enable migration into hypoxic inflamed tissues, they use glycolysis rather than oxidative phosphorylation for ATP production constitutively, even during normoxia. Seiki's group found that MT1-MMP regulated macrophage motility by increasing hypoxia inducible factor (HIF)-1α-mediated glycolysis and thus production of energy (ATP) by these cells; previous transcriptomic analysis in tumor cells had suggested regulation of energy metabolism by MT1-MMP, but the mechanism was undefined (Rozanov et al., 2008). Dissection of the mechanism by which the MT1-MMP cytosolic tail regulates macrophage metabolism revealed that this action relies on MT1-MMP localization to the Golgi apparatus, where its cytosolic tail retains factor inhibiting HIF (FIH)-1. FIH-1 acts by hydroxylating a conserved asparagine residue in HIF-1α thus impairing its interaction with its transcriptional co-activator p300 and abrogating

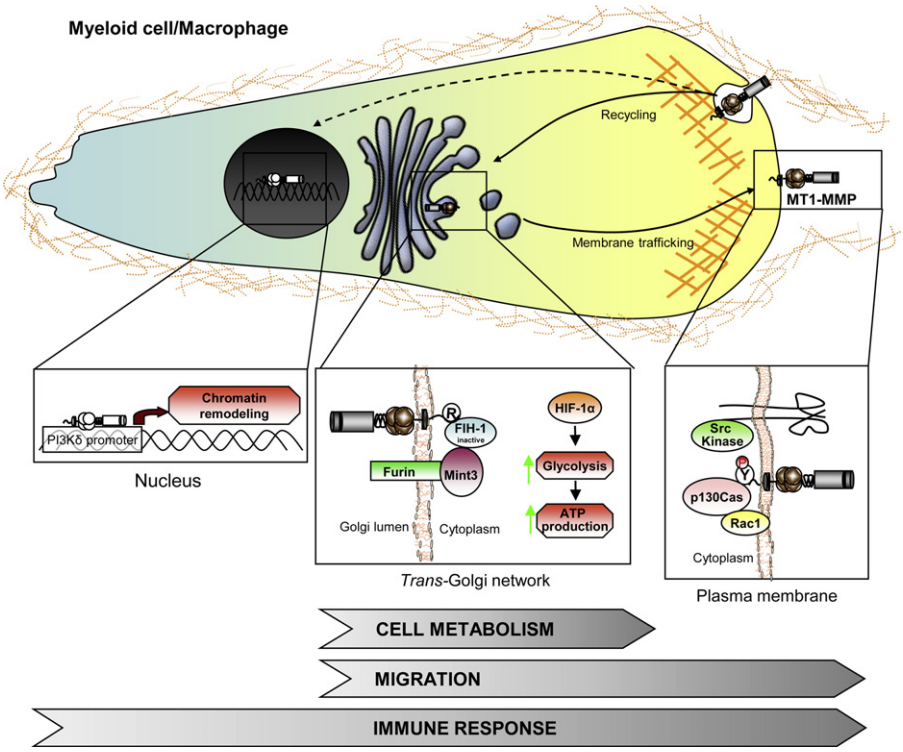

Fig. 2. Site-specific functions of MT1-MMP in macrophages. MT1-MMP is involved in macrophage migration and the immune response in a catalytic-independent manner through at least three site-specific pathways linked to distinct MT1-MMP traffic routes. At the plasma membrane, MT1-MMP can modulate Rac1 activity through binding to p130Cas, thereby regulating migration. The formation of this complex can be regulated by tyrosine phosphorylation of MT1-MMP cytosolic Y^{573} by Src kinase. At the Golgi apparatus, MT1-MMP, through the Arg^{576} in its cytoplasmic tail, binds FIH-1, keeping it close to Mint-3. This inactivation of FIH-1 stabilizes HIF-1α, resulting in the activation of glycolytic ATP production needed for macrophage migration and the immune responses. Upon translocation to the nucleus through as-yet undefined mechanisms, MT1-MMP induces PI3Kδ expression and regulates the transcription of genes critical for the inflammatory response.

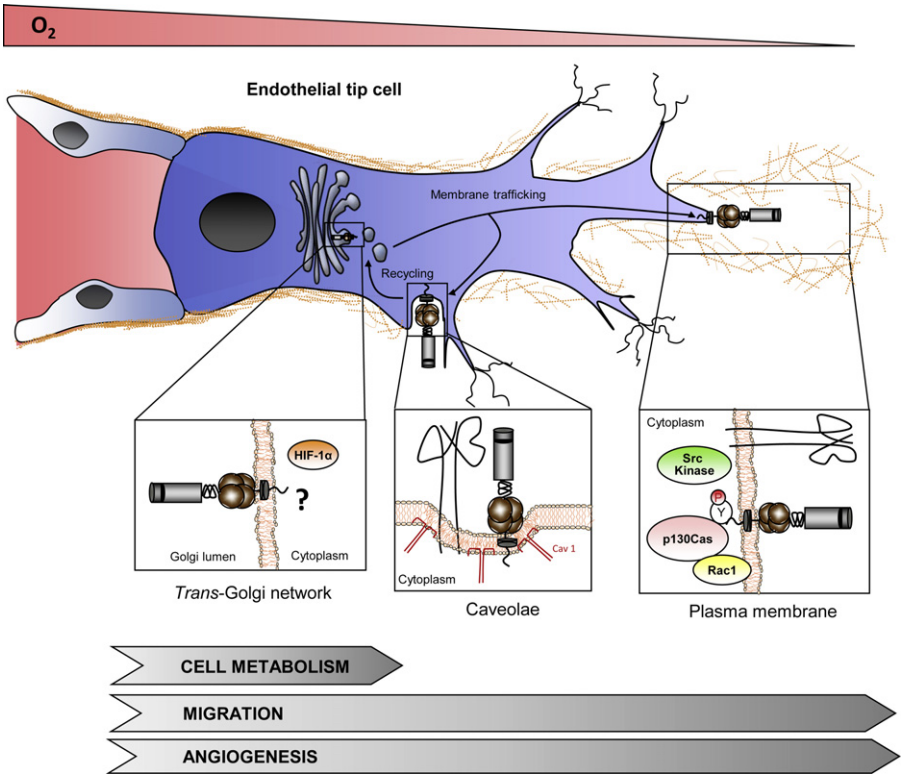

Fig. 3. Site-specific functions of MT1-MMP in endothelial cells. MT1-MMP can affect endothelial cell migration, metabolism and therefore angiogenesis through different pathways involving distinct cytosolic tail interactions and subcellular locations. These actions could be especially relevant in endothelial tip cells, which are exposed to low O_2 levels. In endothelial cells, MT1-MMP association to caveolae can regulate its traffic and function at different cellular locations. In addition, interaction of the MT1-MMP cytosolic tail with p130Cas at the plasma membrane might regulate Rac1 membrane targeting and migration, similar to the situation in macrophages. At the Golgi apparatus, the MT1-MMP cytosolic tail might interact with FIH-1 as reported for macrophages, thereby promoting HIF-1α-mediated cell metabolism.

induction of HIF-1α-dependent genes (Fraisl et al., 2009). MT1-MMP is normally processed by the pro-convertase furin at the Golgi. In macrophages, MT1-MMP at the Golgi interacts through its cytosolic tail Arg^{576} with FIH-1, thereby favoring FIH-1 proximity to Mint-3/APBA3 (another furin partner). Mint-3 in turn forms a complex with FIH-1, retaining it at this site and reducing its available cytoplasmic levels. In the presence of the MT1-MMP/FIH-1/Mint-3 complex at the Golgi, HIF-1α will be free and stabilized, and thus able to induce glycolysis and final production of ATP (Sakamoto and Seiki, 2010). In this manner MT1-MMP might coordinate its pro-invasive activity with the HIF machinery and thereby the cellular metabolism that is also required for migration (Fig. 2); in fact, it is possible that a feedback loop might be operative between hypoxia and MT1-MMP in macrophages since at least in tumor cells both MT1-MMP transcription and mobilization to the plasma membrane can in turn be regulated by HIF-2 and by hypoxia, respectively (Li et al., 2012; Munoz-Najar et al., 2006; Petrella et al., 2005). Points that remain to be defined include whether MT1-MMP exerts this function at the Golgi during its secretory path to the plasma membrane or upon its recycling from the plasma membrane after clathrin or caveolae-mediated endocytosis (Poincloux et al., 2009). Support for the idea that MT1-MMP localization at the Golgi modulates or provides additional MT1-MMP functions is given by the recently reported interactions of MT1-MMP with other Golgi proteins. In tumor cells the peripheral Golgi matrix protein GRASP55 associates with the LLY^{573} motif in the MT1-MMP cytoplasmic domain and favors its furin-dependent activation (Kuo et al., 2000; Roghi et al., 2010). LIM kinase 1 (LIMK1), a modulator of actin dynamics, also co-localizes and associates with MT1-MMP at the Golgi vesicles, facilitating its transport to the plasma membrane in tumor cells (Tapia et al., 2011).

More recently, Weiss's group has uncovered a novel MT1-MMP function in macrophages, dependent on its translocation to the nucleus by an as-yet undefined mechanism (Shimizu-Hirota et al., 2012). MT1-MMP traffics to the nucleus and triggers the activation of the promoter of phosphoinositide 3-kinase δ (PI3Kδ), thus activating the Akt/GSK3β signaling cascade (Fig. 2). This in turn controls the immunoregulatory Mi-2/NuRD complex of nucleosome remodeling enzymes responsible for limiting the transcription of genes involved in the immune response. In this manner, in the absence of MT1-MMP genes belonging to the Mi-2/NuRD complex like *Mi-2β*, *HDAC2* and *MBD3* are down-regulated and genes related to pro-inflammatory responses like *Mx1*, *Mx2*, *Saa3*, *CXCL10* and *CCL5* are up-regulated. The mechanism of MT1-MMP translocation to the nucleus remains unclear, although transfection with various MT1-MMP constructs points to a requirement for MT1-MMP anchorage to the membrane but not for its cytosolic or hemopexin domains or for its catalytic activity (Shimizu-Hirota et al., 2012). The possible role of MT1-MMP in ATP production may also contribute to its transcriptional function, since the Mi-2/NuRD axis is an ATP-dependent nucleosome remodeling complex.

Thus in macrophages, a highly plastic cell type with special metabolic features, the functional repertoire of MT1-MMP has expanded to adapt its functions to cellular responses required for optimal cell function during inflammation and its resolution.

Site-specific functions of MT1-MMP in endothelial cells

During an inflammatory response macrophages constitute the first-line sensors of damage, producing a number of soluble factors, including TNF-α. TNF-α in turn can activate endothelial cells to engage in an angiogenic program aimed at forming new vessels and resolving the inflammation. MT1-MMP, in addition to its important functions in macrophages, is also a key protease in endothelial cells that plays important roles in various steps of the angiogenic response. MT1-MMP proteolytic activity in endothelial cells is closely linked to its regulated presence at specific domains of the plasma membrane, in particular at lamellipodia and filopodia protrusions in which MT1-MMP associates with caveolin-1 and integrin αvβ3 and is catalytically active (Galvez et al., 2002, 2004; Fig. 3). Caveolae constitute the main route for MT1-MMP internalization in endothelial cells but they might also contribute to its mobilization to invadopodia as reported for tumor cells (Frittoli et al., 2011; Galvez et al., 2004; Poincloux et al., 2009). Consistently, MT1-MMP is expressed in endothelial tip cells, specialized cells at the nascent vascular sprout that contain many filopodia, are highly migratory and invasive and are enriched in caveolin-1 and αvβ3 integrin expression as shown by recent transcriptomic analysis (Aplin et al., 2009; del Toro et al., 2010; Gerhardt et al., 2003; Kachgal et al., 2012; Strasser et al., 2010; Yana et al., 2007).

The possibility that MT1-MMP might play additional site-specific functions in endothelial cells is supported by several observations. First, MT1-MMP deficiency reduces the targeting of p130Cas and Rac1 to the plasma membrane, similar to previous findings in myeloid progenitors (Fig. 2; Gonzalo et al., 2010). In endothelial cells, the MT1-MMP/p130Cas/Rac1 complex might contribute to migration, especially in endothelial tip cells, where Rac1 activity has been shown to be relevant (De Smet et al., 2009;

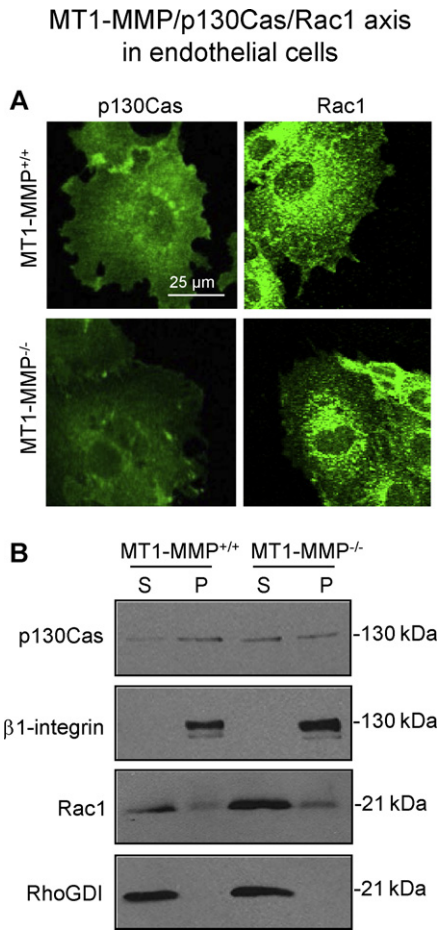

Fig. 4. p130Cas and Rac1 membrane levels are reduced in MT1-MMP null endothelial cells. (A) Mouse lung endothelial cells (MLEC) from wild type or MT1-MMP deficient mice were cultured to 70% confluence and after serum deprivation for 16 h were stained for p130Cas and Rac1 (green). Images show representative confocal microscopy maximal projections. (B) MLEC cultured as in A were separated into particulate (P) and soluble (S) fractions, and analyzed by Western blot for p130Cas and Rac1 expression. β1 integrin and RhoGDI are included as controls of particulate and soluble fractions. A representative blot is shown ($n = 5$).

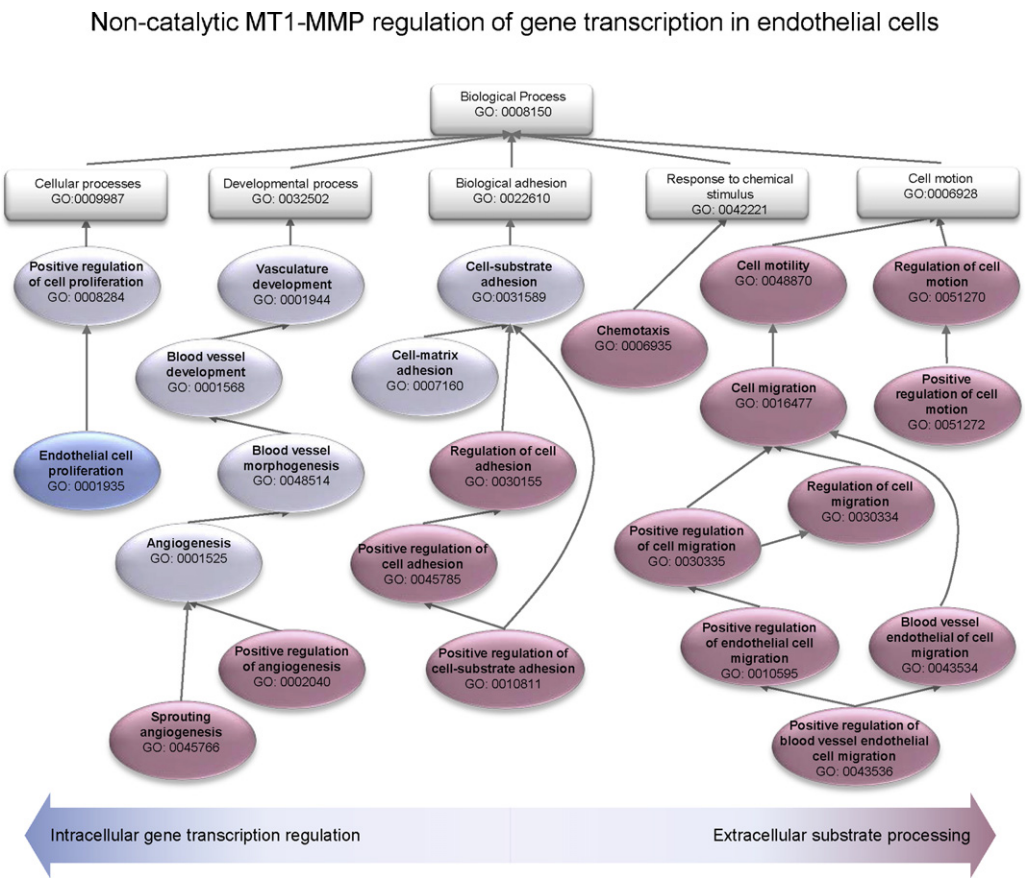

Fig. 5. Selected biological processes (GO annotations) regulated by MT1-MMP. Transcriptome and degradome analysis of inflammatory-activated mouse primary endothelial cells identified genes and proteins positively regulated by MT1-MMP that can affect a number of biological processes related to angiogenesis. Upregulated genes in the transcriptome analysis were predominantly enriched in processes related to proliferation, vasculature development and adhesion, while proteins identified in the MT1-MMP degradome mostly affect processes related to extracellular matrix degradation during neovessel formation (cell motility, adhesion, chemotaxis and vessel morphogenesis). Processes regulated only by intracellular transcription are shown in blue, those regulated only by extracellular processing (degradome) are in red, and processes regulated by both routes are in gray.

Figs. 3 and 4). This new MT1-MMP function might also be conserved in other cell types; for example, MT1-MMP has been shown to associate with a p130Cas/focal adhesion kinase complex upon Src kinase-dependent Tyr^{573} phosphorylation, thus favoring degradation of the matrix at focal adhesions in tumor cells (Wang and McNiven, 2012).

Second, MT1-MMP could be expected to regulate HIF-1 machinery in endothelial cells. The MT1-MMP/HIF-1 axis is active in tumor cells, which also use 'aerobic' glycolysis (the Warburg effect) (Hara et al., 2011), and more recently this axis was reported in bone marrow hematopoietic progenitors exposed to low oxygen tension (Nishida et al., 2012). Like these cell types, endothelial cells are equipped with metabolic mechanisms to enable survival in highly hypoxic conditions, including deriving most of their energy anaerobically through glycolysis (Fraisl et al., 2009). Moreover, the HIF-1α inhibitor FIH-1 is expressed in certain endothelial cells and might inhibit Notch activity, which is critical for endothelial tip cell fate specification. It will be interesting to explore whether MT1-MMP can also associate with FIH-1/Mint-3 in endothelial tip cells, thereby modulating FIH-1 availability and regulating HIF-1α-dependent genes such as Dll4 and Notch signaling (Fig. 3).

Finally, bioinformatics analysis of the MT1-MMP transcriptome and degradome (the collection of its substrates) in cytokine-activated primary mouse lung endothelial cells points to a role of MT1-MMP in regulating gene transcription in endothelial cells in a proteolytic-independent manner. Although most of the Gene Ontology Biological Processes related to angiogenesis, such as chemotaxis, motility, migration, adhesion or vasculature development, are enriched in MT1-MMP degradome or in both MT1-MMP degradome and transcriptome, endothelial cell proliferation was only enriched in the transcriptome. This analysis indicates that there is a minor contribution from non-catalytic MT1-MMP-driven gene regulation to angiogenesis (Fig. 5). MT1-MMP nuclear translocation is not exclusive of macrophages since it has also been observed in hepatocellular carcinoma cells in which caveolin-mediated endocytosis was proposed as the underlying mechanism (Ip et al., 2007). Moreover, MT1-MMP can modulate the expression of components of chromatin remodeling complexes in several cell types including HMGA2 in tumor cells through ERK signaling and Mi-2/NuRD in macrophages through the PI3Kδ/Akt/GSK3 pathway (Dangi-Garimella et al., 2011; Shimizu-Hirota et al., 2012). Although MT1-MMP nuclear translocation has not been confirmed in endothelial cells, we can thus speculate that MT1-MMP might directly or indirectly regulate chromatin remodeling, and thereby gene transcription, in endothelial cells. It will be important to investigate this point further given the current interest in epigenetic regulation in vascular biology and angiogenesis (Aurora et al., 2010; Yan et al., 2010).

Concluding remarks and future perspectives

Interdependence between location and function has been claimed as a mechanism for diversification of protein functions and improvement of their ability to coordinate extracellular cues and intracellular responses. MT1-MMP has become a

prime example of such a site-specific, multi-task protein, able to coordinate extracellular proteolytic modification with non-proteolytic-mediated cellular responses including cell motility and metabolism, ultimately leading to inflammatory responses and angiogenesis.

Open questions remain about the mechanisms by which cells and their metabolic needs regulate the distinct subcellular locations and functions of MT1-MMP. There are several possibilities; for example different metabolic or inflammatory conditions might trigger distinct traffic routes of MT1-MMP. Thus, environmental metabolic needs might change the manner in which MT1-MMP is endocytosed, steering its fate away from degradation to active roles in the Golgi or other compartments such as the nucleus; alternatively, MT1-MMP and its partners might meet at the Golgi/TGN as a result of altered synthesis and secretion. In support of regulated traffic of MT1-MMP under metabolic stress, in addition to transcriptional regulation of MT1-MMP by HIF-2 in tumor cells (Petrella et al., 2005), hypoxia can also promote the mobilization of MT1-MMP from cytosolic storage pools to the plasma membrane involving different molecular mechanisms such as RhoA activation (Li et al., 2012; Munoz-Najar et al., 2006). Interestingly, RhoA activation induced MT1-MMP location at cell-cell contacts and inhibited its caveolae-mediated traffic in endothelial cells (Galvez et al., 2004); it will be interesting to explore whether hypoxia in a RhoA-dependent or independent manner, can impact caveolae traffic routes since at least in tumor cells HIF-1 and -2 induce caveolin-1 transcription and caveolae formation (Wang et al., 2012). Notably, hypoxia also stimulates the formation of invadopodia in tumor cells (Lucien et al., 2011; Munoz-Najar et al., 2006) supporting the concept that a decrease in oxygen availability might trigger a coordinated cellular response involving increased MT1-MMP traffic to the plasma membrane together with induction of caveolae and invadopodia formation resulting in higher levels of MT1-MMP at these invasive structures. This response might be relevant not only in the tumor context but also in hypoxic inflammatory foci leading to endothelial tip cell and macrophage invasion. Moreover, in pathological contexts such as pulmonary arterial hypertension, hypoxia can also lead to trapping of vesicle tethers (SNAREs and SNAPs) in the Golgi (Sehgal and Lee, 2011); it is tempting to speculate that inflammatory hypoxic environments could also regulate Golgi-dependent MT1-MMP traffic to endow cells with appropriate adaptive responses. Understanding these new mechanisms of action of MT1-MMP has the potential to provide further insights into the complex networks activated under stressful inflammatory conditions and open new avenues for therapeutic intervention.

Acknowledgments

We thank S. Bartlett for English editing. This work was supported by grants from the Ministerio de Economia y Competitividad (MINECO; SAF2008-02104, SAF2011-25619 and RD06/0014/1016) and the Fundación Genoma España to A.G.A. AK and MMA are funded by fellowships from the Spanish Ministry of Education and Science and MINECO, respectively. The CNIC is supported by the MINECO and the Pro-CNIC Foundation.

References

Aplin, A.C., Zhu, W.H., Fogel, E., Nicosia, R.F., 2009. Vascular regression and survival are differentially regulated by MT1-MMP and TIMPs in the aortic ring model of angiogenesis. Am. J. Physiol. Cell Physiol. 297, C471–C480.

Artym, V.V., Zhang, Y., Seillier-Moiseiwitsch, F., Yamada, K.M., Mueller, S.C., 2006. Dynamic interactions of cortactin and membrane type 1 matrix metalloproteinase at invadopodia: defining the stages of invadopodia formation and function. Cancer Res. 66, 3034–3043.

Aurora, A.B., Biyashev, D., Mirochnik, Y., Zaichuk, T.A., Sanchez-Martinez, C., Renault, M.A., Losordo, D., Volpert, O.V., 2010. NF-kappaB balances vascular regression and angiogenesis via chromatin remodeling and NFAT displacement. Blood 116, 475–484.

Butler, G.S., Dean, R.A., Tam, E.M., Overall, C.M., 2008. Pharmacoproteomics of a metalloproteinase hydroxamate inhibitor in breast cancer cells: dynamics of membrane type 1 matrix metalloproteinase-mediated membrane protein shedding. Mol. Cell. Biol. 28, 4896–4914.

Cauwe, B., Opdenakker, G., 2010. Intracellular substrate cleavage: a novel dimension in the biochemistry, biology and pathology of matrix metalloproteinases. Crit. Rev. Biochem. Mol. Biol. 45, 351–423.

Cauwe, B., Van den Steen, P.E., Opdenakker, G., 2007. The biochemical, biological, and pathological kaleidoscope of cell surface substrates processed by matrix metalloproteinases. Crit. Rev. Biochem. Mol. Biol. 42, 113–185.

Dangi-Garimella, S., Krantz, S.B., Barron, M.R., Shields, M.A., Heiferman, M.J., Grippo, P.J., Bentrem, D.J., Munshi, H.G., 2011. Three-dimensional collagen I promotes gemcitabine resistance in pancreatic cancer through MT1-MMP-mediated expression of HMGA2. Cancer Res. 71, 1019–1028.

De Smet, F., Segura, I., De Bock, K., Hohensinner, P.J., Carmeliet, P., 2009. Mechanisms of vessel branching: filopodia on endothelial tip cells lead the way. Arterioscler. Thromb. Vasc. Biol. 29, 639–649.

del Toro, R., Prahst, C., Mathivet, T., Siegfried, G., Kaminker, J.S., Larrivee, B., Breant, C., Duarte, A., Takakura, N., Fukamizu, A., Penninger, J., Eichmann, A., 2010. Identification and functional analysis of endothelial tip cell-enriched genes. Blood 116, 4025–4033.

Fraisl, P., Mazzone, M., Schmidt, T., Carmeliet, P., 2009. Regulation of angiogenesis by oxygen and metabolism. Dev. Cell 16, 167–179.

Frittoli, E., Palamidessi, A., Disanza, A., Scita, G., 2011. Secretory and endo/exocytic trafficking in invadopodia formation: the MT1-MMP paradigm. Eur. J. Cell Biol. 90, 108–114.

Galvez, B.G., Matias-Roman, S., Yanez-Mo, M., Sanchez-Madrid, F., Arroyo, A.G., 2002. ECM regulates MT1-MMP localization with beta1 or alphavbeta3 integrins at distinct cell compartments modulating its internalization and activity on human endothelial cells. J. Cell Biol. 159, 509–521.

Galvez, B.G., Matias-Roman, S., Yanez-Mo, M., Vicente-Manzanares, M., Sanchez-Madrid, F., Arroyo, A.G., 2004. Caveolae are a novel pathway for membrane-type 1 matrix metalloproteinase traffic in human endothelial cells. Mol. Biol. Cell 15, 678–687.

Gerhardt, H., Golding, M., Fruttiger, M., Ruhrberg, C., Lundkvist, A., Abramsson, A., Jeltsch, M., Mitchell, C., Alitalo, K., Shima, D., Betsholtz, C., 2003. VEGF guides angiogenic sprouting utilizing endothelial tip cell filopodia. J. Cell. Biol. 161, 1163–1177.

Gingras, D., Beliveau, R., 2010. Emerging concepts in the regulation of membrane-type 1 matrix metalloproteinase activity. Biochim. Biophys. Acta 1803, 142–150.

Gingras, D., Michaud, M., Di Tomasso, G., Beliveau, E., Nyalendo, C., Beliveau, R., 2008. Sphingosine-1-phosphate induces the association of membrane-type 1 matrix metalloproteinase with p130Cas in endothelial cells. FEBS Lett. 582, 399–404.

Golubkov, V.S., Boyd, S., Savinov, A.Y., Chekanov, A.V., Osterman, A.L., Remacle, A., Rozanov, D.V., Doxsey, S.J., Strongin, A.Y., 2005. Membrane type-1 matrix metalloproteinase (MT1-MMP) exhibits an important intracellular cleavage function and causes chromosome instability. J. Biol. Chem. 280, 25079–25086.

Gonzalo, P., Guadamillas, M.C., Hernandez-Riquer, M.V., Pollan, A., Grande-Garcia, A., Bartolome, R.A., Vasanji, A., Ambrogio, C., Chiarle, R., Teixido, J., Risteli, J., Apte, S.S., del Pozo, M.A., Arroyo, A.G., 2010. MT1-MMP is required for myeloid cell fusion via regulation of Rac1 signaling. Dev. Cell 18, 77–89.

Grass, G.D., Bratoeva, M., Toole, B.P., 2012. Regulation of invadopodia formation and activity by CD147. J. Cell Sci. 125, 777–788.

Hara, T., Mimura, K., Seiki, M., Sakamoto, T., 2011. Genetic dissection of proteolytic and non-proteolytic contributions of MT1-MMP to macrophage invasion. Biochem. Biophys. Res. Commun. 413, 277–281.

Ip, Y.C., Cheung, S.T., Fan, S.T., 2007. Atypical localization of membrane type 1-matrix metalloproteinase in the nucleus is associated with aggressive features of hepatocellular carcinoma. Mol. Carcinog. 46, 225–230.

Itoh, Y., Seiki, M., 2006. MT1-MMP: a potent modifier of pericellular microenvironment. J. Cell. Physiol. 206, 1–8.

Kachgal, S., Carrion, B., Janson, I.A., Putnam, A.J., 2012. Bone marrow stromal cells stimulate an angiogenic program that requires endothelial MT1-MMP. J. Cell. Physiol.

Kuo, A., Zhong, C., Lane, W.S., Derynck, R., 2000. Transmembrane transforming growth factor-alpha tethers to the PDZ domain-containing, Golgi membrane-associated protein p59/GRASP55. EMBO J. 19, 6427–6439.

Labrecque, L., Nyalendo, C., Langlois, S., Durocher, Y., Roghi, C., Murphy, G., Gingras, D., Beliveau, R., 2004. Src-mediated tyrosine phosphorylation of caveolin-1 induces its association with membrane type 1 matrix metalloproteinase. J. Biol. Chem. 279, 52132–52140.

Li, J., Zucker, S., Pulkoski-Gross, A., Kuscu, C., Karaayvaz, M., Ju, J., Yao, H., Song, E., Cao, J., 2012. Conversion of stationary to invasive tumor initiating cells (TICs): role of hypoxia in membrane type 1-matrix metalloproteinase (MT1-MMP) trafficking. PLoS One 7, e38403.

Lucien, F., Brochu-Gaudreau, K., Arsenault, D., Harper, K., Dubois, C.M., 2011. Hypoxia-induced invadopodia formation involves activation of NHE-1 by the p90 ribosomal S6 kinase (p90RSK). PLoS One 6, e28851.

Matias-Roman, S., Galvez, B.G., Genis, L., Yanez-Mo, M., de la Rosa, G., Sanchez-Mateos, P., Sanchez-Madrid, F., Arroyo, A.G., 2005. Membrane type 1-matrix metalloproteinase is involved in migration of human monocytes and is regulated through their interaction with fibronectin or endothelium. Blood 105, 3956–3964.

Munoz-Najar, U.M., Neurath, K.M., Vumbaca, F., Claffey, K.P., 2006. Hypoxia stimulates breast carcinoma cell invasion through MT1-MMP and MMP-2 activation. Oncogene 25, 2379–2392.

Nishida, C., Kusubata, K., Tashiro, Y., Gritli, I., Sato, A., Ohki-Koizumi, M., Morita, Y., Nagano, M., Sakamoto, T., Koshikawa, N., Kuchimaru, T., Kizaka-Kondoh, S., Seiki, M., Nakauchi, H., Heissig, B., Hattori, K., 2012. MT1-MMP plays a critical role in hematopoiesis by regulating HIF-mediated chemo-/cytokine gene transcription within niche cells. Blood 119, 5405–5416.

Nusblat, L.M., Dovas, A., Cox, D., 2011. The non-redundant role of N-WASP in podosome-mediated matrix degradation in macrophages. Eur. J. Cell Biol. 90, 205–212.

Nyalendo, C., Michaud, M., Beaulieu, E., Roghi, C., Murphy, G., Gingras, D., Beliveau, R., 2007. Src-dependent phosphorylation of membrane type I matrix metalloproteinase on cytoplasmic tyrosine 573: role in endothelial and tumor cell migration. J. Biol. Chem. 282, 15690–15699.

Page-McCaw, A., Ewald, A.J., Werb, Z., 2007. Matrix metalloproteinases and the regulation of tissue remodelling. Nat. Rev. Mol. Cell Biol. 8, 221–233.

Petrella, B.L., Lohi, J., Brinckerhoff, C.E., 2005. Identification of membrane type-1 matrix metalloproteinase as a target of hypoxia-inducible factor-2 alpha in von Hippel–Lindau renal cell carcinoma. Oncogene 24, 1043–1052.

Poincloux, R., Lizarraga, F., Chavrier, P., 2009. Matrix invasion by tumour cells: a focus on MT1-MMP trafficking to invadopodia. J. Cell Sci. 122, 3015–3024.

Radisky, D.C., Stallings-Mann, M., Hirai, Y., Bissell, M.J., 2009. Single proteins might have dual but related functions in intracellular and extracellular microenvironments. Nat. Rev. Mol. Cell Biol. 10, 228–234.

Ratnikov, B.I., Rozanov, D.V., Postnova, T.I., Baciu, P.G., Zhang, H., DiScipio, R.G., Chestukhina, G.G., Smith, J.W., Deryugina, E.I., Strongin, A.Y., 2002. An alternative processing of integrin alpha(v) subunit in tumor cells by membrane type-1 matrix metalloproteinase. J. Biol. Chem. 277, 7377–7385.

Roghi, C., Jones, L., Gratian, M., English, W.R., Murphy, G., 2010. Golgi reassembly stacking protein 55 interacts with membrane-type (MT) 1-matrix metalloprotease (MMP) and furin and plays a role in the activation of the MT1-MMP zymogen. FEBS J. 277, 3158–3175.

Rozanov, D.V., Deryugina, E.I., Monosov, E.Z., Marchenko, N.D., Strongin, A.Y., 2004. Aberrant, persistent inclusion into lipid rafts limits the tumorigenic function of membrane type-1 matrix metalloproteinase in malignant cells. Exp. Cell Res. 293, 81–95.

Rozanov, D.V., Savinov, A.Y., Williams, R., Liu, K., Golubkov, V.S., Krajewski, S., Strongin, A.Y., 2008. Molecular signature of MT1-MMP: transactivation of the downstream universal gene network in cancer. Cancer Res. 68, 4086–4096.

Sakamoto, T., Seiki, M., 2009. Cytoplasmic tail of MT1-MMP regulates macrophage motility independently from its protease activity. Genes Cells 14, 617–626.

Sakamoto, T., Seiki, M., 2010. A membrane protease regulates energy production in macrophages by activating hypoxia-inducible factor-1 via a non-proteolytic mechanism. J. Biol. Chem. 285, 29951–29964.

Sehgal, P.B., Lee, J.E., 2011. Protein trafficking dysfunctions: role in the pathogenesis of pulmonary arterial hypertension. Pulm. Circ. 1, 17–32.

Shimizu-Hirota, R., Xiong, W., Baxter, B.T., Kunkel, S.L., Maillard, I., Chen, X.W., Sabeh, F., Liu, R., Li, X.Y., Weiss, S.J., 2012. MT1-MMP regulates the PI3Kdelta.Mi-2/NuRD-dependent control of macrophage immune function. Genes Dev. 26, 395–413.

Shirvaikar, N., Marquez-Curtis, L.A., Shaw, A.R., Turner, A.R., Janowska-Wieczorek, A., 2010. MT1-MMP association with membrane lipid rafts facilitates G-CSF-induced hematopoietic stem/progenitor cell mobilization. Exp. Hematol. 38, 823–835.

Shofuda, T., Shofuda, K., Ferri, N., Kenagy, R.D., Raines, E.W., Clowes, A.W., 2004. Cleavage of focal adhesion kinase in vascular smooth muscle cells overexpressing membrane-type matrix metalloproteinases. Arterioscler. Thromb. Vasc. Biol. 24, 839–844.

Smith-Pearson, P.S., Greuber, E.K., Yogalingam, G., Pendergast, A.M., 2010. Abl kinases are required for invadopodia formation and chemokine-induced invasion. J. Biol. Chem. 285, 40201–40211.

Strasser, G.A., Kaminker, J.S., Tessier-Lavigne, M., 2010. Microarray analysis of retinal endothelial tip cells identifies CXCR4 as a mediator of tip cell morphology and branching. Blood 115, 5102–5110.

Tapia, T., Ottman, R., Chakrabarti, R., 2011. LIM kinase1 modulates function of membrane type matrix metalloproteinase 1: implication in invasion of prostate cancer cells. Mol. Cancer 10, 6.

Wang, Y., McNiven, M.A., 2012. Invasive matrix degradation at focal adhesions occurs via protease recruitment by a FAK–p130Cas complex. J. Cell Biol. 196, 375–385.

Wang, Y., Roche, O., Xu, C., Moriyama, E.H., Heir, P., Chung, J., Roos, F.C., Chen, Y., Finak, G., Milosevic, M., Wilson, B.C., Teh, B.T., Park, M., Irwin, M.S., Ohh, M., 2012. Hypoxia promotes ligand-independent EGF receptor signaling via hypoxia-inducible factor-mediated upregulation of caveolin-1. Proc. Natl. Acad. Sci. U.S.A. 109, 4892–4897.

Yamaguchi, H., Takeo, Y., Yoshida, S., Kouchi, Z., Nakamura, Y., Fukami, K., 2009. Lipid rafts and caveolin-1 are required for invadopodia formation and extracellular matrix degradation by human breast cancer cells. Cancer Res. 69, 8594–8602.

Yan, M.S., Matouk, C.C., Marsden, P.A., 2010. Epigenetics of the vascular endothelium. J. Appl. Physiol. 109, 916–926.

Yana, I., Sagara, H., Takaki, S., Takatsu, K., Nakamura, K., Nakao, K., Katsuki, M., Taniguchi, S., Aoki, T., Sato, H., Weiss, S.J., Seiki, M., 2007. Crosstalk between neovessels and mural cells directs the site-specific expression of MT1-MMP to endothelial tip cells. J. Cell Sci. 120, 1607–1614.

The protease MT1-MMP drives a combinatorial proteolytic program in activated endothelial cells

Agnieszka Koziol,* Pilar Gonzalo,* Alba Mota,* Ángela Pollán,* Cristina Lorenzo,* Nuria Colomé,† David Montaner,‡ Joaquín Dopazo,‡ Joaquín Arribas,† Francesc Canals,† and Alicia G. Arroyo*,[1]

*Vascular Biology Department, Centro Nacional de Investigaciones Cardiovasculares (CNIC), Madrid, Spain; †Proteomics Laboratory and Medical Oncology Research Program, Vall d'Hebron Institute of Oncology, Vall d'Hebron University Hospital Research Institute, Barcelona, Spain; and ‡Bioinformatics Department, Centro de Investigación Príncipe Felipe, Valencia, Spain

ABSTRACT **The mechanism by which proteolytic events translate into biological responses is not well understood. To explore the link of pericellular proteolysis to events relevant to capillary sprouting within the inflammatory context, we aimed at the identification of the collection of substrates of the protease MT1-MMP in endothelial tip cells induced by inflammatory stimuli. We applied quantitative proteomics to endothelial cells (ECs) derived from wild-type and MT1-MMP-null mice to identify the substrate repertoire of this protease in TNF-α-activated ECs. Bioinformatics analysis revealed a combinatorial MT1-MMP proteolytic program, in which combined rather than single substrate processing would determine biological decisions by activated ECs, including chemotaxis, cell motility and adhesion, and vasculature development. MT1-MMP-deficient ECs inefficiently processed several of these substrates (TSP1, CYR61, NID1, and SEM3C), validating the model. This novel concept of MT1-MMP-driven combinatorial proteolysis in angiogenesis might be extendable to proteolytic actions in other cellular contexts.—Koziol, A., Gonzalo, P., Mota, A., Pollán, Á., Lorenzo, C., Colomé, N., Montaner, D., Dopazo, J., Arribas, J., Canals, F., Arroyo, A. G. The protease MT1-MMP drives a combinatorial proteolytic program in activated endothelial cells. *FASEB J.* 26, 4481–4494 (2012). www.fasebj.org**

Key Words: angiogenesis · degradome · inflammation · SILAC

Proteolysis governs biological processes such as angiogenesis, the formation of new vessels from preexisting ones; however, the mechanisms by which proteolytic events actually translate into defined cellular responses remain poorly characterized. Angiogenesis requires the presence of invasive endothelial tip cells at the nascent sprout. The endothelial tip cell transcriptome during postnatal retinal vascularization was reported recently (1, 2), but the proteome has not been characterized. Angiogenesis in adults is often linked to inflammation, and factors such as tumor necrosis factor α (TNF-α), sphingosine-1-phosphate (S1P), and bradykinin induce formation of endothelial tip-like cells *in vitro* (3–5). The protease membrane type-1 matrix metalloproteinase (MT1-MMP) is likely active at the developing sprout during inflammation, since it is required for capillary formation induced by nitric oxide (a downstream effector of bradykinin), prostaglandin E2 (PGE2), and the chemokine monocyte chemoattractant protein-1 (MCP-1)/chemokine (C-C motif) ligand 2 (CCL2) (3). Moreover, MT1-MMP is expressed in endothelial tip cells *in vitro* (6), and mathematical models suggest that MT1-MMP contributes to endothelial tip cell guidance (7). Thus, a global analysis of MT1-MMP proteolytic activity in endothelial tip cells

Abbreviations: 2D, 2-dimensional; 3D, 3-dimensional; ADAM, a disintegrin and metalloproteinase; ADAMTS, a disintegrin and metalloproteinase with thrombospondin motifs; BP, biological process; CCL2, chemokine (C-C motif) ligand 2; CSUP, culture supernatant; CXCR4, C-X-C chemokine receptor type 4; CYR61, cysteine-rich angiogenic inducer 61; DAVID, Database for Annotation, Visualization, and Integrated Discovery; Dll4, delta-like ligand 4; EC, endothelial cell; ECM, extracellular matrix; EDTA, ethylenediaminetetraacetic acid; GO, Gene Ontology; H/L, heavy/light; HUVEC, human umbilical vein endothelial cell; ICAM, intercellular adhesion molecule; iMLEC, immortalized mouse lung endothelial cell; Jag1, Jagged 1; MCP-1, monocyte chemoattractant protein-1; MLEC, mouse lung endothelial cell; MMP, matrix metalloproteinase; MS/MS, tandem mass spectrometry; MT1-MMP, membrane type-1 matrix metalloproteinase; NID1, nidogen 1; P, postnatal day; PECAM-1, platelet endothelial cell adhesion molecule 1; PFA, paraformaldehyde; pMLEC, primary mouse lung endothelial cell; S1P, sphingosine-1-phosphate; SEM3C, semaphorin 3C; SILAC, stable isotope labeling of amino acids in cell culture; siRNA, small interfering RNA; TNF-α, tumor necrosis factor α; TSP1, thrombospondin 1; VEGF, vascular endothelial growth factor; VEGFR, vascular endothelial growth factor receptor; VCAM-1, vascular cell adhesion molecule 1; WT, wild type

[1] Correspondence: Matrix Metalloproteinases Laboratory, Centro Nacional de Investigaciones Cardiovasculares (CNIC), Melchor Fernández Almagro 3, 28029 Madrid, Spain. E-mail: agarroyo@cnic.es

doi: 10.1096/fj.12-205906

This article includes supplemental data. Please visit *http://www.fasebj.org* to obtain this information.

should provide deeper understanding of the link between proteolysis and angiogenesis.

The fingerprint of a protease is its full set of substrates in a given cellular context (also known as the protease degradome; ref. 8). Shotgun and quantitative proteomics approaches have significantly advanced this field. Stable isotope labeling of amino acids in cell culture (SILAC) is a powerful quantitative proteomics approach (9), but the need for several cell doublings limits its use in slowly proliferating primary cells. Bioinformatic analysis of identified substrate sets can provide additional information about protease action in specific cell contexts. We have used an inflammatory tip cell model system to integrate SILAC-identified MT1-MMP substrates in TNF-α-activated endothelial cells (ECs) with bioinformatics analysis. This global analysis reveals a combinatorial MT1-MMP proteolytic program that governs EC chemotaxis, motility, and adhesion, ultimately leading to angiogenesis.

MATERIALS AND METHODS

Mice

MT1-MMP-deficient mice were generated as described previously (10). MT1-MMP heterozygotes on the C57BL/6 background were crossed, and wild-type (WT) and null littermates were used for experiments. Mice were kept in the Centro Nacional de Investigaciones Cardiovasculares (CNIC) Animal Facility under pathogen-free conditions and according to institutional guidelines.

Cells

Isolation of mouse lung ECs (MLECs) was described previously (11). Briefly, lungs from WT or MT1-MMP-null mice were excised, disaggregated, and digested in 0.1% collagenase for 1 h at 37°C. The cell suspension was seeded onto plates coated with 10 μg/ml fibronectin (Sigma, St. Louis, MO, USA), 10 μg/ml collagen I (PureCol; Advanced BioMatrix, San Diego, CA, USA), and 0.1% gelatin (Sigma). After attachment, cells were negatively selected with anti-CD16/CD32 mAb (BD Biosciences, San Jose, CA, USA) coupled to magnetic beads (Dynal; Invitrogen, Carlsbad, CA, USA), and then positively selected with anti-intercellular adhesion molecule 2 (ICAM-2; BD Biosciences) coupled to magnetic beads. Primary MLECs were immortalized using the polyoma virus middle T by overnight infection with conditioned medium from the virus-producing Gpmt cell line supplemented with antibiotics, 10 mM HEPES, 8 μg/ml of polybrene (Sigma), and 50 μg/ml EC growth supplement. The Gpmt cell line was a kind gift from Dr. Reinhard Fässler (Max Planck Institute of Biochemistry, Munich, Germany).

Human umbilical vein ECs (HUVECs) from different donors (cultured up to passage 6) were purchased from Lonza (Basel, Switzerland) or isolated from freshly harvested umbilical cords, as described previously (12). Cells were cultured in M199 medium (Lonza) supplemented with 20% fetal bovine serum, 100 U/ml penicillin, 100 μg/ml streptomycin, 2.5 μg/ml fungizone, 10 UI/ml heparin, and 50 μg/ml of EC growth supplement extracted from bovine brain.

Flow cytometry

Immortalized MLECs were left untreated or treated with 20 ng/ml of the angiogenic factors vascular endothelial growth factor (VEGF) or TNF-α (both from PeproTech, Rocky Hill, NJ, USA). For surface expression analysis, cells were harvested using Cell Dissociation Buffer (Gibco, Carlsbad, CA, USA) and stained with rat anti-mouse vascular cell adhesion molecule 1 (VCAM-1; BD Biosciences), biotinylated hamster anti-mouse ICAM-1 (BD Biosciences), hamster anti-mouse platelet EC adhesion molecule 1 (PECAM-1; Millipore, Bedford, MA, USA), rabbit anti-mouse Jagged 1 (Jag1; Cell Signaling Technology, Danvers, MA, USA), rabbit anti-mouse VEGF receptor 2 (VEGFR2; Abcam, Cambridge, MA, USA), rabbit anti-mouse delta-like ligand 4 (Dll4; Santa Cruz Biotechnology, Santa Cruz, CA, USA), hamster anti-mouse β3 integrin (BD Bioscience), rat anti-mouse C-X-C chemokine receptor type 4 (CXCR4; BD Biosciences), and rabbit anti-mouse MT1-MMP (HR; Abcam), followed by incubation with appropriate fluorescent-labeled secondary antibodies. Cell surface expression was determined in a flow cytometer (FACScanto; Beckton Dickinson, Franklin Lakes, NJ, USA), and data were analyzed with FACSDiva software (Beckton Dickinson).

Hierarchical clustering analysis

Regulatory patterns were compared using the platform-independent Java suite Genesis (13).

Immunofluorescence staining

MLECs were plated on matrix-coated glass coverslips. Cells were then fixed with 4% paraformaldehyde (PFA) for 10 min. After blocking with 2% BSA for 30 min at room temperature, coverslips were incubated with Texas Red-phalloidin, rabbit anti-mouse thrombospondin 1 (TSP1; clone 7280; kindly provided by Dr. M. Luisa Iruela-Arispe, University of California, Los Angeles, CA, USA), goat anti-mouse cysteine-rich angiogenic inducer 61 (CYR61), goat anti-mouse nidogen 1 (NID1), or goat anti-mouse semaphorin 3C (SEM3C; Santa Cruz Biotechnology), followed by fluorescent-labeled secondary antibodies. Mouse anti-human TSP1 (Thermo Fisher Scientific, Waltham, MA, USA), rabbit anti-human CYR61, and rabbit anti-human NID1 or goat anti-human SEM3C (Santa Cruz Biotechnology) were used for immunostaining of human ECs. Coverslips were mounted with ProLong Gold antifade reagent (Invitrogen). Samples were examined under a Zeiss LSM700 confocal microscope (Plan-Apochromat 63×1.4 or 40×1.3 Oil DIC M27; Carl Zeiss, Oberkochen, Germany) and images were analyzed with ZEN software (Zeiss).

Three-dimensional (3D) endothelial tip-like cell sprouting assay

MLECs were plated at confluence in Ibidi angiogenic chambers with Matrigel (BD Biosciences) on top; medium containing TNF-α was then added, and the chamber was kept at 37°C for ≥18 h. At the end of incubation, medium was removed, and the cells were fixed with freshly prepared 4% PFA for 20 min, followed by permeabilization in 0.3% Triton X-100. Samples were washed with PBS/Triton X-100 and stained with phalloidin, anti-PECAM-1, anti-TSP1, anti-CYR61, anti-NID1, or anti-SEM3C antibodies. Samples were examined under a Zeiss LSM700 confocal microscope, and images were analyzed with ZEN software.

SILAC

MLECs were grown in complete SILAC Advance D-MEM F-12 Flex Medium (Invitrogen) supplemented with "light" and "heavy" amino acids and dialyzed serum to exclude the possibility of incorporating nonlabeled amino acids. We used nonlabeled lysine and the $^{13}C_6$ form of arginine (light conditions) for cell cultures derived from MT1-MMP-null mice, and isotopes of lysine ($^{13}C_6$) and arginine ($^{13}C_6$ $^{15}N_4$) for cells derived from WT mice (heavy conditions). Cells were cultured for 7 d, corresponding to ~6 doublings, and appropriate amounts of isotopic lysine and arginine were used to optimize isotopic incorporation while minimizing the risk of arginine to proline conversion. For the last 48 h of culture, medium was replaced by serum-free medium, to reduce the serum protein background, and for the last 24 h, cells were stimulated with 20 ng/ml TNF-α. At the end of the 7-d period, conditioned medium from null and WT cultures was collected, and the cells were harvested with cold PBS and 10 mM ethylenediaminetetraacetic acid (EDTA). Supernatants from null (light condition) and WT (heavy condition) were pooled 1:1 after bicinchoninic acid protein determination (BCA Protein Assay; Pierce, Rockford, IL, USA). The pooled media were incubated for 3 h at 4°C with wheat germ agglutinin (WGA)-agarose beads to extract glycoproteins, and the glycoproteins were eluted by incubation with 0.5 M *N*-acetyl-D-glucosamine. The glycoprotein mixture was concentrated on a 3-kDa cutoff centrifugal filter (Amicon Ultra-4; Millipore) to a final volume of 200 μl. Urea was added to a final concentration of 8 M (pH 8.5). Proteins were reduced by addition of 50 mM dithiothreitol (DTT; Amersham Biosciences, Piscataway, NJ, USA), followed by carbamidomethylation with 125 mM iodoacetamide (Sigma). Finally, the protein mixture was purified by acetone–trichloroacetic acid precipitation (2D-CleanUp kit; GE Healthcare, Piscataway, NJ, USA). For microsomal fraction analysis, cells were detached nonenzymatically with cold PBS and 10 mM EDTA, and equal amounts of cells from WT and MT1-MMP-null culture were pooled, left in sucrose buffer, and cracked by sequential passes through a 25-gauge needle. The pooled fraction was spun to pellet nuclei, and the supernatant was ultracentrifuged for 2 h at 55,000 rpm to separate cytosol from the microsomal fraction. The microsomal pellet was resuspended in guadininium chloride (6 M; Sigma). Supernatant and microsomal fractions were resuspended in loading buffer, and proteins were separated by 10% SDS-PAGE.

Mass spectrometry

After separation of glycoproteins by 10% SDS-PAGE, Coomassie-stained gel was cut into 20 slices, and each one was in-gel digested with modified porcine trypsin (Promega, Madison, WI, USA). The digests were dried in a vacuum centrifuge, extracted with formic acid solution, and analyzed on an Esquire Ultra IT mass spectrometer (Bruker, Bremen, Germany) coupled to a nano-HPLC system (Ultimate; LC Packings, Amsterdam, The Netherlands). Peptide mixtures were first concentrated on a 300-mm i.d. and 1-mm PepMap nanotrapping column and then loaded onto a 75-mm i.d., 15-cm PepMap nanoseparation column (LC Packings). Peptides were then eluted with an acetonitrile (ACN) gradient (0–60% B in 150 min, where B is 80% ACN, 0.1% formic acid in water; flow rate ~300 nl/min) through a PicoTip emitter nanospray needle (New Objective, Woburn, MA, USA) onto the nanospray ionization source of the IT mass spectrometer. Tandem mass spectrometry (MS/MS) fragmentation (1.9 s, 100–2800 *m/z*) was performed on three of the most intense ions, as determined from a 1.2-s MS survey scan (310–1500 *m/z*), using a dynamic exclusion time of 1.2 min for precursor selection and excluding single-charged ions.

Protein identification and data analysis

Data were processed for protein identification and quantification with Protein Scape 2.1 and WARP-LC 1.2 (Bruker), a software platform that integrates processing of LC-MS run data, protein identification through database search of MS/MS spectra, and protein quantification based on the integration of the chromatographic peaks of MS-extracted ion chromatograms for each precursor. Proteins were identified using Mascot (Matrix Science, London, UK) to search the SwissProt database, restricting the search to mouse proteins. MS/MS spectra were searched with a precursor mass tolerance of 1.5 Da, fragment tolerance of 0.5 Da, trypsin specificity with a maximum of 1 missed cleavage, cysteine carbamidomethylation as a fixed modification, and methionine oxidation and the N-terminal and corresponding Lys and Arg SILAC labels as variable modifications. A positive identification criterion was set as an individual Mascot score for each peptide MS/MS spectrum higher than the corresponding homology threshold score. The false-positive rate for Mascot protein identification was measured by searching a randomized decoy database, as described previously (14), and estimated to be <4%. For protein quantification, heavy/light (H/L) ratios were calculated by averaging the measured H/L ratio for the observed peptides, after discarding outliers. For selected proteins of interest, quantitative data obtained from

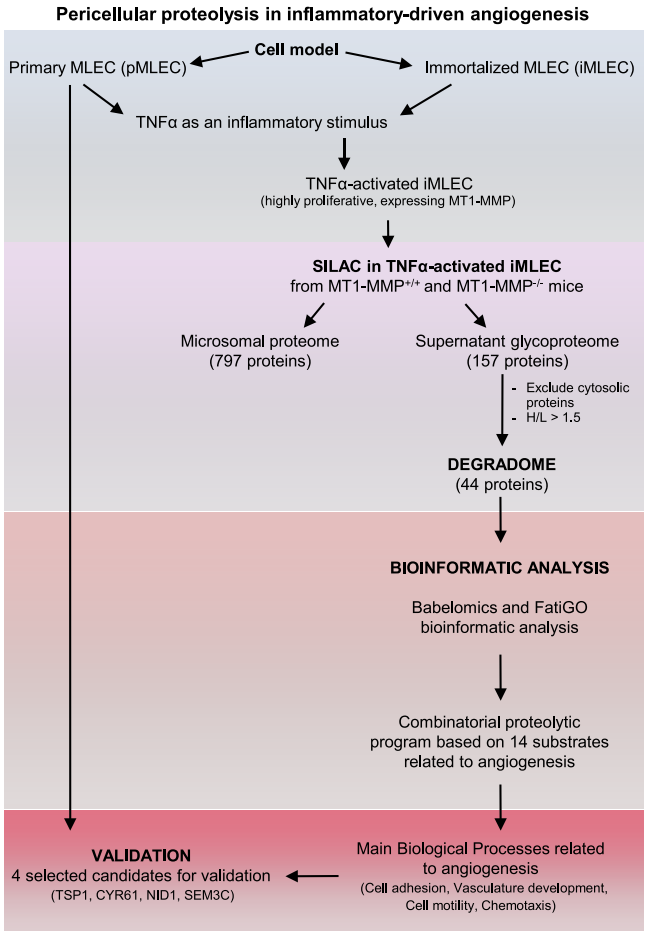

Figure 1. Experimental approach to analyze proteolysis in inflammation-activated ECs. Flow chart depicts experimental design to identify and analyze the substrate collection of the protease MT1-MMP in endothelial tip cells stimulated in inflammatory conditions by quantitative proteomics and bioinformatics.

the automated Protein Scape software analysis were manually reviewed. Further protein analysis was conducted with Protein Knowledgebase UniProtKB (http://www.uniprot.org) and the GeneCards database (http://www.genecards.org).

Bioinformatic data analysis with Babelomics

The Babelomics Web tool (http://www.babelomics.org) is a freely available program suited to analysis of large-scale experiments (microarrays, proteomics) with functional annotation (15). The FatiGO module (16) was used for enrichment analysis of selected proteins. This functional profiling was performed by comparing two lists of genes, the first being the genes encoding the proteins with an H/L ratio > 1.5 in the SILAC analysis unless otherwise stated, and the second being the rest of the genome.

Overlap analysis

Overlap analysis and generation of Venn diagrams was performed using an online application (http://www.pangloss.com/seidel/Protocols/venn4.cgi).

Microarrays

Primary MLECs were treated with 20 ng/ml MCP-1 for 6 h. The experiments were conducted using 1-color mouse whole-genome oligomicroarrays (Applied Biosystems, Foster City, CA, USA), and differential expression analyses was performed using the linear modeling features of the Limma package (Bioconductor; http://www.bioconductor.org/).

RT-PCR

For relative quantitation of expression, quantitative real-time PCR analysis was performed using the AB7900 FAST 384 Detection System (Applied Biosystems), according to the manufacturer's instructions. Total cellular RNA was extracted from cultured confluent MLECs using TRIzol reagent (Invitrogen), according to the manufacturer's protocol, and quantified using a Nanodrop ND-1000 (Thermo Fisher Scientific). cDNA synthesis was performed with 1 μg of total RNA using an RNA synthesis kit (RNeasy Plus mini kit; Qiagen, Valencia, CA, USA). Predesigned qPCR primers for mouse Mmp14, Thbs1, Cyr61, Nid1, Sema3c, Tbp, and Hrpt1 were selected from TaqMan Gene Expression Assay database (Applied Biosystems). Relative quantitation of each target gene was performed using comparative threshold multiplex PCR in gene expression relative to the Tbp and Hrpt1. The data were analyzed by the qBASE program (http://www.biogazelle.com), obtaining the C_t of the amplification products.

For HUVECs, after RNA extraction, cDNA synthesis was also performed with 1 μg of total RNA using an RNA synthesis kit (RNeasy Plus mini kit; Qiagen). cDNAs were subjected to PCR amplification using the following primer pairs for human MT1-MMP: 5′-CGCTACGCCATCCAGGGTCTC-3′ and 5′-CGGTCATCATCGGGCAGCACAAAA-3′ (Isogen Bioscience, Maarssen, The Netherlands). The PCR products were visualized using ethidium bromide in 1% agarose gel.

Western blot

Cells were lysed in RIPA buffer containing protease inhibitors, and culture supernatants (CSUPs) were collected and enriched for glycoproteins as described above. Culture (50 μg) supernatant and 20 μg of total cell lysate were loaded and separated by SDS-PAGE, and proteins were transferred to nitrocellulose membrane; protein loading of CSUPs was checked by Ponceau red staining of the blotted membrane. Blots were incubated with anti-mouse or anti-human antibodies overnight at 4°C, washed, and followed by secondary HRP-conjugated antibody. Signal was detected by chemiluminescence (Amersham ECL Signal Detection Reagent; GE Healthcare) or enhanced chemiluminescence (Immobilon Western, Chemiluminescent HRP Substrate; Millipore). Protein amount in the supernatants was quantified by densitometry using ImageJ software (U.S. National Institutes of Health, Bethesda, MD, USA). All the experiments were performed at

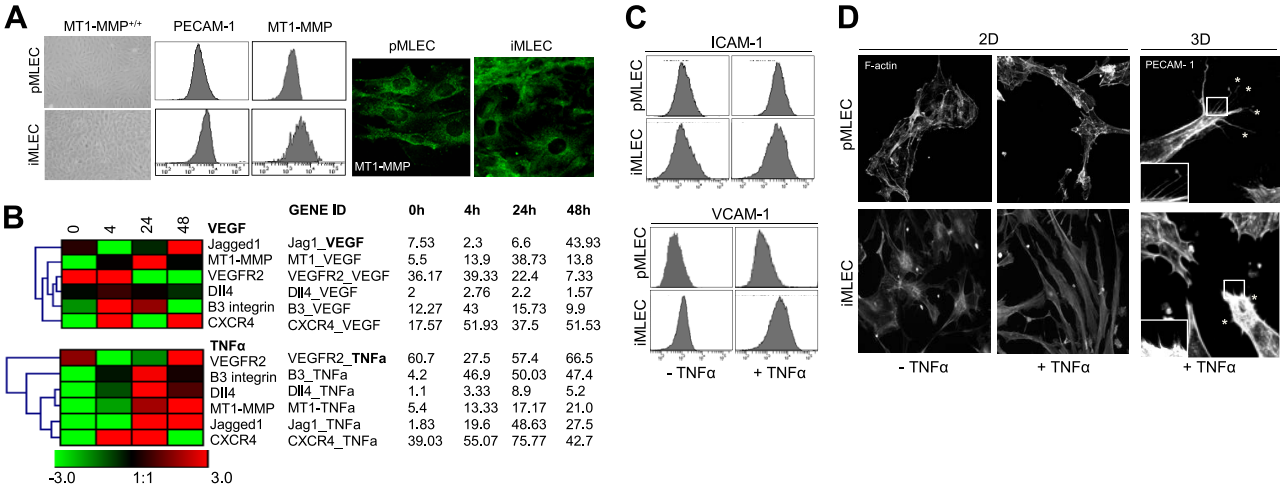

Figure 2. iMLECs respond similarly to pMLECs to TNF-α stimulation. *A*) Morphology of pMLECs and iMLECs (left panels); levels of PECAM-1 and MT1-MMP in pMLECs and iMLECs assessed by flow cytometry (middle panels) and immunostaining (right panels). *B*) iMLECs were left untreated (0 h) or treated with 20 ng/ml of VEGF or TNF-α, and the expression of the tip cell markers VEGFR2, Jag1, Dll4, MT1-MMP, integrin β3, and CXCR4 was analyzed at the cell surface by flow cytometry at 4, 24, and 48 h (n=3). Left panel: hierarchical schemes were obtained. Right panel: average percentages of positive population for each marker and condition were analyzed by the high-content analysis software Genesis on normalization of data. *C*) Cell surface levels of ICAM-1 and VCAM-1 were assessed by flow cytometry in pMLECs and iMLECs left untreated or treated with 20 ng/ml TNF-α for 24h; *D*) TNF-α-stimulated pMLECs or iMLECs were cultured in 2D or 3D conditions and stained with phalloidin or anti-PECAM-1 antibody, respectively.

least in triplicate. Data are represented as means ± SE, and unpaired Student's *t* test was applied. Differences were considered significant at values of $P < 0.05$.

Whole-mount retina staining

Eyes from postnatal day 6–8 (P6–P8) mice were removed and fixed with 4% PFA at 4°C. Fixed retinas were flat-mounted and blocked in 2% BSA, PBS, and 0.3% Triton X-100, followed by overnight incubation with primary antibodies (anti-CYR61 or rat anti-mouse NID1; Abcam) and isolectin IB4 (Sigma) to visualize vasculature. The next day, retinas were extensively washed and incubated with fluorescent-conjugated secondary antibodies. Images were acquired with a Zeiss LSM700 confocal microscope (Plan-Apochromat 63×1.4 Oil DIC M27), and images were analyzed with ZEN software.

Transfection of small interfering RNA (siRNA)

Silencer siRNA constructs were purchased from Ambion (Applied Biosystems). Specific oligonucleotide sequences targeting human MT1-MMP were as follows: 5′-CAUCUGUGACGGGAACUUU-3′ and 5′-GGAAUGAGGAUCUGAAUGG-3′ and a nontargeting siRNA control, which bears no homology with relevant human genes. For siRNA transfection, cells were seeded in 6-well plates at 2.5×10^5 cells/well and grown to reach 60–70% confluence. The different amounts of siRNAs and Oligofectamine reagent (Invitrogen) were diluted in Opti-MEM I (Gibco; Invitrogen). The diluted siRNA-liposome complex was added to cells and incubated for 4 h. Following the transfection, fresh Opti-MEM I containing 30% FBS was added, and cells were grown for 24 h. After that, cells were rinsed with fresh M199 medium and cultured with TNF-α for 24 h for analysis.

RESULTS

Pericellular proteolysis in inflammation-induced endothelial tip cells

To understand the link of pericellular proteolysis to events relevant to capillary sprouting within the

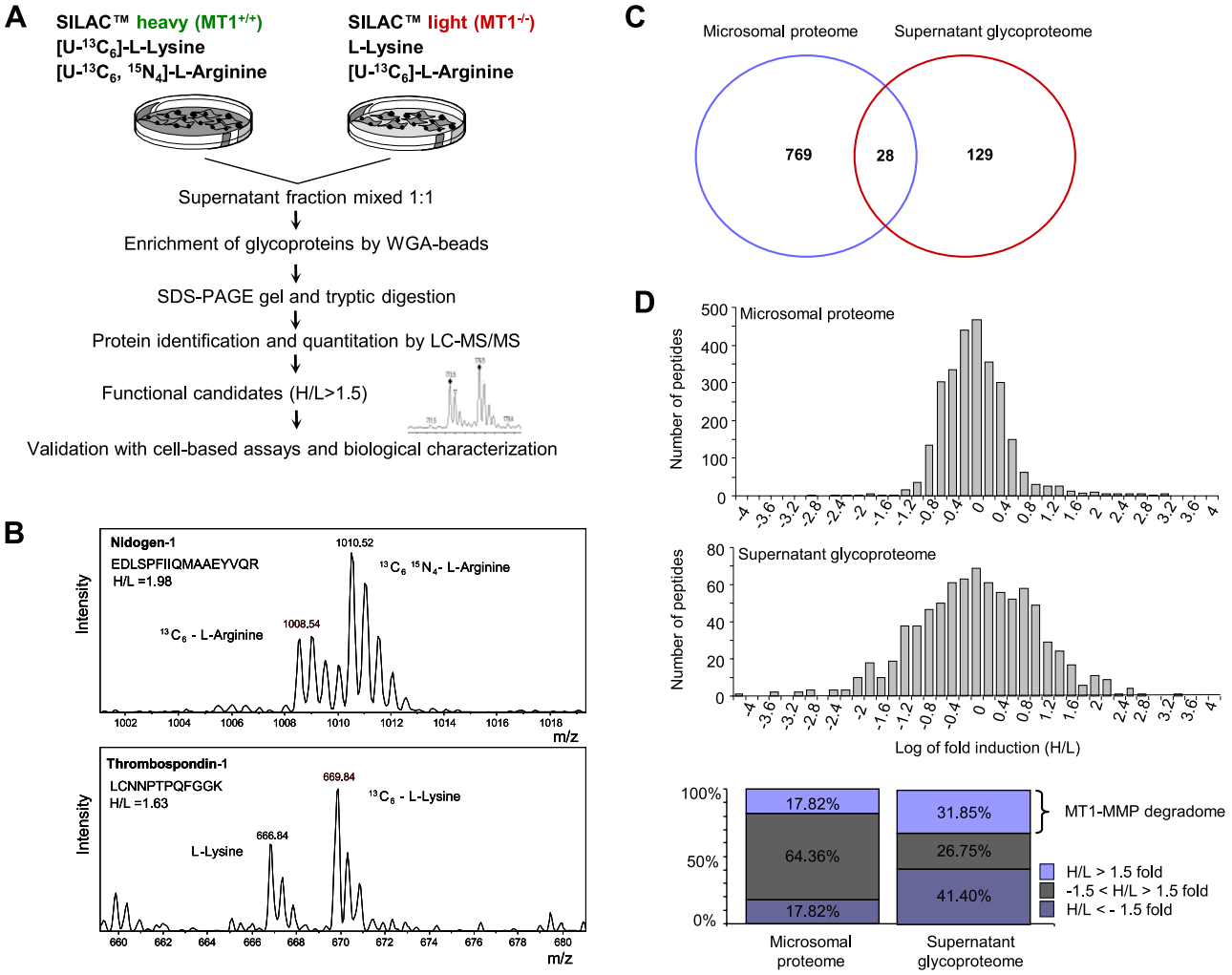

Figure 3. SILAC in TNF-α-stimulated iMLECs. *A*) SILAC strategy for comparing the supernatant proteome of WT ($MT1^{+/+}$) and MT1-MMP-null ($MT1^{-/-}$) iMLECs stimulated with TNF-α (20 ng/ml) for 24 h. *B*) Peptide mass spectra for NID1 and TSP1, with relative abundance of heavy and light labeled forms. *C*) Venn diagram showing proteins identified in both microsomal proteome and supernatant glycoproteome. *D*) Normal distribution of H/L ratios of labeled peptides in microsomal proteome and supernatant glycoproteome. Histogram shows the percentage of quantified proteins with H/L ratio = 1, and <1.5- or >1.5-fold change in the microsomal proteome and the supernatant glycoproteome.

TABLE 1. *MT1-MMP degradome glycoproteins grouped in relation to their reported function in angiogenesis*

Protein	Name	Function	H/L ratio	Processed by MMP/ADAM proteases
Angiogenesis related				
ITPR1	Inositol 1,4,5-trisphosphate receptor type 1	Calcium signaling pathway	18.04	*
TSP2	Thrombospondin-2	Cell adhesion, ECM-receptor interaction	8.68	ADAMTS1, MMP-2, MMP-9
MMP3	Stromelysin-1	Proteolysis	6.04	–
LYOX	Protein-lysine 6-oxidase	Vasculature development, extracellular matrix organization	5.68	*
PCOC1	Procollagen C-endopeptidase enhancer 1	Proteolysis	5.53	MMP-2
TRPM2	Transient receptor potential cation channel subfamily M member 2	Ion transport	5.33	–
EGFR	Epidermal growth factor receptor	Proliferation, protein interaction	4.60	–
SODE	Extracellular superoxide dismutase [Cu-Zn]	Oxygen metabolism	4.37	*
PTX3	Pentraxin-related protein PTX3	Membrane organization, endocytosis	4.20	MT1-MMP
PR2C2	Prolactin-2C2	Vascular development, cell migration	4.14	–
IC1	Plasma protease C1 inhibitor	Immune response	3.70	–
CNTN1	Contactin-1	Cell adhesion	3.67	–
STC1	Stanniocalcin-1	Cellular ion homeostasis	3.59	MT1-MMP
SFRP1	Secreted frizzled-related protein 1	Development, differentiation	3.34	–
TIMP1	Metalloproteinase inhibitor 1	Enzyme inhibitor activity	3.14	MMP-9
SEM3C	Semaphorin-3C	Vasculature development, axon guidance	2.94	ADAMTS1, ADAMTS13
CO6A1	Collagen α-1(VI) chain	Cell adhesion	2.88	MMP-9, MMP-13
FBN1	Fibrillin-1	Metal ion binding	2.76	MT1-MMP, MMP-2, MMP-3, MMP-7, MMP-9, MMP-12, MMP-13
SLIT3	Slit homolog 3 protein	Axon guidance	2.51	–
LIF	Leukemia inhibitory factor	Receptor interaction, Jak-STAT signaling pathway	2.37	MMP-9
CERU	Ceruloplasmin	Metal ion binding	2.29	–
NID1	Nidogen-1	Cell adhesion, binding	2.26	MT1-MMP, ADAMTS1, MMP-15, MMP-19
NGAL	Neutrophil gelatinase-associated lipocain	Response to virus	2.11	–
MMP19	Matrix metalloproteinase-19	Vascular development, differentiation	2.10	–
CSF1	Macrophage colony-stimulating factor 1	Cytokine-cytokine receptor interaction	2.06	–
GELS	Gelsolin	Cytoskeleton organization	2.06	MT1-MMP
TENA	Tenascin	Focal adhesion, ECM-receptor interaction	2.04	MT1-MMP
FBLN2	Fibulin-2	Cell adhesion, matrix binding	2.04	–
CO3	Complement C3	Immune response, ECM-receptor interaction	1.96	MT1-MMP
CCL2	C-C motif chemokine 2	Proliferation. Immune response, chemotaxis	1.86	–
TIMP3	Metalloproteinase inhibitor 3	Enzyme inhibitory activity	1.80	–
SLIT2	Slit homolog 2 protein	Axon guidance, cell motion	1.73	–
TSP1	Thrombospondin-1	Migration, cell adhesion, immune response	1.68	MT1-MMP, ADAMTS1, ADAMTS13
CYR61	Protein CYR61	Vasculature development, adhesion, proliferation	1.68	MT1-MMP, *
CO3A1	Collagen α-1(III) chain	Vasculature development	1.67	MT1-MMP
TIMP2	Metalloproteinase inhibitor 2	Enzyme inhibitory activity	1.67	–

(*continued on next page*)

TABLE 1. *(continued)*

Protein	Name	Function	H/L ratio	Processed by MMP/ADAM proteases
Unrelated to angiogenesis				
KLRA4	Killer cell lectin-like receptor 4	Cell adhesion, NK mediated cytotoxicity	14.90	−
KPBB	Phosphorylase b kinase regulatory subunit β	Calcium signaling pathway	11.58	−
SNED1	Sushi, nidogen and EGF-like domain-containing protein 1	Cell adhesion	7.05	−
CPXM1	Probable carboxypeptidase X1	Adhesion, proteolysis	6.12	−
IGS10	Immunoglobulin superfamily member 10	Receptor signaling	5.85	−
GDN	Glia-derived nexin	Enzyme inhibitory activity, developmental protein	1.95	−
AEBP1	Adipocyte enhancer-binding protein 1	Regulation of transcription, cell adhesion	1.77	−
LOXL3	Lysyl oxidase homolog 3	Oxidoreductase activity	1.73	−

Information about reported protein function was obtained from the DAVID annotation database and PubMed (search keywords: protein or gene name AND angiogenesis, vasculogenesis, endothelial cell migration, endothelial cell adhesion OR endothelial cell proliferation). Reported processing of each protein by MT1-MMP or other MMP/ADAM proteases is indicated. Asterisks indicate proteins reported to be processed by other protease families (serine proteases, *etc.*).

inflammatory context, we aimed at the identification of the collection of MT1-MMP substrates in endothelial tip cells induced by inflammatory stimuli. **Figure 1** outlines the experimental design undertaken in this study.

We first compared the behavior of primary MLECs (pMLECs; ref. 17) *vs.* polyoma virus middle T-immortalized MLECs (iMLECs) from WT mice. iMLECs maintained EC morphology and similar expression of PECAM-1 (>95% in both iMLECs and pMLECs); MT1-MMP cell surface levels were slightly higher in iMLECs (**Fig. 2*A***). To choose the appropriate inflammatory stimulus for inducing endothelial tip cells, we evaluated the effect of the main angiogenic factor VEGF and of the proangiogenic cytokine TNF-α on the expression of the endothelial tip cell markers Jag1, VEGFR2, Dll4, MT1-MMP, integrin β3, and CXCR4 in iMLECs (Fig. 2*B*). Hierarchical clustering analysis of these data performed with Genesis (13) showed that TNF-α regulated the expression of the tip cell markers Dll4 + MT1-MMP and Jag1 + CXCR4 but in a different manner than VEGF, which mainly regulated Dll4 + VEGFR2, as reported previously (5). This analysis confirmed TNF-α as an inflammatory inducer of endothelial tip cells (4). TNF-α induced a similar increase of the endothelial activation markers ICAM-1 and VCAM-1 and enhanced MT1-MMP expression in both pMLECs and iMLECs (Fig. 2*C* and not shown). TNF-α stimulation also resulted in similar elongation and induction of filopodia-like membrane protrusions in both pMLECs and iMLECs cultured in 2D or 3D conditions (Fig. 2*D*). Since iMLECs responded similarly to TNF-α and displayed higher MT1-MMP levels and proliferative capacity than pMLECs, iMLECs were chosen as the proper cellular model to perform quantitative proteomics of MT1-MMP activity in inflammation-activated ECs.

SILAC identification of MT1-MMP degradome in TNF-α-induced endothelial tip cells

Proteolysis by transmembrane proteases mainly affects other transmembrane or secreted glycoproteins (18). We therefore used SILAC to analyze lectin-enriched glycoproteins in mixed supernatants of TNF-α-activated WT (labeled with heavy amino acids) and MT1-MMP-null iMLECs (labeled with light isotopes). Proteins in mixed microsomal fractions were also analyzed; for details of the SILAC procedure and examples of mass spectra, see **Fig. 3*A***, ***B*** and Materials and Methods. Totals of 157 glycoproteins in conditioned medium and 797 proteins in the microsomal fraction were identified and quantified (relative H/L ratios; complete list of proteins available at http://www.cnic.es/doc/metaloproteinasas/SILACproteinlist.pdf), with only 28 proteins found in both proteomes (Fig. 3*C*). Interpretation of H/L ratios in the supernatant glycoproteome is complex; a transmembrane protein or a matrix-bound secreted protein shed by MT1-MMP will yield an H/L ratio >1, but degraded secreted proteins might give H/L ratios <1 or >1 (ref. 8 and Supplemental Fig. S1). Peptide H/L ratio frequencies show a gaussian distribution, with a peak at log H/L = 0, indicating equivalent labeling of WT and MT1-MMP-null cells (Fig. 3*D*). Notably, lack of MT1-MMP altered H/L ratios more in the supernatant glycoproteome than in the microsomal proteome (31.85 *vs.* 17.02% H/L>1.5; Fig. 3*D*). Since H/L > 1 is the more likely outcome for protease action on the supernatant glycoproteome (Supplemental Fig. S1), we defined the MT1-MMP endothelial degradome as the set of glycoproteins with H/L > 1.5 (Fig. 3*D*). Categorization of these identified proteins based on their generic assigned function [Database for Annotation, Visualization, and Integrated Discovery (DAVID); ref. 19) and PubMed search defined a group of angiogen-

esis-related proteins and a smaller group of unrelated proteins (**Table 1**). Most identified proteins are exclusively MT1-MMP substrates, including extracellular matrix (ECM)/matricellular proteins (CYR61, FBLN2, SNED1), and non-ECM proteins (PR2C2, SLIT2, EGFR, SFRP1) (Table 1). Nonexclusive substrates include TSP1, NID1, and SEM3C.

Bioinformatic analysis reveals a combinatorial MT1-MMP proteolytic program in angiogenesis

Gene Ontology (GO) enrichment analysis of the MT1-MMP endothelial degradome (H/L>1.5) was carried out with the FatiGO module (16) in the open-source bioinformatics Web tool Babelomics (15), which compares genes of interest with the rest of the mouse genome. This set of proteins was enriched in cellular components of extracellular and matrix-related compartments (**Fig. 4*A***) correlating with exposure of these proteins to the protease. The MT1-MMP endothelial degradome was also enriched in molecular functions related to binding, particularly matrix binding, and enzyme activity (Fig. 4*B*) and was highly-enriched in biological processes (BPs) related to cellular adhesion, motility, and chemotaxis, key steps in endothelial tip cell function, and to vasculature development (Fig. 4*C*).

Several substrates appeared in more than one BP (Supplemental Table S1). Overlap analysis and Venn diagrams of proteins annotated in these BPs revealed a proteolytic program of 14 substrates, in which combined rather than single substrate processing by MT1-MMP would control key steps of the angiogenic response, in particular cell motility, chemotaxis, cell adhesion, and vasculature development (Fig. 4*D*). In this combinatorial program, processing of TSP1 is common to these 4 BPs; CYR61 processing is the second branch point, excluding motility and steering toward one of the other fates. Processing of TSP1 and CYR61, combined with CCL2 and SLIT2, determines chemotaxis. Within the MT1-MMP-combinatorial program, adhesion and vasculature development would be more closely related, with motility showing the least overlap, being determined by combined processing of TSP1, SEM3C, EGFR, PR2C2, and CSF1.

The SILAC-analyzed microsomal fraction lacked most MT1-MMP substrates (Fig. 3*C*). However, the 24 h of iMLEC TNF-α stimulation is enough for transcrip-

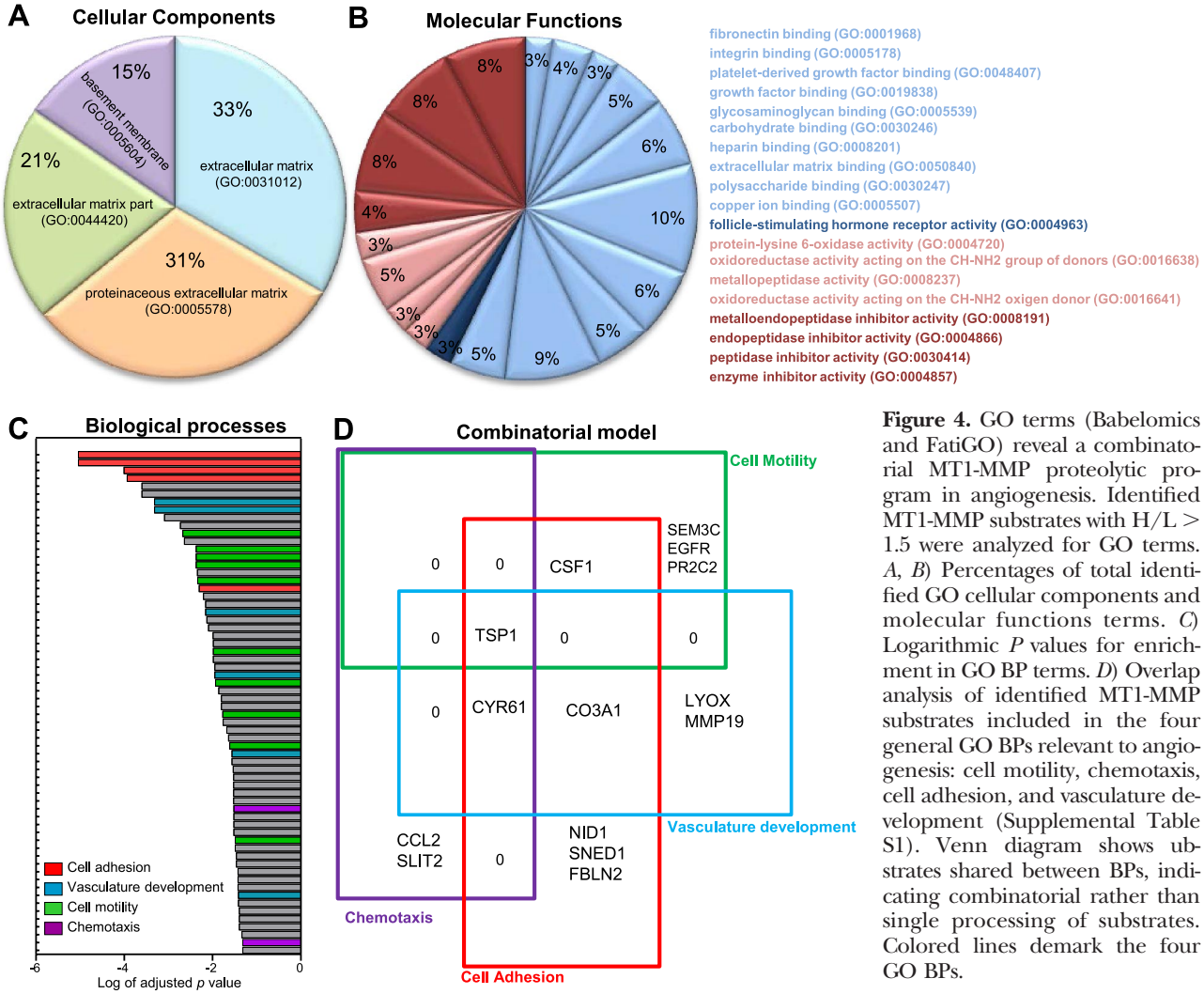

Figure 4. GO terms (Babelomics and FatiGO) reveal a combinatorial MT1-MMP proteolytic program in angiogenesis. Identified MT1-MMP substrates with H/L > 1.5 were analyzed for GO terms. *A*, *B*) Percentages of total identified GO cellular components and molecular functions terms. *C*) Logarithmic *P* values for enrichment in GO BP terms. *D*) Overlap analysis of identified MT1-MMP substrates included in the four general GO BPs relevant to angiogenesis: cell motility, chemotaxis, cell adhesion, and vasculature development (Supplemental Table S1). Venn diagram shows substrates shared between BPs, indicating combinatorial rather than single processing of substrates. Colored lines demark the four GO BPs.

tional regulation to occur, and genes encoding 4 of the 14 proteins in the combinatorial model (CO3A1, FBLN2, protein-lysine 6-oxidase and MMP19) are found up-regulated in MCP-1-stimulated WT but not MT1-MMP-null pMLECs (Supplemental Table S2 and Supplemental Fig. S2); thus, their H/L > 1 in iMLEC supernatant might partly reflect transcriptional regulation.

Biological validation of MT1-MMP combinatorial proteolysis in TNF-α-stimulated primary ECs

For further validation, we selected substrates within each of the 4 main BPs. *In vitro* digestion assays had previously shown the ability of MT1-MMP to cleave TSP1, CYR61, and NID1 (20, 21), and we further confirmed by *in silico* analysis that TSP1, CYR61, and NID1 and also SEM3C contain putative MT1-MMP cleavage sequences [R(F/K)-nonP-X(polar)-X(hydrophobic); ref. 22] at positions that predict the peptides identified by SILAC (Supplemental Fig. S3).

Based on the SILAC analysis performed in CSUPs and on the ability of the identified proteins TSP1, CYR61, NID1, and SEM3C to bind the ECM and/or the basement membrane, we next hypothesized that the absence of MT1-MMP might affect cleavage of these proteins from the ECM and therefore their release to the supernatant and their cellular distribution. No major differences were observed in mRNA and protein levels of TSP1, CYR61, NID1, and SEM3C in total lysates of WT and MT1-MMP-null pMLECs treated with TNF-α (24 h), pointing to similar abundance of these substrates (**Fig. 5*A, B***). In accordance with SILAC data, lower levels of TSP1, NID1, and SEM3C were detected in the supernatants of MT1-MMP-null MLECs, indicating that MT1-MMP proteolytic action releases TSP1, NID1, and SEM3C from the ECM; consistent with cleavage of NID1 at the N or C terminus, the molecular mass of NID1 in supernatants from WT MLECs was slightly smaller (Fig. 5*A*). Higher levels of CYR61 were, however, found in supernatants from MT1-MMP-deficient pMLECs, correlating with a more complex SILAC peptide profile and pointing to an active processing of the intact soluble form of CYR61 by MT1-MMP. Impaired processing in the absence of MT1-MMP led to accumulation of TSP1, CYR61, NID1, and SEM3C in

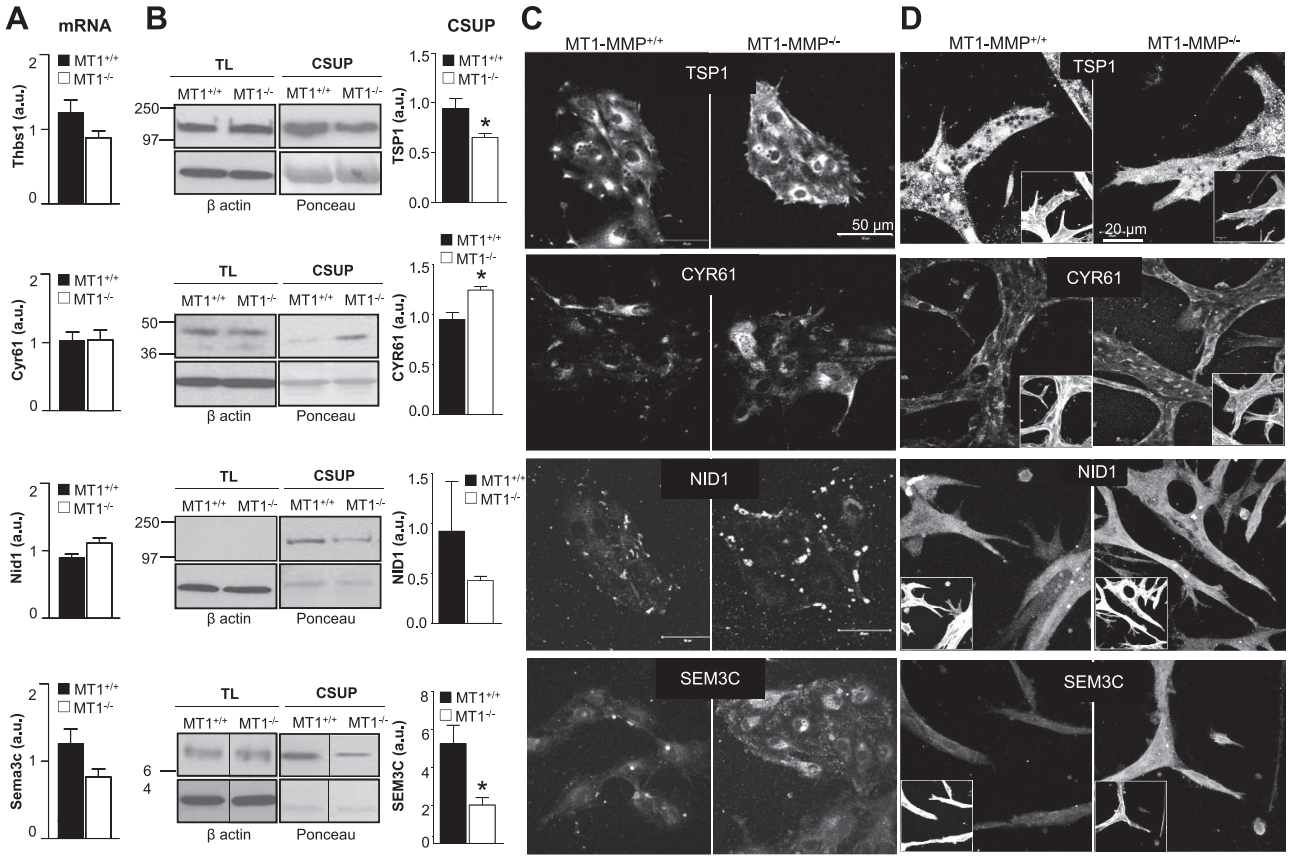

Figure 5. Impaired processing of TSP1, CYR61, NID1, and SEM3C in MT1-MMP-null pMLECs. *A*) Bar charts show mRNA levels of Thbs1, Cyr61, Nid1, and Sema3c in TNF-α-stimulated WT ($MT1^{+/+}$) and null ($MT1^{-/-}$) pMLECs analyzed by quantitative PCR (n=5). *B*) Immunoblots show detection of TSP1, CYR61, NID1, and SEM3C in total lysates (TL) and CSUPs of TNF-α-stimulated WT ($MT1^{+/+}$) and null ($MT1^{-/-}$) pMLECs; bar charts show densitometric quantification of proteins in supernatants (n=3). *C*) Confocal microscopy analysis was performed in TNF-α-stimulated WT and MT1-MMP-null pMLECs immunostained for TSP1, CYR61, NID1, or SEM3C; representative maximal projections are shown (n=5). *D*) Confocal immunofluorescence of TSP1, CYR61, NID1, or SEM3C in TNF-α-stimulated WT and null pMLECs grown in Ibidi chambers covered by 3D-Matrigel; representative maximal projections are shown (n=5). Insets: F-actin staining.

pericellular clusters in contact with the matrix and/or adhesion sites in MT1-MMP-null pMLECs (Fig. 5*C*).

TSP1, CYR61, NID1, and SEM3C have been related to angiogenesis and vascular development (23–26), and we therefore analyzed the effect of MT1-MMP-mediated processing of these substrates in models better mimicking vascular development, such as 3D-Matrigel MLEC cultures and retina postnatal vascularization. Although no major differences were observed in TSP1, CYR61, NID1, and SEM3C signal along EC 3D tubes, enrichment and/or pericellular clusters of these substrates, especially of CYR61 and NID1, were observed along the endothelial tip cells formed by MT1-MMP-null pMLECs compared with WT (Fig. 5*D*). Accordingly, accumulation of CYR61 and NID1 was also detected along endothelial tip cells at the vascular front of retinas from MT1-MMP-null neonates, but not their WT counterparts, indicating that this newly identified MT1-MMP processing axis is also relevant to *in vivo* angiogenesis (**Fig. 6**). SEM3C and TSP1 were undetectable in the vasculature of mouse neonate retinas (not shown).

We next investigated whether the MT1-MMP proteolytic program identified in mouse ECs could be extendable to the human model. To this purpose, MT1-MMP expression was inhibited by two independent siRNA oligonucleotides in HUVECs; the efficiency of MT1-MMP interference was >70% assessed by RT-PCR and Western blot (**Fig. 7*A***). TSP1, CYR61, NID1, and SEM3C levels in total lysates from negative siRNA and MT1-MMP-inhibited HUVECs were similar (not shown). Lower levels of TSP1, CYR61, and NID1 were, however, found in supernatants from MT1-MMP-inhibited compared with negative siRNA-inhibited HUVECs, pointing to decreased processing of these substrates in cells with reduced levels of MT1-MMP (Fig. 7*B*). No differences could be detected in supernatant levels of SEM3C (Fig. 7*B*). In a complementary approach, we compared substrate subcellular distribution in MT1-MMP-inhibited HUVECs. As shown in Fig. 7*C*, the subcellular distribution of TSP1, CYR61, NID1, and SEM3C was changed in HUVECs with reduced expression of MT1-MMP; in particular, CYR61 and SEM3C appeared more intense and NID1 formed pericellular clusters in HUVECs with lower expression of MT1-MMP. These data support the hypothesis that the identified MT1-MMP combinatorial program is also operative in human ECs.

DISCUSSION

SILAC performed in TNF-α-activated primary ECs has provided an integrated view of the contribution of the protease MT1-MMP to inflammatory capillary sprouting through combinatorial cleavage of defined sets of substrates and a mechanistic link between proteolytic events and biological responses by ECs during angiogenesis (**Fig. 8**).

Largely known for a long time, the link between angiogenesis and inflammation is not well understood. TNF-α is an early tissue-damage signal for angiogenesis and can induce morphological and molecular changes compatible with induction of the endothelial tip cell phenotype (4, 27); we confirmed this ability in iMLECs. Endothelial tip cells are crucial to initiate an efficient angiogenic response (5). The molecular fingerprint of these tip cells has started to be elucidated by recent transcriptomics analysis in retinal tip cells; matrix and matrix-related genes as well as secreted proteins, such as apelin, seemed to be particularly represented (2). MT1-MMP gene was not found to be enriched in the microarray assays performed in retinal tip cells (1, 2); low levels of MT1-MMP might have been missed, or MT1-MMP might be especially relevant in inflammatory angiogenesis. We then hypothesized that identification of MT1-MMP collection of substrates in inflammatory tip cells will provide insights into their function and into the link between proteolytic events and biological responses during angiogenesis.

We have circumvented SILAC limited use in primary cells by immortalizing mouse lung ECs, allowing us to perform this approach for the first time in ECs obtained from genetically modified mice. Our results showed larger variations in the supernatant glycoproteome than in the microsomal proteome in the absence of MT1-MMP; this highlights the power of performing

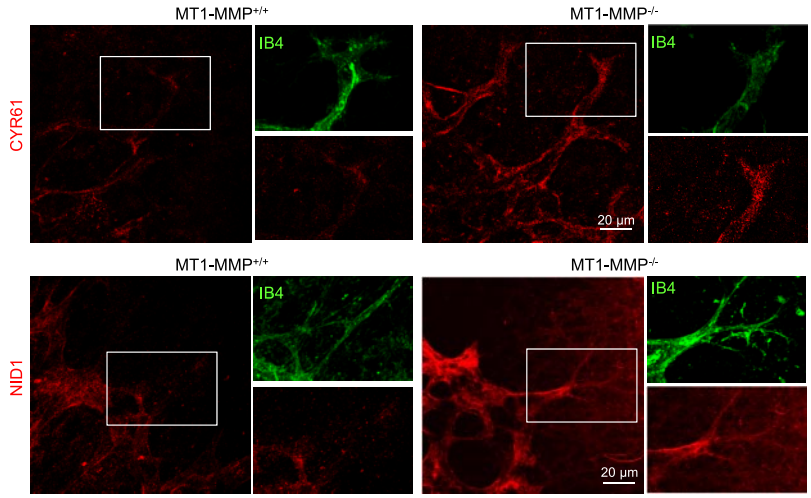

Figure 6. Accumulation of CYR61 and NID1 in endothelial tip cells of retinas from MT1-MMP-null mouse neonates. Whole-mount confocal immunofluorescence of CYR61 or NID1 (red) and isolectin B4 (green) in retinas of P6 WT (MT1-MMP$^{+/+}$) and null (MT1-MMP$^{-/-}$) mice; representative maximal projections are shown (n=4).

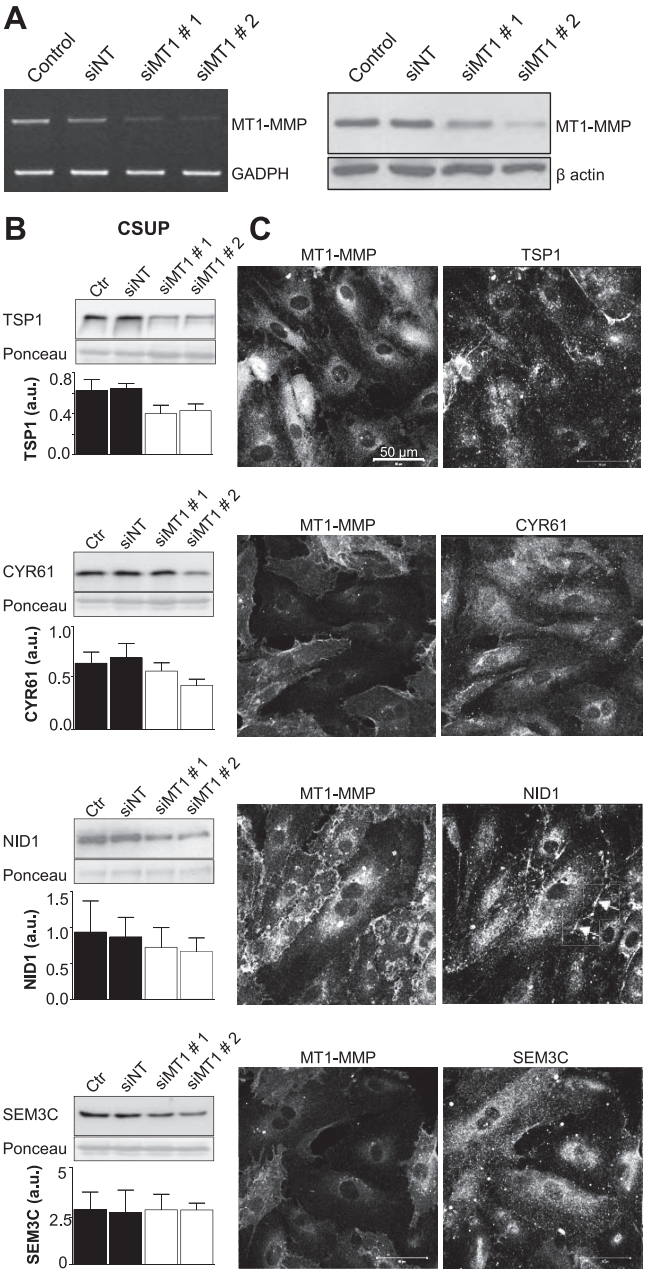

Figure 7. Impaired processing of TSP1, CYR61, NID1 and SEM3C in MT1-MMP-inhibited human ECs. *A*) MT1-MMP expression was inhibited by siRNA transfection of two different MT1-MMP siRNA oligonucleotides (siMT1 #1 and siMT1 #2) or a negative siRNA (siNT) in HUVECs; MT1-MMP mRNA and protein levels were assessed by RT-PCR and Western blot, respectively. *B*) Immunoblots show detection of TSP1, CYR61, NID1, and SEM3C in CSUPs of TNF-α-stimulated HUVECs transfected with siNT or siMT1 #1 and #2; bar charts show densitometric quantification of proteins in supernatants (n=4–6). *C*) Confocal microscopy analysis was performed in TNF-α-stimulated MT1-MMP-siRNA HUVECs immunostained for MT1-MMP and TSP1, CYR61, NID1, or SEM3C; representative maximal projections are shown (n=4); arrows indicate NID1 pericellular deposits.

SILAC in CSUPs for protease analysis, since catalytic activity mostly affects secreted glycoproteins that are a small fraction of the total proteome (28). A few SILAC MT1-MMP substrates were identified previously by isobaric tags for relative and absolute quantitation-(iTRAQ)/isotope-coded affinity tag (ICAT) in tumor cells (29) and by differential gel electrophoresis (DIGE) in human plasma incubated with the MT1-MMP catalytic domain (30), supporting the robustness of these techniques and pointing to MT1-MMP cleavage of a given substrate in different contexts. MT1-MMP can affect angiogenesis through the processing of matrix components (31) but also of transmembrane molecules such as semaphorin 4D and endoglin (32, 33). Although we used SILAC to identify transmembrane glycoproteins, most of the identified MT1-MMP substrates in inflammatory endothelial tip cells are ECM and secreted proteins, in accordance with reported retinal endothelial tip cell transcriptome (2), and reinforcing the idea that matrix and its remodeling are essential for modulating endothelial tip cells. Further optimization of cell surface protein labeling (34) might still expand MT1-MMP repertoire to include endothelial transmembrane proteins. SILAC also provided insight into redundancy *vs.* specificity of substrate cleavage by MMP/a disintegrin and metalloproteinase (ADAM) family members. MT1-MMP mainly shares substrates such as TSP1, NID1, and SEM3C with ADAM with thrombospondin motifs 1 (ADAMTS1), suggesting cooperation among these proteolytic pathways in angiogenesis. Accordingly, ADAMTS1 is up-regulated in the transcriptome of retinal endothelial tip cells (2) and down-regulated in MCP-1-stimulated MT1-MMP-null pMLECs (Supplemental Table S2).

One of the most novel aspects of our study involves the identification of a combinatorial proteolytic program by overlap analysis and Venn diagram representation of the MT1-MMP endothelial degradome. In this combinatorial program, TSP1 and/or CYR61 processing is central to processes such as cell adhesion, motility, chemotaxis, and vasculature development (35). Matricellular proteins, such as TSP1 and CYR61, are interesting because they act as a bridge between cells and the ECM, thus modulating cell behavior; therefore, it is not unexpected that MT1-MMP action relies mainly on processing of members of this family. Outcome of angiogenesis will then depend on combined rather than individual processing of substrates, whose fragments might act in a competitive, synergistic, or sequential manner to fine-tune the angiogenic response; for example, TSP1 and CYR61 share domains that directly or indirectly bind integrin $\alpha_v\beta_3$, an adhesion receptor expressed in endothelial tip cells that cooperates with endothelial MT1-MMP (2, 12). Overlap analysis also showed that EC adhesion and vasculature development are molecularly closer and that cell motility is the most unique in the combination of processed substrates.

Increased abundance of a given protein in the supernatant of WT cells might also be related to higher expression of the protein. Although no major changes were found in the microsomal fraction, 4 of the 14 genes encoding for proteins represented in the combinatorial proteolytic program were up-regulated in MCP-1-stimulated pMLECs expressing MT1-MMP *vs.*

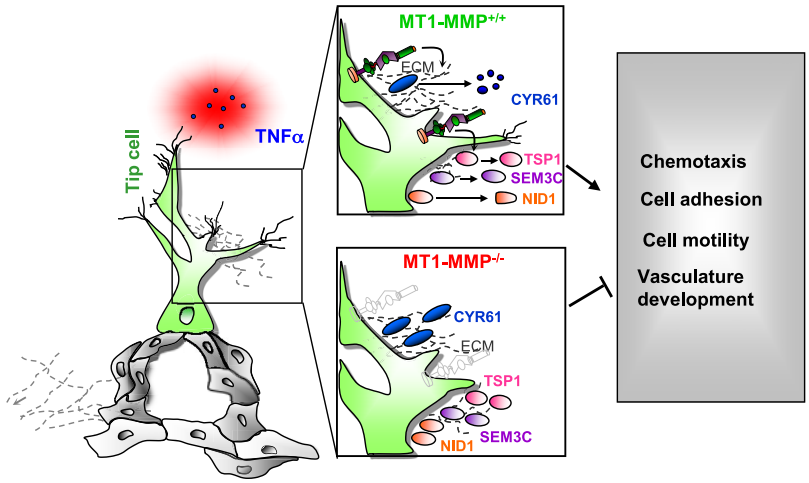

Figure 8. MT1-MMP combined substrate processing in inflammatory angiogenesis. Combined processing of TSP1, CYR61, NID1, SEM3C, and other substrates by MT1-MMP has a major effect on the regulation of EC adhesion and motility and chemotaxis, ultimately leading to vasculature development. This proteolytic program is activated by inflammatory stimuli, such as TNF-α. The absence of MT1-MMP in stimulated ECs results in impaired processing and accumulation of the identified substrates dampening the capillary sprouting process and favoring quiescence of the vasculature.

null cells; in particular, genes and proteins related to cell adhesion and vasculature development, complex responses that likely require activation of a given transcriptional program. These data indicate a bimodal contribution of MT1-MMP to inflammatory angiogenesis, including regulation of a restricted gene set but dominated by combinatorial processing of defined substrates related to motility, chemotaxis, and adhesion.

We next biologically validated the processing of selected substrates involved in the four main BPs, cell motility, chemotaxis, cell adhesion, and vasculature development (TSP1, CYR61, NID1, and SEM3C), whose cleavage would likely occur within the same time frame, cooperating in driving cellular responses leading to inflammatory capillary sprouting. Conversely, as we demonstrated in TNF-α-stimulated MT1-MMP-null pMLECs, in the absence of MT1-MMP simultaneous accumulation of these substrates in ECs might contribute to defective angiogenesis (10, 17). Whether the proteolytic effect of MT1-MMP on the identified substrates in cells is only due to direct processing or to additional indirect effects, for instance, through the combined action of other proteases, such as ADAMTS1, remains to be defined. Notably, we have also confirmed that the combinatorial program driven by MT1-MMP identified in mouse cells is also acting in human ECs, since decreasing MT1-MMP expression affects on the processing and subcellular distribution of TSP1, CYR61, NID1, and SEM3C in HUVECs; however, milder effects were observed and were likely related to the experimental approach and possibly to a different repertoire of proteases expressed by human ECs. The multidomain structure of matricellular proteins contributes to their pleiotropic functions in angiogenesis. Thus, TSP1 effects on angiogenesis largely depend on whether it is soluble or matrix-bound (23); during inflammatory angiogenesis, MT1-MMP could modulate these angiogenic properties by cooperating with ADAMTS1 (35) or acting at a different cleavage site and possibly affecting interaction with integrin $\alpha_v\beta_3$. Matrix-bound TSP1 accumulation in the absence of MT1-MMP might contribute to the reduced angiogenesis reported in MT1-MMP-null cells (11, 17). Moreover, accumulation of CYR61/CCN1 might impair its induction of EC adhesion, migration, and proliferation (24) likely by altering its binding to integrins $\alpha_6\beta_1$ or $\alpha_v\beta_3$ (36). CYR61 was also accumulated in MT1-MMP-deficient retinas pointing to a key role for MT1-MMP in CYR61 processing *in vivo* and suggesting that loss of this processing might mimic vascular defects observed in the absence of CYR61 (24). However, since CYR61 can play dual roles in physiological and pathological vascularization in the retina (37), functional consequences of CYR61 processing would deserve further investigation. Likewise, pericellular deposits of NID1, a protein normally associated to laminin and fibulin at the basement membrane (25) might confer basement membrane-like "quiescence" signals hindering EC active sprouting. We also observed NID1 deposition along the filopodia of endothelial tip cells at the retinal vascular front of MT1-MMP-null neonates in contrast to the restricted distribution of NID1 to the posterior pole of retinal tip cells in WT (2); this points to an active role of MT1-MMP in NID1 processing during vascular sprouting also *in vivo*. Finally, SEM3C processing by ADAMTS1 can contribute to tumor cell migration (26), and therefore we can envision that MT1-MMP-processing of SEM3C might affect EC migration required for capillary sprouting; in the absence of this processing, impaired migration might lead to defective angiogenesis. In sum, TSP1, CYR61, NID1, and SEM3C can modulate EC adhesive and migratory behavior through complementary mechanisms including binding to integrins; the synergistic or competitive action of these accumulated substrates in the absence of MT1-MMP would impair migration and adhesion, yielding a more quiescent endothelial state and defective angiogenesis (ref. 17 and Fig. 8).

We have established a valid cell model system for studying the mechanistic link between proteolysis and biological responses in the context of inflammation-activated ECs. SILAC-based proteomics identified the supernatant glycoproteome as the main protein set targeted by the protease MT1-MMP. Combination of SILAC with bioinformatics revealed that the main con-

tribution of MT1-MMP to inflammatory angiogenesis is a combinatorial processing of defined substrates impacting early and rapid responses such as motility, chemotaxis, and adhesion, finally leading to new vessel formation. Profiling of MT1-MMP-processed substrates in plasma could be used as a surrogate marker of angiogenic activity in chronic inflammatory disease such as rheumatoid arthritis, inflammatory bowel disease, psoriasis, and atherosclerosis, potentially identifying patients who might benefit from antiangiogenic therapies. FJ

The authors thank Suneel S. Apte (Lerner Research Institute, Cleveland, OH, USA) and Karl Tryggvason (Karolinska Institute, Stockholm, Sweden) for MT1-MMP-null mice, R. Álvarez and A. Dopazo for microarray analysis, A. Luque for help in EC immortalization, J. Vázquez for critical reading of the manuscript, and S. Bartlett for English editing. This work was supported by grants from the Spanish Ministry of Economy and Competitivity (MINECO; SAF2008-02104, SAF2011-25619 and RD06/0014/1016) and the Fundación Genoma España to A.G.A. A.K. is funded by a Formación de Profesorado Universitario fellowship and P.G. by a Fondo de Investigación Sanitaria contract from the former Ministry of Science and Innovation (MICINN). The Vall d'Hebron Institute of Oncology Proteomics Laboratory is a member of the ProteoRed–Instituto de Salud Carlos III network (MICINN). Work at the Centro de Investigación Príncipe Felipe was partly supported by the Instituto Nacional de Bioinformática (MICINN). The CNIC is supported by the MINECO and the Pro-CNIC Foundation. A.K. and P.G. designed and performed research, data analysis and interpretation, and contributed to the manuscript; A.M., A.P., C.L., and N.C. performed specific assays; D.M. and J.D. helped with bioinformatics analysis; J.A. and F.C. provided conceptual and technical support in proteomics analysis; and A.G.A. designed and supervised research and wrote the paper. Data presented are under patent application review.

REFERENCES

1. Strasser, G. A., Kaminker, J. S., and Tessier-Lavigne, M. (2010) Microarray analysis of retinal endothelial tip cells identifies CXCR4 as a mediator of tip cell morphology and branching. *Blood* **115,** 5102–5110
2. Del Toro, R., Prahst, C., Mathivet, T., Siegfried, G., Kaminker, J. S., Larrivee, B., Breant, C., Duarte, A., Takakura, N., Fukamizu, A., Penninger, J., and Eichmann, A. (2010) Identification and functional analysis of endothelial tip cell-enriched genes. *Blood* **116,** 4025–4033
3. Arroyo, A. G., and Iruela-Arispe, M. L. (2010) Extracellular matrix, inflammation, and the angiogenic response. *Cardiovasc. Res.* **86,** 226–235
4. Sainson, R. C., Johnston, D. A., Chu, H. C., Holderfield, M. T., Nakatsu, M. N., Crampton, S. P., Davis, J., Conn, E., and Hughes, C. C. (2008) TNF primes endothelial cells for angiogenic sprouting by inducing a tip cell phenotype. *Blood* **111,** 4997–5007
5. De Smet, F., Segura, I., De Bock, K., Hohensinner, P. J., and Carmeliet, P. (2009) Mechanisms of vessel branching: filopodia on endothelial tip cells lead the way. *Arterioscler. Thromb. Vasc. Biol.* **29,** 639–649
6. Yana, I., Sagara, H., Takaki, S., Takatsu, K., Nakamura, K., Nakao, K., Katsuki, M., Taniguchi, S., Aoki, T., Sato, H., Weiss, S. J., and Seiki, M. (2007) Crosstalk between neovessels and mural cells directs the site-specific expression of MT1-MMP to endothelial tip cells. *J. Cell Sci.* **120,** 1607–1614
7. Karagiannis, E. D., and Popel, A. S. (2006) Distinct modes of collagen type I proteolysis by matrix metalloproteinase (MMP) 2 and membrane type I MMP during the migration of a tip endothelial cell: insights from a computational model. *J. Theor. Biol.* **238,** 124–145
8. Doucet, A., Butler, G. S., Rodriguez, D., Prudova, A., and Overall, C. M. (2008) Metadegradomics: toward in vivo quantitative degradomics of proteolytic post-translational modifications of the cancer proteome. *Mol. Cell. Proteomics* **7,** 1925–1951
9. Ong, S. E., Blagoev, B., Kratchmarova, I., Kristensen, D. B., Steen, H., Pandey, A., and Mann, M. (2002) Stable isotope labeling by amino acids in cell culture, SILAC, as a simple and accurate approach to expression proteomics. *Mol. Cell. Proteomics* **1,** 376–386
10. Zhou, Z., Apte, S. S., Soininen, R., Cao, R., Baaklini, G. Y., Rauser, R. W., Wang, J., Cao, Y., and Tryggvason, K. (2000) Impaired endochondral ossification and angiogenesis in mice deficient in membrane-type matrix metalloproteinase I. *Proc. Natl. Acad. Sci. U. S. A.* **97,** 4052–4057
11. Oblander, S. A., Zhou, Z., Galvez, B. G., Starcher, B., Shannon, J. M., Durbeej, M., Arroyo, A. G., Tryggvason, K., and Apte, S. S. (2005) Distinctive functions of membrane type 1 matrix-metalloprotease (MT1-MMP or MMP-14) in lung and submandibular gland development are independent of its role in pro-MMP-2 activation. *Dev. Biol.* **277,** 255–269
12. Galvez, B. G., Matias-Roman, S., Yanez-Mo, M., Sanchez-Madrid, F., and Arroyo, A. G. (2002) ECM regulates MT1-MMP localization with beta1 or alphavbeta3 integrins at distinct cell compartments modulating its internalization and activity on human endothelial cells. *J. Cell Biol.* **159,** 509–521
13. Sturn, A., Quackenbush, J., and Trajanoski, Z. (2002) Genesis: cluster analysis of microarray data. *Bioinformatics* **18,** 207–208
14. Elias, J. E., and Gygi, S. P. (2007) Target-decoy search strategy for increased confidence in large-scale protein identifications by mass spectrometry. *Nat. Methods* **4,** 207–214
15. Medina, I., Carbonell, J., Pulido, L., Madeira, S. C., Goetz, S., Conesa, A., Tarraga, J., Pascual-Montano, A., Nogales-Cadenas, R., Santoyo, J., Garcia, F., Marba, M., Montaner, D., and Dopazo, J. (2010) Babelomics: an integrative platform for the analysis of transcriptomics, proteomics and genomic data with advanced functional profiling. *Nucleic Acids Res.* **38,** W210–W213
16. Al-Shahrour, F., Diaz-Uriarte, R., and Dopazo, J. (2004) FatiGO: a web tool for finding significant associations of Gene Ontology terms with groups of genes. *Bioinformatics* **20,** 578–580
17. Galvez, B. G., Genis, L., Matias-Roman, S., Oblander, S. A., Tryggvason, K., Apte, S. S., and Arroyo, A. G. (2005) Membrane type 1-matrix metalloproteinase is regulated by chemokines monocyte-chemoattractant protein-1/ccl2 and interleukin-8/CXCL8 in endothelial cells during angiogenesis. *J. Biol. Chem.* **280,** 1292–1298
18. Butler, G. S., and Overall, C. M. (2007) Proteomic validation of protease drug targets: pharmacoproteomics of matrix metalloproteinase inhibitor drugs using isotope-coded affinity tag labelling and tandem mass spectrometry. *Curr. Pharm. Des.* **13,** 263–270
19. Huang da, W., Sherman, B. T., Stephens, R., Baseler, M. W., Lane, H. C., and Lempicki, R. A. (2008) DAVID gene ID conversion tool. *Bioinformation* **2,** 428–430
20. Butler, G. S., Dean, R. A., Tam, E. M., and Overall, C. M. (2008) Pharmacoproteomics of a metalloproteinase hydroxamate inhibitor in breast cancer cells: dynamics of membrane type 1 matrix metalloproteinase-mediated membrane protein shedding. *Mol. Cell. Biol.* **28,** 4896–4914
21. D'Ortho, M. P., Will, H., Atkinson, S., Butler, G., Messent, A., Gavrilovic, J., Smith, B., Timpl, R., Zardi, L., and Murphy, G. (1997) Membrane-type matrix metalloproteinases 1 and 2 exhibit broad-spectrum proteolytic capacities comparable to many matrix metalloproteinases. *Eur. J. Biochem.* **250,** 751–757
22. Kridel, S. J., Sawai, H., Ratnikov, B. I., Chen, E. I., Li, W., Godzik, A., Strongin, A. Y., and Smith, J. W. (2002) A unique substrate binding mode discriminates membrane type-1 matrix metalloproteinase from other matrix metalloproteinases. *J. Biol. Chem.* **277,** 23788–23793
23. Iruela-Arispe, M. L., Luque, A., and Lee, N. (2004) Thrombospondin modules and angiogenesis. *Int. J. Biochem. Cell Biol.* **36,** 1070–1078
24. Kubota, S., and Takigawa, M. (2007) CCN family proteins and angiogenesis: from embryo to adulthood. *Angiogenesis* **10,** 1–11

25. Ho, M. S., Bose, K., Mokkapati, S., Nischt, R., and Smyth, N. (2008) Nidogens-Extracellular matrix linker molecules. *Microsc. Res. Tech.* **71,** 387–395
26. Esselens, C., Malapeira, J., Colome, N., Casal, C., Rodriguez-Manzaneque, J. C., Canals, F., and Arribas, J. (2010) The cleavage of semaphorin 3C induced by ADAMTS1 promotes cell migration. *J. Biol. Chem.* **285,** 2463–2473
27. Ligresti, G., Aplin, A. C., Zorzi, P., Morishita, A., and Nicosia, R. F. (2011) Macrophage-derived tumor necrosis factor-alpha is an early component of the molecular cascade leading to angiogenesis in response to aortic injury. *Arterioscler. Thromb. Vasc. Biol.* **31,** 1151–1159
28. Beck, M., Schmidt, A., Malmstroem, J., Claassen, M., Ori, A., Szymborska, A., Herzog, F., Rinner, O., Ellenberg, J., and Aebersold, R. (2011) The quantitative proteome of a human cell line. *Mol. Syst. Biol.* **7,** 549
29. Tam, E. M., Morrison, C. J., Wu, Y. I., Stack, M. S., and Overall, C. M. (2004) Membrane protease proteomics: Isotope-coded affinity tag MS identification of undescribed MT1-matrix metalloproteinase substrates. *Proc. Natl. Acad. Sci. U. S. A.* **101,** 6917–6922
30. Hwang, I. K., Park, S. M., Kim, S. Y., and Lee, S. T. (2004) A proteomic approach to identify substrates of matrix metalloproteinase-14 in human plasma. *Biochim. Biophys. Acta* **1702,** 79–87
31. Chun, T. H., Sabeh, F., Ota, I., Murphy, H., McDonagh, K. T., Holmbeck, K., Birkedal-Hansen, H., Allen, E. D., and Weiss, S. J. (2004) MT1-MMP-dependent neovessel formation within the confines of the three-dimensional extracellular matrix. *J. Cell Biol.* **167,** 757–767
32. Basile, J. R., Holmbeck, K., Bugge, T. H., and Gutkind, J. S. (2007) MT1-MMP controls tumor-induced angiogenesis through the release of semaphorin 4D. *J. Biol. Chem.* **282,** 6899–6905
33. Hawinkels, L. J., Kuiper, P., Wiercinska, E., Verspaget, H. W., Liu, Z., Pardali, E., Sier, C. F., and ten Dijke, P. (2010) Matrix metalloproteinase-14 (MT1-MMP)-mediated endoglin shedding inhibits tumor angiogenesis. *Cancer Res.* **70,** 4141–4150
34. Conn, E. M., Madsen, M. A., Cravatt, B. F., Ruf, W., Deryugina, E. I., and Quigley, J. P. (2008) Cell surface proteomics identifies molecules functionally linked to tumor cell intravasation. *J. Biol. Chem.* **283,** 26518–26527
35. Lee, N. V., Sato, M., Annis, D. S., Loo, J. A., Wu, L., Mosher, D. F., and Iruela-Arispe, M. L. (2006) ADAMTS1 mediates the release of antiangiogenic polypeptides from TSP1 and 2. *EMBO J.* **25,** 5270–5283
36. Leu, S. J., Chen, N., Chen, C. C., Todorovic, V., Bai, T., Juric, V., Liu, Y., Yan, G., Lam, S. C., and Lau, L. F. (2004) Targeted mutagenesis of the angiogenic protein CCN1 (CYR61). Selective inactivation of integrin alpha6beta1-heparan sulfate proteoglycan coreceptor-mediated cellular functions. *J. Biol. Chem.* **279,** 44177–44187
37. Hasan, A., Pokeza, N., Shaw, L., Lee, H. S., Lazzaro, D., Chintala, H., Rosenbaum, D., Grant, M. B., and Chaqour, B. (2011) The matricellular protein cysteine-rich protein 61 (CCN1/Cyr61) enhances physiological adaptation of retinal vessels and reduces pathological neovascularization associated with ischemic retinopathy. *J. Biol. Chem.* **286,** 9542–9554

Received for publication February 26, 2012.
Accepted for publication July 17, 2012.